# Synthesis, Structures, and Catalytic Reactions of Ring-Substituted Titanium(IV) Complexes

Yanlong Qian,* Jiling Huang, Muhammad D. Bala, Bing Lian, Hao Zhang, and Hao Zhang

*The Laboratory of Organometallic Chemistry, East China University of Science and Technology, 130 Meilong Road, Shanghai 200237, People's Republic of China*

*Received November 6, 2002*

## *Contents*



* Corresponding author (fax +86-21-5428-2375; e-mail qianling@online.sh.cn).

## *I. Introduction*

### A. Background

The subject of metallocenes, their synthesis, structural characterization, and application to catalysis, has been a very active area of research as evidenced by the sheer volume of readily available literature.[1−9] Group IV transition metals (Ti, Zr, and Hf) and group III lanthanide metals (Y and La−Lu) have received special attention as illustrated by the publication of exclusive thematic issues on the two groups by this journal within a span of just two years (2000 and 2002, respectively).[10,11] Despite all of this, to the best of our knowledge, the recently available literature lacks a comprehensive review linking the various aspects of titanium chemistry: synthesis, structural characterization, and a systematic study on the influence of ring substituents on catalysis in a single piece.[12] We particularly observe that discussions on the chemistry and catalytic applications of group IV metallocenes often refer to zirconium-based complexes for illustrations and citing examples. Despite the fact that titanium has a unique chemistry and reactivity that needs frequent review and appraisal to keep in line with the rapid pace of development in research, titanocenes oftentimes feature prominently only in areas where they have proved to be far better than zirconocenes and are therefore well established, such as the cyclopentadienyl-amido complexes. Therefore, we plan to feature titanium-based complexes to narrow the gap.

10.1021/cr020002x CCC: $44.00 
Published on Web 06/21/2003

Yanlong Qian was born in 1940. He received his B.S. degree from the Department of Polymer Chemistry, University of Science and Technology of China, in 1963. Then he joined Shanghai Institute of Organic Chemistry, Chinese Academy of Sciences. In 1992 he moved to East China University of Science and Technology. During 1979–1981 and 1988–1990 he was awarded twice with the Alexander von Humboldt Research Fellowship and did his research on organotitanium chemistry and catalysis at the Max-Planck Institute of Coal Research, Muelheim/Ruhr, Germany, as a Visiting Scholar and Guest Professor, respectively. He is currently a Professor of Organic Chemistry at East China University of Science and Technology. His main research interests include organometallic and coordination chemistry, homogeneous catalysis, organic synthesis of fine chemicals, and polymer chemistry.

Jiling Huang was born in 1941. She received her B.S. degree from the Department of Chemistry, Beijing University of Science and Technology, in 1964. Then she joined Shanghai Institute of Organic Chemistry, Chinese Academy of Sciences. In 1992 she moved to East China University of Science and Technology. During 1986–1988 she worked at Florida State University as a Visiting Scholar. She is currently a Professor of Organic Chemistry at East China University of Science and Technology. Her main research interests include organometallic chemistry, homogeneous catalysis, and the application of organometallics in organic synthesis.

The general interest in academic and industrial laboratories on metallocenes as potential driving forces for the polymer and probably the pharmaceutical industries is illustrated by not only the number of open publications but also the deluge of patent claims made annually on improved synthetic methodology and applications of metallocenes in catalysis.[13] With ∼75% of the total investment in polyolefin research, which is estimated at over a billion dollars per annum, expended on metallocene research alone, the frenzy of activities based on estimations that the olefin industry will churn out >62 million tons of metallocene-based polymer annually is poised to increase.[14,15]

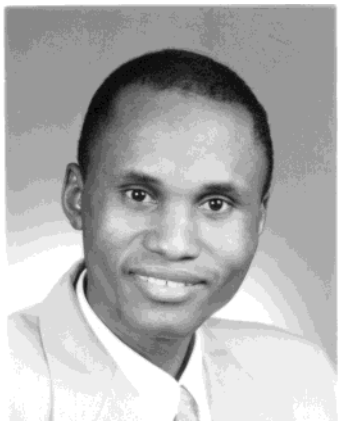

Muhammad Dabai Bala was born in Zuru, Kebbi State, Nigeria, in 1969. He received his B.S. from Ahmadu Bello University in 1991. Then he joined the Chemistry Program of Abubakar Tafawa Balewa University, Bauchi, as a Graduate Assistant, where he obtained his M.S. in Polymer Chemistry in 1997. He obtained his Ph.D. under the supervision of Professor Yanlong Qian at East China University of Science and Technology. His research interests include organometallic chemistry (group III), polymer chemisty, and catalysis.

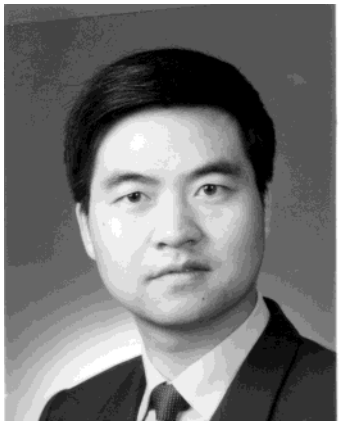

Bing Lian was born in 1975 in Jiangsu, People's Republic of China. He received his B.S. in 1997, M.S. in 2000, and Ph.D. in 2003 under the supervision of Professor Jiling Huang, all from East China University of Science and Technology. His research was mainly focused on the syntheses of organometallic complexes (group IVB) and their application to olefin polymerization.

Therefore, since a predictable relationship was established between metallocene symmetry and polymer tacticity, development of research in metallocene catalysis over the past few years centered largely on the design of new catalysts by varying the electronic and steric influences of the ring substituents on the central metal, with numerous laboratories in academia and industry in active competition.[16−18] The introduction of modifications to the classical ligands is a very effective way of varying the physical and chemical properties of the parent metallocenes over a very wide range in order to incorporate novel reactivity and optimize existing properties, such as catalyst activity and selectivity.[19] In addition, the technique of varying the substituents on the classical cyclopentadienyl (Cp) and indenyl (Ind) ligand serves as an effective means of controlling polymer properties such as stereo- and regioregularity, molecular weight, comonomer incorporation, microstructure, softening point ($T_g$), amount of crystalline/amorphous regions, and even solubility.[20,21] The importance of

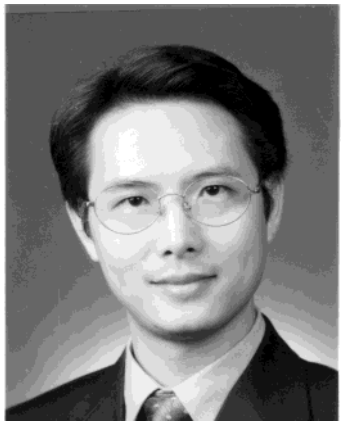

Hao Zhang was born in Jiangxi, People's Republic of China, in 1973. He received his B.S. in 1994 and M.S. in 1997 from Nanchang University. He received his Ph.D. in 2003 from East China University of Science and Technology in the research group of Professor Yanlong Qian. His research interests include synthetic organic chemistry, organometallic chemistry (group IVB), polymer chemistry, and catalysis.

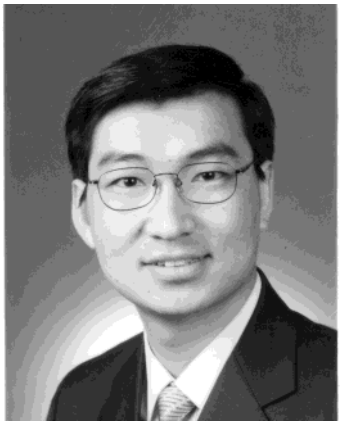

Hao Zhang was born in 1976 in Baotou, People's Republic of China. He received his B.S. from Normal University of Inner Mongolia and his M.S. from the Chemical Engineering College of Inner Mongolia Polytechnic University. He is presently working for the Ph.D. with Professor Yanlong Qian at East China University of Science and Technology in the application of group IVB metals and chromium catalysts for homogeneous polymerization.

ring substituents in metallocene chemistry has been highlighted by several minor and major reviews.[22−27]

At the end of this discussion is a collection of all the abbreviations and an explanation of their meaning (List of Abbreviations).

## B. Scope of Review

We review the chemistry of substituted cyclopentadienyl and indenyl tri- and dihalide complexes of titanium in the +4 oxidation state. This implies that lower oxidation states will be handled only when the species involved is in a transition state. Both titanocenes and half-sandwich complexes that are uniformly or differentially singly and multiply substituted will be covered. Bis(Cp), bis(Ind), and mixed Cp(Ind) *ansa*-metallocenes (Si, O, and C bridged) will be covered. It is also within the scope of the paper to discuss structural features as they affect catalyst efficiency; in particular, we will explore intramolecular coordination between some of the functionalized rings and the central metal, especially coordination from alkoxo and amino groups. Finally, we will discuss the applications of the titanocenes as precursors in conjunction with suitable cocatalysts (methylalumoxane or borane/borate salts) for the activation of the homo- and copolymerization of olefinic monomers; isomerization, polymerization, and hydrogenation of diolefins; and metathesis polymerization of cyclic monomers.

The review will cover only the period from 1995 to date as there are well-reviewed parts of the present topic contained in various media up to the mid 1990s. These we will refer to in due course for background information. As sources of reference we will use information that is available in open scientific media while keeping the use of patents to only when necessary. This is because as Hlatky[28] rightly pointed out, patents, being legal documents not journal articles, delight in presenting results that are different from established trends without offering much explanation to win approval (whereas the main aims of scientific articles are to theorize and proffer explanations on available results). In addition, patents produce only limited data related to the characterization of metallocenes and polymers, the centerpiece of this discussion.[29]

# *II. Bis- or Mono-Cp(Ind) Titanium Complexes*

## A. Bis-Cp(Ind) Titanium Complexes

The utilization of ring substitution theoretically offers the synthetic chemist an almost unlimited possible combination of ligands around the metal enriching the spectrum of titanocenes. The main possible combinations of substituted titanocenes to be encountered in this review are classified in Chart 1. The possibilities increase severalfold if other less

**Chart 1**

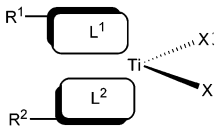


- Uniformly substituted Cp or Ind complexes; $R^1 = R^2$, $L^1 = L^2$.
- Differentially substituted Cp or Ind complexes; $R^1 \neq R^2$, $L^1 = L^2$.
- Uniformly substituted mixed ligand Cp(Ind) complexes; $R^1 = R^2$, $L^1 \neq L^2$.
- Differentially substituted mixed ligand Cp(Ind) complexes; $R^1 \neq R^2$, $L^1 \neq L^2$.
- X = Halide (F, Cl, Br); but is often alkyl (methyl) or aryl (phenyl) for catalyst application.

frequently encountered ligands such as fluorenyl (Flu) monoanion and cyclooctatetraenyl (COT) dianion are considered. The symmetry ($C_{2v}$, $C_2$, $C_s$, or $C_1$) of the different combinations strongly affects metallocene efficiency (activity, stereo- and regioselectivity, etc.) as catalyst precursors. For a more detailed discussion on the role of metallocene symmetry on catalytic application, refer to section III of this paper.

### *1. Bis-Cp(Ind) Titanium Complexes Containing Alkyl and Alkenyl Side Chains*

Synthetic methods for preparing cyclopentadienyl- and indenyl-substituted ligands, especially chiral ligands, have been recently reviewed.[30] The influences of the ring substituents on structure and reactivity have been covered. We first discuss the synthesis of alkyl- and alkenyl-substituted titanocene.

Typical synthetic strategies for the synthesis of titanocene and mixed-sandwich compounds are outlined in Scheme 1.

**Scheme 1**

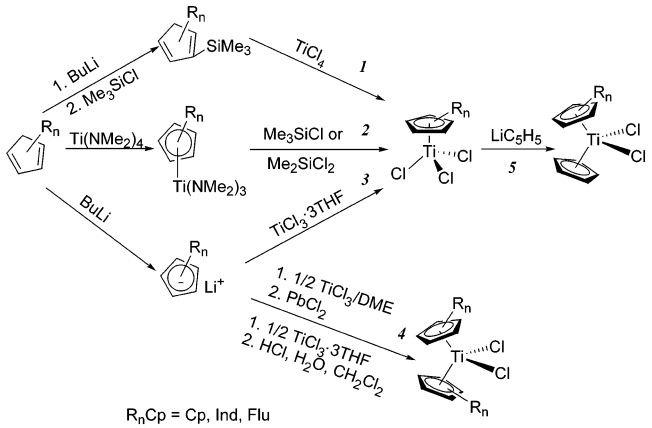


Route 1, Scheme 1: The reaction of RnCpLi in THF with chorotrimethylsilane affords $RnCpSiMe_3$, which is isolated as a distillable oil; subsequent treatment with titanium tetrachloride in hexane yields the red crystalline trichloro complex ($RnCpTiCl_3$) in moderate yield.[31−33]

Route 2, Scheme 1: Treatment of substituted cyclopentadienes with $Ti(NMe_2)_4$ resulted in the formation of amido complexes, which could be transformed to the corresponding trichloride complexes via reaction with appropriate chlorinating reagents.[34]

Route 3, Scheme 1: Half-sandwich titanium derivatives containing the RnCp ligand may also be prepared by treating RnCpLi′ with $TiCl_3$·3THF in THF followed by oxidation of the intermediate Ti(III) complex with HCl to afford $RnCpTiCl_3$, which is isolated as a pure complex in a lower yield.[35,36]

Route 4, Scheme 1: Two equivalents of RnCpLi is treated with titanium trichloride, and the intermediate titanium(III) is oxidized with lead dichloride, thus titanium dichloride ($RnCp_2TiCl_2$) was isolated as pentane-soluble red crystal in moderate yield. A modification of this involves the use of $TiCl_3$·3THF followed by oxidation of the Ti(III) to Ti(IV) by aqueous HCl; drying followed by filtration afforded the desired product.[36−38]

Route 5, Scheme 1: The mixed ring sandwich complex $RnCpCpTiCl_2$ was obtained by the reaction of $RnCpTiCl_3$ with CpLi instead of the reaction of $CpTiCl_3$ with RnCpLi, and the product was isolated as red crystals.[39,40]

These five routes summarize the most common synthetic routes, and most titanium complexes bearing alkyl and alkenyl groups can be thus prepared. In compounds bearing mixed ligands (Cp and Ind) or mixed ligand substituents the general procedure is to introduce the more sterically demanding (in most cases also electronically stable) ligand or substituent. Various authors, in order to improve yield and also explore previously unused reagents, which in some cases may be less expensive or less hazardous to use, claim "slight modifications" to these procedures.

References, characterization, and physical property data of some titanocene complexes bearing the alkyl and $\omega$-alkenyl substituents are presented in Table 1.

### *2. Bis-Cp(Ind) Titanium Complexes Containing Pendant Alkoxyl Chains*

The synthesis of metallocenes with ether functionalized side chains has attracted a great deal of attention because the side chains may be designed to function as reversible or labile coordinating groups during catalysis, thereby helping to stabilize and prolong the lifetime of the hitherto unstable active species. Also, static intramolecular coordination of ether side groups has been used to alter the electronic and steric properties around the titanium metal. Some researchers have also used the ether point to heterogenize the metallocene by anchorage to silica supports.[44]

Alkoxyl functionalized metallocenes have been the subject of several reviews.[25] The coordination chemistry[26] and synthesis[23] have been covered. Complex **1** has been typically obtained by simple metathetical reactions involving the alkoxyalkyl-substituted ligand

**Table 1. Alkyl- and $\omega$-Alkenyl-Substituted $Cp_2TiCl_2$ Complexes**

| complex | color, characterization, etc. |
|---|---|
| $(\eta^5\text{-}C_5H_4{}^t\!Bu)_2TiCl_2$ | red solid, $^1$H NMR, EI-MS, IR[37,38] |
| $(1,3\text{-}{}^t\!Bu_2\text{-}\eta^5\text{-}C_5H_3)_2TiCl_2$ | red solid, $^1$H NMR, EI-MS, IR[37] |
| $(1,2\text{-}{}^t\!Bu_2\text{-}\eta^5\text{-}C_5H_3)_2TiCl_2$ | brownish red solid, mp, $^1$H NMR, $^{13}$C NMR, IR, EA, X-ray[41] |
| $(1,3\text{-}{}^t\!Bu_2\text{-}\eta^5\text{-}C_5H_3)_2TiI_2$ | dark red-brown solid, $^1$H NMR, EA[34] |
| $(\eta^5\text{-}C_5H_4{}^t\!Bu)(\eta^5\text{-}C_5H_5)TiCl_2$ | red solid, mp, $^1$H NMR, $^{13}$C NMR[43] |
| $(\eta^5\text{-}C_5Me_4CH_2CH_2CH{=}CH_2)_2TiCl_2$ | red needles, mp, $^1$H NMR, $^{13}$C{$^1$H}NMR, IR, EI-MS, EA[36] |
| $(\eta^5\text{-}C_5Me_4CH_2CH_2CH{=}CH_2)(\eta^5\text{-}C_5H_5)TiCl_2$ | bright red crystals, mp, $^1$H NMR, $^{13}$C{$^1$H}NMR, IR, EI-MS, EA[36] |
| $(\eta^5\text{-}C_5H_4CMe_2CHMe_2)_2TiCl_2$ | red crystals, $^1$H NMR, $^{13}$C{$^1$H}NMR, HRMS, MS-FAB, EA, X-ray[39] |
| $(\eta^5\text{-}C_5H_4CMe_2CHMe_2)(\eta^5\text{-}C_5H_5)TiCl_2$ | red microcrystals, $^1$H NMR, $^{13}$C{$^1$H}NMR[39] |
| $[\eta^5\text{-}C_5H_4CR^1R^2\text{-}(1\text{-cyclo-}C_6H_9)]_2TiCl_2$ | |
| $R^1$ = Me, $R^2$ = Me | $^1$H NMR, $^{13}$C NMR, IR[40] |
| $R^1$ = Me, $R^2$ = Et | $^1$H NMR, $^{13}$C NMR, IR[40] |
| $R^1$ = Me, $R^2$ = Pr | $^1$H NMR, $^{13}$C NMR, IR[40] |
| $R^1$ = Me, $R^2$ = $^i$Bu | $^1$H NMR, $^{13}$C NMR, IR[40] |
| $R^1$ = Et, $R^2$ = Et | $^1$H NMR, $^{13}$C NMR, IR[40] |

**Table 2. Titanocenes Containing an Oxygen Atom in the Side Chain**

| complex | | color, characterization, etc. |
|---|---|---|
| $[\eta^5\text{-}C_5H_4CMe_2(2\text{-}OMe\text{-}C_6H_4)]_2TiCl_2$ | **1** | red crystals, mp, $^1$H NMR, MS, EA[45] |
| $[\eta^5\text{-}C_5H_4CMe(Et)(2\text{-}OMe\text{-}C_6H_4)]_2TiCl_2$ | | red crystals, mp, $^1$H NMR, MS, EA[45] |
| $(\eta^5\text{-}C_5H_4CEt_2C_6H_4\text{-}4\text{-}OMe)_2TiCl_2$ | | red solid, mp, $^1$H NMR, MS, EA[45] |
| $(\eta^5\text{-}C_5H_4CH_2CH_2OMe)_2TiCl_2$ | **2** | violet-red solid, mp, $^1$H NMR, $^{13}$C NMR, MS, EA, X-ray,[46] IR[48] |
| $(\eta^5\text{-}C_5H_4CH_2CH_2OMe)(\eta^5\text{-}C_5H_5)TiCl_2$ | | mp, $^1$H NMR, MS, EA[46] |
| $[\eta^5\text{-}C_5H_4(CH_2)_3OMe]_2TiCl_2$ | | purple needle, mp, $^1$H NMR, MS, IR, EA[49] |
| $(\eta^5\text{-}C_5H_4(CH_2)_3OMe)(\eta^5\text{-}C_5H_5)TiCl_2$ | | red solid, mp, $^1$H NMR, MS, IR, EA[49] |
| $[\eta^5\text{-}C_5H_4(CH_2)_3OMe](\eta^5\text{-}C_5H_4CH_2CH_2OMe)TiCl_2$ | | red solid, mp, $^1$H NMR, MS, IR, EA[49] |
| $(\eta^5\text{-}C_5H_4CH_2CH_2OR)_2TiCl_2$ | | |
| R = isobornyl | | brick red solid, $^1$H NMR, $^{13}$C NMR, EA[50] |
| R = menthyl | | $^1$H NMR, $^{13}$C NMR, MS[50] |
| R = fenchyl | | $^1$H NMR, $^{13}$C NMR, MS, EA[50] |
| $[\eta^5\text{-}C_5H_4(CH_2)_6OC_6H_4\text{-}4\text{-}C_6H_{10}\text{-}4\text{-}C_5H_{11}]_2TiCl_2$ | | brown solid, IR, EA[51] |
| $(\eta^5\text{-}C_5H_4OSiEt_3)_2TiCl_2$ | | red solid, mp, $^1$H NMR, $^{13}$C NMR[47] |
| $(\eta^5\text{-}C_5H_4OSiMe_2{}^t\text{Bu})_2TiCl_2$ | | orange powder, mp, $^1$H NMR, $^{13}$C NMR, EA[47] |
| $(\eta^5\text{-}C_5H_4OSi{}^i\text{Pr}_3)_2TiCl_2$ | | red solid, mp, $^1$H NMR, $^{13}$C NMR[47] |
| $[\eta^5\text{-}C_5H_4CH_2(2\text{-}C_4H_7O)]_2TiCl_2$ | | red, mp, [α], $^1$H NMR, $^{13}$C NMR, MS, EA, X-ray[52] |
| $(\eta^5\text{-}C_5H_4OSiEt_3)(\eta^5\text{-}C_5H_5)TiCl_2$ | **3** | red crystals, mp, $^1$H NMR, $^{13}$C NMR[47] |
| $(\eta^5\text{-}C_5H_4OSiEt_3)(\eta^5\text{-}C_5Me_5)TiCl_2$ | | red solid, mp, $^1$H NMR, $^{13}$C NMR[47] |
| $(\eta^5\text{-}C_5H_4OH)(\eta^5\text{-}C_5Me_5)TiCl_2$ | | violet powder, mp (dec), $^1$H NMR, $^{13}$C NMR, EA[47] |
| $[\eta^5\text{:}\eta^1\text{-}C_5H_4CEt_2(2\text{-}C_6H_4O)](\eta^5\text{-}C_5H_5)TiCl$ | **4** | orange crystals, mp, $^1$H NMR, MS, EA, X-ray[45] |
| $[\eta^5\text{:}\eta^1\text{-}C_5H_4CEt_2(2\text{-}C_6H_4O)](\eta^5\text{-}C_5H_4CH_2CH_2OMe)TiCl$ | | orange crystals, mp, $^1$H NMR, MS, EA[45] |
| $[\eta^5\text{:}\eta^1\text{-}C_5H_4CPr_2(2\text{-}C_6H_4O)](\eta^5\text{-}C_5H_5)TiCl$ | | orange solid, mp, $^1$H NMR, MS, EA[45] |
| $[\eta^5\text{-}C_5H_4CH_2(2\text{-}C_4H_7O)](\eta^5\text{-}C_5H_4CH_2C_6H_5)TiCl_2$ | | red solid, mp, $^1$H NMR, MS, EA[45] |
| $[\eta^5\text{-}C_5H_4CH_2(2\text{-}C_4H_7O)](\eta^5\text{-}C_5H_4CMe_2C_6H_5)TiCl_2$ | | red solid, mp, $^1$H NMR, MS, EA[45] |
| $[\eta^5\text{-}C_5H_4CH_2(2\text{-}C_4H_7O)][\eta^5\text{-}C_5H_4CMe(Et)C_6H_5]TiCl_2$ | | dark red solid, mp, $^1$H NMR, MS, EA[45] |
| $[\eta^5\text{-}C_5H_4CH_2(2\text{-}C_4H_7O)](\eta^5\text{-}C_5H_4CEt_2C_6H_5)TiCl_2$ | | dark red solid, mp, $^1$H NMR, MS, EA[45] |
| $(\eta^5\text{-}C_5H_4CH_2CH_2OMe)(\eta^5\text{-}C_5H_4CMe_2C_6H_5)TiCl_2$ | | red solid, mp, $^1$H NMR, MS, EA, X-ray[45] |
| $[\eta^5\text{-}C_5H_4CMe_2(2\text{-}OMe\text{-}C_6H_4)](\eta^5\text{-}C_5H_5)TiCl_2$ | | orange crystals, mp, $^1$H NMR, MS, EA[45] |
| $[\eta^5\text{-}C_5H_4CMe(Et)(2\text{-}OMe\text{-}C_6H_4)](\eta^5\text{-}C_5H_5)TiCl_2$ | | orange solid, mp, $^1$H NMR, MS, EA[45] |
| $[\eta^5\text{-}C_5H_4CMe(Pr)(2\text{-}OMe\text{-}C_6H_4)](\eta^5\text{-}C_5H_5)TiCl_2$ | | red crystals, mp, $^1$H NMR, MS, EA[45] |
| $[\eta^5\text{-}C_5H_4CMe(Bu)(2\text{-}OMe\text{-}C_6H_4)](\eta^5\text{-}C_5H_5)TiCl_2$ | | red crystals, mp, $^1$H NMR, MS, EA[45] |
| $[\eta^5\text{-}C_5H_4CMe({}^i\text{Bu})(2\text{-}OMe\text{-}C_6H_4)](\eta^5\text{-}C_5H_5)TiCl_2$ | | red crystals, mp, $^1$H NMR, MS, EA[45] |
| $[\eta^5\text{-}C_5H_4(1,1\text{-cyclo-}C_6H_{10})(2\text{-}OMe\text{-}C_6H_4)](\eta^5\text{-}C_5H_5)TiCl_2$ | **5** | red solid, mp, $^1$H NMR, MS, EA, X-ray[45] |
| $[\eta^5\text{-}C_5H_4(1,1\text{-cyclo-}C_6H_{10})(4\text{-}OMe\text{-}C_6H_4)](\eta^5\text{-}C_5H_5)TiCl_2$ | | dark red crystals, mp, X-ray[53] |
| $[\eta^5\text{-}C_5H_4CMe_2(2\text{-}OMe\text{-}C_6H_4)](\eta^5\text{-}C_5H_4CH_2C_6H_5)TiCl_2$ | | red solid, mp, $^1$H NMR, MS, EA[45] |
| $[\eta^5\text{-}C_5H_4CMe_2(2\text{-}OMe\text{-}C_6H_4)](\eta^5\text{-}C_5H_4CH_2CH_2OMe)TiCl_2$ | | dark red solid, mp, $^1$H NMR, MS, EA[45] |
| $[\eta^5\text{-}C_5H_4CEt_2(3\text{-}OMe\text{-}C_6H_4)](\eta^5\text{-}C_5H_5)TiCl_2$ | | red solid, mp, $^1$H NMR, MS, EA[45] |
| $[\eta^5\text{-}C_5H_4CEt_2(2\text{-}OMe\text{-}C_6H_4)](\eta^5\text{-}C_5H_5)TiCl_2$ | | red solid, mp, $^1$H NMR, MS, EA[45] |
| $[\eta^5\text{-}C_5H_4CR^1R^2(2\text{-}OMe\text{-}C_6H_4)](\eta^5\text{-}C_5H_5)TiBr_2$ | | |
| $R^1 = R^2 = Me$ | | ref 26 |
| $R^1, R^2 = (CH_2)_5$ | | ref 26 |
| $[\eta^5\text{:}\eta^1\text{-}C_5H_4CR^1R^2(2\text{-}C_6H_4O)](\eta^5\text{-}C_5H_5)TiBr$ | | |
| $R^1 = R^2 = Me$ | | ref 26 |
| $R^1, R^2 = (CH_2)_5$ | | ref 26 |
| $[\eta^5\text{-}C_5H_4CH(CH_3)CH_2OMe]_2TiCl_2$ | | red solid, mp, [α], $^1$H NMR, $^{13}$C NMR, MS, EA, X-ray[54] |
| $[\eta^5\text{-}C_5H_4CH_2CH(CH_3)OMe]_2TiCl_2$ | | red solid, mp, $^1$H NMR, $^{13}$C NMR, MS, IR, EA[54] |

**Scheme 2**

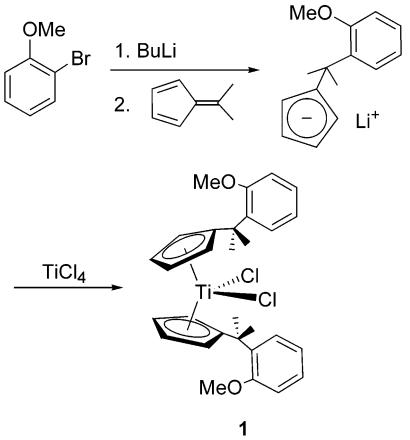


1

anion and $TiCl_4$ ($TiCl_4$·2THF) in a 2:1 molar ratio as shown in Scheme 2.[45]

Directly the sodium salt of the ligand has also been used with $TiCl_4$ to produce the required product

**Scheme 3**

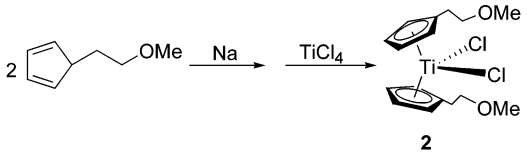


2

**Scheme 4**

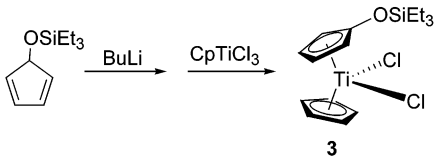


3

in a good yield as shown in Scheme 3.[46]

The mixed ligand complex **3** was readily formed by the direct reaction of Cp′$TiCl_3$ with $CpOSiEt_3$ anion according to Scheme 4.[47]

In some cases, the methoxyaryl cyclopentadienyl titanium complex **4** yielded a titanoxacycle complex by the elimination of 1 equiv of MeCl (Scheme 5). [45]

**Scheme 5**

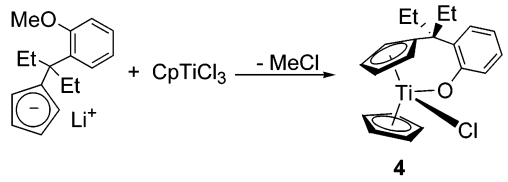


**4**

Table 2 presents uniformly substituted Cp or mixed Cp complexes, highlighting the physical properties reported and the characterization.

Qian et al. reported the X-ray structure of complex **2**, shown in Figure 1, which was found to be similar

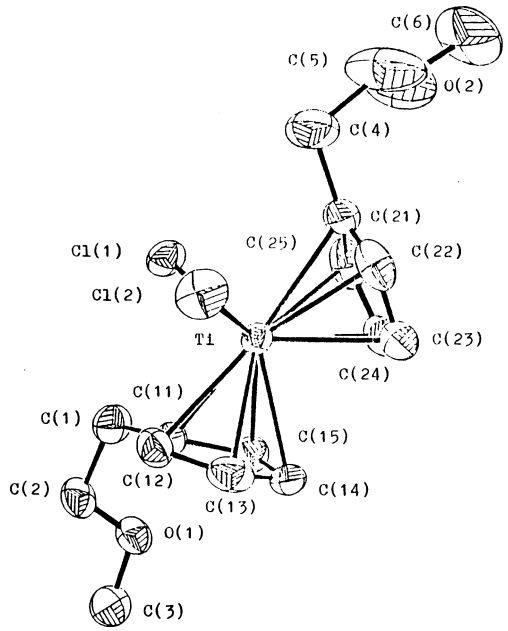


**Figure 1.** Structure of ($\eta^5$-$C_5H_4CH_2CH_2OMe)_2TiCl_2$ (**2**) in the crystal.[46]

to that of the unsubstituted $Cp_2TiCl_2$ complex.[55] Here the two oxygen atoms in the side chains have no intramolecular coordination with the metal center, and the two 2-methoxyl substituents are directed away from the central titanium atom.

The structure of [$\eta^5$-$C_5H_4$(1,1-cyclo-$C_6H_{10}$)(2-OMe-$C_6H_4$)]($\eta^5$-$C_5H_5$)$TiCl_2$ (**5**) also shows that the MeO group on the benzene ring in the complex is quite far away from the titanium center, and there is no

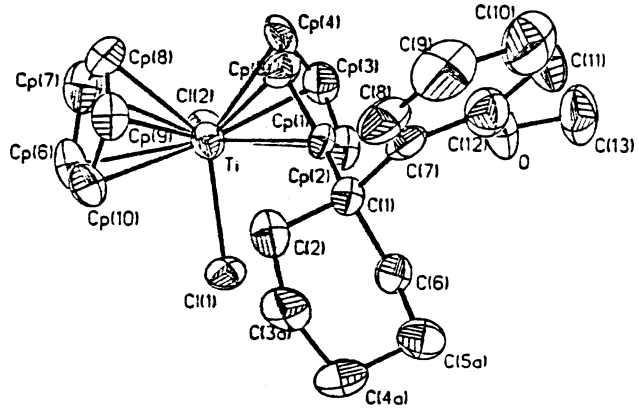


**Figure 2.** Structure of [$\eta^5$-$C_5H_4$(1,1-cyclo-$C_6H_{10}$)(2-OMe-$C_6H_4$)]($\eta^5$-$C_5H_5$)$TiCl_2$ (**5**) in the crystal.[45]

interaction between the O atom and the Ti center due to steric restrictions (Figure 2).

### *3. Bis-Cp(Ind) Titanium Complexes Containing Pendant Dialkylamino Side Groups*

The chemistry of amino alkyl functionalized metallocenes has been the subject for a microreview and has also featured in most reviews on metallocenes in general.[22] A recent review by Qian and Huang focused on the intramolecular coordination chemistry of these complexes.[27] Titanocene(IV) complexes containing the *N*,*N*-dimethylaminoalkyl-cyclopentadienyl ligands have been synthesized following classical metathetical procedures similar to route 4 (Scheme 6); refer to section II.A.1 (Scheme 1 and following discussion) for details.

**Scheme 6**

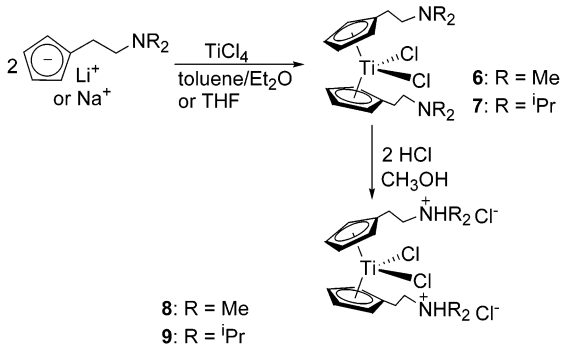


Complexes with R = methyl[56] **6** and isopropyl[57] **7** have been reported. The preparation of the former complex is quite difficult due to the interaction of the amino group with the metal substrate and also the presence of intermolecular coordination in the product leading to oligomeric species and coordination polymers that are difficult to characterize (Chart 2).[27]

**Chart 2**

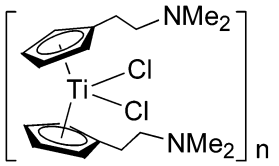


These complexes can be readily converted into the corresponding hydrochloride derivatives[56,57] by treatment with 2 equiv of hydrogen chloride in a methanolic solution with the protonation of the amino group to give the titanocene dihydrochlorides **8** as red, amorphous solids in quantitative yield. The complexes are excellently soluble in polar solvents such as methanol, dimethyl sulfoxide, and acetonitrile but are insoluble in nonpolar solvents. It is remarkable that, unlike the corresponding metallocene dichlorides, the dihydrochlorides are stable to air and moisture and were observed to be water stable for several hours.

Mixed-ring titanocene dichloride complexes ($\eta^5$-$C_5H_4CH_2CH_2NMe_2$)($\eta^5$-$C_5H_5$)$TiCl_2$ (**10**),[56] ($\eta^5$-$C_5Me_4$-$CH_2CH_2NMe_2$)($\eta^5$-$C_5H_5$)$TiCl_2$ (**11**),[58] ($\eta^5$-$C_5Me_4CH_2$-$CH_2NMe_2$)($\eta^5$-$C_5Me_5$)$TiCl_2$ (**12**),[58] and ($\eta^5$-$C_5H_4CH_2$-$CH_2N^iPr_2$)($\eta^5$-$C_5H_4SiMe_3$)$TiCl_2$ (**13**)[59] have been syn-

**Scheme 7**

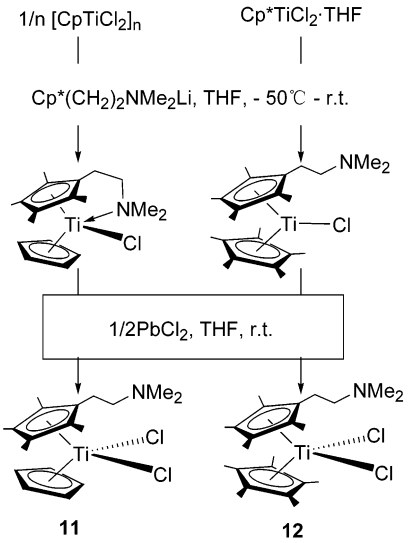


thesized via the appropriate combinations of the various ligands by synthetic procedures already outlined (see section II.A.1, routes 1 and 4) with slight modifications when necessary (Scheme 7).

Rausch et al.[60] reported a different route to the synthesis of ($\eta^5$-$C_5H_4CH_2CH_2NMe_2$)($\eta^5$-$C_5H_5$)$TiCl_2$ (**10**) via metathesis of the corresponding [$CpCH_2CH_2N(Me)_2$]$TiCl_3$ (**14**) (see Table 16) with CpTl in boiling toluene to yield a garnet red microcystalline solid after recrystallization from $CH_2Cl_2$ (Scheme 8). The compound was exceedingly moisture sensitive, a stark contrast to the stability of $Cp_2TiCl_2$.

Qian and co-workers[61] synthesized a series of mixed cyclopentadienyl titanocenes containing terminal amino substituents (**15**, **16**; **17**, **18**; and **19**−**24**; see Table 4) via the general synthetic route outlined in Scheme 9:

**Scheme 8**

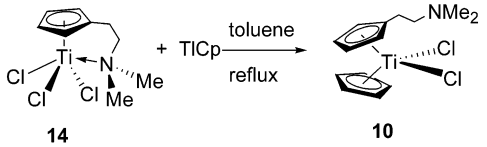


**Scheme 9**

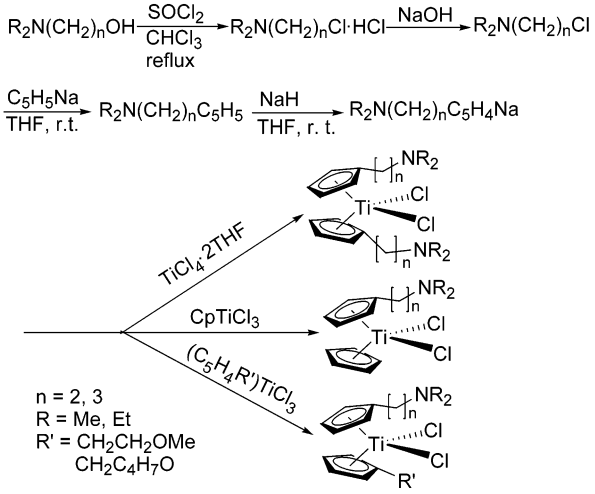


Here, we discuss the structural features of titanocene complexes containing pendant $NR_2$ ligand. Spectroscopic and single-crystal X-ray analytical data show intramolecular coordination of pendant amino ligands toward the metal center in nitrogen functionalized cyclopentadienyl trichlorotitanium (see section II.B.3.a). However, no coordination of the additional (dialkylamino-ethyl or propyl) function could be assumed for the dichlorotitanium complexes **6**, **7**, and **15** because the chemical shift of $CH_2$ and CH attached to the nitrogen atom in these complexes shows only a little change in the compound compared

**Table 3. $^1$H NMR Spectra of Titanocenes Containing a Pendant $NR_2$ Ligand**

| | | δ | | |
|---|---|---|---|---|
| | | δ $CH_2N$ | δ $NCHCH_3$ | δ $NCH_3$ |
| $C_5H_5(CH_2CH_2N^iPr_2)$[a] | | 2.65 | 2.92 | |
| ($\eta^5$-$C_5H_4CH_2CH_2N^iPr_2)_2TiCl_2$[a] | **7** | 2.93 | 2.93 | |
| ($\eta^5$-$C_5H_4CH_2CH_2N^iPr_2)_2TiCl_2$·HCl[a] | **9** | 3.32 | 3.63 | |
| $C_5H_5(CH_2CH_2NMe_2)$[b] | | 2.53 | | 2.27 |
| ($\eta^5$-$C_5H_4CH_2CH_2NMe_2)_2TiCl_2$[b] | **6** | 2.71 | | 2.36 |
| ($\eta^5$-$C_5H_4CH_2CH_2NMe_2)_2TiCl_2$·HCl[c] | **8** | 3.02 | | 2.89 |
| ($\eta^5$-$C_5H_4CH_2CH_2N^iPr_2$)($\eta^5$-$C_5H_4SiMe_3$)$TiCl_2$[a] | **13** | 2.93 | 2.93 | |
| ($\eta^5$-$C_5H_4CH_2CH_2N^iPr_2$)($\eta^5$-$C_5H_4SiMe_3$)$TiCl_2$·HCl[b] | **25** | 3.50 | 3.64 | |

[a] $C_6D_6$. [b] $CDCl_3$. [c] $CD_3OD$.

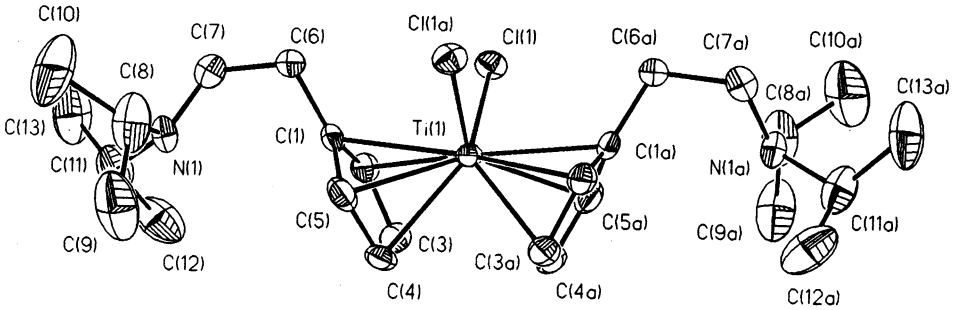


**Figure 3.** Structure of ($\eta^5$-$C_5H_4CH_2CH_2N^iPr_2)_2TiCl_2$ (**7**) in the crystal.[57] (Reprinted with permission from ref 57. Copyright 1996 American Chemical Society.)

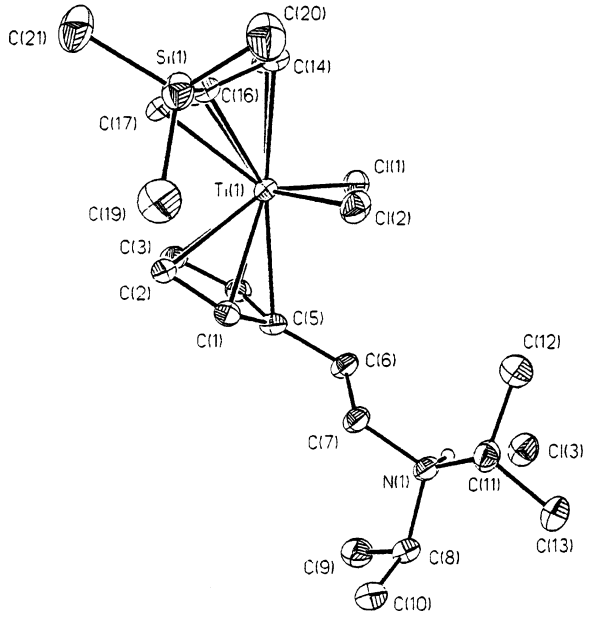


**Figure 4.** Structure of ($\eta^5$-$C_5H_4CH_2CH_2N^iPr_2$)($\eta^5$-$C_5H_4$-$SiMe_3$)$TiCl_2$·HCl (**25**) in the crystal.[59] (Reprinted with permission from ref 59. Copyright 1996 VCH.)

with the corresponding ligand (see Table 3); the combined effects of the two Cp rings and chloride atoms may account for these slight changes.[58]

Structural analysis also shows that, in **7** (Figure 3), neither an intramolecular nor an intermolecular coordination of the additional di(isopropyl)aminoethyl side chain was observed. The molecule possesses a crystallographic 2-fold axis of symmetry passing through the titanium atom. The chlorine atoms together with the centroids of the cyclopentadienyl ring form a considerably distorted pseudo-tetrahedral coordination geometry around the titanium with angles ranging from 94.4° (Cl−Ti−Cl′) to 132.6° (Ce)−Ti−(Ce). The Cp rings are slightly staggered with the di(isopropyl)aminoethyl groups arranged at the open side of the sandwich. The detailed data show that this molecular structure is similar to that observed for $(C_5H_5)_2TiCl_2$ and $(C_5H_4Me)_2TiCl_2$, demonstrating that the introduction of the two di(isopropyl)aminoethyl functions does not significantly affect the basic molecular structure. Hence, by extrapolation, similar mixed-ring complexes **10** and **19** exhibit analogous structural patterns.[61]

Values of the signals due to the protons surrounding nitrogen and the Cp ring in complex **7** are very similar to those of the ligand di(isopropyl)aminoethyl-substituted cyclopentadiene, indicating the absence of any major structural change such as intramolecular coordination as a result.

A single-crystal X-ray diffraction study of **25** (Figure 4) established the expected bent-metallocene type structure. The structural framework is similar to that of ($\eta^5$-$C_5H_4CH_2CH_2N^iPr_2)_2TiCl_2$ (**7**). The di(isopropyl)-aminoethyl group is situated at the open side of the sandwich, whereas the trimethylsilyl substituent is found occupying a lateral position. This orientation minimizes the steric interaction between the trimethylsilyl group and the chlorine atoms, on the one hand, and with the other cyclopentadienyl ring, on the other. All other average bond parameters for ($\eta^5$-$C_5H_4CH_2CH_2N^iPr_2$)($\eta^5$-$C_5H_4SiMe_3$)$TiCl_2$·HCl (**25**) are within the range established for the complexes **7** and $Cp_2TiCl_2$, demonstrating that the different Cp ring substitutions in **25** and **7** do not significantly affect the basic molecular structure.[62]

Physical properties and characterization for bis-Cp(Ind) titanium complexes functionalized by $NR_2$ ligands are presented in Table 4.

### *4. Bis-Cp(Ind) Titanium Complexes Containing Pendant Phospho Side Groups*

Butenschön and co-workers have extensively studied the chemistry and coordination behavior of phospho-substituted metallocenes, and his recent review

**Table 4. Dimethylaminoalkyl−Cyclopentadienyl Titanium Complexes**

| complex | | color, characterization, etc. |
|---|---|---|
| ($\eta^5$-$C_5H_4CH_2CH_2NMe_2)_2TiCl_2$ | **6** | dark red solid, mp,[61,63] $^1$H NMR,[56,61,63] $^{13}$C NMR, EI-MS, EA[63] |
| | **8** | complex with HCl: $^1$H NMR[56] |
| ($\eta^5$-$C_5H_4CH_2CH_2N^iPr_2)_2TiCl_2$ | **7** | red solid, mp, $^1$H NMR, $^{13}$C NMR, MS, EA, X-ray[57] |
| | **9** | complex with HCl: deep red crystals, mp, $^1$H NMR, $^{13}$C NMR, MS, EA[57] |
| [$\eta^5$-$C_5H_4(CH_2)_3NMe_2]_2TiCl_2$ | **15** | dark red solid, mp (dec), $^1$H NMR[61] |
| ($\eta^5$-$C_5H_4CH_2CH_2NEt_2)_2TiCl_2$ | **16** | red solid, mp (dec), $^1$H NMR[61] |
| ($\eta^5$-$C_5H_4CH_2CH_2NMe_2$)($\eta^5$-$C_5H_5$)$TiCl_2$ | **10** | garnet solid, mp (dec),[61,63] $^1$H NMR,[60,61,63] $^{13}$C NMR, EA[60] |
| [$\eta^5$-$C_5H_4(CH_2)_3NMe_2$]($\eta^5$-$C_5H_5$)$TiCl_2$ | **17** | dark red solid, mp( dec),$^1$H NMR[61] |
| ($\eta^5$-$C_5H_4CH_2CH_2NEt_2$)($\eta^5$-$C_5H_5$)$TiCl_2$ | **18** | red solid, mp (dec), $^1$H NMR[61] |
| ($\eta^5$-$C_5Me_4CH_2CH_2NMe_2$)($\eta^5$-$C_5H_5$)$TiCl_2$ | **11** | red solid, $^1$H NMR, $^{13}$C{$^1$H}NMR[58] |
| ($\eta^5$-$C_5Me_4CH_2CH_2NMe_2$)($\eta^5$-$C_5Me_5$)$TiCl_2$ | **12** | red solid, mp, $^1$H NMR, $^{13}$C{$^1$H} NMR, MS, EA, X-ray[58] |
| ($\eta^5$-$C_5H_4CH_2CH_2N^iPr_2$)($\eta^5$-$C_5H_4SiMe_3$)$TiCl_2$ | **13** | orange-red solid, mp, $^1$H NMR, $^{13}$C NMR, $^{29}$Si NMR, MS, EA[59] |
| | **25** | complex with HCl: red solid, $^1$H NMR, $^{13}$C NMR X-ray[59] |
| | | complex with $B[3,5\text{-}(CF_3)_2C_6H_3]^-_4$: red solid, mp, $^1$H NMR, $^{13}$C NMR, EA[59] |
| ($\eta^5$-$C_5H_4CH_2CH_2NMe_2$)($\eta^5$-$C_5H_4CH_2CH_2OMe$)$TiCl_2$ | **19** | red solid, mp (dec), $^1$H NMR[61] |
| ($\eta^5$-$C_5H_4CH_2CH_2NEt_2$)($\eta^5$-$C_5H_4CH_2CH_2OMe$)$TiCl_2$ | **20** | red solid, mp (dec), $^1$H NMR[61] |
| [$\eta^5$-$C_5H_4(CH_2)_3NMe_2$]($\eta^5$-$C_5H_4CH_2CH_2OMe$)$TiCl_2$ | **21** | red solid, mp (dec), $^1$H NMR[61] |
| [$\eta^5$-$C_5H_4CH(CH_3)CH_2NMe_2$]($\eta^5$-$C_5H_4CH_2CH_2OMe$)$TiCl_2$ | **22** | dark red solid, mp (dec), $^1$H NMR[61] |
| ($\eta^5$-$C_5H_4CH_2CH_2NMe_2$)[$\eta^5$-$C_5H_4CH_2$-(2-$C_4H_7O$)]$TiCl_2$ | **23** | red solid, mp (dec), $^1$H NMR[61] |
| ($\eta^5$-$C_5H_4(CH_2)_3NMe_2$)[$\eta^5$-$C_5H_4CH_2$-(2-$C_4H_7O$)]$TiCl_2$ | **24** | red solid, mp (dec), $^1$H NMR[61] |
| [2-($C_5H_{10}N$)-$\eta^5$-$C_9H_6]_2TiCl_2$ | | $^1$H NMR, $^{13}$C{$^1$H} NMR[64] |
| [2-($NMe_2$)-$\eta^5$-$C_9H_6]_2TiCl_2$ | | lustrous black crystals, $^1$H NMR, $^{13}$C NMR, EA, HRMS[65] |
| | | complex with $Li(THF)_2$: X-ray[65] |

has highlighted these complexes as well as the less studied sulfur and arsenic pendant groups.[24]

Titanocene complexes of the type $(Ph_2PC_5H_4)_2TiX_2$ (**26**) or $Ph_2PCpCpTiX_2$ (**27**) are easily obtained via ordinary metathesis methods described above; typical routes are presented in Schemes 10[66] and 11,[67] respectively.

**Scheme 10**

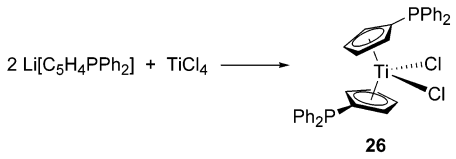


**26**

**Scheme 11**

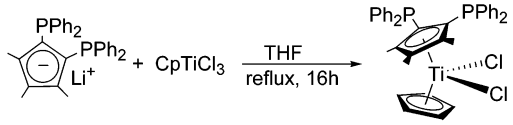


**27**

The molecular structure of $[\eta^5\text{-}C_5H_4P(S)PPh_2](\eta^5\text{-}C_5H_4SiMe_3)TiCl_2$ (**28**) is presented in Figure 5. The bond distance of Ti−Cl [2.350(1) and 2.318(1) Å] and bond angle of Cl−Ti−Cl [95.74(5)°] are similar to those of $Cp_2TiCl_2$[55] or $(^iPr_2NCH_2CH_2C_5H_4)(Me_3SiC_5H_4)$-$TiCl_2$ (**13**).[59] There is no evidence that the phosphorus atom in the side chain interacts with the central Ti atom due to the steric limitation coming from two phenyl rings stuck to the P atom. However, it is interesting to note that the phosphorus atom was involved in intermolecular coordination forming a bimetallic complex **29** (Figure 6).[69]

A list of titanocenes containing a phosphorus atom in the side chain is given in Table 5.

### *5. Bis-Cp(Ind) Titanium Compounds Containing a Bulky Group in the Side Chain*

The interest in aryl side chain functionalized cyclopentadienyl ligands is focused on the steric and electronic effects (as a $\pi$-aromatic system and planar structure) on the corresponding metal complexes. In addition, aromatic substituents play a major role in the design of styrene and propylene polymerization catalysts, such as the conformationally dynamic catalysts reported by Waymouth.[72]

Alt et al.[42] reported the benzyl-substituted titanocene dichloride **30** by using a one-pot reaction (Scheme 12). Hence, 6,6-dimethylfulvene was reacted with phenyllithium to form the substituted Cp lithium salt, which without further purification was reacted with titanium tetrachloride, yielding the target compound.

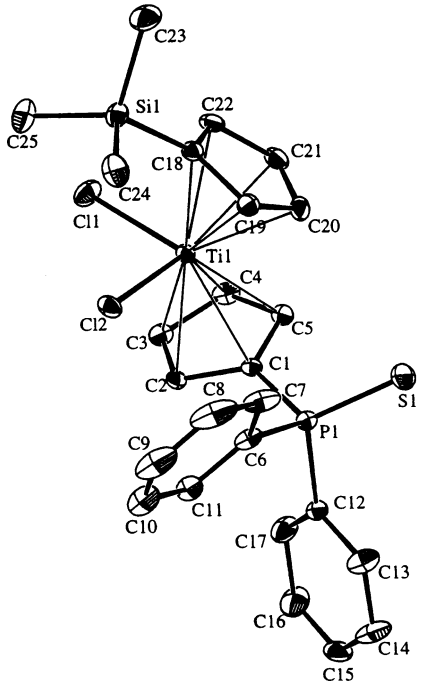


**Figure 5.** Structure of $[\eta^5\text{-}C_5H_4P(S)Ph_2][\eta^5\text{-}C_5H_4SiMe_3)$-$TiCl_2$ (**28**) in the crystal.[68] (Reprinted with permission from ref 68. Copyright 1998 Elsevier Sequoia.)

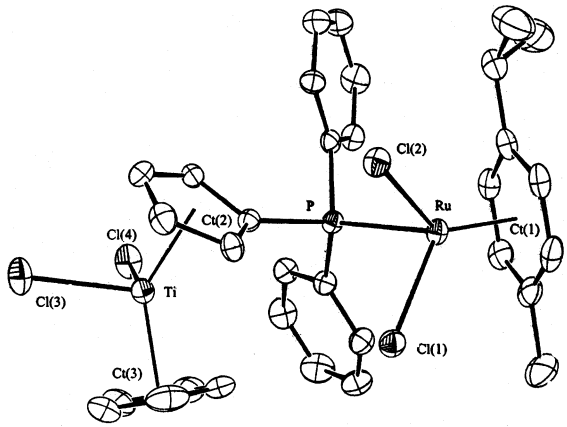


**Figure 6.** Structure of $Cl_2Ti(Cp)CpP(Ph)_2Ru(p\text{-cymene})$-$Cl_2$ (**29**) in the crystal.[69] (Reprinted with permission from ref 69. Copyright 2000 Elsevier Sequoia.)

**Table 5. Titanocenes Containing a Pendant Phospho Side Groups**

| complex | | color, characterization, etc. |
|---|---|---|
| $(\eta^5\text{-}C_5H_4PPh_2)_2TiCl_2$ | **26** | red brown solid, $^1$H NMR, $^{31}$P NMR[66] |
| $(\eta^5\text{-}C_5H_4CH_2PPh_2)_2TiCl_2$ | | red powder, $^1$H NMR, $^{31}$P NMR, EA[70] |
| $(\eta^5\text{-}C_5H_4CH_2CH_2PPh_2)_2TiCl_2$ | | red powder, $^1$H NMR, $^{31}$P NMR, EA[70, 69] |
| $[\eta^5\text{-}C_5H_4P(S)Ph_2]_2TiCl_2$ | | red microcrystalline solid, $^1$H NMR, $^{13}$C NMR, $^{31}$P NMR, EA,[71] MS[68] |
| $\{[\eta^5\text{-}C_5H_4P(S)Ph_2]_2TiCl_2\cdot TiCl_4\}_n$ | | yellow microcrystalline solid, $^1$H NMR, $^{31}$P NMR, EA[71] |
| $(\eta^5\text{-}C_5H_4PPh_2)(\eta^5\text{-}C_5H_5)TiCl_2$ | | red solid, $^1$H NMR, $^{31}$P NMR, EA[69] |
| $(\eta^5\text{-}C_5H_4CH_2CH_2PPh_2)(\eta^5\text{-}C_5H_5)TiCl_2$ | | $^1$H NMR, $^{31}$P NMR, EA[69] |
| $[\eta^5\text{-}C_5H_4P(S)Ph_2](\eta^5\text{-}C_5H_5)TiCl_2$ | | red microcrystalline solid, $^1$H NMR, $^{13}$C NMR, $^{31}$P NMR, EA[71] |
| $[4,5\text{-}(PPh_2)_2\text{-}\eta^5\text{-}C_5Me_3](\eta^5\text{-}C_5H_5)TiCl_2$ | **27** | $^1$H NMR, $^{13}$C NMR, $^{31}$P NMR, EA[67] |
| $(\eta^5\text{-}C_5H_4PPh_2)(\eta^5\text{-}C_5H_4SiMe_3)TiCl_2$ | | brown solid, $^1$H NMR, $^{31}$P NMR, MS, EA[68] |
| $[\eta^5\text{-}C_5H_4P(S)Ph_2](\eta^5\text{-}C_5H_4SiMe_3)TiCl_2$ | **28** | red-orange crystals, $^1$H NMR, $^{31}$P NMR, IR, MS, EA, X-ray[68] |
| $Cl_2Ti(\eta^5\text{-}C_5H_5)[\eta^5\text{-}C_5H_4P(Ph)_2]Ru(p\text{-cymene})Cl_2$ | **29** | ref 69 |

**Scheme 12**

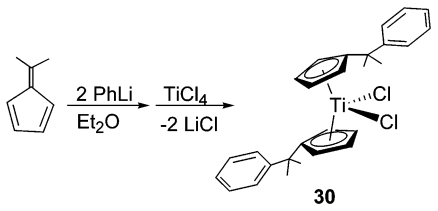


**30**

**Scheme 13**

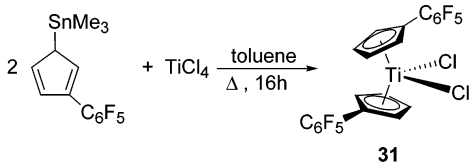


**31**

However, by using a different synthetic route (Scheme 13) involving a trimethyltinylated Cp′ intermediate with titanium tetrachloride in refluxing toluene for 16 h, Rausch et al.[73] obtained the titanocene complex **31** in 54% yield after recrystallization from hot toluene.

Other researchers have started from Ti(III) and the corresponding salt of the ligand followed by oxidation using a stoichiometric amount of $PbCl_2$ as oxidant, forming the desired product (Scheme 14).[74]

**Scheme 14**

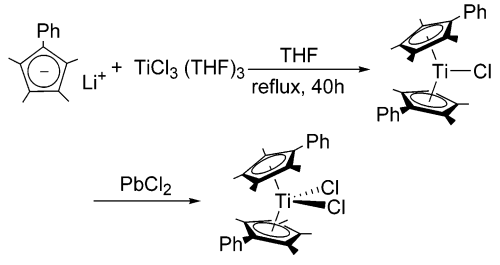


**32**

Single-crystal [3-$CMe_2$Ph-$\eta^5$-$C_5H_3$Me]$_2TiCl_2$ (**33**) suitable for X-ray diffraction was recrystallized from toluene and presented in Figure 7. The molecule is $C_2$-symmetric with a tetrahedral geometry around the central titanium atom formed by the centroids of the Cp rings and the two chlorine atoms.[75]

The bond angle of Cl(1)−Ti−Cl(2) (90.4°) is similar to that in $Cp_2TiCl_2$ (94.6°), and the phenyl groups are pointed away from the central Ti metal in the solid state. Although there is much speculation on the existence of some labile interaction in solution (important for catalysis), concrete evidence from X-ray crystallography as noted above implies that there is no firm intramolecular coordination between the phenyl groups and the metal center. A similar conclusion is arrived at in the crystal structure of $(PhC_5Me_4)_2TiCl_2$ (**32**) (Figure 8).[74]

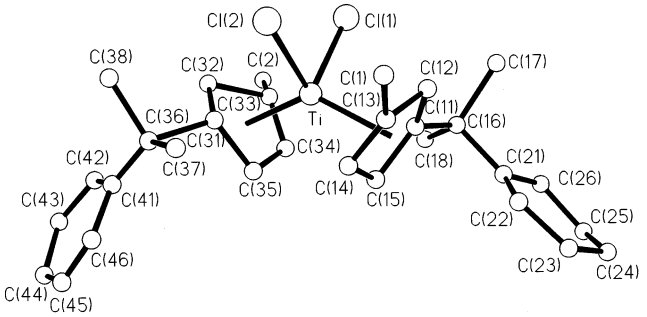


**Figure 7.** Structure of [3-$CMe_2$Ph-$\eta^5$-$C_5H_3$Me]$_2TiCl_2$ (**33**) in the crystal.[75]

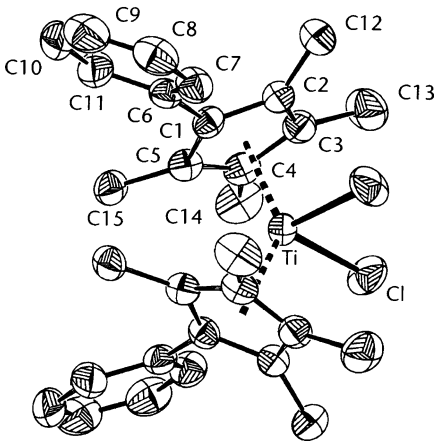


**Figure 8.** Structure of ($\eta^5$-$C_5Me_4Ph)_2TiCl_2$ (**32**) in the crystal.[74] (Reprinted with permission from ref 74. Copyright 1999 CCCC.)

Bis 2-methylbenz[*e*]indenyltitanium dichloride (**34**) (Scheme 15) is also prepared largely by way of route 3 (see section II.A.1).[77]

**Scheme 15**

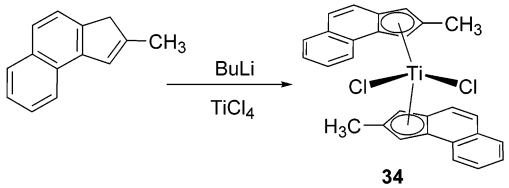


**34**

Physical properties and references for titanocenes containing a bulky functionalized group are listed in Table 6.

### *6. Bridged or ansa-Titanocenes*

In 1982 a rigid, $C_2$-symmetric chelating ligand [ethylene-1,2-bis(3-indene)], originally reported by Lappert,[81] was metalated by Brintzinger[82] to prepare the first *ansa*-titanocenes. Later in 1984 Ewen[83] published the first use of a chiral metallocene as a catalyst in the polymerization of propene. Using a mixture of *meso*- and *dl*-isomers of Brintzinger's ethylene-bridged *ansa*-bis(1-indenyl)titanium dichloride, Ewen reported that a mixture of 63% isotactic and 37% atactic poly(propy1ene) was produced. This report was quickly followed by Kaminsky and Brintzinger,[84] who used *rac*-ethylene-bridged bis(tetrahydro-1-indenyl)zirconium dichloride to obtain highly isotactic poly(propy1ene) with high molecular weight and narrow molecular weight distribution. Since the appearance of these studies, research on the development of novel bridged ligands and the corresponding metal complexes has intensified and expanded by several groups to include silicon, alkyl (chiral and achiral), aryl (chiral and achiral), and oxygen bridges.

**Table 6. Titanocenes Containing a Bulky Group in the Side Chain**

| complex | | color, characterization, etc. |
|---|---|---|
| $[\eta^5\text{-}C_5H_4C(CH_3)_2Ph]_2TiCl_2$ | **30** | $^1$H NMR, $^{13}$C NMR, MS[42] |
| $(\eta^5\text{-}C_5H_4C_6F_5)_2TiCl_2$ | **31** | $^1$H NMR, EA[73] |
| $(\eta^5\text{-}C_5Me_4Ph)_2TiCl_2$ | **32** | dark red crystals, mp, MS, IR, $^1$H NMR, $^{13}$C NMR, UV−vis, X-ray[74] |
| $[\eta^5\text{-}C_5H_4CMe_2(C_{13}H_9)^b](\eta^5\text{-}C_5H_5)TiCl_2$ | | air stable, red crystals, $^1$H NMR, $^{13}$C NMR, MS, EA[76] |
| $[\eta^5\text{-}C_5H_4CMe_2(C_{13}H_9)^b](\eta^5\text{-}C_5Me_5)TiCl_2$ | | air stable, dark red crystals, $^1$H NMR, $^{13}$C NMR, MS, EA[76] |
| $[\eta^5\text{-}C_5H_4CMe_2(C_{13}H_9)^b]_2TiCl_2$ | | air stable, deep red crystals, $^1$H NMR, $^{13}$C NMR, MS, EA, X-ray[76] |
| $(\eta^5\text{-}C_5H_4CPh_3)(\eta^5\text{-}C_5H_5)TiCl_2$ | | $^1$H NMR[78] |
| $[3\text{-}CMe_2R\text{-}\eta^5\text{-}C_5H_3Me]_2TiCl_2$ | | |
| R = Ph | **33** | red crystals, mp, $^1$H NMR, IR, MS, EA, X-ray[75] |
| R = *p*-MePh | | red solid, mp, $^1$H NMR, IR, MS, EA[75] |
| $(3\text{-}CMe_2R\text{-}\eta^5\text{-}C_5H_3Me)(\eta^5\text{-}C_5H_5)TiCl_2$ | | |
| R = *p*-MePh | | red solid, mp, $^1$H NMR, IR, MS, EA[75] |
| $(\eta^5\text{-}C_{26}H_{37})^a(\eta^5\text{-}C_5Me_4CH_2C_6H_5)TiCl_2$ | | red solid, mp, $^1$H NMR, $^{13}$C NMR, IR, MS[79] |
| $[2\text{-}CH_3\text{-}\eta^5\text{-}(C_{13}H_8)^b]_2TiCl_2$ | **34** | red solid, $^1$H NMR, EA[77] |
| $(1\text{-Bn-}\eta^5\text{-}C_9H_7)_2TiCl_2$ | | purple-black solid, IR[80] |
| $(\eta^5\text{-}C_5H_4CH_2Ph)_2TiCl_2$ | | ref 45 |

[a] **a** in the Table =  **b** = 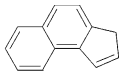

**Table 7. Silicon-Bridged *ansa*-Titanocenes**

| complex | | color, characterization, etc. |
|---|---|---|
| $\mu\text{-}Me_2Si(\eta^5\text{-}C_5H_4)(\eta^5\text{-}C_5Me_4)TiCl_2$ | | red crystals, mp, $^1$H NMR, MS, EA, X-ray[88] |
| $\mu\text{-}Me_2Si(\eta^5\text{-}C_5Me_4)_2TiCl_2$ | **35** | brown-red crystals, $^1$H NMR, $^{13}$C NMR, MS, IR, X-ray[85] |
| $rac\text{-}\mu\text{-}SiMe_2(3\text{-}^t\text{Bu-}5\text{-}SiMe_3\text{-}\eta^5\text{-}C_5H_2)_2TiCl_2$ | | green crystals, $^1$H NMR, $^{13}$C NMR, IR, UV, EA, X-ray[85] |
| $\mu\text{-}SiMe_2(3\text{-}SiMe_3\text{-}\eta^5\text{-}C_5H_3)(\eta^5\text{-}C_5H_4)TiCl_2$ | | mp, $^1$H NMR, $^{13}$C NMR, IR, MS, EA[89] |
| $\mu\text{-}SiMe_2(3\text{-R-}\eta^5\text{-}C_5H_3)(\eta^5\text{-}C_5Me_4)TiCl_2$ | | |
| R = menthyl (*R*) | | red crystals, mp, [α], $^1$H NMR, $^{13}$C NMR, MS, EA, X-ray[90] |
| R = neomenthyl (*R*) | | red, mp, [α], $^1$H NMR, $^{13}$C NMR, MS, EA[90] |
| R = menthyl (*S*) | | red-brown crystals, $^1$H NMR, $^{13}$C NMR, MS, EA, X-ray[90] |
| $\mu\text{-}(Me_2SiSiMe_2)(3\text{-}^t\text{Bu-}\eta^5\text{-}C_5H_3)(\eta^5\text{-}C_5H_4)TiCl_2$ | | red crystals, mp, $^1$H NMR, MS, EA, X-ray[87] |
| $\mu\text{-}(Me_2SiSiMe_2)(3\text{-Me-}\eta^5\text{-}C_5H_3)(\eta^5\text{-}C_5H_4)TiCl_2$ | | red crystals, mp, $^1$H NMR, MS, X-ray[87] |
| $\mu\text{-}(Me_2SiSiMe_2)(\eta^5\text{-}C_5H_3\text{−}3\text{-Me})_2TiCl_2$ | | mp, $^1$H NMR, MS, EA[87] |
| $\mu\text{-}(Me_2Si)_2(3\text{-}^t\text{Bu-}\eta^5\text{-}C_5H_3)_2TiCl_2$ | **36** | |
| *rac* | | deep red, cube-shaped crystals, mp, $^1$H NMR, MS[86] |
| *meso* | | deep red, needle crystals, mp, $^1$H NMR, MS, EA, X-ray[86] |
| $\mu,\mu\text{-}(SiMe_2)_2(3\text{-Me-}5\text{-}^i\text{Pr-}\eta^5\text{-}C_5H)_2TiCl_2$ | | |
| *rac* | | bright red crystals, $^1$H NMR, EA, X-ray[91] |
| *meso* | | $^1$H NMR[91] |
| $\mu\text{-}(Me_2SiSiMe_2)(\eta^5\text{-}1\text{-}C_9H_6)_2TiCl_2$ | | brownish black crystals, mp,$^1$HNMR, EA, MS[92] |
| $\mu\text{-}(Me_2SiSiMe_2)(\eta^5\text{-}1\text{-}C_9H_{10})_2TiCl_2$ | | deep red crystals, mp,$^1$H NMR, EA, MS[92] |

**a. Silicon-Bridged *ansa*-Titanocenes.** The *ansa*-$Cp_2TiX_2$ (**35**) complex was obtained by eliminating 2 equiv of LiCl during the metathetical reaction of the dilithium salt of bridged Cp ligand with titanium tetrachloride (Scheme 16).[85]

**Scheme 16**

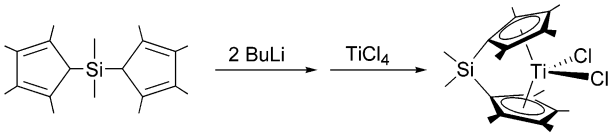


**35**

However, a mixture **36** of *meso*- and *rac*-isomers forms in the final product (Scheme 17).[86] These are separated by fractional recrystallization from suitable solvents, with the *meso* form separated first. In some cases, separation is much more difficult due to the close similarity in solubility behaviors of the two isomers.[87]

**Scheme 17**

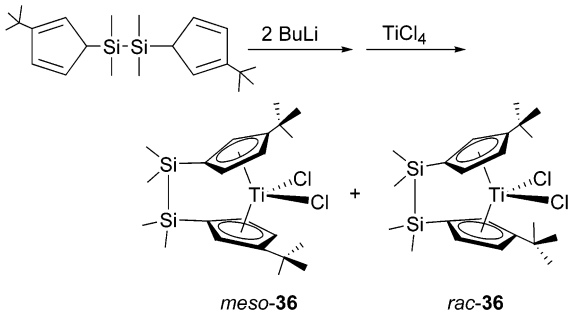


Some physical data and references for metallocenes bearing a silicon-bridging atom are summarized in Table 7.

**b. Carbon-Bridged *ansa*-Titanocenes.** Symmetrical and uniformly substituted *ansa*-indenyltitanocenes are obtained by similar metathetical techniques used for the cyclopentadienyl counterparts, discussed above.

$C_2$ symmetric tetrahydroindenyl titanium complex **37** was prepared from the *ansa*-titanocene complex

**Scheme 18**

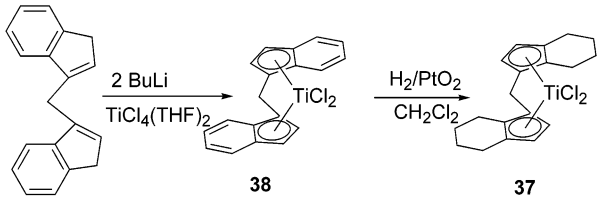


methylenebis(indenyl)titanium dichloride (**38**) after catalytic hydrogenation (Scheme 18).[93] The structure of the methylenebis(4,5,6,7-tetrahydro-1-indenyl)-titanium dichloride (Figure 9) was determined by an X-ray diffraction analysis.

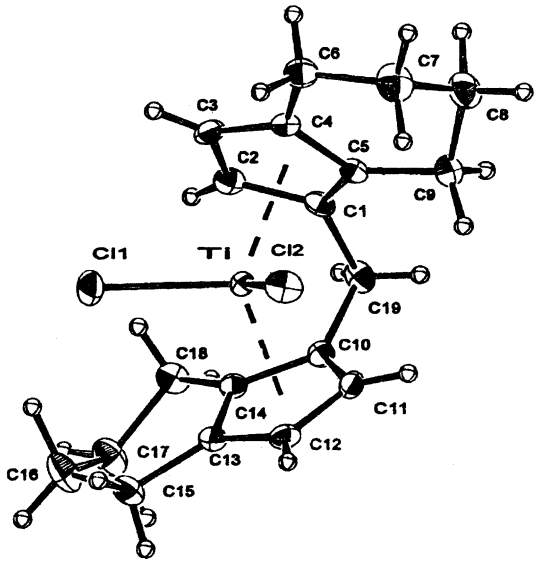


**Figure 9.** Structure of $\mu$-$CH_2(\eta^5$-1-$C_9H_{10})_2TiCl_2$ (**37**) in the crystal.[93] Ti−Ce, 2.077, 2.078 Å; Cl−Ti−Cl, 96.70(4)°; Ind−Ti−Ind, 121.0°. (Reprinted with permission from ref 93. Copyright 1997 Elsevier Sequoia.)

Voskoboynikov[94] reported the synthesis of bis-(indenyl)methane ligand and the corresponding *ansa*-titanium complex, methylene-bis(indenyl)titanium(IV) dichloride, by two different pathways. The common metalation of the dilithium salt of bis(indenyl)-methane in THF yielded only 16% of the *rac*-$H_2C(indenyl)_2TiCl_2$ (**38**). An alternative route involving the treatment of $TiCl_4$ with bis[3-(tri-*n*-butyltin)indenyl]methane results in 38% yield of the *rac*-$H_2C(indenyl)_2TiCl_2$ (**38**) isomer (Scheme 19). X-ray

**Scheme 19**

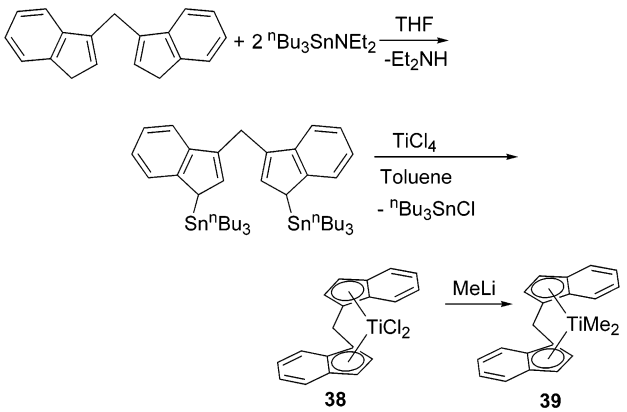


crystal structural analysis of the *rac*-$H_2C(indenyl)_2$-$TiMe_2$ (**39**) obtained by the treatment of *rac*-$H_2C(indenyl)_2TiCl_2$ (**38**) with 2 equiv of MeLi in diethyl ether is shown in Figure 10.

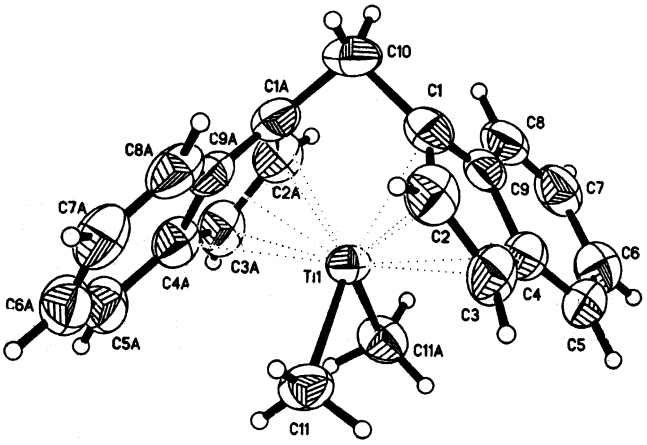


**Figure 10.** Structure of $\mu$-$CH_2(\eta^5$-1-$C_9H_6)_2TiMe_2$ (**39**) in the crystal.[94] Cl−Ti−Cl, 94.0(2)°; Ind−Ti−Ind, 121.6°. (Reprinted with permission from ref 94. Copyright 2001 Elsevier Sequoia.)

Metalation of bis(4,6-dimethylinden-7-yl)methane with BuLi and titanium tetrachloride gave the $C_2$ symmetric [*dl*-bis(4,6-dimethylinden-7-yl)methyl-idene]titanium dichloride (**40**) (Scheme 20). [95]

**Scheme 20**

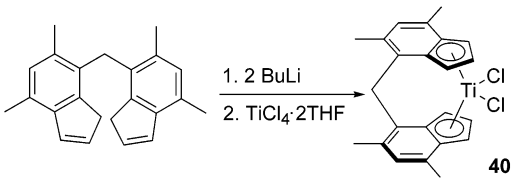


Nantz et al.[96] reported the synthesis of the ethylene-bridged *ansa*-titanocene dichlorides **41** and **42**, which were prepared as a mixture of racemic and meso diastereomers by treating the dianion of 1,2-bis(2-indenyl)ethane ligand with $TiCl_3$·3THF followed by addition of 6 M HC1 and subsequent aeration (Scheme 21). This is the first example of ethylene-

**Scheme 21**

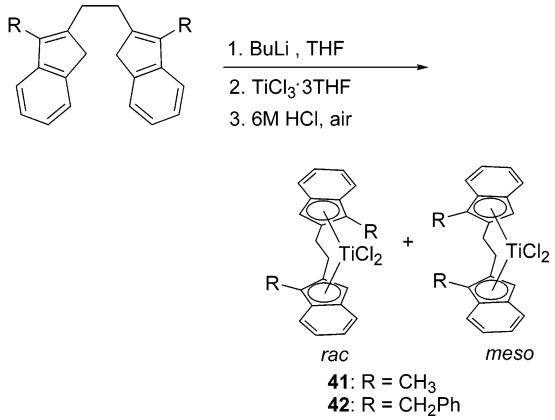


bridged titanocenes in which the indenyl ligands are attached at the 2-position and have alkyl substituents in the 1-position. The structure of complex **41**

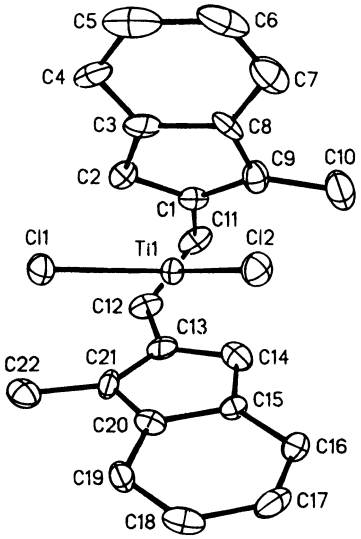


**Figure 11.** Structure of *rac*-$\mu$-$(CH_2CH_2)(1\text{-}CH_3\text{-}\eta^5\text{-}2\text{-}C_9H_5)_2TiCl_2$ (**41**) in the crystal.[96] Ti−Ce, 2.118, 2.122 Å; Cl−Ti−Cl, 96.2°; Ind−Ti−Ind, 128.0°. (Reprinted with permission from ref 96. Copyright 1995 American Chemical Society.)

(Figure 11) and [ethylenebis($\eta^5$-4,5,6,7-tetrahydro-2-indenyl)]titanium dichloride (**43**) was analyzed by X-ray analysis (Figure 12).

Later the same group[97] reported new examples of chiral, α-substituted *ansa*-titanocenes **44**−**47** derived from 1,2-bis(2-indenyl)ethane (Scheme 22). They

**Scheme 22**

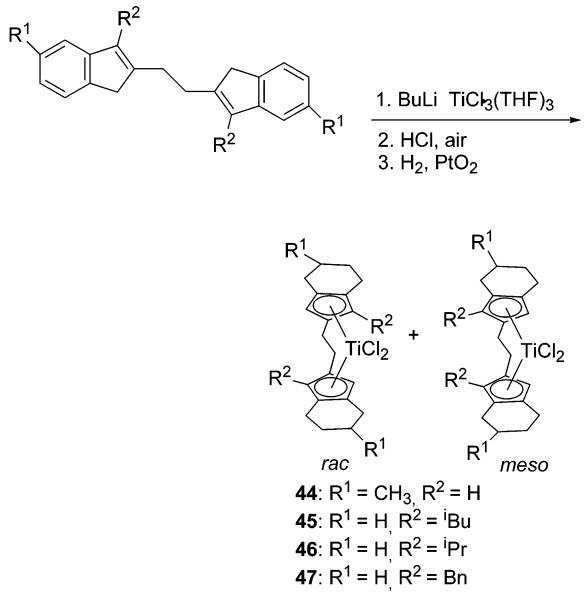


found that the α-substituent is more sterically encumbered and, hence, slightly favors formation of the racemic isomer. The X-ray structure of all three *ansa*-titanocenes was deterimined to follow predictable patterns as shown in Figures 13−15.

Halterman and his group have been very active in the design of new chiral bridged ligands and the preparation of metallocene complexes thereof and have reviewed a large portion of these findings.[30] Some of their more exciting and elegant findings on the use of aryl and bulky bridging groups for the synthesis of *ansa*-bis(indene)titanium dichlorides are

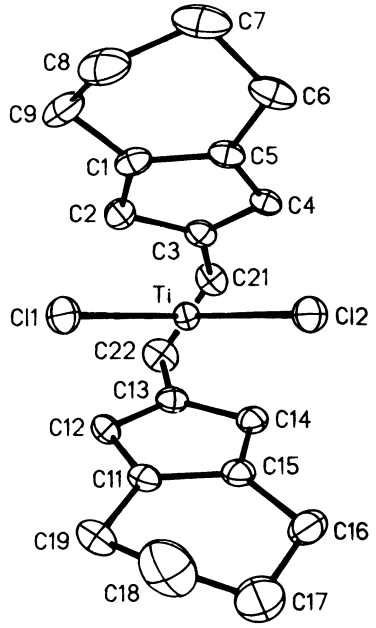


**Figure 12.** Structure of $\mu$-$(CH_2CH_2)(\eta^5\text{-}2\text{-}C_9H_{10})_2TiCl_2$ (**43**) in the crystal.[96] Ti−Ce, 2.098, 2.096 Å; Cl−Ti−Cl, 94.8°; Ind−Ti−Ind, 129.5°. (Reprinted with permission from ref 96. Copyright 1995 American Chemical Society.)

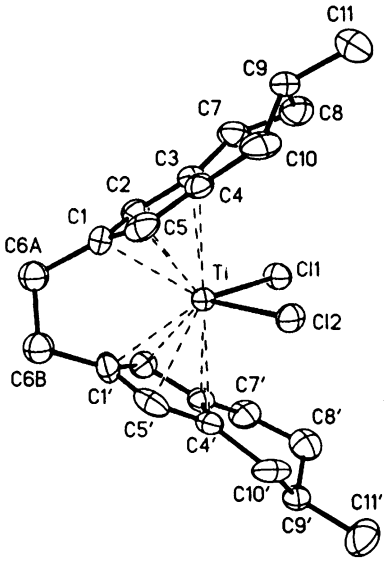


**Figure 13.** Structure of *meso*-$\mu$-$(CH_2CH_2)(5\text{-}CH_3\text{-}\eta^5\text{-}2\text{-}C_9H_8)_2TiCl_2$ (**44**) in the crystal.[97] (Reprinted with permission from ref 97. Copyright 1999 Elsevier Sequoia.)

discussed in the following paragraphs. In 1997 they reported the biaryl-bridged bis(indene) titanium complex, which was obtained from the deprotonation of the ligand by BuLi and then with $TiCl_3$ followed by oxidation to give the titanocene **48** (Scheme 23).[98]

The complexes *ansa*-[2,2'-bis[(4,7-dimethyl-inden-1-yl)methyl]-1,1'-binaphthyl]titanium dichloride (**49**) (Scheme 24), *ansa*-[2,2′-bis[(4,5,6,7-tetrahydroinden-1-yl)methyl]-1,1′-binaphthyl]titanium dichloride (**51**), and *ansa*-[2,2′-bis[(4,5,6,7-tetrahydroinden-1-yl)-methyl]-5,5′,6,6′,7,7′,8,8′-octahydro-1,1′-binaphthyl]-titanium dichloride (**52**) were synthesized from the same starting materials by progressive hydrogenation using $PtO_2$ as a catalyst in a varying $H_2$ pressure as shown in Scheme 25. The crystal structure of

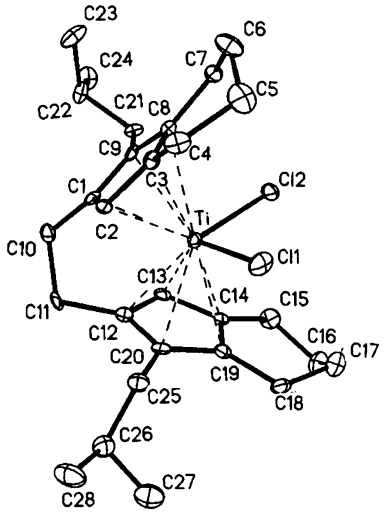


**Figure 14.** Structure of *rac*-$\mu$-$(CH_2CH_2)(1\text{-}^i\text{Bu-}\eta^5\text{-2-}C_9H_8)_2$-$TiCl_2$ (**45**) in the crystal.[97] (Reprinted with permission from ref 97. Copyright 1999 Elsevier Sequoia.)

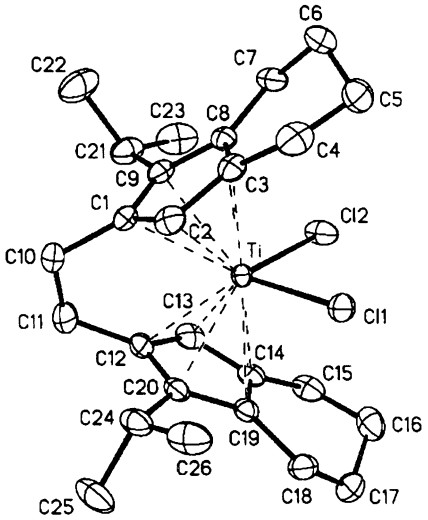


**Figure 15.** Structure of *rac*-$\mu$-$(CH_2CH_2)(1\text{-}^i\text{Pr-}\eta^5\text{-2-}C_9H_8)_2$-$TiCl_2$ (**46**) in the crystal.[97] **44**: Ti−Ce, 2.111, 2.115 Å; Cl−Ti−Cl, 96.70°; Ind-Ti−Ind, 129.7°. **45**: Ti−Ce, 2.111, 2.116 Å; Cl−Ti−Cl, 92.48°; Ind−Ti−Ind, 129.2°. **46**: Ti-Ce, 2.092, 2.092 Å; Cl−Ti−Cl, 94.96°; Ind-Ti−Ind, 129.9°. (Reprinted with permission from ref 97. Copyright 1999 Elsevier Sequoia.)

**Scheme 23**

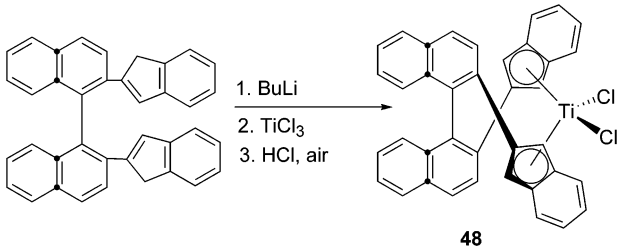


48

complex **52** has been determined and is shown in Figure 16.[99]

The new phenyl-bridged *ansa*-bis(indenyl)titanium dichlorides **53** were obtained in a good yield (89%) from the corresponding ligands by lithiation followed by the addition of $TiCl_3$ (Scheme 26).[100]

Deprotonation of bis(indene) with BuLi followed by metalation with $TiCl_3$ and oxidative workup (HCl, air, chloroform) was reported to give the single stereoisomeric 2,5-diisopropylcyclohexane-1,4-diyl-bridged bis(indenyl)titanium dichloride (**54**) in 80% yield. Catalytic hydrogenation of bis(indenyl)titanium dichloride gave the 2,5-diisopropylcyclohexane-1,4-diyl-bridged bis(tetrahydroindenyl)titanium dichloride (**55**) in 76% yield (Scheme 27). The solid-state structure of **55** was determined by X-ray crystallographic methods (Figure 17).[101,102]

**Scheme 24**

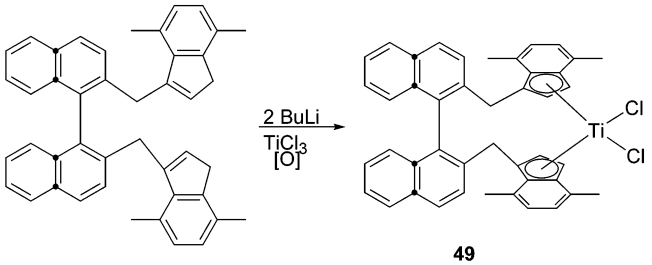


49

**Scheme 25**

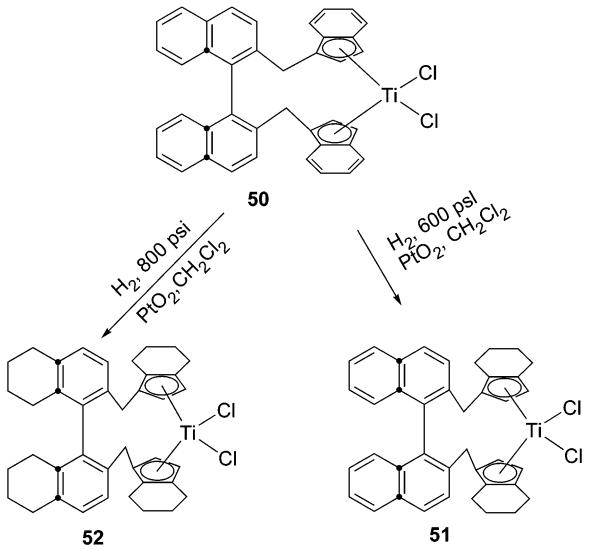


Erker et al.[103] synthesized *ansa*-cycloalkylene-bis(indenyl)titanium dichloride **56** through the reaction of dilithiated salt of the cycloalkylene-bridged indene ligand with $TiCl_3$. Transformation to the corresponding bis(tetrahydroindenyl)titanium dichloride (**57**) was achieved in good yields by catalytic hydrogenation (Scheme 28).

References, characterization, and some physical data of titanocenes bearing various carbon-bridging atoms are presented in Table 8.

**c. *ansa*-Titanocenes Containing Miscellaneous Bridging Groups.** The disiloxane-bridged bis(indenyl)titanium complex **62** was prepared as shown in Scheme 29 and the structure determined by X-ray diffraction analysis (Figure 18). Using $PtO_2$, **62** was converted to the corresponding tetrahydroindenyl complex **63**.[111]

Table 9 presents data on *ansa*-titanocenes bearing miscellaneous bridging atoms.

**d. Titanocenes Containing Mixed Cp (Ind) Ligands.** Unbridged mixed-ligand titanocenes having Cp and Ind moieties on the same metal are prepared in a way analogous to the procedures

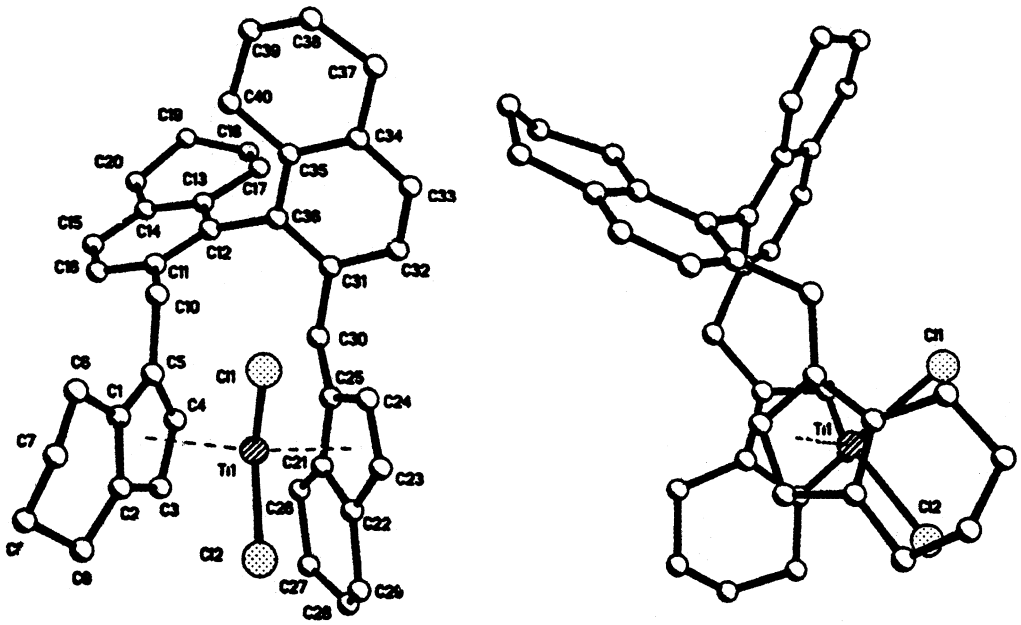

**Figure 16.** Structure of [2,2′-($\eta^5$-1-$C_9H_{10}CH_2$)$_2$($C_{20}H_{20}$)]$TiCl_2$ (**52**) in the crystal.[99] (Reprinted with permission from ref 99. Copyright 1996 Elsevier Sequoia.)

**Scheme 26**

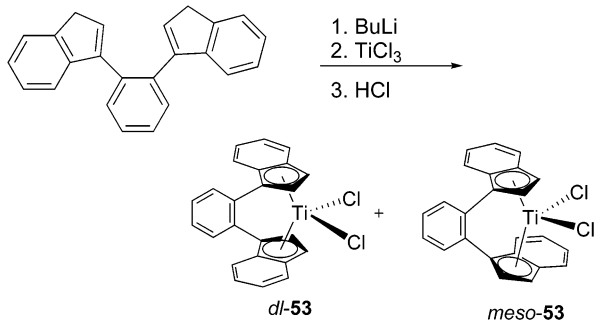


**Scheme 27**

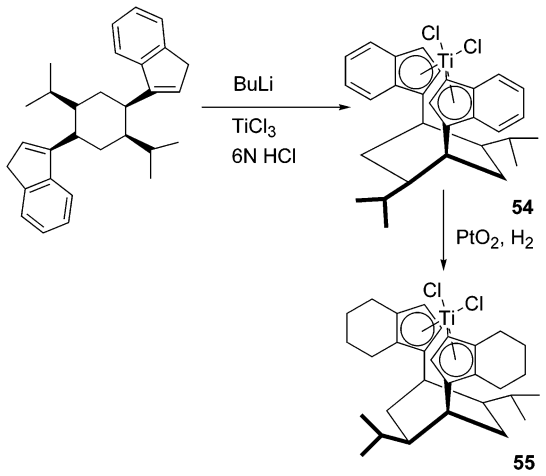


described in section II.A.1 for differently substituted Cp or Ind ligands.

Either Cp[117] or Ind[43] and substituted Ind[80] may be introduced first to prepare the mixed-ligand $C_s$ symmetric titanocene **64** (Scheme 30).

Chien and Rausch[77] synthesized mixed-ring titanium complexes **65** through benz[*e*]indenyltitanium trichloride and CpTl in toluene (Scheme 31).

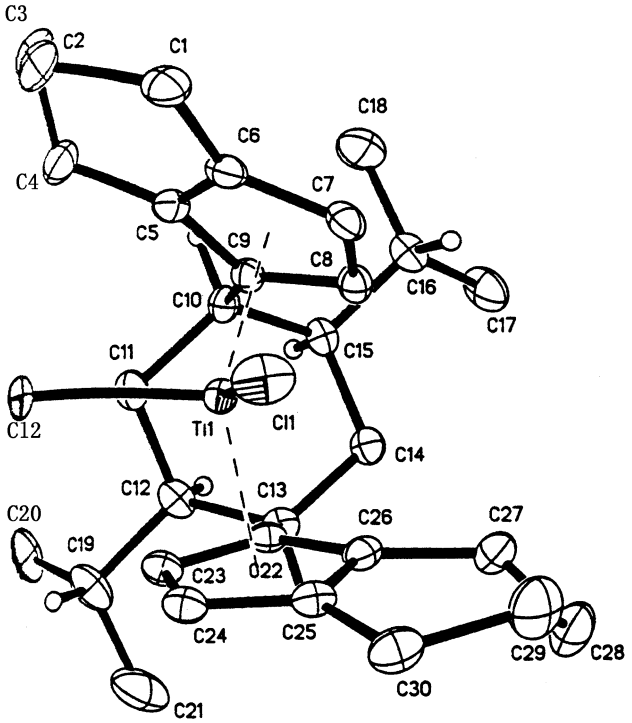

**Figure 17.** Structure of (+)-(1*S*,2*R*,4*R*,5*R*)-[2,5-$^i$Pr$_2$-1,4-($\eta^5$-1-$C_9H_{10}$)$_2$$C_6H_8$]$TiCl_2$ (**55**) in the crystal.[102] Ti−Ce, 2.093(2), 2.094(2) Å; Cl−Ti−Cl, 93.01°; Ind−Ti−Ind, 133.4(1)°. (Reprinted with permission from ref 102. Copyright 2000 American Chemical Society.)

Buchwald used X-ray diffraction to determine the structure of a titanocene **66** containing a mixed cyclopentadienyl (indenyl) *ansa*-ligand as illustrated in Scheme 32.[118]

Miyake et al.[119] synthesized a novel unsymmetrical *ansa*-metallocene $Me_2C$(3-$^t$Bu-$C_5H_3$)(3-$^t$Bu-$C_9H_5$)$TiCl_2$ (*threo*) (**68**). The titanium complex was prepared by the reaction of $TiC1_4(THF)_2$ with the dilithium salt in THF at −78 °C, yielding dark green crystals (Scheme 33).

**Table 8. Carbon-Bridged Titanocenes**

| complex | | color, characterization, etc. |
|---|---|---|
| $\mu$-$CMe_2$(3-$^t$Bu-$\eta^5$-$C_5H_3$)$_2TiCl_2$ | | |
| *rac* | | dark green polycrystalline, mp, $^1$H NMR, EA[104] |
| *meso* | | dark green needle, mp, $^1$H NMR, EA[104] |
| $\mu$-($CH_2CH_2$)[$\eta^5$-1-($C_9H_{10}$)$^a$]$_2TiCl_2$ | | refs 82 and 105 |
| *dl*-[1,2-($\eta^5$-1-$C_9H_{10}$)$^a_2C_6H_4$]$TiCl_2$ | | red solid, mp, $^1$H NMR, $^{13}$C NMR, IR, MS, EA, X-ray[106] |
| *S*-[2,2′-($\eta^5$-2-$C_9H_{10}$)$^a_2$($C_{14}H_{12}$)$^b$]$TiCl_2$ | | purple crystals, [$\alpha$], EA[107] |
| [2,2′-(3,4-$R_2$-$\eta^5$-$C_5H_2$)$_2$($C_{12}H_8$)$^c$]$TiCl_2$ | | |
| R = Me | | dark red cube, $^1$H NMR, MS, EA, X-ray[108] |
| R = $(CH_2)_4$ | | dark red crystals, $^1$H NMR, $^{13}$C NMR, MS, EA, X-ray[109] |
| R = Ph | | dark red powder, $^1$H NMR, $^{13}$C NMR, MS, EA[109] |
| (*R*)-(+)-[2,2′-($\eta^5$-2-$C_9H_{10}$)$^a_2$($C_{20}H_{12}$)$^d$]$TiCl_2$ | | tan powder, mp (dec), [$\alpha$], $^1$H NMR, $^{13}$C NMR, IR, MS, EA[98] |
| (*R*)-(+)-[2,2′-($\eta^5$-2-$C_{10}H_{12}$)$^e_2$($C_{20}H_{12}$)$^d$]$TiCl_2$ | | tan solid, mp (dec), [$\alpha$], $^1$H NMR, $^{13}$C NMR, IR, MS, EA[98] |
| $\mu$-$CH_2$($\eta^5$-1-$C_9H_{10}$)$^a_2TiCl_2$ | **37** | dark red crystals, $^1$H NMR, $^{13}$C NMR, MS, X-ray[93] |
| $\mu$-$CH_2$($\eta^5$-1-$C_9H_6$)$_2TiCl_2$ | **38** | greenish brown crystalline solid, $^1$H NMR, EA[94], MS[93] |
| $\mu$-$CH_2$($\eta^5$-1-$C_9H_6$)$_2TiMe_2$ | **39** | dark green crystalline solid, $^1$H NMR, EA, X-ray[94] |
| $\mu$-$CH_2$(5,7-$Me_2$-$\eta^5$-4-$C_9H_4$)$_2TiCl_2$ | **40** | green precipitate, mp, $^1$H NMR, MS[95] |
| $\mu$-($CH_2CH_2$)(1-R-$\eta^5$-2-$C_9H_5$)$_2TiCl_2$ | | |
| R = $CH_3$ (*rac*) | **41** | IR, $^1$H NMR,$^{13}$C NMR, EI-MS, HRMS, X-ray[96] |
| R = $CH_3$ (*meso*) | | $^1$H NMR[96] |
| R = $CH_2$Ph (*rac*) | **42** | IR,$^1$H NMR,$^{13}$C NMR, MS, HRMS[96] |
| R = $CH_2$Ph (*meso*) | | $^1$H NMR[96] |
| $\mu$-($CH_2CH_2$)($\eta^5$-2-$C_9H_{10}$)$^a_2TiCl_2$ | **43** | red-gold solid, mp, IR,$^1$H NMR,$^{13}$C NMR, EA, X-ray[96] |
| $\mu$-($CH_2CH_2$)(1-$R^2$-5-$R^1$-$\eta^5$-2-$C_9H_8$)$_2TiCl_2$ | | |
| $R^1$ = $CH_3$, $R^2$ = H (*rac*) | **44** | $^1$H NMR[97] |
| $R^1$ = $CH_3$, $R^2$ = H (*meso*) | | red solid, IR,$^1$H NMR,$^{13}$C NMR, X-ray[97] |
| $R^1$ = H, $R^2$ = $^i$Bu (*rac*) | **45** | bright red solid, mp, IR, $^1$H NMR,$^{13}$C NMR, HRMS, X-ray[97] |
| $R^1$ = H, $R^2$ = $^i$Pr (*rac*) | **46** | red solid, IR, $^1$H NMR, $^{13}$C NMR, HRMS, X-ray[97] |
| $R^1$ = H, $R^2$ = Bn (*rac*) | **47** | red solid, mp, IR, $^1$H NMR,$^{13}$C NMR, HRMS[97] |
| *dl*-[$\mu$-($CH_2CH_2$)(4-$^i$Pr-$\eta^5$-7-$C_9H_5$)$_2TiCl_2$] | | fine green precipitate, mp, IR, $^1$H NMR,$^{13}$CNMR, EA, MS, X-ray[95] |
| $\mu$,$\mu$-($CH_2CH_2$)$_2$($\eta^5$-1,2-$C_9H_5$)$_2TiCl_2$ | | dark green powder, mp (dec), IR, $^1$H NMR,$^{13}$C NMR, MS[110] |
| [2,2′-($\eta^5$-2-$C_9H_{10}$)$_2$($C_{20}H_{12}$)$^d$]$TiCl_2$ | **48** | tan powder, mp (dec), [$\alpha$], IR, $^1$H NMR,$^{13}$C NMR, EA, MS[98,107] |
| [2,2′-(4,7-$Me_2$-$\eta^5$-1-$C_9H_4CH_2$)$_2$($C_{20}H_{12}$)$^d$]$TiCl_2$ | **49** | dark green powder, mp, [$\alpha$], IR, $^1$H NMR,$^{13}$C NMR, MS[99] |
| [2,2′-($\eta^5$-1-$C_9H_6CH_2$)$_2$($C_{20}H_{12}$)$^d$]$TiCl_2$ | **50** | ref 99 |
| [2,2′-($\eta^5$-1-$C_9H_{10}CH_2$)$_2$($C_{20}H_{12}$)$^d$]$TiCl_2$ | **51** | red solid, mp (dec), IR,$^1$H NMR,$^{13}$C NMR, MS[99] |
| [2,2′-($\eta^5$-1-$C_9H_{10}CH_2$)$_2$($C_{20}H_{20}$)$^g$]$TiCl_2$ | **52** | fine red powder, mp (dec), IR,$^1$H NMR,$^{13}$C NMR, MS, X-ray[99] |
| [1,2-($\eta^5$-1-$C_9H_6$)$_2C_6H_4$]$TiCl_2$ | **53** | dark brown solid, IR,$^1$H NMR,$^{13}$C NMR, MS[100] |
| [1,2-(4,7-$Me_2$-$\eta^5$-1-$C_9H_4$)$_2C_6H_4$]$TiCl_2$ (*dl*) | | green solid, mp (dec), IR, $^1$H NMR,$^{13}$C NMR, EA, MS[100] |
| [1,2-(4,7-$Me_2$-$\eta^5$-1-$C_9H_4$)$_2C_6H_4$]$TiCl_2$ (*meso*) | | brown solid, mp (dec), IR, $^1$H NMR,$^{13}$C NMR, MS[100] |
| [1,2-($\eta^5$-1-$C_{12}H_{10}$)$^f_2C_6H_4$]$TiCl_2$ | | dark brown solid, IR, $^1$H NMR,$^{13}$C NMR, MS[100] |
| (+)−(*1S,2R,4R,5R*)- | **54** | dark green solid, mp, [$\alpha$], $^1$H NMR,$^{13}$C NMR, IR, EA, MS,[102] |
| [2,5-$^i$$Pr_2$−1,4-($\eta^5$-1-$C_9H_6$)$_2C_6H_8$]$TiCl_2$ | | X-ray[101] |
| (+)−(*1S,2R,4R,5R*)- | **55** | red crystals, mp, [$\alpha$], $^1$H NMR,$^{13}$C NMR, IR, EA, MS, X-ray[102] |
| [2,5-$^i$$Pr_2$−1,4-($\eta^5$-1-$C_9H_{10}$)$_2C_6H_8$]$TiCl_2$ | | |
| [1,2-($\eta^5$-3-$C_9H_6$)$_2$-cyclo-$C_5H_8$]$TiCl_2$ | **56** | EA[103] |
| [1,2-($\eta^5$-3-$C_9H_6$)$_2$-cyclo-$C_6H_{10}$]$TiCl_2$ | **57** | EA[103] |
| [1,2-($\eta^5$-3-$C_9H_6$)$_2$-cyclo-$C_7H_{12}$]$TiCl_2$ | **58** | EA[103] |
| [1,2-($\eta^5$-3-$C_9H_{10}$)$_2$-cyclo-$C_5H_8$]$TiCl_2$ (*rac*) | **59** | mp (dec), $^1$H NMR, $^{13}$C NMR[103] |
| [1,2-($\eta^5$-3-$C_9H_{10}$)$_2$-cyclo-$C_5H_8$]$TiCl_2$ (*meso*) | | mp (dec), IR, $^1$H NMR, $^{13}$C NMR, EA, X-ray[103] |
| [1,2-($\eta^5$-3-$C_9H_{10}$)$_2$-cyclo-$C_6H_{10}$]$TiCl_2$ (*rac*) | **60** | red solid, mp (dec), $^1$H NMR, X-ray[103] |
| [1,2-($\eta^5$-3-$C_9H_{10}$)$_2$-cyclo-$C_6H_{10}$]$TiCl_2$ (*meso*) | | red solid, mp (dec), IR, $^1$H NMR, $^{13}$C NMR, EA, X-ray[103] |
| [1,2-($\eta^5$-3-$C_9H_{10}$)$_2$-cyclo-$C_7H_{12}$]$TiCl_2$ (*rac*) | **61** | mp (dec), $^1$H NMR, $^{13}$C NMR[103] |
| [1,2-($\eta^5$-3-$C_9H_{10}$)$_2$-cyclo-$C_7H_{12}$]$TiCl_2$ (*meso*) | | mp (dec), IR, $^1$H NMR, $^{13}$C NMR, EA, X-ray[103] |

$^a$

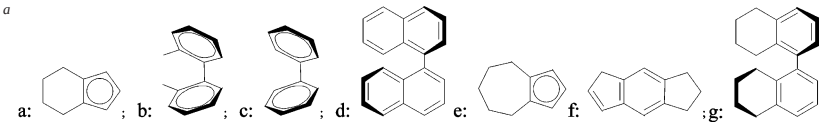


**Table 9. Miscellaneous Bridged *ansa*-Titanocenes**

| complex | | color, characterization, etc. |
|---|---|---|
| $\mu$-($Me_2SiOSiMe_2$)($\eta^5$-$C_5H_4$)$_2TiCl_2$ | | red microcrystalline solid, $^1$H NMR, $^{13}$C NMR, MS, EA[112] |
| $\mu$-($Me_2SiOSiMe_2$)($\eta^5$-$C_5H_4$)$_2TiBr_2$ | | dark green solid, $^1$H NMR, $^{13}$C NMR, EA[113] |
| $\mu$-($Me_2SiOSiMe_2$)($\eta^5$-1-$C_9H_6$)$_2TiCl_2$ | **62** | burgundy[114] or brownish black[111] crystals, mp,[111] $^1$H NMR,[111,114] MS,[111] EA,[111,114] X-ray[111] |
| $\mu$-($Me_2SiOSiMe_2$)($\eta^5$-1-$C_9H_{10}$)$_2TiCl_2$ | **63** | deep red crystals, mp,$^1$H NMR, EA, MS, X-ray[111] |
| $\mu$-[$Me_2SiN$(Bu)$SiMe_2$]($\eta^5$-$C_5H_4$)$_2TiCl_2$ | | $^1$H NMR, $^{13}$C NMR, $^{29}$Si NMR, MS[115] |
| $\mu$-PPh($\eta^5$-$C_5Me_4$)$_2TiCl_2$ | | red brown solid, $^1$H NMR, $^{13}$C NMR, $^{31}$P NMR, IR, EA, X-ray[116] |
| $\mu$-$GeMe_2$($\eta^5$-$C_5Me_4$)($\eta^5$-$C_5H_4$)$TiCl_2$ | | purple crystals, mp, $^1$H NMR, MS, EA[88] |

**Scheme 28**

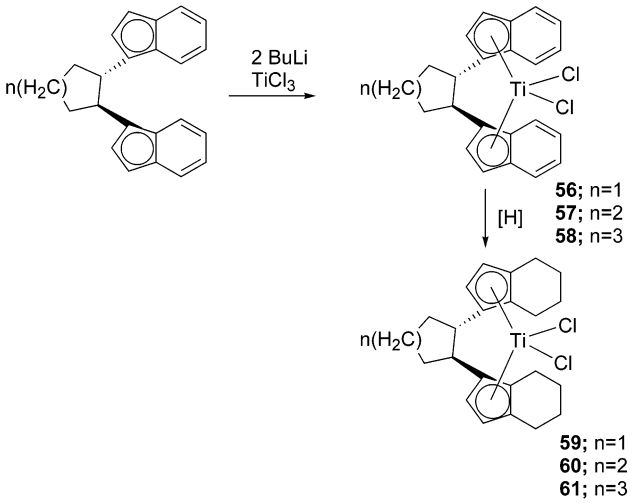


**Scheme 29**

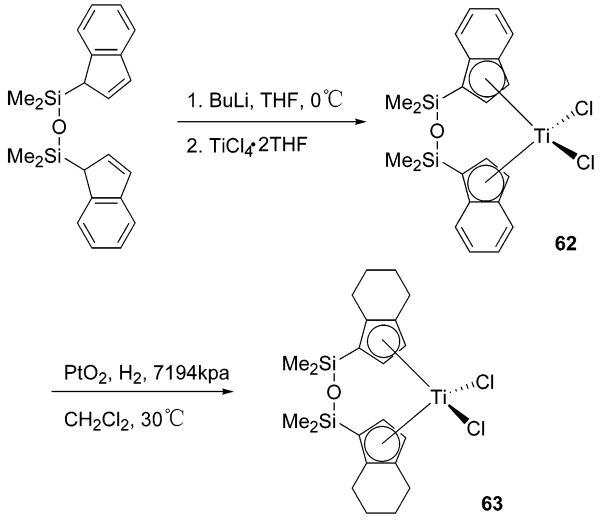


Collins and co-workers[120] prepared the titanium complexes **69** (Table 10) through reaction of the dilithium salt of the propylidene-bridged metallocene ligand with the metal tetrachloride suspended in dichloromethane (Chart 3). The synthetic yields were very low, ∼4%.

### *7. Bimetallic Complexes Containing Titanium*

Researchers have used tremendous imagination through the linkage of various parts of two metal

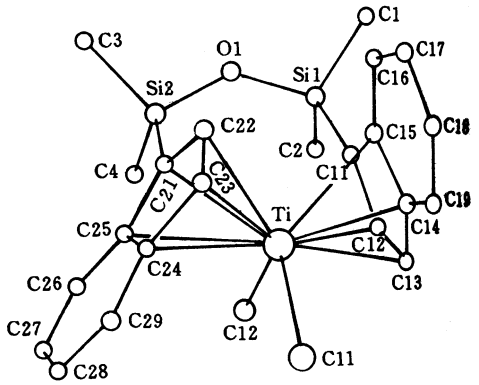


**Figure 18.** Structure of $\mu$-($Me_2SiOSiMe_2$)($\eta^5$-1-$C_9H_6$)$_2TiCl_2$ (**62**) in the crystal.[111]

**Scheme 30**

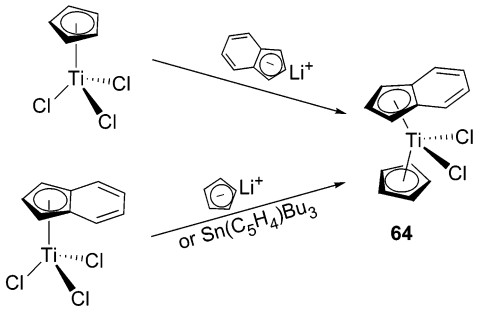


**Scheme 31**

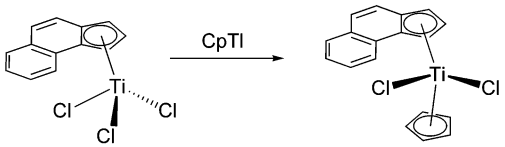


**Scheme 32**

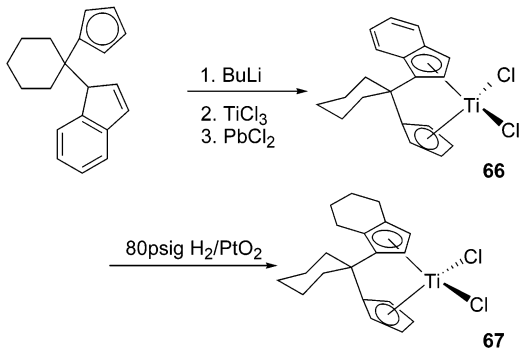


**Scheme 33**

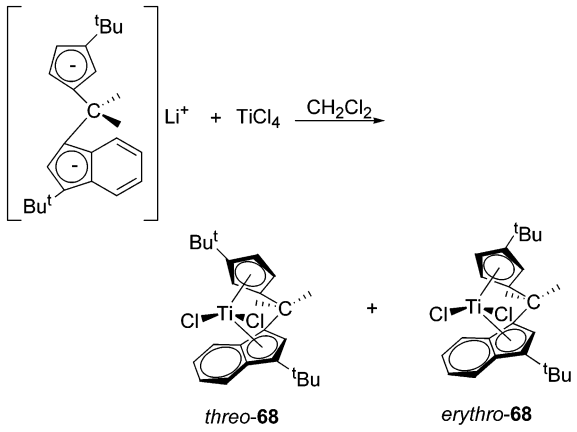


centers in order to vary the chemical and physical properties of what is regarded as a bimetallic unity. Bimetallic complexes may be characterized as either homonuclear or heteronuclear depending on whether the two metal centers are the same (e.g., Ti−Ti) or different (e.g., Ti−Zr), respectively. The complexes may be further classified on the basis of the type of linkage binding the two metal centers:

(a) Bimetallic complexes contain links between a Cp or Ind moiety on one metal and another Cp or Ind moiety on the other metal (Chart 4).

**Table 10. Titanocenes Containing Mixed Cp (Ind) Ligands**

| complex | | color, characterization, etc. |
|---|---|---|
| $(\eta^5\text{-}C_5H_5)(\eta^5\text{-}C_9H_7)TiCl_2$ | **64** | brown crystals,[117] mp (dec),[43] $^1$H NMR, $^{13}$C NMR, MS[117] |
| $(\eta^5\text{-}C_5H_5)[\eta^5\text{-}(C_{13}H_9)^a]TiCl_2$ | **65** | red crystals, $^1$H NMR, EA[77] |
| cyclo-$C(CH_2)_5(\eta^5\text{-}C_5H_4)(\eta^5\text{-}C_9H_6)TiCl_2$ | **66** | dark green crystals, $^1$H NMR, $^{13}$C NMR, EA[118] |
| cyclo-$C(CH_2)_5(\eta^5\text{-}C_5H_4)(\eta^5\text{-}C_9H_{10})TiCl_2$ | **67** | black crystals, $^1$H NMR, $^{13}$C NMR, EA, X-ray[118] |
| $\mu$-$CMe_2$(3-$^t$Bu-$\eta^5$-$C_5H_4$)(3-$^t$Bu-$\eta^5$-$C_9H_6$)$TiCl_2$ | **68** | green powder, $^1$H NMR, EA[119] |
| $\mu$-$CMe_2(\eta^5\text{-}C_5H_4)(\eta^5\text{-}C_9H_6)TiCl_2$ | **69** | green solid, IR, $^1$H NMR, $^{13}$C NMR, EA, MS[120] |
| $(\eta^5\text{-}C_5H_5)$(1-Bn-$\eta^5$-$C_9H_7$)$TiCl_2$ | | purple-black solid, IR, MS[80] |

**Chart 3. Structure of $\mu$-$CMe_2(\eta^5\text{-}C_5H_4)(\eta^5\text{-}C_9H_6)TiCl_2$ 69[120]**

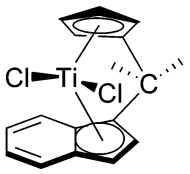

**69**

**Chart 4**

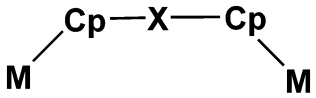

**Chart 5**

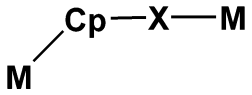

**Chart 6**



(b) Bimetallic complexes contain a Cp or Ind moiety on one metal linked to the second metal center via the link atoms or ligands (X) (Chart 5).

(c) Bimetallic complexes contain links between two metal centers via the link atoms or ligands (X) without the involvement of any Cp or Ind ligands on either metal (Chart 6).

Noh et al.[121] reported the homonuclear bimetallic titanocene with one polysiloxane bridge **70**−**71** or two disiloxane bridges[122] **72** linked between the different Cp moieties, which is illustrated in Schemes 34 and 35, respectively.

**Scheme 34**

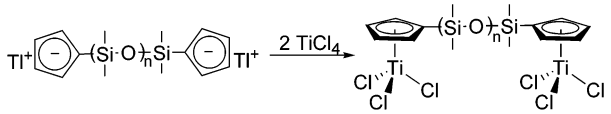

**70**: n = 1
**71**: n = 2

**Scheme 35**

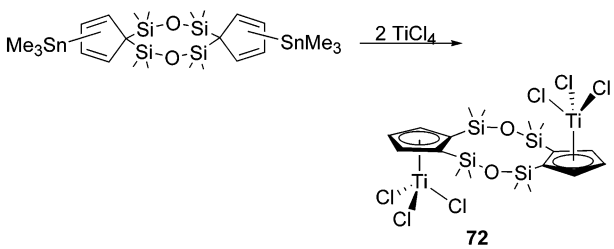

**72**

In the same year, Royo[123] and Churakov[124] independently obtained the same binuclear complex **73** with a link between the Cp moiety and titanium center according to Scheme 36.

**Scheme 36**

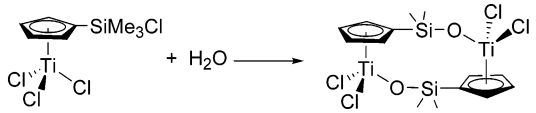

**73**

The oxo-complex $[(C_5Me_4Ph)TiCl_2]_2(\mu\text{-O})$ (**74**) was prepared by Björgvinsson et al.[125] via the hydrolysis of $(C_5Me_4Ph)TiCl_3$ in the presence of $HNEt_2$ or $Ag_2O$, which is a typical complex with a simple $\mu$-O link between two titanium centers according to Scheme 37.

**Scheme 37**

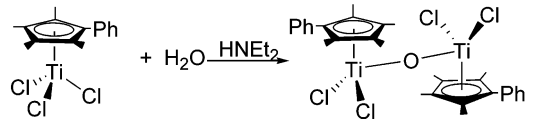

**74**

Qian et al.[126] successfully obtained the doubly $\mu$-N-linked binuclear titanocenes **75** and **76** by the reaction of $Cp'TiX_3$ with RNHLi in the presence of $Et_3N$ according to Scheme 38.

**Scheme 38**

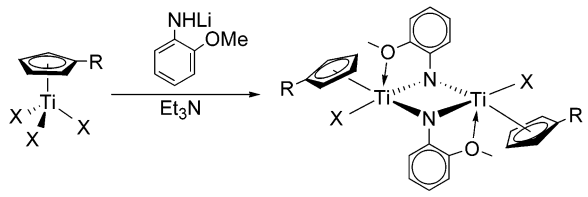

**75**: R = $BrCH_2CH_2$, X = Br
**76**: R = $CH_3OCH_2CH_2$, X = Cl

With so much flexibility, it is not surprising that numerous homonuclear bimetallic titanocenes have been synthesized in recent years; some of these are listed in Table 11, outlining the physical properties and characterization.

The first homobinuclear monoindenyl-titanium complex **77** was synthesized by the stepwise reaction of 2 equiv of $ClTi(O^iPr)_3$ and $[1,2\text{-}C_2H_4(1\text{-Ind})_2]Li_2$, giving a 1:1 *rac* and *meso* mixture of $1,2\text{-}C_2H_4[1\text{-IndTi}(O^iPr)_3]_2$, followed by an in situ chlorination reaction with $CH_3C(O)Cl$ in ethyl ether to form $1,2\text{-}C_2H_4[1\text{-IndTi}(O^iPr)Cl_2]_2$. Further reaction of 1,2-

**Table 11. Bimetallic Titanocenes**

| complex | | color, characterization, etc. |
|---|---|---|
| $[\mu\text{-}(\eta^5\text{-}C_5H_4)]_2[(\eta^5\text{-}C_5H_5)TiCl_2]_2$ | | IR, MS, EA[127] |
| $[\mu\text{-}Me_2Si(\eta^5\text{-}C_5H_4)_2][(\eta^5\text{-}C_5H_5)TiCl_2]_2$ | | crystalline, $^1$H NMR, EA[128] |
| $[\mu\text{-}(Me_2SiCH_2SiMe_2)(\eta^5\text{-}C_5H_4)_2][(\eta^5\text{-}C_5H_5)TiCl_2]_2$ | | orange microcrystal, mp (dec), $^1$H NMR, $^{13}$C NMR, $^{29}$Si NMR, EA[129] |
| $[\mu\text{-}(Me_2SiCH_2CH_2SiMe_2)(\eta^5\text{-}C_5H_4)_2][(\eta^5\text{-}C_5H_5)TiCl_2]_2$ | | orange-red microcrystal, mp (dec), $^1$H NMR, $^{13}$C NMR, $^{29}$Si NMR, EA[129] |
| $[\mu\text{-}(Me_2SiO)_nSiMe_2](\eta^5\text{-}C_5H_4)_2(TiCl_3)_2$ | | |
| $n = 1$ | **70** | pale green solid,[89] IR, $^1$H NMR, MS[121] |
| $n = 2$ | **71** | bright yellow solid, $^1$H NMR, IR, EA[121] |
| $[\mu\text{-}(Me_2SiOSiMe_2)(3\text{-}R\text{-}\eta^5\text{-}C_5H_3)_2][(\eta^5\text{-}C_5H_5)TiCl_2]_2$ | | |
| R = H | | red solid, mp, $^1$H NMR, EA,[116] MS, $^{13}$C NMR[130] |
| R = Si(CH$_3$)$_3$ | | red solid, mp, $^1$H NMR, EA[131] |
| $[\mu\text{-}(Me_2SiOSiMe_2)(\eta^5\text{-}C_5H_4)_2][(\eta^5\text{-}C_5H_4R)TiCl_2]_2$ | | red microcrystalline, $^1$H NMR, $^{13}$C NMR, MS, EA[130] |
| R = SiMe$_3$ | | |
| $[\mu\text{-}(Me_2SiO)_2SiMe_2(\eta^5\text{-}C_5H_4)_2][(\eta^5\text{-}C_5H_5)TiCl_2]_2$ | | $^1$H NMR[132] |
| $[\mu\text{-}\eta^5\text{:}\eta^5\text{-}(C_5H_3)_2(Me_2Si)_2][(\eta^5\text{-}C_5H_5)TiCl_2]_2$ (*trans*) | | pale red microcrystal, mp (dec), $^1$H NMR, $^{29}$Si NMR, EA[133] |
| $[\mu\text{-}\eta^5\text{:}\eta^5\text{-}(C_5H_3)_2(Me_2Si)_2][(\eta^5\text{-}C_5Me_5)TiCl_2]_2$ (*trans*) | | dark brown plates, mp (dec), $^1$H NMR, $^{13}$C NMR, $^{29}$Si NMR, EA, X-ray[133] |
| | | dark red crystals, mp (dec), $^1$H NMR, $^{13}$C NMR, $^{29}$Si NMR, X-ray[133] |
| $[\mu\text{-}\eta^5\text{:}\eta^5\text{-}(C_5H_3)_2(Me_2Si)_2][(\eta^5\text{-}C_5Me_5)TiCl_2]_2$ (*cis*) | | mp, $^1$H NMR, MS, EA [133] |
| $[\mu\text{-}\eta^5\text{:}\eta^5\text{-}(C_5H_3)_2(Me_2Si)_2][(\eta^5\text{-}C_5H_4SiMe_3)TiCl_2]_2$ (*trans*) | | |
| $[\mu\text{-}\eta^5\text{:}\eta^5\text{-}(C_5H_3)_2(Me_2SiOSiMe_2)_2](TiCl_3)_2$ | **72** | yellow crystalline, mp, $^1$H NMR, $^{13}$C NMR, MS[122] |
| $\{[\mu\text{-}(OSiMe_2\text{-}\eta^5\text{-}C_5H_4)]TiCl_2\}_2$ | **73** | pale yellow microcrystalline, $^1$H NMR, $^{13}$C NMR, MS, EA,[130] X-ray[130, 124] |
| $\{\mu\text{-}[\eta^5\text{-}C_5H_4(\eta^5\text{-}OSiMeCl)]TiCl_2\}_2$ | | yellow microcrystalline, $^1$H NMR, $^{13}$C NMR, EA[134a] |
| $[(TiCl_2)_2(\mu^2\text{-}O)\text{-}(\eta^5\text{-}C_5H_4)_2\text{-}\mu^2\text{-}(SiMe_2O)_nSiMe_2]$ | | |
| $n = 1$ | | bright yellow, $^1$H NMR, IR, EA[121] |
| $n = 2$ | | yellow solid, $^1$H NMR, IR, EA[121] |
| $[Ti(\eta^5\text{-}C_5H_4SiMe_2Cl)Cl_2]_2(\mu\text{-}O)$ | | yellow solid, $^1$H NMR, $^{13}$C NMR, MS, EA[130] |
| $[Ti(\eta^5\text{-}C_5H_4CH_2C_6H_5)Cl_2]_2(\mu\text{-}O)$ | | yellow solid, MS, EA[45] |
| $[Ti(\eta^5\text{-}C_5Me_4C_6H_5)Cl_2]_2(\mu\text{-}O)$ | **74** | red solid, $^1$H NMR, $^{13}$C NMR, MS, EA, X-ray[125] |
| $[(\mu\text{-}NC_6H_4OMe\text{-}2)(\eta^5\text{-}C_5H_4R)Ti(X)]_2$ | | |
| R = BrCH$_2$CH$_2$, X = Br | **75** | dark red crystals, mp, $^1$H NMR, IR, MS, EA, X-ray[126] |
| R = CH$_3$OCH$_2$CH$_2$, X = Cl | **76** | dark red crystals, mp, $^1$H NMR, IR, MS, EA[126] |
| $[(\mu\text{-}NC_6H_4NMe_2\text{-}2)(\eta^5\text{-}C_5H_5)Ti(Cl)]_2$ | | dark red solid, mp, $^1$H NMR, IR, MS, EA[126] |
| $[(\mu\text{-}NC_6H_4R^2\text{-}2)(\eta^5\text{-}C_5H_4R^1)Ti(X)]_2$ | | |
| $R^1$ = BrCH$_2$CH$_2$, $R^2$ = H, X = BR | | dark red crystals, mp, $^1$H NMR, IR, MS, EA[126] |
| $R^1$ = CH$_3$OCH$_2$CH$_2$, $R^2$ = H, X = Cl | | dark red crystals, mp, $^1$H NMR, IR, MS, EA[126] |
| $R^1$ = H, $R^2$ = CH$_3$, X = Cl | | dark red crystals, mp, $^1$H NMR, IR, MS, EA[126] |
| $R^1$ = CH$_3$OCH$_2$CH$_2$, $R^2$ = CH$_3$, X = Cl | | dark red crystals, mp, $^1$H NMR, IR, MS, EA[126] |
| $[(\mu\text{-}NC_6H_4Me_2\text{-}2,6)(\eta^5\text{-}C_5H_5)Ti(Cl)]_2$ | | dark red solid, mp, $^1$H NMR, IR, MS, EA[126] |
| $[(\mu\text{-}NPy\text{-}2)(\eta^5\text{-}C_5H_4R)Ti(X)]_2$ | | |
| R = H, X = Cl | | red crystals, mp, $^1$H NMR, IR, MS, EA[126] |
| R = CH$_3$OCH$_2$CH$_2$, X = Cl | | red crystals, mp, $^1$H NMR, IR, MS, EA[126] |
| R = BrCH$_2$CH$_2$, X = Br | | red crystals, mp, $^1$H NMR, IR, MS, EA[126] |
| $\mu$-PhB$[(\eta^5\text{-}C_5H_4)TiCl_3]_2$ | | yellow green, $^1$H NMR, $^{13}$C NMR, EA, X-ray[134b] |
| 1,2-$[(1\text{-}\eta^5\text{-}C_9H_6)TiCl_3]_2(CH_2CH_2)$ | **77** | purple-black solid, $^1$H NMR, EA[135] |
| $\mu\text{-}(CH_2)_n[(\eta^5\text{:}\eta^1\text{-}C_9H_5SiMe_2NCMe_3)TiCl_2]_2$ | | |
| $n = 6$ | | reddish brown solid, $^1$H NMR, $^{13}$C NMR, HRMS[357] |
| $n = 9$ | | reddish brown solid, $^1$H NMR, $^{13}$C NMR, HRMS[357] |
| $n = 12$ | | reddish brown solid, $^1$H NMR, $^{13}$C NMR, HRMS[357] |
| $\mu\text{-}Me_2Si[(\eta^5\text{-}C_5H_4)(\eta^5\text{-}C_5H_5)ZrCl_2][(\eta^5\text{-}C_5H_4)(\eta^5\text{-}C_5H_5)TiCl_2]$ | **78** | red crystals, $^1$H NMR, EA[136a] |
| $\mu\text{-}Me_2Si[(\eta^5\text{-}C_5H_4)(\eta^5\text{-}C_5H_5)ZrCl_2][(\eta^5\text{-}C_5H_4)(\eta^5\text{-}C_5H_4)TiCl_2]$ | **79** | red solid, $^1$H NMR, IR, MS, EA[136b] |

$C_2H_4[1\text{-}IndTi(O^iPr)Cl_2]_2$ with $CH_3C(O)Cl$ in $CH_2Cl_2$ afforded $1,2\text{-}C_2H_4[1\text{-}IndTiCl_3]$ (**77**), and the entire reaction pathway is represented in Scheme 39.[135]

Many papers have focused on the heteronuclear bimetallic complexes. Nifant'ev[136a] reported the heteronuclear bimetallic complex $\mu\text{-}Me_2Si[(\eta^5\text{-}C_5H_4)(\eta^5\text{-}C_5H_5)ZrCl_2]$ $[(\eta^5\text{-}C_5H_4)(\eta^5\text{-}C_5H_5)TiCl_2]$ (**78**) with one $Me_2Si$ bridge linked between different Cp moieties. More recently, Qian et al.[136b] successfully obtained the heteronuclear bimetallic titanocene with the substituent on the Cp ring, such as $\mu\text{-}Me_2Si[(\eta^5\text{-}C_5H_4)(\eta^5\text{-}C_5H_5)ZrCl_2]$ $[(\eta^5\text{-}C_5H_4)(\eta^5\text{-}PhCH_2C_5H_4)TiCl_2]$ (**79**).

**Scheme 39**

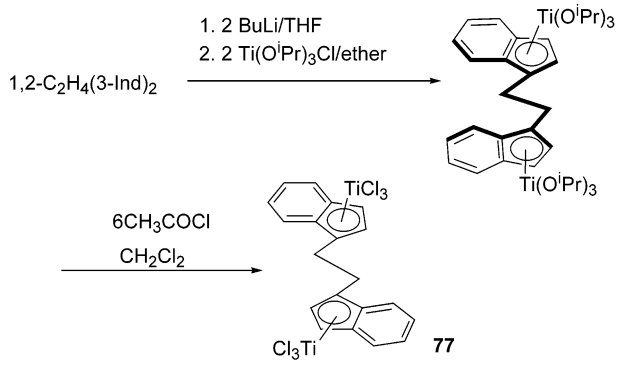

## B. Mono-Cp(Ind) Titanium Complexes

### *1. Mono-Cp(Ind) Titanium Complexes Containing Pendant Alkyl and Alkenyl Side Chains*

Substituted Cp and Ind complexes [R-Cp(Ind)]$TiCl_3$ (R = alkenyl, amino, or alkoxo substituent) are generally prepared by reacting the substituted ligands with an organolithium compound (mostly BuLi) followed by chlorotrimethylsilane in $CH_2Cl_2$ to obtain the trimethylsilyl derivatives, which are highly reactive for transmetalation with metal halides ($TiX_4$). Thus, a series of 1-(alkyl)indenyltrichlorotitanium (alkyl = H, Me, Et, *tert*-butyl, $Me_3Si$, *n*-propyl, *n*-butyl) and 2-(methyl)indenyltrichlorotitanium were synthesized.[137,138] To investigate the effects the numbers and relative positions of ring substituents with different electronic and steric factors have on catalytic activity, exhaustive studies were carried out by Chien and Rausch employing multimethylated indenes (Scheme 40).[138,139]

**Scheme 40**

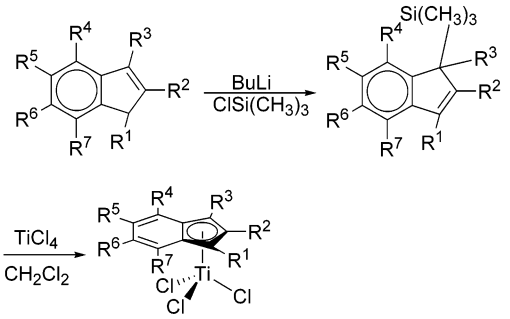


**80**: $R^1 = CH_3$, $R^{2-7} = H$
**81**: $R^1 = CH_2CH_3$, $R^{2-7} = H$
**82**: $R^1 = C(CH_3)_3$, $R^{2-7} = H$
**83**: $R^1 = CH(CH_3)_2$, $R^{2-7} = H$
**84**: $R^1 = (CH_2)_2CH_3$, $R^{2-7} = H$
**85**: $R^1 = (CH_2)_3CH_3$, $R^{2-7} = H$
**86**: $R^1 = H$, $R^2 = CH_3$, $R^{3-7} = H$
**87**: $R^{1,2} = CH_3$; $R^{3-7} = H$
**88**: $R^{1,3} = CH_3$; $R^{2,4-7} = H$
**89**: $R^{1-3} = CH_3$; $R^{4-7} = H$
**90**: $R^{1,3,4,7} = CH_3$; $R^{2,5,6} = H$
**91**: $R^{4-7} = CH_3$; $R^{1-3} = H$
**92**: $R^{1,2,4-7} = CH_3$; $R^3 = H$
**93**: $R^{1-7} = CH_3$

The alkenyl-substituted indenyltrichlorotitanium complexes were similarly obtained (Scheme 41).[138]

Trialkyltinhalides ($R_3SnX$; R = alkyl, X = halide) have also been employed as effective transmetalation alternatives when the trimethylsilyl intermediate failed to yield the required results or when yields were too low. Morris et al.[140] have used the technique with great success (Scheme 42).

**Scheme 41**

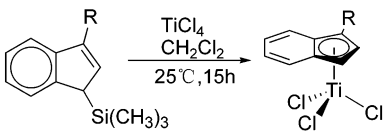


**94**: R = ($CH_2$=$CHCH_2$)
**95**: R = ($CH_2$=$CHCH_2CH_2$)

**Scheme 42**

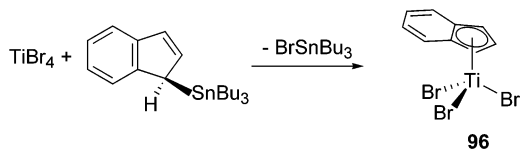


**96**

The structure of **96** has been determined by X-ray analysis and is characterized by the well-established (distorted) piano-stool structure (Figure 19).

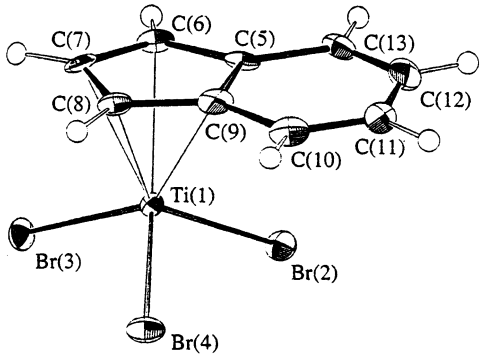


**Figure 19.** Structure of ($\eta^5$-$C_9H_7$)$TiBr_3$ (**96**) in the crystal.[140] (Reprinted with permission from ref 140. Copyright 1999 Elsevier Sequoia.)

To study the effects of changing the chloride atoms in the half-sandwich titanocene to the more reactive fluoride atoms, Xu and Ruckenstein[141] have synthesized a series of fluorinated indenyl titanium complexes, obtained from the corresponding chloride species using $Me_3SnF$ as fluorinating agent (Scheme 43). A similar procedure was earlier used by Roesky et al. to obtain an *n*-propyltetramethyl-substituted cyclopentadienyl titanium trifluoride complex.[142]

**Scheme 43**

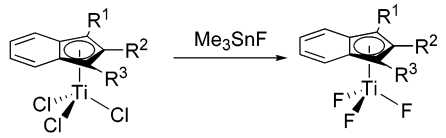


**97**: $R^1 = R^2 = R^3 = H$
**98**: $R^1 = Me$, $R^2 = R^3 = H$
**99**: $R^1 = Et$, $R^2 = R^3 = H$
**100**: $R^1 = {}^tBu$, $R^2 = R^3 = H$
**101**: $R^1 = Me_3Si$, $R^2 = R^3 = H$
**102**: $R^1 = {}^iPr$, $R^2 = R^3 = H$
**103**: $R^2 = H$, $R^1 = R^3 = Me$
**104**: $R^1 = Ph$, $R^2 = R^3 = H$
**105**: $R^2 = H$, $R^1 = R^3 = Ph$

Table 12 presents a list of the properties, references, and characterization of recently reported complexes bearing alkyl and alkenyl side groups.

### *2. Mono-Cp(Ind) Titanium Complexes Containing Functional Alkoxyl Side Chains*

Qian et al. synthesized and elucidated by X-ray the structure of the first intramolecularly coordinated methoxyethyltitanium complex **106**, Scheme 44.[46,48]

Over the years many alkoxyl functionalized titanocenes have been synthesized by this group. A typical example is presented in Chart 7 to illustrate the general structural features of these complexes.

Borrowing Pearson's formalism of hard and soft acids and bases (HSAB), it could be observed that the crystal structures of **106**, **107**, and **110** (Figures 20−22) illustrate a typical case of intramolecular coordination between a hard donor group (pendant

**Table 12. Half-Sandwich Complexes Bearing Alkyl and Alkenyl Side Groups**

| complex | | color, characterization, etc. |
|---|---|---|
| ($\eta^5$-$C_5H_4{}^t$Bu)$TiCl_3$ | | orange solid, mp, $^1$H NMR, $^{13}$C NMR, EA, X-ray[43] |
| (1,3-$R^1_2$-2-$R^2$-$\eta^5$-$C_5H_2$)$TiCl_3$ | | |
| $R^1$ = Me, $R^2$ = Bu | | yellowish red solid, $^1$H NMR, $^{13}$C NMR, HRMS, EA[31] |
| $R^1$ = Me, $R^2$ = $^t$Bu | | red solid, $^1$H NMR, $^{13}$C NMR, HRMS[31] |
| ($\eta^5$-$C_5Me_4CH_2CH_2CH{=}CH_2$)$TiCl_3$ | | red solid, mp, $^1$H NMR, $^{13}$C NMR,[35,36] EI-MS, IR,[36] EA[35, 36] |
| (1-$CH_2{=}CH(CH_2)_n$-$\eta^5$-$C_9H_6$)$TiCl_3$ | | |
| $n$ = 1 | | crystal, $^1$H NMR, $^{13}$C NMR[356] |
| $n$ = 2 | | crystal, $^1$H NMR, $^{13}$C NMR[356] |
| $n$ = 3 | | crystal, $^1$H NMR, $^{13}$C NMR[356] |
| (1-R-$\eta^5$-$C_9H_6$)$TiCl_3$ | | |
| R = $CH_3$ | **80** | dark red crystals, mp, IR, UV,[139] $^1$H NMR,[137,139] $^{13}$C{$^1$H} NMR,[139] EA,[137,139] MS[139] |
| | | dark red crystals, mp, IR, UV,[139] $^1$H NMR,[137,139] $^{13}$C{$^1$H} NMR,[139] EA,[137,139] MS[139] |
| R = $CH_2CH_3$ | **81** | dark red crystals, $^1$H NMR, EA[137] |
| | | dark red crystals, $^1$H NMR, EA[137] |
| R = $C(CH_3)_3$ | **82** | dark red crystals, mp, IR, UV, $^1$H NMR, $^{13}$C{$^1$H} NMR, EA, MS[139] |
| R = $Si(CH_3)_3$ | | dark red crystals, $^1$H NMR, EA[138] |
| R = $CH(CH_3)_2$ | **83** | dark red crystals, $^1$H NMR, EA[138] |
| | | dark red crystals, $^1$H NMR, EA[138] |
| R = $CH_2CH_2CH_3$ | **84** | dark red crystals, $^1$H NMR, EA[138] |
| R = $CH_2CH_2CH_2CH_3$ | **85** | |
| R = $CH_2CH{=}CH_2$ | **94** | |
| R = $CH_2CH_2CH{=}CH_2$ | **95** | |
| (2-Me-$\eta^5$-$C_9H_6$)$TiCl_3$ | **86** | dark red crystals, $^1$H NMR, EA[137] |
| (2-$CH_3CH_2CH_2$-$\eta^5$-$C_9H_6$)$TiCl_3$ | | crystal, $^1$H NMR, $^{13}$C NMR[356] |
| (2-$CH_2{=}CH(CH_2)_n$-$\eta^5$-$C_9H_6$)$TiCl_3$ | | |
| $n$ = 1 | | crystal, $^1$H NMR, $^{13}$C NMR[356] |
| $n$ = 2 | | crystal, $^1$H NMR, $^{13}$C NMR[356] |
| $n$ = 3 | | crystal, $^1$H NMR, $^{13}$C NMR[356] |
| ($\eta^5$-$C_9H_{11}$)$TiCl_3$ | | orange crystals, $^1$H NMR, EA[137] |
| (1-$R^1$-2-$R^2$-3-$R^3$-4-$R^4$-5-$R^5$-6-$R^6$-7-$R^7$-$\eta^5$-$C_9$)$TiCl_3$ | | |
| $R^{1,2}$ = $CH_3$; $R^{3-7}$ = H | **87** | burgundy crystals, $^1$H NMR,$^{13}$C NMR, EA[138] |
| $R^{1,3}$ = $CH_3$; $R^{2,4-7}$ = H | **88** | burgundy crystals, mp, $^1$H NMR,[137,139] $^{13}$C{$^1$H} NMR,[139] IR, UV,[139] EA,[137,139] MS[139] |
| | | purple crystals,$^1$H NMR,$^{13}$C NMR, EA[138] |
| $R^{1-3}$ = $CH_3$; $R^{4-7}$ = H | **89** | purple crystals,$^1$H NMR, EA[138] |
| $R^{1,3,4,7}$ = $CH_3$; $R^{2,5,6}$ = H | **90** | purple crystals,$^1$H NMR, EA[138] |
| $R^{4-7}$ = $CH_3$; $R^{1-3}$ = H | **91** | purple crystals,$^1$H NMR,EA[138] |
| $R^{1,2,4-7}$ = $CH_3$; $R^3$ = H | **92** | green crystals,$^1$H NMR,EA[138] |
| $R^{1-7}$ = $CH_3$ | **93** | |
| ($\eta^5$-$C_9H_7$)$TiBr_3$ | **96** | dark red crystals, mp, IR, $^1$H NMR, $^{13}$C NMR, EA, X-ray[140] |
| ($\eta^5$-$C_5Me_4{}^n$Pr)$TiF_3$ | | yellow-orange solid, mp, $^1$H NMR, $^{19}$F NMR, IR, EA, MS[142] |
| (1-$R^1$-2-$R^2$-3-$R^3$-$\eta^5$-$C_9H_4$)$TiF_3$ | | |
| $R^1$ = $R^2$ = $R^3$ = H | **97** | orange-yellow solid, $^1$H NMR, $^{19}$F NMR, EA, MS[141] |
| $R^1$ = Me, $R^2$ = $R^3$ = H | **98** | orange-yellow, $^1$H NMR, $^{19}$F NMR, EA, MS[141] |
| $R^1$ = Et, $R^2$ = $R^3$ = H | **99** | $^1$H NMR, $^{19}$F NMR, EA, MS[141] |
| $R^1$ = $^t$Bu, $R^2$ = $R^3$ = H | **100** | $^1$H NMR, $^{19}$F NMR, EA, MS[141] |
| $R^1$ = $Me_3Si$, $R^2$ = $R^3$ = H | **101** | orange yellow solid, $^1$H NMR, $^{19}$F NMR, EA, MS[141] |
| $R^1$ = $^i$Pr, $R^2$ = $R^3$ = H | **102** | $^1$H NMR, $^{19}$F NMR, EA, MS[141] |
| $R^2$ = H, $R^1$ = $R^3$ = Me | **103** | $^1$H NMR, $^{19}$F NMR, EA, MS[141] |
| $R^1$ = Ph, $R^2$ = $R^3$ = H | **104** | $^1$H NMR, $^{19}$F NMR, EA, MS[141] |
| $R^2$ = H, $R^1$ = $R^3$ = Ph | **105** | dark green crystals, $^1$H NMR, $^{19}$F NMR, EA, MS[141] |

**Scheme 44**

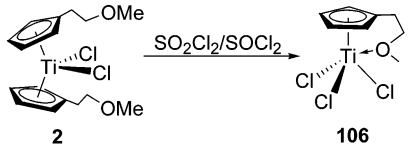


**2** **106**

oxygen atom) and an unsaturated hard titanium metal center.

Although an attempt to obtain a suitable single crystal of **108** and **109** for X-ray diffraction was unsuccessful, we can firmly conclude from the IR spectra of the C−O−C bond from Table 13 that, in contrast to the other three cases, these two show no intramolecular Ti−O coordination, because as a result of the intramolecular coordination of Ti−O the

**Chart 7**

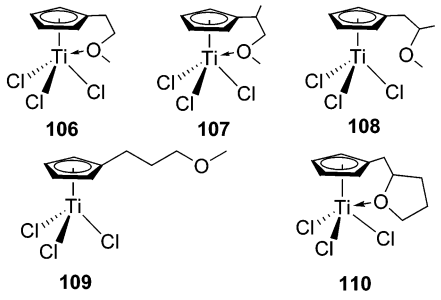


**106** **107** **108**

**109** **110**

stretching vibration frequencies of the C−O bonds in **106**, **107**, and **110** have been observed to decrease by ∼60−100 cm$^{-1}$ when compared to those of the corresponding ligands. Therefore, this is used in

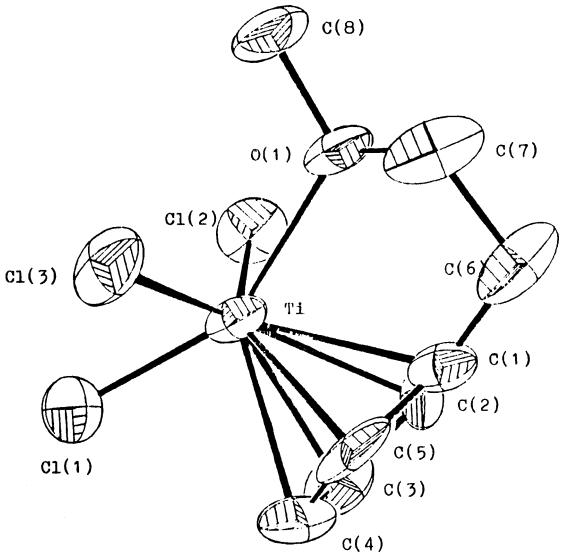


**Figure 20.** Structure of ($\eta^5$-$C_5H_4CH_2CH_2OCH_3$)$TiCl_3$ (**106**) in the crystal.[26]

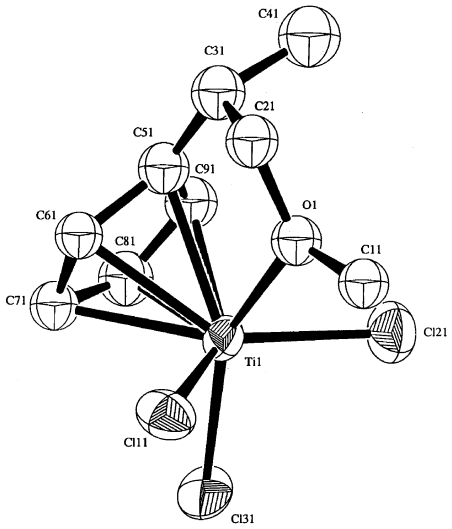


**Figure 21.** Structure of [$\eta^5$-$C_5H_4CH(CH_3)CH_2OCH_3$]$TiCl_3$ (**107**) in the crystal.[26]

combination with other structural considerations as a standard for detecting the presence of such coordination. Hence, it could be observed that in **108** and **109**, the stretching vibration frequencies of the C−O bond are almost unchanged from those of the ligands

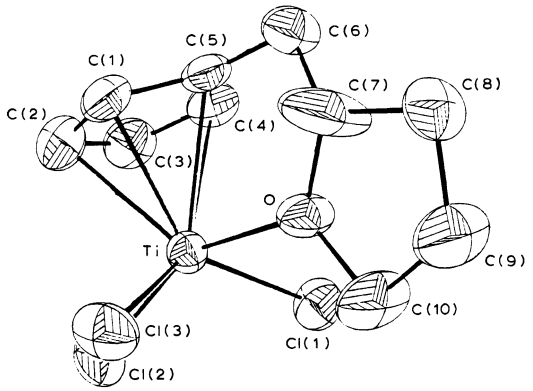


**Figure 22.** Structure of [$\eta^5$-$C_5H_4CH_2$(2-$C_4H_7O$)]$TiCl_3$ (**110**) in the crystal.[26]

and the slight variations may be rationalized on the basis of ligand geometry and steric effects. In addition, it seems that in **108** the presence of a methyl group bonded to a carbon atom next to the oxygen atom inhibits the formation of a Ti−O coordination bond, whereas in **109** the extra $-CH_2-$ unit in the spacer unit has directed the −O− atom too far away for any interaction to occur.

Recently, van der Zeijden et al.[143] also investigated the intramolecular coordination of **106** by using a temperature-dependent NMR technique. They found that the coordination of the ethereal oxygen atom in the side chain of the complex is fluxional, ∼30% in $CD_2Cl_2$ at room temperature, and for the bulkier substituents this figure is significantly lower.

Due to the open nature of the coordination environment around mono-Cp Ti complexes, thermocyclization often takes place between Ti−Cl and O−$CH_3$ in ($\eta^5$-$C_5H_4ROR'$)$TiCl_3$ complexes; for example, **111** yields a more stable titanoxacycle complex **112**, Scheme 45.[26,45]

**Scheme 45**

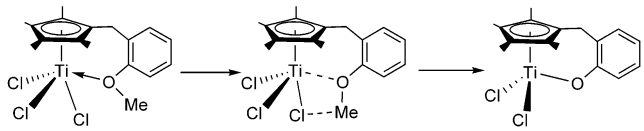


**111** **112**

Rau et al.[144] successfully obtained a similar complex, **113**, by a one-pot procedure, Scheme 46. An

**Table 13. Spectral Data of the C−O−C Bond and Ti−O Lengths**

| compound | | $\nu$(C−O−C) ($cm^{-1}$) | Ti−O (Å) |
|---|---|---|---|
| $CH_3OCH_2CH_2C_5H_4SiMe_3$ | | 1120 s | |
| ($\eta^5$-$C_5H_4CH_2CH_2OCH_3$)$_2TiCl_2$ | | 1100 s | |
| ($\eta^5$-$C_5H_4CH_2CH_2OCH_3$)$TiCl_3$ | **106** | 1035 s | 2.217−2.211 |
| $CH_3OCH_2CH(CH_3)C_5H_4SiMe_3$ | | 1100 s | |
| [$\eta^5$-$C_5H_4CH(CH_3)CH_2OCH_3$]$_2TiCl_2$ | | 1100 s | |
| [$\eta^5$-$C_5H_4CH(CH_3)CH_2OCH_3$]$TiCl_3$ | **107** | 1040 s | 2.22−2.26 |
| $CH_3OCH(CH_3)CH_2C_5H_4SiMe_3$ | | 1100 s | |
| [($\eta^5$-$C_5H_4CH_2CH(CH_3)OCH_3$)]$_2TiCl_2$ | | 1100 s | |
| [$\eta^5$-$C_5H_4CH_2CH(CH_3)OCH_3$]$TiCl_3$ | **108** | 1100 s | |
| $CH_3OCH_2CH_2CH_2C_5H_4SiMe_3$ | | 1100 s | |
| ($\eta^5$-$C_5H_4CH_2CH_2CH_2OCH_3$)$_2TiCl_2$ | | 1118 s | |
| ($\eta^5$-$C_5H_4CH_2CH_2CH_2OCH_3$)($\eta^5$-$C_5H_5$)$TiCl_2$ | | 1125 s | |
| ($\eta^5$-$C_5H_4CH_2CH_2CH_2OCH_3$)$TiCl_3$ | **109** | 1100 m | |
| (2-$C_4H_7O$)$CH_2C_5H_4SiMe_3$ | | 1065 s | |
| [$\eta^5$-$C_5H_4CH_2$(2-$C_4H_7O$)]$_2TiCl_2$ | | 1060 s | |
| [$\eta^5$-$C_5H_4CH_2$(2-$C_4H_7O$)]$TiCl_3$ | **110** | 960 s | 2.615 |

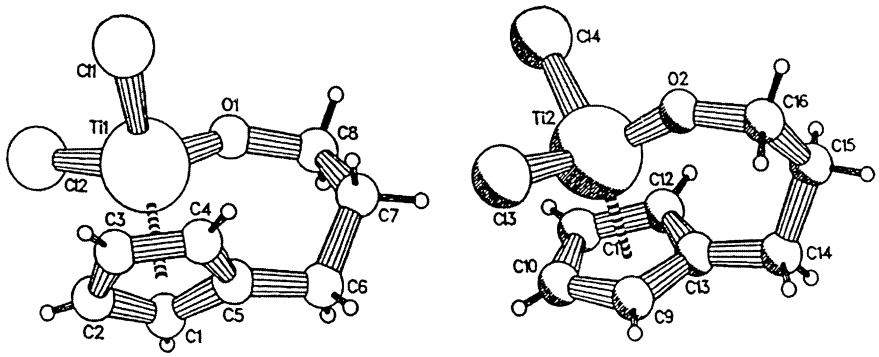


**Figure 23.** PLUTO drawing of $[\eta^5:\eta^1\text{-}C_5H_4(CH_2)_3O]TiCl_2$ (**115**).[146] (Reprinted with permission from ref 146. Copyright 1996 Elsevier Sequoia.)

**Scheme 46**

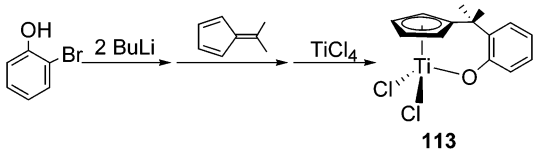


**113**

atypical procedure starting from a metallocene is a common method of obtaining half-metallocenes characterized by intramolecular coordination[48] (Scheme 47) or cyclization[145] (Scheme 48).

**Scheme 47**

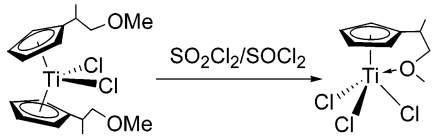


**107**

**Scheme 48**

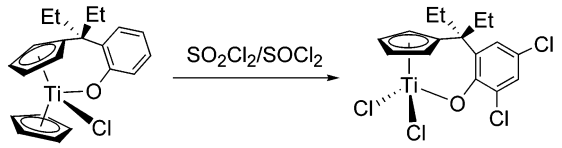


**4** **114**

An effective single-step procedure to cyclopentadienyl-alkoxy titanium complex **115** involves simultaneous double substitution using a bis(trimethylsilyl) ligand ($Me_3SiC_5H_4CH_2CH_2CH_2OSiMe_3$), Scheme 49.[146]

**Scheme 49**

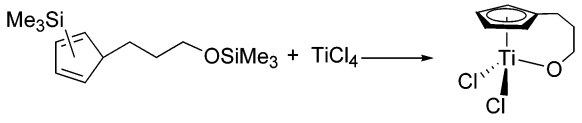


**115**

In the molecular structure of the complex $[\eta^5:\eta^1\text{-}C_5H_4(CH_2)_3O]TiCl_2$ (**115**), which is indicated in Figure 23, in the asymmetric unit there are two crystallographically independent molecules as forms 1 and 2. To the structure of complex **116**, it shows that $[[\eta^5:\eta^1\text{-}C_5H_4(CH_2)_2O]TiCl_2]_2$ in Figure 24 is a dimeric form with bridged oxygen atoms acting as a normal

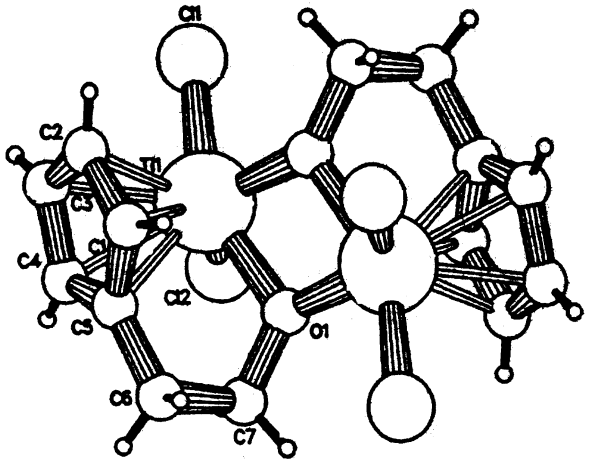


**Figure 24.** PLUTO drawing of $[[\eta^5:\eta^1\text{-}C_5H_4(CH_2)_2O]TiCl_2]_2$ (**116**).[146] (Reprinted with permission from ref 146. Copyright 1996 Elsevier Sequoia.)

alkoxy−Ti bond [Ti(1)−O(1)a, 1.9472(17) Å] and one coordinate O→Ti bond [Ti(1)−O(1), 2.0726(17) Å]. Two Ti−O−Ti bridges in complex **116** form a nonsymmetric quadrangle in the center of the molecular.

Because the open molecular structure of the alkoxy functionalized half-titanocenes in addition to being capable of demonstrating novel structural patterns also allows the incorporation of a large variety of monomers, many researchers have prepared them by employing commonly used metathetical procedures with the aim of developing highly active catalysts for the polymerization of styrenic monomers and the copolymerization of ethylene with larger α-olefins.

Thus, Whitby et al.[147] reported the bifunctional half-sandwich titanium complex **117**, Scheme 50.

**Scheme 50**

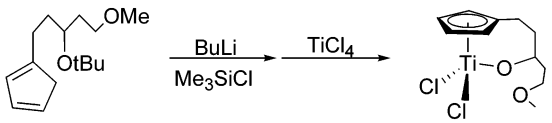


**117**

Similarly, the corresponding indenyl titanoxacyclic complexes have been obtained by reacting a trimethylsilyl-substituted indene with $TiCl_4$; in an unprecedented finding the authors also obtained the

bidentate oxacyclic compounds (**118**−**120**) directly from the lithium salt of the ligand and an excess of $TiCl_4$ (Scheme 51), evidenced by single-crystal X-ray

**Scheme 51**

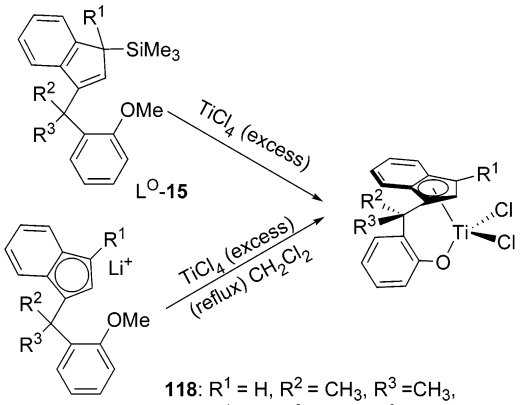


diffraction analysis (Figure 25). They found that the Me−O bonds in $[\eta^5\text{-}C_9H_6C(R^2)(R^3)\text{-}o\text{-}C_6H_4OMe]TiCl_3$ are sensitive to heat and Lewis acid conditions such as treatment with $BBr_3$ and sequentially formed an intramolecular cyclic structure through the elimination of $CH_3Cl$ or $CH_3Br$.[148]

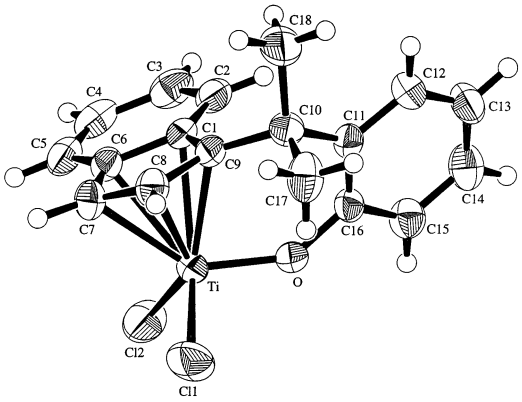


**Figure 25.** Structure of $[\eta^5\text{:}\eta^1\text{-}C_9H_6C(CH_3)_2(C_6H_4\text{-}2\text{-}O)]TiCl_2$ (**118**) in the crystal.[148]

Rausch et al.[149] also synthesized a variety of methoxy-substituted indenyl trichlorotitanium complexes **121** and **122** (Schemes 52 and 53).

**Scheme 52**

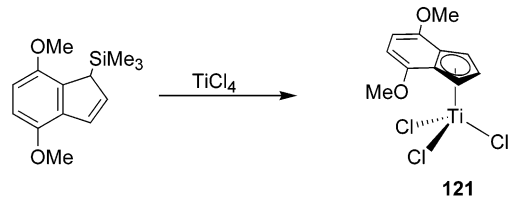


**Scheme 53**

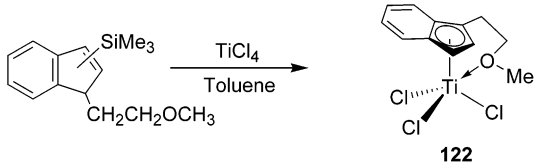


In addition, Zhou et al.[150] also reported the synthesis of the siloxy-substituted indenyl trichlorotitanium complex **123** (Scheme 54).

**Scheme 54**

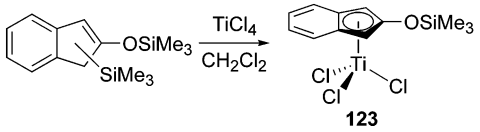


Recently reported new half-sandwich titanium complexes that contain an alkoxyl atom in the side chain are listed in Table 14.

### *3. Mono-Cp(Ind) Titanium Complexes Containing Functional Dialkylamino Side Chains, Including Those with Constrained Geometry*

**a. Mono-Cp(Ind) Titanium Complexes Containing a Dialkylamino Side Group.** The following discussion briefly outlines the various routes to mono-Cp titanium compounds bearing $NR_2$ ring substitutions from the corresponding ligands and titanium halides.

The treatment of $Me_3SiC_5H_4CH_2CH_2NMe_2$ or $Me_3SiC_5Me_4CH_2CH_2NMe_2$ with $TiCl_4$ in $CH_2Cl_2$ or toluene yielded the corresponding $C_5H_4CH_2CH_2NMe_2TiCl_3$ (**14**) and $C_5Me_4CH_2CH_2NMe_2TiCl_3$ (**125**) complexes.[60,153,154]

Reacting $TiCl_4$ with $(C_5H_4CH_2CH_2N^iPr_2)Li$ easily forms a coordination polymer $(C_5H_4CH_2CH_2N^iPr_2)TiCl_3$ (**124**) unit, which is highly sensitive to moisture (Scheme 55).[155] Its monomeric hydrochloride $[(C_5H_4CH_2CH_2N(H)^iPr_2)TiCl_3]^+Cl^-$ (**126**), that shows excellent solubility in polar solvents, was obtained by treatment with 1 equiv of HCl via protonation of the amino group.

Herrmann[156] synthesized the dialkylaminocyclopentadienyl complexes **127** and **128**, which contain pyrrolidine(N) and piperidine(N) functions as $\sigma$-donating pendant groups from their silylated cyclopentadiene precursor compound and $TiCl_4$ (Scheme 56).

Enders and co-workers[157,158] succeeded in the synthesis of 8-quinolylcyclopentadienyl trichlorotitanium (**129** and **130**) from the trimethylsilyl derivative in toluene (Scheme 57).

The reaction of trimethylsilyl ligand with $TiCl_4$ in $CH_2Cl_2$ (or toluene, but not in THF) affords the complex **131** in a moderate yield.[159] The yellow titanium compound is much more air-sensitive than the parent unsubstituted compound $CpTiCl_3$ (Scheme 58).

Trialkyltinhalides ($R_3SnX$; R = alkyl, X = halide) have also been employed as good leaving groups, especially when the trimethylsilyl intermediate failed to yield the required results or when yields are too low. Chien et al.[154] has employed the technique to prepare dialkylamino functionalized complex **132** (Scheme 59).

$^1H$ NMR spectral analysis is a versatile tool for establishing coordination of chelating pendant ligand (amino-) to the central Ti metal. For example (see Table 15), it has been established that in the $^1H$ NMR spectra for $\eta^5\text{-}C_5H_4CH_2CH_2NMe_2TiCl_3$ (**14**) there is

**Table 14. Half-Sandwich Titanium Complexes Containing an Oxygen Atom in the Side Chain**

| complex | | color, characterization, etc. |
|---|---|---|
| ($\eta^5$-$C_5H_4CH_2CH_2OMe$)$TiCl_3$ | **106** | orange crystals,[46,149] mp, $^1$H NMR, MS, IR, EA,[46] X-ray[46,26] |
| [$\eta^5$-$C_5H_4CH(CH_3)CH_2OMe$]$TiCl_3$ | **107** | IR, X-ray[48] |
| [$\eta^5$-$C_5H_4CH_2CH(CH_3)OMe$]$TiCl_3$ | **108** | IR[48] |
| ($\eta^5$-$C_5H_4CH_2CH_2CH_2OMe$)$TiCl_3$ | **109** | yellow oil, $^1$H NMR, $^{13}$C NMR, IR[147] |
| [$\eta^5$-$C_5H_4CH_2$(2-$C_4H_7O$)]$TiCl_3$ | **110** | orange crystals, mp, $^1$H NMR, MS, IR, EA, X-ray[151] |
| ($\eta^5$-$C_5H_4CH_2CH_2OR$)$TiCl_3$ | | |
| R = menthyl | | brown oil, $^1$H NMR, $^{13}$C NMR[143] |
| R = fenchyl | | $^1$H NMR, $^{13}$C NMR[143] |
| [$\eta^5$-$C_5H_4CMe_2$(2-MeO-$C_6H_4$)]$TiCl_3$ | | deep red solid, $^1$H NMR, MS[144] |
| [$\eta^5$-$C_5Me_4CH_2$(2-MeO-$C_6H_4$)]$TiCl_3$ | | $^1$H NMR[26] |
| ($\eta^5$-$C_5Me_4OSiMe_3$)$TiCl_3$ | | red needle crystals, $^1$H NMR, MS, EA[150] |
| ($\eta^5$-$C_5H_4OSiMe_2{}^t$Bu)$TiCl_3$ | | red crystals, mp, $^1$H NMR, $^{13}$C NMR, EA[47] |
| [$\eta^5$-$C_5Me_4CH_2$(2-MeO-$C_6H_4$)]$TiCl_3$ | **111** | ref 26 |
| [$\eta^5$:$\eta^1$-$C_5Me_4CH_2$($C_6H_4$-2-O)]$TiCl_2$ | **112** | X-ray[26] |
| [$\eta^5$:$\eta^1$-$C_5Me_4CH_2$($C_6H_4$-2-O)]$TiBr_2$ | | ref 26 |
| [$\eta^5$:$\eta^1$-$C_5H_4C$(Ph)H($C_6H_4$-2-O)]$TiCl_2$ | | yellow crystals, X-ray[152] |
| [$\eta^5$:$\eta^1$-$C_5H_4CMe_2$($C_6H_4$-2-O)]$TiCl_2$ | **113** | orange crystals, $^1$H NMR, $^{13}$C NMR, MS, EA[144] |
| [$\eta^5$:$\eta^1$-$C_5H_4CEt_2$(3,5-$Cl_2$-$C_6H_2$-2-O)]$TiCl_2$ | **114** | orange crystals, mp, $^1$H NMR, $^{13}$C NMR, IR, MS, EA, X-ray[145] |
| [$\eta^5$:$\eta^1$-$C_5H_4(CH_2)_3O$]$TiCl_2$ | **115** | yellow-green crystals, $^1$H NMR, $^{13}$C NMR, MS, IR, EA, X-ray[146] |
| [{$\eta^5$:$\eta^1$-$C_5H_4(CH_2)_2O$}$TiCl_2$]$_2$ | **116** | orange-red crystals, mp, $^1$H NMR, $^{13}$C NMR, MS, IR, EA, X-ray[146] |
| [$\eta^5$:$\eta^1$-$C_5H_4CH_2CH_2CR^1R^2O$]$TiCl_2$ | | |
| $R^1$ = Me, $R^2$ = H | | yellow solid, mp, $^1$H NMR, $^{13}$C NMR, MS, IR, EA[147] |
| $R^1$ = $R^2$ = Me | | mp, $^1$H NMR, $^{13}$C NMR, MS, IR, EA[147] |
| [$\eta^5$:$\eta^1$-$C_5H_4CH(CH_2CH{=}CH_2)(CH_2)_2O$]$TiCl_2$ | | yellow solid, mp, $^1$H NMR, $^{13}$C NMR, MS, EA[147] |
| [$\eta^5$:$\eta^1$-$C_5H_4CH_2CH_2CH(CH_2CH_2OMe)O$]$TiCl_2$ | **117** | yellow crystalline solid, mp, $^1$H NMR, $^{13}$C NMR, IR, MS, X-ray[147] |
| [$\eta^5$:$\eta^1$-$C_5Me_4CH(R)CH_2CH_2O$]$TiCl_2$ | | |
| R = H | | yellow crystals, $^1$H NMR, $^{13}$C NMR, MS, EA[147] |
| R = $CH_2CH{=}CH_2$ | | bright yellow solid, $^1$H NMR, $^{13}$C NMR, IR, MS, EA[147] |
| [$\eta^5$:$\eta^1$-$C_9H_5$-1-$R^1$-$CR^2R^3$($C_6H_4$-2-O)]$TiCl_2$ | | |
| $R^1$ = H, $R^2$ = $R^3$ = $CH_3$ | **118** | dark red crystals, mp, $^1$H NMR, EA, MS, IR, X-ray[148] |
| $R^1$ = H, $R^2$ = $CH_3$, $R^3$ = Et | **119** | dark red crystals, mp, $^1$H NMR, EA, MS, IR[148] |
| $R^1$ = $^t$Bu, $R^2$ = $R^3$ = $CH_3$ | **120** | dark red crystals, mp, $^1$H NMR, EA, MS, IR[148] |
| [4,7-$(OMe)_2$-$\eta^5$-$C_9H_5$]$TiCl_3$ | **121** | green crystals, $^1$H NMR, EA[149] |
| (1-$CH_2CH_2OMe$-$\eta^5$-$C_9H_6$)$TiCl_3$ | **122** | dark red crystals, $^1$H NMR, EA[149] |
| (1-$C_6H_4$−2-OMe-$\eta^5$-$C_9H_6$)$TiCl_3$ | | dark blue crystals, $^1$H NMR, EA[149] |
| (2-$OSiMe_3$-$\eta^5$-$C_9H_6$)$TiCl_3$ | **123** | dark red needle crystals, $^1$H NMR, EA, MS[150] |

**Scheme 55**

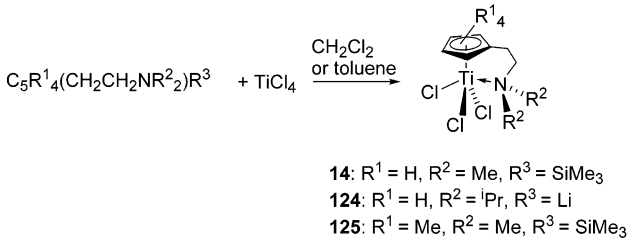


**14**: $R^1$ = H, $R^2$ = Me, $R^3$ = $SiMe_3$
**124**: $R^1$ = H, $R^2$ = $^i$Pr, $R^3$ = Li
**125**: $R^1$ = Me, $R^2$ = Me, $R^3$ = $SiMe_3$

**Scheme 56**

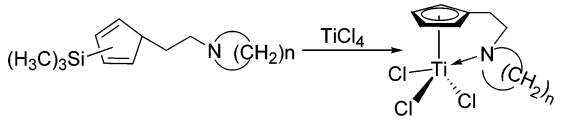


**127**: n = 4
**128**: n = 5

**Scheme 57**

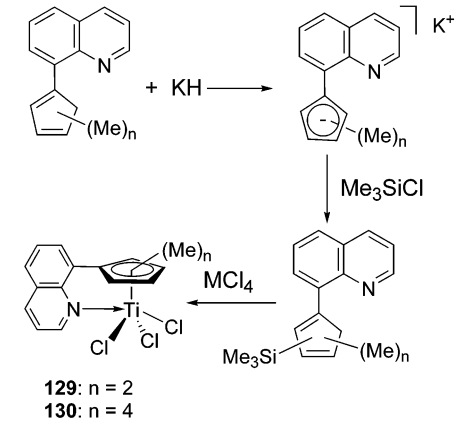


**129**: n = 2
**130**: n = 4

**Scheme 58**

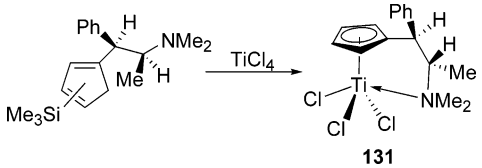


**131**

a downfield shift (~0.4 ppm) for the signal of the methyl group linked to the nitrogen ($\delta$ 2.69) compared to analogous resonances in the spectra of the ligands $C_5H_5(CH_2CH_2NMe_2)$ ($\delta$ 2.27) and $Me_3Si$-$C_5H_4(CH_2CH_2NMe_2)$ ($\delta$ 2.28). Furthermore, a more significant downfield shift (~0.7 ppm) was also observed for the nitrogen methylene signal in **14** ($\delta$ 3.26) as compared to the values in the ligands $C_5H_5(CH_2CH_2NMe_2)$ ($\delta$ 2.53) and [$Me_3SiC_5H_4(CH_2$-$CH_2NMe_2)$] ($\delta$ 2.51), respectively. Finally, the ethylene group exhibits two distinct triplets instead of a multiplet. Similar patterns observed in cobalt[160] and molybdenium[161] complexes have already been confirmed to be due to intramolecular coordination of the amino side chain to the central metal; hence, Chien and co-workers[153] proposed an intramolecular dimethylamino-to-titanium coordination in **14**.

In Table 15 the values of $\Delta\delta(NMe_2)$ and $\Delta\delta(CH_2N)$ in **125** are significantly smaller than those found for

**Table 15. Comparisons of $^1$H NMR ($CDCl_3$) Data for Various $NR_2$ Functionalized Complexes**

| | | δ | | | | |
|---|---|---|---|---|---|---|
| | | δ $CH_2N$ | δ $NMe_2$ | δ CHN | δ $N(CH_2)_4$ | δ $NHMe_2$ |
| $C_5H_5(CH_2CH_2NMe_2)$ | | 2.53 | 2.27 | | | |
| $C_5H_4(CH_2CH_2NMe_2)SiMe_3$ | | 2.51 | 2.28 | | | |
| ($\eta^5$-$C_5H_4CH_2CH_2NMe_2$)$TiCl_3$ | **14** | 3.26 | 2.69 | | | |
| $C_5Me_4H(CH_2CH_2NMe_2)$ | | 2.29 | 2.24 | | | |
| $C_5Me_4(CH_2CH_2NMe_2)SiMe_3$ | | 2.43 | 2.21 | | | |
| ($\eta^5$-$C_5Me_4CH_2CH_2NMe_2$)$TiCl_3$ | **125** | 2.96 | 2.36 | | | |
| $C_5H_5(CH_2CH_2N(CH_2)_4)$ | | 2.43−2.55 | | | 1.64, 2.40 | |
| $C_5H_4(CH_2CH_2N(CH_2)_4)SiMe_3$ | | 2.56 | | | 1.75, 2.51 | |
| ($\eta^5$-$C_5H_4CH_2CH_2N(CH_2)_4$)$TiCl_3$ | **127** | 3.30, 3.41 | | | 1.85, 3.00 | |
| $C_5H_5CH(Ph)CH(Me)NMe_2$ | | | 2.20 | 3.22 | | |
| $Me_3SiC_5H_4CH(Ph)CH(Me)NMe_2$ | | | 2.25 | 3.26 | | |
| [$\eta^5$-$C_5H_4CH(Ph)CH(Me)NMe_2$]$TiCl_3$ | **131** | | 2.75 | 4.64 | | |
| [$\eta^5$-$C_5H_4CH(Ph)CH(Me)NMe_2$]$TiCl_3$ (−80 °C) | | | 2.60−2.78 | 4.64 | | |
| $C_5H_5(CH_2CH_2N^iPr_2)$ | | 2.56 | | | | 2.93−3.23[a] |
| $C_5H_4(CH_2CH_2N^iPr_2)SiMe_3$ | | 2.47−2.57 | | | | 2.94−3.24[a] |
| ($\eta^5$-$C_5H_4CH_2CH_2N^iPr_2$)$TiCl_3$ | **124** | 2.88 | | | | 2.99 |

[a] Coupled with the $sp^3$ signal of the $C_5$ ring.

**Scheme 59**

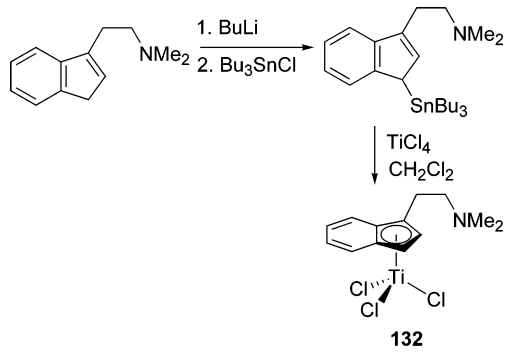


**14**, probably due to the finding that methyl substitution on the Cp ring of an organometallic compound increases the electron density around the central metal. Permethylation of the ring in **125** led to lower Lewis acidity of the titanium center, thereby weakening the Ti−$NMe_2$ interaction, with the result that the change in the electronic environment around the nitrogen in **14** is much smaller than in **125**.

From the foregoing discussion and the values from Table 15, compounds with intramolecularly coordinated Ti−N bonds such as **127** are easily discernible, and the X-ray diffraction studies conducted by Herrmann and co-workers,[156] which was the first single-crystal X-ray structure of a titanium complex with intramolecular N-donor stabilization, strongly confirm the NMR data (Figure 26).

The $^1$H NMR spectrum of **131** shows only one broad signal for the $NMe_2$ group, but at low temperature the signal splits into two resonances. van der Zeijden[159] believes therefore that this indicates a fluxional coordination of the amino sidearm as the existence of this chemical shift, which is attributable to an intramolecular coordination of the dimethylamino group to titanium at low temperatures. Considering **129** and **130**, Enders et al. appointed the $^1$H NMR signal of the hydrogen adjacent to the quinoline nitrogen as a probe for coordination to the nitrogen atom. This $^1$H NMR signal appears at δ 8.81 and δ 8.9 for free quinoline and the ligand $C_5HMe_4(8\text{-}C_9H_6N)$, respectively, whereas it shifted to δ 9.22 in **129** and δ 9.13 in **130**, indicating that the nitrogen

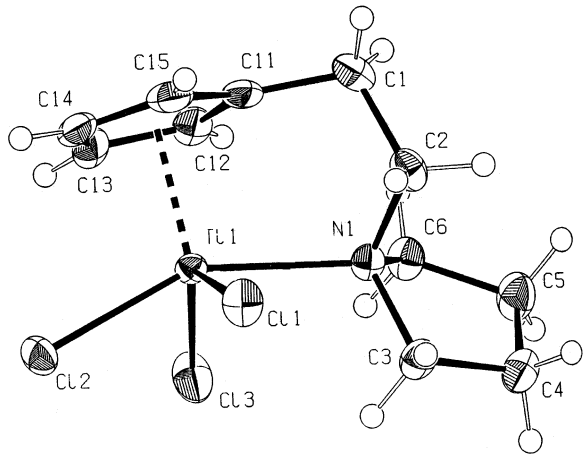


**Figure 26.** Structure of [$\eta^5$-$C_5H_4CH_2CH_2N(CH_2)_4$]$TiCl_3$ (**127**) in the crystal.[156] (Reprinted with permission from ref 156. Copyright 1995 Elsevier Sequoia.)

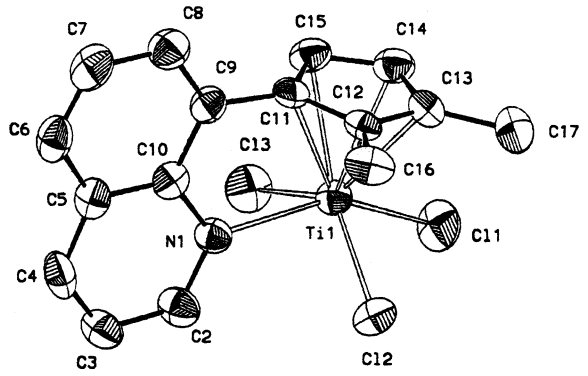


**Figure 27.** Structure of [2,3-$Me_2$-1-(8-$C_9H_6N$)-$\eta^5$-$C_5H_2$]-$TiCl_3$ (**129**) in the crystal.[158] (Reprinted with permission from ref 158. Copyright 1997 Elsevier Sequoia.)

atom is coordinated just as confirmed by the single-crystal structural analysis, in which **129** was found to be monomeric in the solid state (Figure 27).[157,158]

The Ti−N distance of 2.274(4) Å is within the usual range for a dative nitrogen−titanium bond. Because of the additional nitrogen atom, the Ti−Cl bonds [2.300(1)−2.326(1) Å] are elongated by ∼0.1 Å compared to ($\eta^5$-$C_5H_5$)$TiCl_3$ or ($\eta^5$-$C_5Me_4Et$)$TiCl_3$. The angles around the nitrogen are 118.1° ($C_2-N_1-C_{10}$),

**Table 16. Alkyl Amino Functionalized Half-Sandwich Titanium Compounds**

| complex | | color, characterization, etc. |
|---|---|---|
| ($\eta^5$-$C_5H_4CH_2CH_2NMe_2$)$TiCl_3$ | **14** | yellow solid, $^1$H NMR, EA[153, 154] |
| ($\eta^5$-$C_5H_4CH_2CH_2N^iPr_2$)$TiCl_3$ | **124** | yellow solid, $^1$H NMR, MS[155] |
| | **126** | complex with HCl: $^1$H NMR, $^{13}$C NMR, EA[155] |
| ($\eta^5$-$C_5Me_4CH_2CH_2NMe_2$)$TiCl_3$ | **125** | red-orange solid, $^1$H NMR, EA[60] |
| [$\eta^5$-$C_5H_4CH_2CH_2N(CH_2)_4$]$TiCl_3$ | **127** | $^1$H NMR, $^{13}$C{$^1$H} NMR, EA[156] |
| [$\eta^5$-$C_5H_4CH_2CH_2N(CH_2)_5$]$TiCl_3$ | **128** | ref 156 |
| [2,3-$Me_2$-1-(8-$C_9H_6N$)[a]-$\eta^5$-$C_5H_2$]$TiCl_3$ | **129** | red solid, $^1$H NMR, $^{13}$C NMR, MS, EA, X-ray[158] |
| [$\eta^5$-$C_5Me_4$-(8-$C_9H_6N$)]$TiCl_3$ | **130** | red solid, $^1$H NMR, $^{13}$C{$^1$H} NMR, MS, EA, X-ray[157] |
| [$\eta^5$-$C_5H_4CH(Ph)CH(Me)NMe_2$]$TiCl_3$ | **131** | yellow solid, $^1$H NMR, $^{13}$C NMR, EA[159] |
| [1-($Me_2NCH_2CH_2$)-$\eta^5$-$C_9H_6$]$TiCl_3$ | **132** | green solid, $^1$H NMR[154] |

[a] a: 

121.7° ($C_2-N_1-Ti_1$), and 120.6° ($C_{10}-N_1-Ti_1$), summing to 360.4°; this shows that the nitrogen atom is in a planar arrangement with the lone pair pointing directly to the metal.[157,158]

On the other hand, Jutzi et al.[155] found that **124** easily forms a coordination polymer, which converts into the monomeric hydrochloride [{$\eta^5$-$C_5H_4CH_2CH_2N(H)^iPr_2$}$TiCl_3$]$^+Cl^-$ (**126**) in the presence of acidified methanolic solvent.

Table 16 presents the physical properties, references, and characterization for some recently prepared half-titanocenes bearing the $NR_2$ functional group on the Cp moeity.

**b. Mono-Cp(Ind) Titanium Complexes Constrained Geometry Catalysts (CGC).** CGC first reported by Bercaw[162] for organoscandium olefin polymerization catalysts were later extended by Okuda and co-workers[18] to the titanium-linked amido cyclopentadienyltitanium dichloride catalyst in 1990.[163] CGC have the advantages of a relatively open active site, which can easily incorporate higher olefins in forming copolymers with polyethylene, resistance toward counterions such as methylalumoxane (MAO), temperature stability up to 160 °C, and giving higher molecular weight polymers when compared to Britzinger-type *ansa*-metallocenes. The topic has been extensively reviewed covering literature up to 1998.[1,18,164] As evidenced by the shear volume of published data and patent applications, the chemistry and applications of CGC are presently some of the most dynamic and constantly evolving areas of organotitanium chemistry and catalysis.

The generalized structure for the CGC is shown in Chart 8.

**Chart 8**

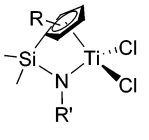


RCp = Cp, Ind, Flu
R' = alkyl, aryl

Three main strategies are employed for efficient CGC synthesis in Scheme 60:

Route A[165−175] is based on a metathetical reaction using the dilithium salt of [(RCp)$SiMe_2NR'$]$^{2-}$ dianions and $TiCl_3$·3THF to afford the dichloro derivatives of the type [$\eta^5$:$\eta^1$-(RCp)$SiMe_2NR'$]$TiCl_2$.

**Scheme 60**

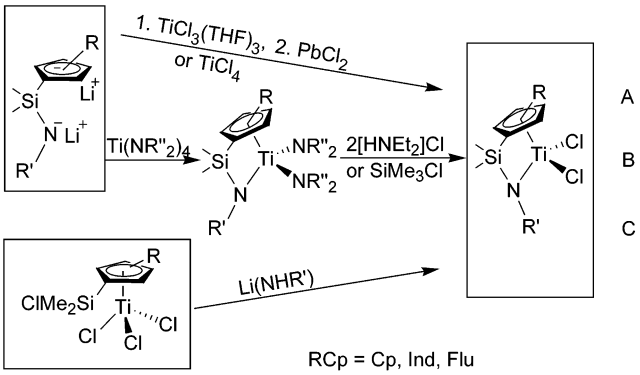


RCp = Cp, Ind, Flu

Route B[176−179] is based on the reaction of homoleptic metal amides $Ti(NR_2)_4$ with the bifunctional [(RCp)-$SiMe_2NHR'$] ligand via amine elimination to produce the diamido [$\eta^5$:$\eta^1$-(RCp)$SiMe_2NR'$]$Ti(NR_2)_2$ compounds; these are then converted to the desired complexes in the presence of $NEt_3$·HCl or $SiMe_3Cl$.

Route C,[134a,179−186] introduced by Royo and adopted by Okuda (see below), assembles the ligand framework on a metal template. In this procedure, reaction of (RCp)($SiMe_2Cl$)$SiMe_3$ with $TiCl_4$ gives [$\eta^5$-(RCp)($SiMe_2Cl$)]$TiCl_3$, and it is subsequently reacted with LiNHR to give the CGC titanium complexes.

Route B gives the diamido half-sandwich derivatives in a good yield, but subsequent treatment with HCl or $NEt_3$·HCl to the corresponding dichlorides may lead to the formation of a mixture or amine adducts, which are undesirable for catalytic purposes and have to be removed by the addition of a Lewis acid. Later, Petersen et al. developed a suitable quantitative route to the dichloro complexes using $Me_2SiCl_2$ as an alternative to the protic reagents. The intermediary product [$RCpSiMe_2NHR'$] is readily obtained via either route 1 or 2 (Scheme 61).[187−189]

Due to poor complex yields (20−40%) as a result of incomplete amine elimination and lower reactivity

**Scheme 61. Synthetic Route to CGC Ligand**


RCp = Cp, Ind, Flu

for $TiCl_4$ to ligand, advancement has focused on developing more efficient metalation strategies by taking advantage of the acidity of the fully protonated CGC ligand (Scheme 61). In this regard, Petersen[177] and Waymouth[166] treated bis(dialkylamide)s with ammonium chlorides or excess $Me_3SiCl$, giving clean conversion to the dichlorides, although in the former case amine adducts were produced. This strategy was also employed by Okuda to produce chiral CGC complexes based on method A.

Since the first reported synthesis of a CGC complex suitable as an olefin polymerization catalyst capable of producing high-density polyethylenes and also able to activate both isotactic and syndiotactic polymerizations, there has been a surge in interest in the development of the chemistry of such *ansa*-metallocene-based systems; replacement of the cyclopentadienyl ring hydrogen by various substituents R′ has been shown to result in significant changes in both steric and electronic effects on the metal center. In addition, variation of substituents R linked to nitrogen with a bulkier donor or chiral group also modifies the properties of resulting compounds.

An early attempt to directly synthesize amido-indenyl complexes bearing indenyl ring substitution by reacting $C_9H_6(SiMe_3)(SiMe_2Cl)$ with titanium tetrachloride, followed by reaction of the trichloro compound with LiNHR, did not yield the desired result.[187] Hence, the authors had to use the conventional method (route C) of first assembling the dilithium derivative of ligand $Li_2[C_9H_6SiMe_2NCMe_3]$, which was subsequently reacted with $TiCl_3$·3THF followed by oxidation to yield the desired product $[\eta^5:\eta^1\text{-}C_9H_6SiMe_2N^tBu]TiCl_2$ **133** (Scheme 62).

**Scheme 62**

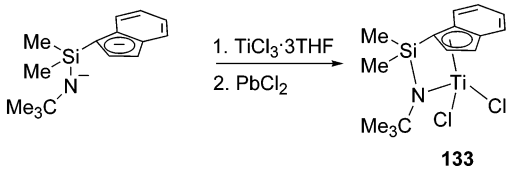


In addition, Royo and co-workers[185] synthesized a series of similar amido-Cp complexes by varying the group R attached to the amido group, via a slightly modified route C, Scheme 63.

**Scheme 63**

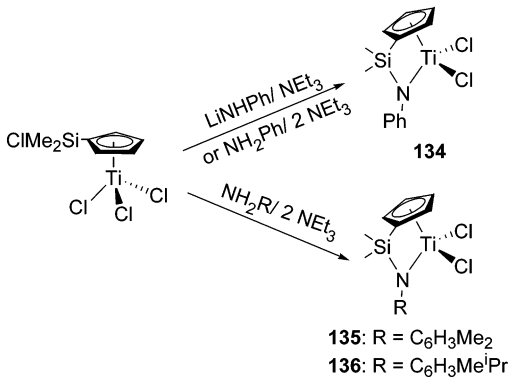


Treatment of $(\eta^5\text{-}C_5H_4SiMe_2Cl)TiCl_3$ with 1 equiv of $NH_2R$ (R = $C_6H_5$, 2,6-$Me_2C_6H_3$, or 2-Me-6-$^i$Pr$C_6H_3$) in the presence of 2 equiv of $NEt_3$ results in the corresponding constrained geometry derivatives $(\eta^5:\eta^1\text{-}C_5H_4SiMeNR)TiCl_2$ (**134**−**136**), which after standard workup were isolated as orange (R = $C_6H_5$) or yellow (R = 2,6-$Me_2C_6H_3$ and 2-Me-6-$^i$Pr$C_6H_3$) crystals. The yield of compound **134** improved slightly (40 vs 30%) using the lithium amide Li(NHPh) in the presence of 1 equiv of $NEt_3$. Complexes **134**−**136** are thermally stable in $C_6D_6$ after 24 h at 120 °C but extremely oxygen and moisture sensitive and insoluble in aliphatic, but readily soluble in aromatic and polar, solvents, with the greater solubility for the systems containing the larger branched aryl ligands. Similarly, compounds **137**−**141** were synthesized[167] with the aim to study the influence of varying the R in the linked amido-cyclopentadienyl ligand on olefin polymerization performance. It was realized that due to steric reasons during coordination of the bidentate ligand to the titanium center, the size of R is critically important not only in catalysis but also in determining the yield of $Ti(\eta^5:\eta^1\text{-}C_5Me_4SiMe_2NR)Cl_2$ (**137**−**141**) (Chart 9).

**Chart 9**

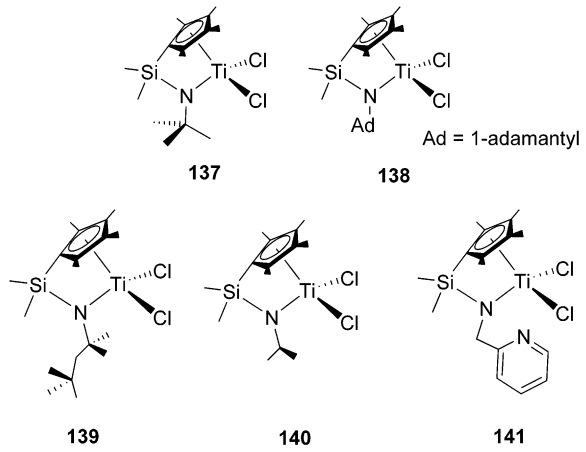


Investigation of catalyst behavior in the hydrogenation of imine prompted the synthesis of a series of titanium complexes $(\eta^5:\eta^1\text{-}C_5H_4SiMe_2NR')TiCl_2$ (**142**−**148**) and $(\eta^5:\eta^1\text{-}C_5Me_4SiMe_2NR')TiCl_2$ (**149**−**155**) [R′ = CHMePh, $CHMeC_{10}H_7$, $CHMeCMe_3$, $CHPhCMe_3$, $CHMeC_6H_{11}$, (1*S*)-pinayl-3, or (1*R*)-bornyl-2] containing an enantiomerically pure linked amido-cycopentadienyl ligand in which both R and R′ were varied.[182]

Following established synthetic methodologies (routes A and C), two series of titanium dichloride complexes (*Sc*)-$(\eta^5:\eta^1\text{-}C_5R_4SiMe_2NR')TiCl_2$ [R = H (**142**−**148**) or Me (**149**−**155**)] with various optically active amido substituents R′ were synthesized (Chart 10). It seems that the nature of the Cp ring is very important in determining the synthetic route; hence, the authors reported synthesizing $C_5H_4$- and $C_5Me_4$-based complexes via routes A and C, respectively (**156**−**159**). Chart 11 represent a group of CGC complexes with various substituents on the trimethylated cyclopentadienyl ligand in the position adjacent to the dimethylsilene bridge. Mach and coworkers produced these compounds with the employment of route C. Similarly, CGC bearing $\omega$-alkenyl

**Chart 10**

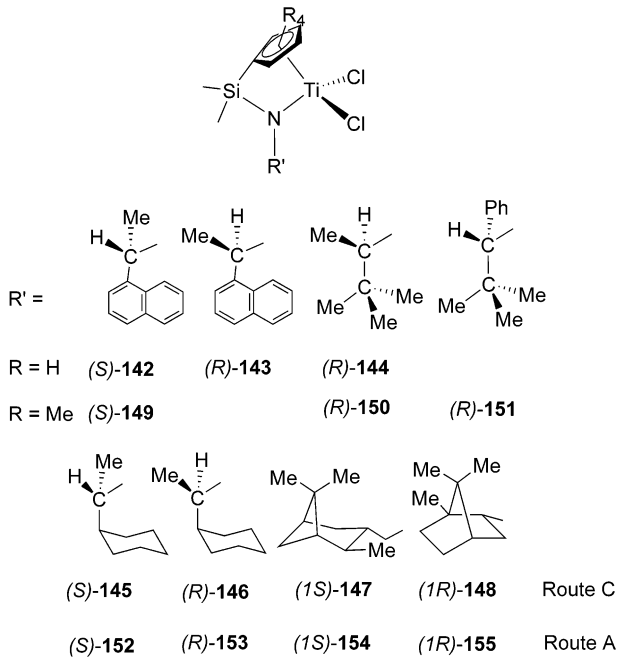


**Chart 11**

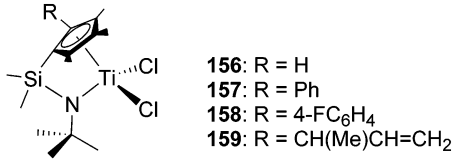


substituent groups **160**−**162** (Chart 12) on the cyclopentadienyl or indenyl moiety (R) with various spacer lengths were prepared to investigate the effect of the catalyst structure on olefin polymerization and polymer properties.[168,171]

**Chart 12**

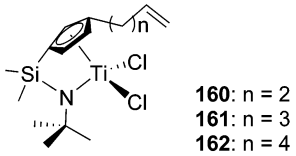


The synthesis by the way of route C to the CGC having 3-*tert*-butylcyclopentadienyl linked to a (*S*)-1-phenylamido group **163** (Chart 13) through a dimethylsilanediyl group serves as a simple means of determining diastereoselectivity during the formation of linked amido-cyclopentadienyl complexes, where it was found that the crude reaction mixtures reveal the formation of a mixture of diastereomers in a 1:1 ratio (approx).[182]

**Chart 13**

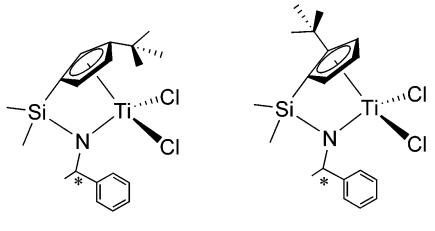


Royo[179] first introduced the synthesis of ($\eta$:$^5\eta^1$-$C_5H_4SiMe_2NCHMePh)TiCl_2$ **164** via route C also developed by his group, as an efficient synthetic route to CGC complexes from a suitable starting material ($\eta^5$-$C_5H_4SiMe_2Cl)TiCl_3$. The reaction of ($\eta^5$-$C_5H_4SiMe_2Cl)TiCl_3$ with LiNHCHMePh (1:1) in the presence of $NEt_3$ results in the precipitation of $NEt_3$·HCl and formation of the desired compound ($\eta$:$^5\eta^1$-$C_5H_4SiMe_2NCHMePh)TiCl_2$ **164** (Scheme 64).

**Scheme 64**

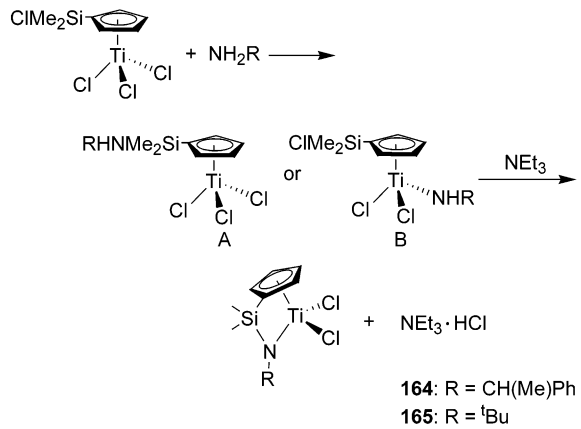


The mechanism was proposed to produce two possible intermediate species, [($\eta^5$-$C_5H_4SiMe_2$-NHCHMePh)$TiCl_3$] (**A**) and [($\eta^5$-$C_5H_4SiMe_2Cl)TiCl_2$-NHCHMePh] (**B**), formed by the aminolysis of the Si−Cl or Ti−Cl bond. In the presence of $NEt_3$, **A** and **B** convert into the desired complex via an intramolecular elimination of HCl involving the second chlorine atom from the Ti−Cl (A) or Si−Cl (B) bond, with the precipitation of $Et_3N$·HCl (Scheme 64).

Okuda et al.[165,169,181,184] also introduced a tridentate variation of the linked amidocyclopentadienyl ligand. They proposed that the two-electron donor functional groups X = OMe and $NMe_2$ may act as labile ligands, thereby temporarily coordinating to the central metal during catalytic reactions and hence stabilizing the highly electrophilic centers. A synthetic strategy following routes A and C was employed to produce the tridentate linked-amido cyclopentadienyltitanium

**Chart 14**

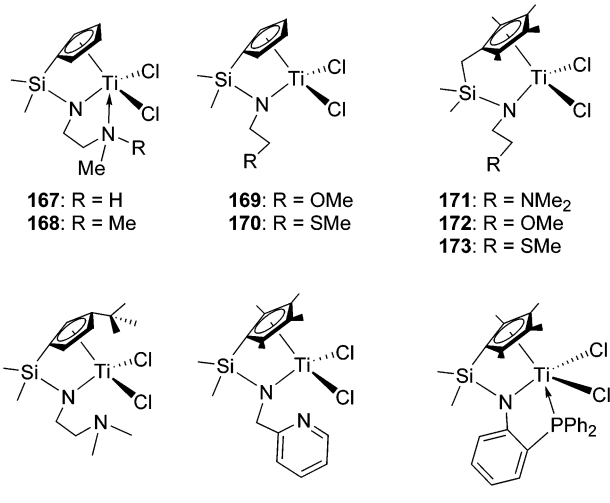

complexes containing OMe, $NMe_2$, SMe, and $PPh_2$ groups (Chart 14), and the mechanism is believed to be similar to that established by Royo et al.[183] (Scheme 65).

**Scheme 65**

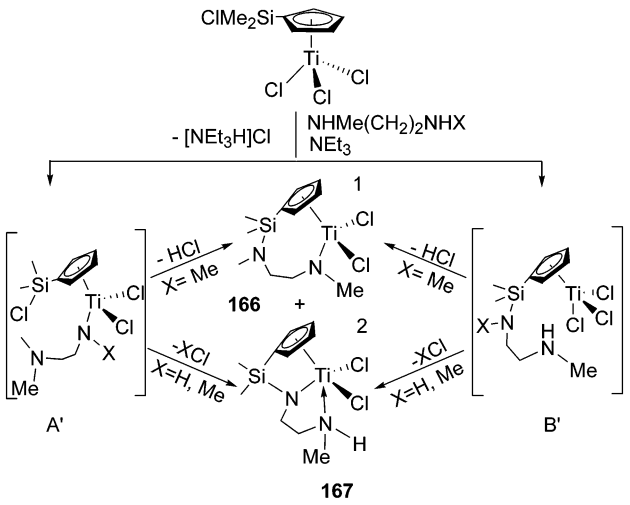


As an extension of the structural variations in constrained geometry titanium complexes, Parket al.[176,178] have employed the hydrazido moiety as a donor group instead of the amido ligand. The hydrazido moiety was thought to readily stabilize the catalytically active cationic species compared to the amido ligand due to its strong donor nature. Route B was adopted in synthesizing these complexes. An *N*,*N*-dimethyl hydrazido ligand $(C_5Me_4H)SiMe_2(NHNMe_2)$ was obtained by the reaction between $LiNHNMe_2$ and $(C_5Me_4H)SiMe_2Cl$ in the presence of $Et_3N$. The $\eta^1$-hydrazido bis(dimethylamido) complex $[(\eta^5\text{-}C_5Me_4)SiMe_2(\eta^1\text{-}NNMe_2)]Ti(NMe_2)_2$ (**176**) was prepared by the reaction of $C_5HMe_4Si(Me)_2NHNMe_2$ and $Ti(NMe_2)_4$ at 130 °C, followed by treatment with excess $Me_3SiCl$ in dichloromethane, yielding the $\eta^2$-hydrazido dichloride compound **177** as an orange solid (Scheme 66).

**Scheme 66**

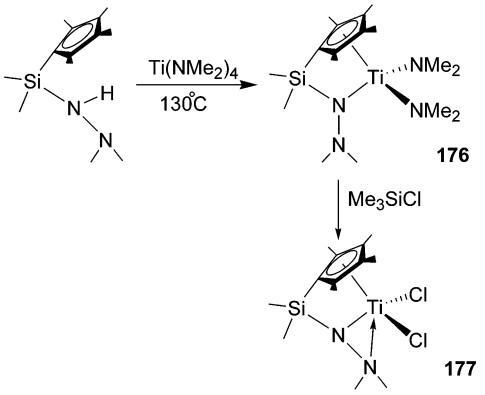


The third possible variable option for synthetic chemists interested in exploring the linked-amido titanium CGC complexes is to replace the Si bridge with another group, and along this line $C_2$ and $C_3$ carbon bridges have been most favored as alternatives for linking the Cp ring and nitrogen (Chart 15).[190−196]

**Chart 15**

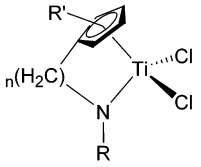

| R'Cp = $C_5Me_4$, n = 2 | R'Cp = $C_5H_4$, n = 2 | R'Cp = $C_5H_4$, n = 3 |
|---|---|---|
| **178**: R = Me | **181**: R = Me | **185**: R = Me |
| **179**: R = $^i$Pr | **182**: R = $^i$Pr | **186**: R = $^i$Pr |
| **180**: R = $^i$Bu | **183**: R = $^i$Bu | **187**: R = $SiMe_3$ |
| | **184**: R = $SO_2C_6H_4CH_3$ | |

Teuben et al.[190,191] reported the preparation of complexes **181**−**184** and **185** and **186** by reaction of the ligand $(C_5H_5(CH_2)_nNHR)$ with metal halides $TiX_4$ in the presence of a base ($Et_3N$) to trap the generated HX (Scheme 67).

**Scheme 67**

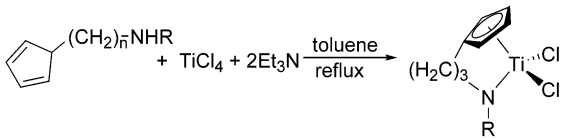


**185**: R = Me
**186**: R = $^i$Pr

Later, they also reported the synthesis of complexes **178**−**180** via a synthetic strategy analogous to route C (Scheme 68).

**Scheme 68**

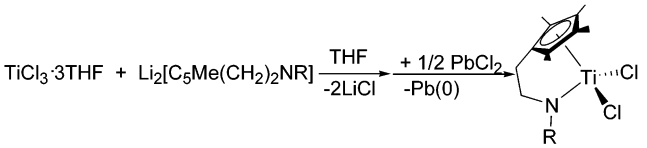


**178**: R = Me
**179**: R = $^i$Pr
**180**: R = $^i$Bu

Complex **178** was obtained by the thermal decomposition of $[\eta^5\text{-Cp*Ti}(NMe_2)Cl_2]$ (Scheme 69).[194]

In 1997, Green and co-workers[192,193] synthesized **187** via treatment of $TiCl_4$ in toluene with $Me_3SiC_5H_4(CH_2)_3N(SiMe_3)_2$ (Scheme 70) as an easier, one-step

**Scheme 69**

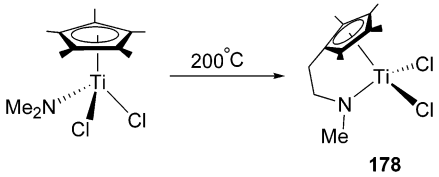


**178**

**Scheme 70**

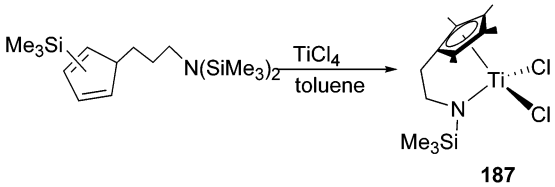


**187**

alternative to Scheme 68 mentioned above. The elimination of $SiMe_3Cl$ from $Me_3SiC_5H_4(CH_2)_3N(SiMe_3)_2$ occurs readily in toluene at 60 °C to give **187**.

Ethylene-bridged "bis-CGC" titanocenes **188** and **189** were obtained by treatment of a titanocene−bis(trimethylsilyl)acetylene complex with acetone azine $Me_2C{=}N{-}N{=}Me_2$ (Scheme 71).[196,197]

**Scheme 71**

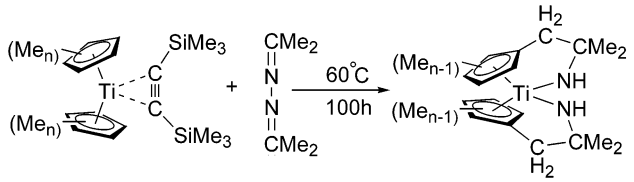


**188**: n = 3
**189**: n = 4

The structures of compounds **137** and **158** were determined by single-crystal X-ray diffraction (Figures 28 and 29).[171]

The titanium atom is in a pseudo-tetrahedral environment defined by one silylamido $\sigma$-N coordinated Cp ligand and two chloro ligands. The amido nitrogen is planar (the sum of bond angles around the N atom is 360°) with $sp^2$ hybridization. The Ti−N length [1.910 Å (04)] of **137** and **158** is consistent with a N−Ti $p\pi-d\pi$ bonding orbital interaction. However, the magnitude of this interaction is controlled by both the constrained geometry of the molecule and electronic and steric properties of substituents on the amido group, as observed in other complexes of this type $[(\eta^5{:}\eta^1\text{-}C_5H_4SiMe_2NR)TiCl_2]$.

The N−Ti−Cp bite angle is believed to determine polymerization activity of the catalysts prepared thereof (Chart 16). The magnitude of the bite angle

**Chart 16. Illustration of the Bite Angle in CGC and Related Complexes**

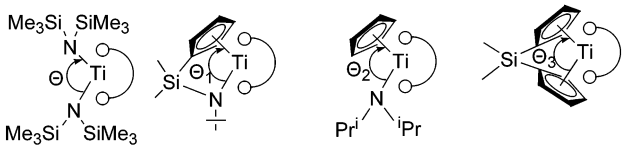


is somewhat more affected by substituents on the nitrogen atoms as their stereoelectronic effect instantly influences the Ti−N bond. The bite angle N−Ti−Cp ($\Theta_1$ = 107.8°) in the prototype CGC molecule **137** is considerably smaller ($\Theta_2$ = 116.2°) than in the Cp-amido complex $[(\eta^5\text{-}C_5H_5)TiCl_2(N^iPr_2)]$ with a missing bridging atom,[198] the diamido complexes such as $[Ti\{N(SiMe_3)_2\}_2(CH_2Ph)_2]$ (Θ = 120.6°),[199] and the Cp−Ti−Cp bond angle ($\Theta_3$ = 128.7°) in $[\{\mu\text{-}SiMe_2(\eta^5\text{-}C_5H_4)_2\}TiCl_2]$.[200] From these data the "open" nature of the metal center in CGC complexes is obvious, and this has been regarded as the reason for their ability to incorporate higher olefins during copolymerization with ethylene and also accounts for the poor stereocontrol with regard to the latter monomer (refer to Figure 30). The

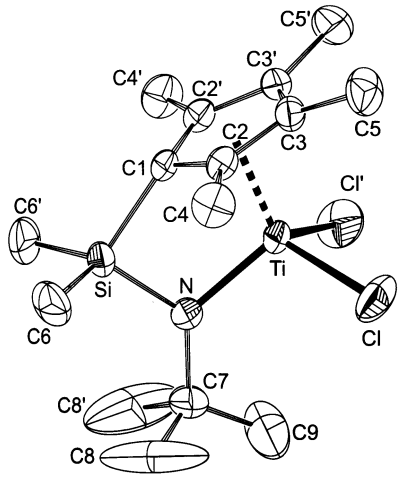


**Figure 28.** Structure of $(\eta^5{:}\eta^1\text{-}C_5Me_4SiMe_2N^tBu)TiCl_2$ (**137**) in the crystal.[171] (Reprinted with permission from ref 171. Copyright 2001 CCCC.)

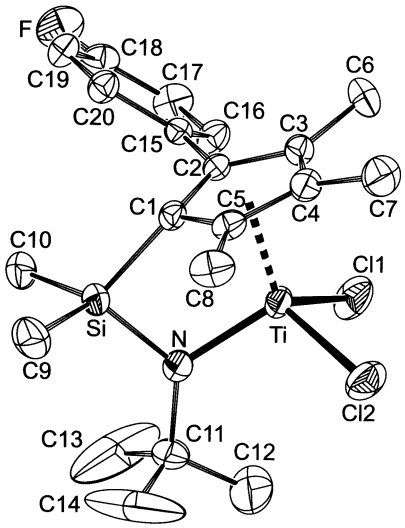


**Figure 29.** Structure of $[2\text{-}(4\text{-}FC_6H_4)\text{-}\eta^5{:}\eta^1\text{-}C_5Me_3SiMe_2N^tBu]TiCl_2$ (**158**) in the crystal.[171] (Reprinted with permission from ref 171. Copyright 2001 CCCC.)

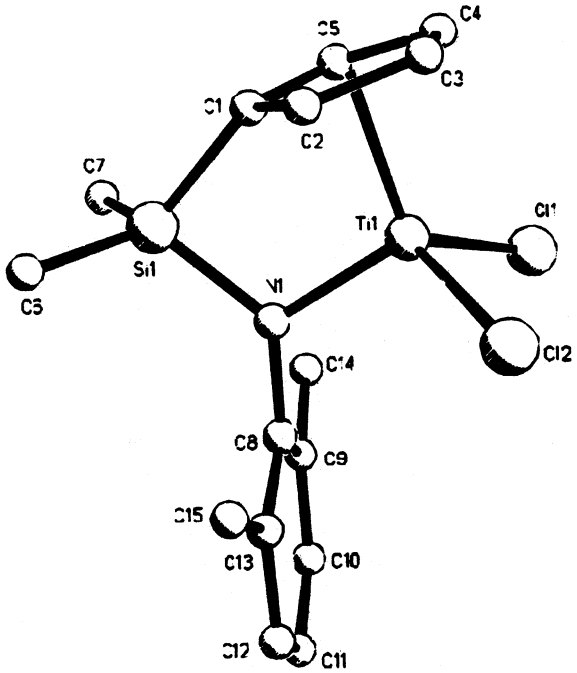


**Figure 30.** Structure of $(\eta^5{:}\eta^1\text{-}C_5H_4SiMe_2NC_6H_3Me_2)TiCl_2$ (**135**) in the crystal.[185] (Reprinted with permission from ref 185. Copyright 1998 Elsevier Sequoia.)

skeleton of CGC complexes is not affected by the substituent R′ on the Cp ligand as seen from a comparison of the bite angle N−Ti−Cp in **137** and **158** [107.6° (2)]; other skeletal angles and bond lengths are virtually equal in both compounds.

The Cp−Ti−N angle of 105.1° observed in **135**[185] is slightly smaller than that found in the prototypical CGC **137** with a R = $^t$Bu,[177] which indicates a tendency toward an increasing "openness" of the active site with the introduction of the bulkier amido sustituent. In the case of CGC complexes with a chiral group linked to nitrogen (complex **154**),[182] the Cp−Ti−N bite angle and Ti−N bond lengths are not different from those of the above-mentioned achiral CGC complexes. The absolute *S* configuration of the stereogenic carbon atom was also confirmed crystallographically (Figure 31).

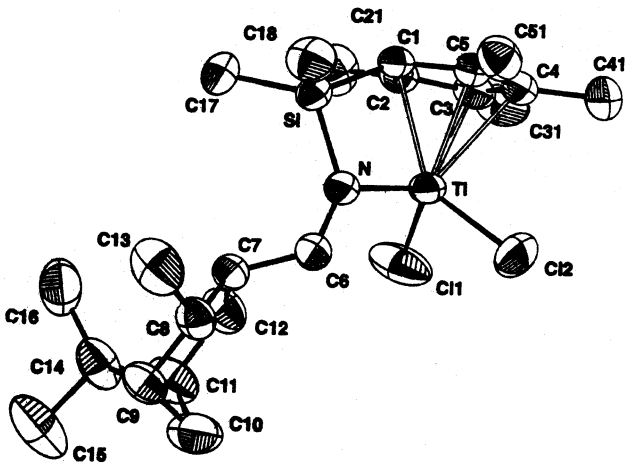


**Figure 31.** Structure of [$\eta^5$:$\eta^1$-$C_5Me_4SiMe_2(CH_2$pinayl-3)]-$TiCl_2$ (**154**) in the crystal.[182] (Reprinted with permission from ref 182. Copyright 2000 Elsevier Sequoia.)

The typical CGC structural conformation is revealed by NOE measurements and further confirmed by single-crystal X-ray analysis as having an orientation of the methylene hydrogen atoms toward the titanium center and the bulky group pointing away from the metal center.

Chiral amino auxiliary ligands R were used as stereocontrol elements by Waymouth et al.[166] to study the potential influence of metal chirality in amidoindenyl titanium complexes on catalytic stereospecificity (Scheme 72). The complexes were synthesized

**Scheme 72**

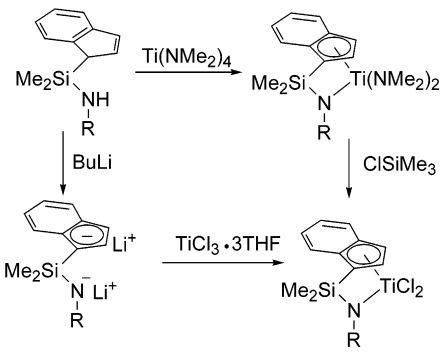


**190**: R = CHMePh
**191**: R = $C_6H_{11}$

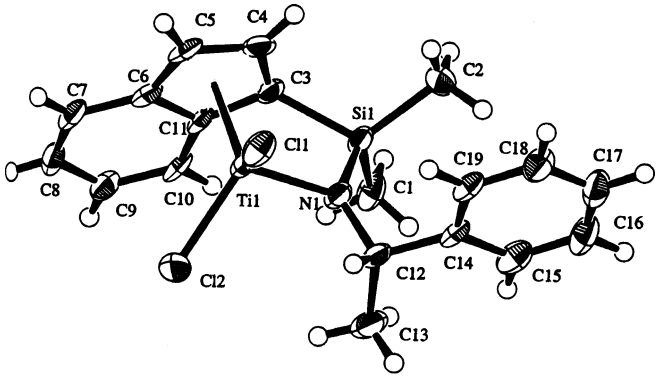


**Figure 32.** Structure of {$\eta^5$:$\eta^1$-$C_9H_6SiMe_2NCHMePh$}-$TiCl_2$ (**190**) in the crystal.[166] (Reprinted with permission from ref 166. Copyright 1997 American Chemical Society.)

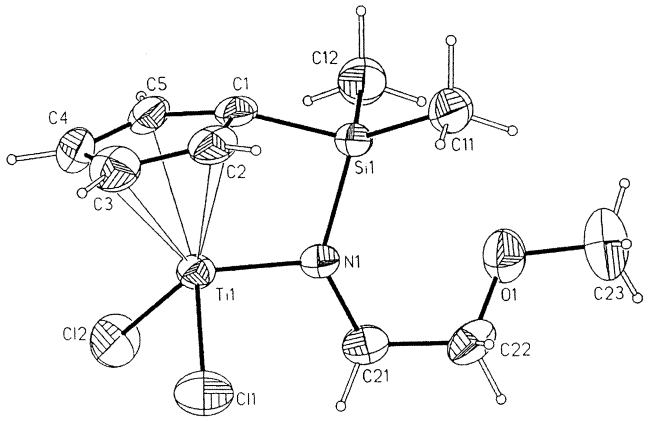


**Figure 33.** Structure of ($\eta^5$:$\eta^1$-$C_5H_4SiMe_2NCH_2CH_2OMe$)-$TiCl_2$ (**169**) in the crystal.[184] (Reprinted with permission from ref 184. Copyright 1996 VCH.)

by the way of routes A and B, and a single-crystal X-ray diffraction analysis is depicted (Figure 32).

The introduction of additional pendant neutral coordination sites (OMe, $NMe_2$, SMe, $PPh_2$, and C=C) to the amido N atom was expected to produce flexible tridentate ligands for CGC titanium complexes with some unprecedented properties. However, variable-temperature $^1$H NMR spectral analysis of the methoxyl[184] or methylthio[181] group signal did not show any significant difference from those of ordinary free ligands, suggesting the absence of any special properties such as coordination of sulfur or oxygen atom toward titanium. An open structure without any intramolecular coordination was confirmed by X-ray structural analysis of **169** and **170** in the crystalline state (Figures 33 and 34).

However, in the case of **175,**[181] the change in the magnitude of the $^1J_{PC}$ and $^2J_{PC}$ values for the *ipso*- and *ortho*-carbon atoms in the $^{13}$C NMR, together with the significant high-field shift of the $^{31}$P NMR resonance, suggests the presence of a coordinating phosphorus atom to the metal center (Scheme 73).

A similar NMR spectroscopic analytical strategy was employed to study the structures of complexes **168**, and Okuda et al.[165,181,184] proposed a possible model of a fluxional coordination (Scheme 74).

Later the argument in favor of intramolecular coordination of the additional donor atom (Scheme 74) was adopted. It was only very recently that this

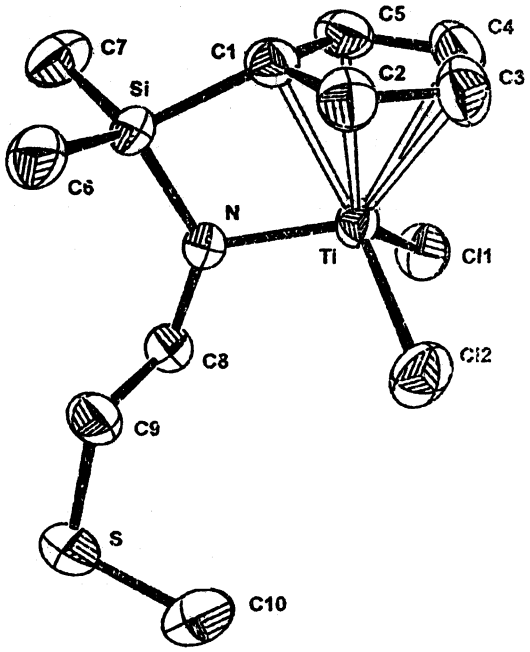


**Figure 34.** Structure of ($\eta^5$:$\eta^1$-$C_5H_4SiMe_2NCH_2CH_2SMe$)-$TiCl_2$ (**170**) in the crystal.[181] (Reprinted with permission from ref 181. Copyright 1999 Elsevier Sequoia.)

**Scheme 73**

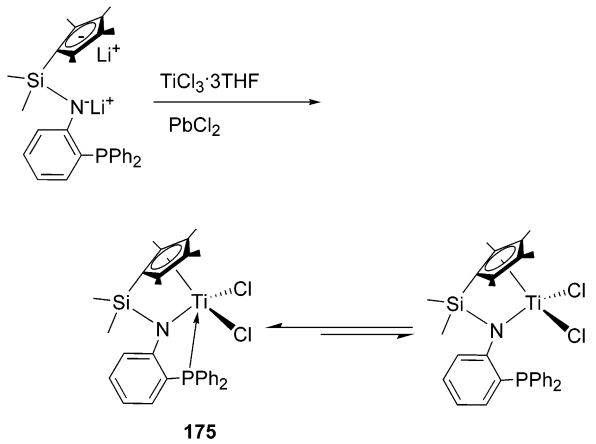


**Scheme 74**

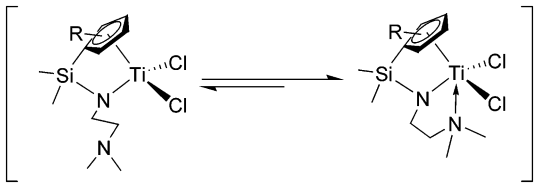


assumption has been conclusively confirmed by X-ray crystal analysis.[186]

NMR spectroscopic analysis was also adopted by Royo and co-workers to determine the structure of complexes **166** and **167** highlighted by extra $NMe_2$ and NHMe groups attached to the amido group (Chart 17).[183] Here, the intramolecular coordination of the terminal nitrogen in **167** was indicated by the significant difference in chemical shifts between NHMe protons and those of the free diamine in **166** ($\delta$ 2.40 NMe and 1.80−1.90 NH).

$^1$H NMR spectral studies of **167** at 25 °C show some broad signal $\delta$ ($CH_2NH$ and BB′ part of $C_5H_4$),

**Chart 17**

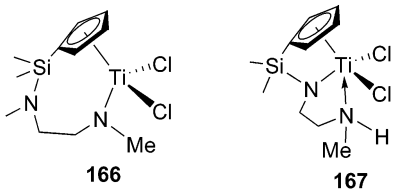


indicating possible fluxional behavior with the relevant rate within the NMR time scale. This process may be described as an interconversion between the two enantiomeric conformations, which can be observed in **166**.[183]

The structure of **166** was confirmed by a single-crystal X-ray diffraction study (Figure 35). The Cp−Ti−N (2) angle of 114.2° (113.9) is significantly larger than the corresponding angle in the prototype CGC **165**. This result suggests that the "open" nature of the active site is lost with the increase of the spacer length as reflected by a Cl−Ti−Cl angle of 101.4° (102.34), which is in the normal range of the value observed for unconstrained monocyclopentadienyl-amido derivatives.

Furthermore, the structure of **177** was confirmed by X-ray crystal structure analysis (Figure 36) to

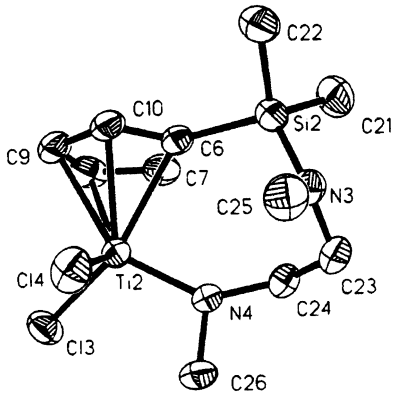


**Figure 35.** Structure of [{$\eta^5$-$C_5H_4SiMe_2NMe(CH_2)_2$-$\eta$-NMe}$TiCl_2$] (**166**) in the crystal.[183] (Reprinted with permission from ref 183. Copyright 2001 American Chemical Society.)

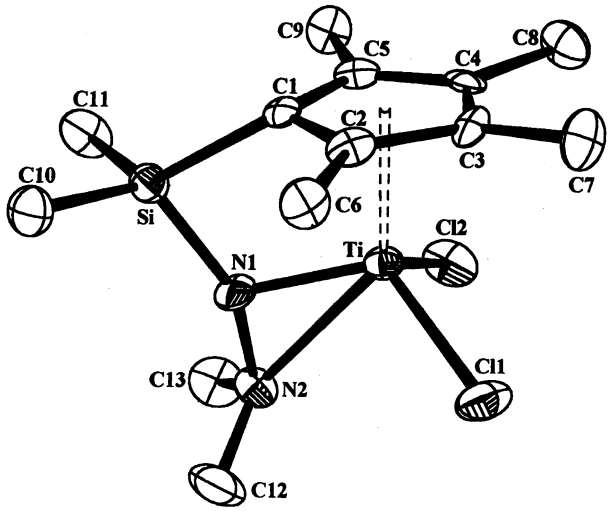


**Figure 36.** Structure of ($\eta^5$:$\eta^1$-$C_5Me_4SiMe_2NNMe_2$)$TiCl_2$ (**177**) in the crystal.[176] (Reprinted with permission from ref 176. Copyright 2000 American Chemical Society.)

**Table 17. Constrained Geometry Complexes (CGC)**

| complex | | color, characterization, etc. |
|---|---|---|
| {$\eta^5$:$\eta^1$-$C_9H_6SiMe_2N$ $^t$Bu }$TiCl_2$ | **133** | red microcrystalline solid, $^1$H NMR,$^{13}$CNMR, EA, MS[166,187] |
| ($\eta^5$:$\eta^1$-$C_5H_4SiMe_2NR$)$TiCl_2$ | | |
| R = phenyl | **134** | orange crystals, $^1$H NMR, $^{13}$C{$^1$H} NMR, EA[185] |
| R = $C_6H_3Me_2$ | **135** | yellow crystals, $^1$H NMR, $^{13}$C{$^1$H} NMR, EA, X-ray[185] |
| R = $C_6H_3Me^iPr$ | **136** | yellow crystals, $^1$H NMR, $^{13}$C{$^1$H} NMR, EA[185] |
| ($\eta^5$:$\eta^1$-$C_5Me_4SiMe_2NR$)$TiCl_2$ | | |
| R = $^t$Bu | **137** | yellow crystals, $^1$H NMR, $^{13}$C NMR,[166] EI-MS,[167] EA,[166] X-ray[171,177] |
| R = 1-adamantyl | **138** | yellow crystals, $^1$H NMR, $^{13}$C{$^1$H} NMR, MS, EA[167] |
| R = $CMe_2CH_2{}^t$Bu | **139** | yellow crystals, $^1$H NMR, $^{13}$C{$^1$H} NMR, MS, EA[167] |
| R = $^i$Pr | **140** | yellow crystals, $^1$H NMR, $^{13}$C{$^1$H} NMR, MS, EA[167] |
| R = $CH_2(C_5H_4N)$-2 | **141** | orange solid, $^1$H NMR, $^{13}$C{$^1$H} NMR, MS, EA[167] |
| R = Ph | | yellow-beige crystals, $^1$H NMR, $^{13}$C NMR, EA[202] |
| R = $C_6F_5$ | | orange crystals, $^1$H NMR, $^{13}$C NMR, EA, X-ray[202] |
| R = $SO_2Ph$ | | orange crystals, $^1$H NMR, $^{13}$C NMR, EA, X-ray[202] |
| R = $SO_2Me$ | | orange powder, $^1$H NMR, $^{13}$C NMR, EA[202] |
| ($\eta^5$:$\eta^1$-$C_5H_4SiMe_2NR$)$TiCl_2$ | | |
| R = $CH_2C_6H_3F$-6-($NHCH_2C_6H_3F_2$-2,6)-2 | | yellow crystals, $^1$H NMR, $^{13}$C{$^1$H} NMR, MS, EA[174] |
| R = $CHMeC_{10}H_7$ (*S*) | **142** | yellow needles, [α], $^1$H NMR, $^{13}$C NMR, MS,EA[182] |
| R = $CHMeC_{10}H_7$ (*R*) | **143** | yellow solid, [α], EA[182] |
| R = $CHMe^tBu$ (*R*) | **144** | yellow needles, [α], $^1$H NMR, $^{13}$C NMR, MS,EA[182] |
| R = $CHMeC_6H_{11}$ (*S*) | **145** | yellow needles, [α], $^1$H NMR, $^{13}$C NMR, MS,EA[182] |
| R = $CHMeC_6H_{11}$ (*R*) | **146** | yellow crystals, [α], EA[182] |
| R = $CH_2$pinayl-3 (*S*) | **147** | yellow solid, [α], $^1$H NMR, $^{13}$C NMR, MS, EA[182] |
| R = bornyl (*R*) | **148** | orange-yellow needles, [α], $^1$H NMR, $^{13}$C NMR, EA[182] |
| R = CHMePh (*R*) | | yellow prisms, [α], $^1$H NMR, $^{13}$C NMR, MS, EA[180] |
| R = CHMePh (*S*) | | yellow crystals, [α], EA, X-ray[180] |
| ($\eta^5$:$\eta^1$-$C_5Me_4SiMe_2NR$)$TiCl_2$ | | |
| R = $CHMeC_{10}H_7$ (*S*) | **149** | orange crystals, [α], $^1$H NMR, $^{13}$C NMR, MS,EA[182] |
| R = $CHMe^tBu$ (*R*) | **150** | orange crystals, [α], $^1$H NMR, $^{13}$C NMR, EA[182] |
| R = $CH^tBuPh$ (*R*) | **151** | dark yellow crystals, $^1$H NMR, $^{13}$C NMR, EA[182] |
| R = $CHMeC_6H_{11}$ (*S*) | **152** | yellow crystals, [α], $^1$H NMR, $^{13}$C NMR, MS,EA[182] |
| R = $CHMeC_6H_{11}$ (*R*) | **153** | orange solid, [α], EA[182] |
| R = $CH_2$pinayl-3 (*S*) | **154** | yellow needles, [α], $^1$H NMR, $^{13}$C NMR, MS,EA, X-ray[182] |
| R = bornyl (*R*) | **155** | yellow powder, $^1$H NMR, $^{13}$C NMR[182] |
| R = CHMePh (*R*) | | yellow-orange needles, [α], $^1$H NMR, $^{13}$C NMR, MS, EA[180] |
| R = CHMePh (*S*) | | yellow crystals, [α],[166,180] $^1$H NMR, $^{13}$C NMR,[166] EA[166,180] |
| R = $CH_2CH{=}CH_2$ | | dark brown powder, mp, EA[165] |
| (2-R-$\eta^5$:$\eta^1$-$C_5Me_3SiMe_2N{}^t$Bu)$TiCl_2$ | | |
| R = H | **156** | bright yellow crystals, mp, $^1$H NMR, $^{13}$C{$^1$H} NMR, IR, MS[171] |
| R = Ph | **157** | yellow crystals, mp, $^1$H NMR, $^{13}$C{$^1$H} NMR, IR, MS[171] |
| R = 4-$FC_6H_4$ | **158** | yellow crystals, mp, $^1$H NMR, $^{13}$C{$^1$H} NMR, IR, MS, X-ray[171] |
| R = $CH_2(CH_3)CH{=}CH_2$ | **159** | yellow crystals, mp, $^1$H NMR, $^{13}$C{$^1$H} NMR, IR, MS[171] |
| {3-[$CH_2{=}CH(CH_2)_n$]-$\eta^5$:$\eta^1$-$C_5H_3SiMe_2N{}^t$Bu}$TiCl_2$ | | |
| *n* = 2 | **160** | $^1$H NMR, $^{13}$C NMR, $^{29}$Si NMR[168] |
| *n* = 3 | **161** | $^1$H NMR, $^{13}$C NMR, $^{29}$Si NMR[168] |
| *n* = 4 | **162** | $^1$H NMR, $^{13}$C NMR, $^{29}$Si NMR[168] |
| (3-$^t$Bu-$\eta^5$:$\eta^1$-$C_5H_3SiMe_2NR$)$TiCl_2$ | | |
| R = CHMePh (*S*) | **163** | dark yellow solid, $^1$H NMR, $^{13}$C NMR, MS, EA[182] |
| R = CHMePh (*R*) | | dark yellow solid, EA[182] |
| ($\eta^5$:$\eta^1$-$C_5H_4SiMe_2NR$)$TiCl_2$ | | |
| R = CHMePh | **164** | orange-brown crystals, $^1$H NMR, $^{13}$C{$^1$H} NMR, MS, EA[179] |
| R = $^t$Bu | **165** | orange crystals, $^1$H NMR,[177,134a,173,179] $^{13}$C NMR,[30,137] $^{29}$Si NMR, $^{15}$N NMR, $^{14}$N NMR,[173] MS,[179] EA,[179,134a] X-ray[177] |
| R = $CH_2Ph$ | | yellow crystals, $^1$H NMR, $^{13}$C{$^1$H} NMR, MS, EA[174] |
| R = $CH_2C_6H_3F_2$ | | yellow crystals, $^1$H NMR, $^{13}$C NMR, MS, EA, X-ray[174] |
| R = $^i$Pr | | yellow crystals, $^1$H NMR, $^{13}$C{$^1$H} NMR, MS, EA, X-ray[174] |
| [{$\eta^5$-$C_5H_4SiMe_2NMe(CH_2)_2$-$\eta$-NMe}$TiCl_2$] | **166** | red crystals, $^1$H NMR, $^{13}$C{H} NMR, $^{29}$Si NMR, EA, X-ray[183] |
| ($\eta^5$:$\eta^1$-$C_5H_4SiMe_2NR$)$TiCl_2$ | | |
| R = $CH_2CH_2NHMe$ | **167** | yellow solid, $^1$H NMR, $^{13}$C{$^1$H} NMR, $^{29}$Si NMR, EA, IR[183] |
| R = $CH_2CH_2NMe_2$ | **168** | orange crystals, mp, MS, $^1$H NMR, $^{13}$C{$^1$H} NMR, EA[184] |
| R = $CH_2CH_2OMe$ | **169** | yellow-brown crystals, mp, $^1$H NMR, $^{13}$C{$^1$H} NMR, MS, EA, X-ray[184] |
| R = $CH_2CH_2SMe$ | **170** | yellow crystals, $^1$H NMR, $^{13}$C{$^1$H} NMR, EA, MS, X-ray[181] |
| ($\eta^5$:$\eta^1$-$C_5Me_4SiMe_2NR$)$TiCl_2$ | | |
| R = $CH_2CH_2NMe_2$ | **171** | orange crystals, mp, $^1$H NMR, $^{13}$C{$^1$H} NMR,[165,169] MS,[169] EA[165,169] |
| R = $CH_2CH_2OMe$ | **172** | light yellow brown solid, mp, $^1$H NMR, $^{13}$C{$^1$H} NMR, MS, EA[169] |
| R = $CH_2CH_2SMe$ | **173** | yellow crystals, $^1$H NMR, $^{13}$C{$^1$H} NMR, MS, EA, X-ray[181] |
| (3-$^t$Bu-$\eta^5$:$\eta^1$-$C_5H_3SiMe_2N$ $CH_2CH_2NMe_2$)$TiCl_2$ | **174** | orange-red oil, $^1$H NMR, $^{13}$C{$^1$H} NMR, MS[165] |
| ($\eta^5$:$\eta^1$-$C_5Me_4SiMe_2NR$)$TiCl_2$ | | |
| R = 1-$C_6H_4$-2-$PPh_2$ | **175** | brown crystals, $^1$H NMR, $^{13}$C{$^1$H} NMR, MS, $^{31}$P{$^1$H} NMR[181] |
| R = $PhCH_2$ | | yellow crystals, $^1$H NMR, $^{13}$C NMR, MS, EA[170,174] |
| [($\eta^5$-$C_5Me_4$)$SiMe_2$($\eta^1$-$NNMe_2$)]$Ti(NMe_2)_2$ | **176** | refs 176 and 178 |
| [($\eta^5$-$C_5Me_4$)$SiMe_2$($\eta^1$-$NNMe_2$)]$TiCl_2$ | **177** | orange crystals, $^1$H NMR, $^{13}$C NMR, EA, X-ray[176,178] |

**Table 17 (Continued)**

| complex | | color, characterization, etc. |
|---|---|---|
| ($\eta^5$:$\eta^1$-$C_5R^1{}_4CH_2CH_2NR^2$)$TiCl_2$ | | |
| $R^1$ = Me, $R^2$ = Me | **178** | orange crystals, $^1$H NMR, $^{13}$C(APT) NMR,[190,194] EA[190] |
| $R^1$ = Me, $R^2$ = $^i$Pr | **179** | orange crystals, $^1$H NMR,$^{13}$C(APT) NMR, EA[190] |
| $R^1$ = Me, $R^2$ = $^t$Bu | **180** | $^1$H NMR, $^{13}$C(APT) NMR, EA[190] |
| $R^1$ = H, $R^2$ = Me | **181** | orange solid, $^1$H NMR, $^{13}$C NMR, IR, MS, EA[191] |
| $R^1$ = H, $R^2$ = $^i$Pr | **182** | orange solid, $^1$H NMR, $^{13}$C NMR, IR, MS, EA, X-ray[191] |
| $R^1$ = H, $R^2$ = $^t$Bu | **183** | red crystals, $^1$H NMR, $^{13}$C NMR, EA[191] |
| $R^1$ = H, $R^2$ = $SO_2C_6H_4CH_3$ | **184** | yellow solid, $^1$H NMR, $^{13}$C NMR, EA, X-ray[195] |
| [$\eta^5$:$\eta^1$-$C_5H_4(CH_2)_3NR$]$TiCl_2$ | | |
| R = Me | **185** | orange-red solid, $^1$H NMR, $^{13}$C NMR, IR, MS, EA[191] |
| R = $^i$Pr | **186** | red solid, $^1$H NMR, $^{13}$C NMR, IR, MS, EA, X-ray[191] |
| R = $SiMe_3$ | **187** | orange solid, $^1$H NMR,[192,193] EA[192] |
| {3-$SiMe_3$-$\eta^5$:$\eta^1$-$C_9H_5SiMe_2NC(Ph)(Me)H$}$TiCl_2$ | | |
| (*p-R,Sc*) | | red crystals, $^1$H NMR,$^{13}$C NMR, EA, MS[182] |
| (*p-S,Sc*) | | red crystals, $^1$H NMR,$^{13}$C NMR, EA, MS[182] |
| {3-[$CH_3CH_2(CH_2)_n$]-$\eta^5$:$\eta^1$-$C_9H_5SiMe_2N^tBu$}$TiCl_2$ | | |
| *n* = 1 | | $^1$H NMR, $^{13}$C NMR, $^{29}$Si NMR[168] |
| *n* = 2 | | $^1$H NMR, $^{13}$C NMR, $^{29}$Si NMR[168] |
| *n* = 3 | | $^1$H NMR, $^{13}$C NMR, $^{29}$Si NMR[168] |
| *n* = 4 | | $^1$H NMR, $^{13}$C NMR, $^{29}$Si NMR[168] |
| {3-[$CH_2$=$CH(CH_2)_n$]-$\eta^5$:$\eta^1$-$C_9H_5SiMe_2N^tBu$}$TiCl_2$ | | |
| *n* = 1 | | $^1$H NMR, $^{13}$C NMR, $^{29}$Si NMR[168] |
| *n* = 2 | | $^1$H NMR, $^{13}$C NMR, $^{29}$Si NMR[168] |
| *n* = 3 | | $^1$H NMR, $^{13}$C NMR, $^{29}$Si NMR[168] |
| *n* = 4 | | $^1$H NMR, $^{13}$C NMR, $^{29}$Si NMR[168] |
| *n* = 5 | | $^1$H NMR, $^{13}$C NMR, $^{29}$Si NMR[168] |
| [3-R-$\eta^5$:$\eta^1$-$C_9H_5SiMe_2N^tBu$]$TiCl_2$ | | |
| R = $CH_2Ph$ | | $^1$H NMR, $^{13}$C NMR, $^{29}$Si NMR[203] |
| R = $(CH_2)_2Ph$ | | $^1$H NMR, $^{13}$C NMR, $^{29}$Si NMR[203] |
| R = $(CH_2)_3Ph$ | | $^1$H NMR, $^{13}$C NMR, $^{29}$Si NMR[203] |
| R = $CMe_2Ph$ | | $^1$H NMR, $^{13}$C NMR, $^{29}$Si NMR[203] |
| {3-[$CH_3(CH_2)_{19}$]-$\eta^5$:$\eta^1$-$C_9H_5SiMe_2N^tBu$}$TiCl_2$ | | $^1$H NMR, $^{13}$C NMR, $^{29}$Si NMR[356] |
| {2-[$CH_2$=$CH(CH_2)_n$]-$\eta^5$:$\eta^1$-$C_9H_5SiMe_2N^tBu$}$TiCl_2$ | | |
| *n* = 1 | | $^1$H NMR, $^{13}$C NMR, $^{29}$Si NMR[356] |
| *n* = 2 | | $^1$H NMR, $^{13}$C NMR, $^{29}$Si NMR[356] |
| *n* = 3 | | $^1$H NMR, $^{13}$C NMR, $^{29}$Si NMR[356] |
| *n* = 4 | | $^1$H NMR, $^{13}$C NMR, $^{29}$Si NMR[356] |
| {2-($CH^2$=$CHCH_2$)-$\eta^5$:$\eta^1$-$C_9H_5Si[(CH_2)_6CH$=$CH_2]$-MeN$^t$Bu}$TiCl_2$ | | $^1$H NMR, $^{13}$C NMR, $^{29}$Si NMR[356] |
| {2-($CH_3CH_2CH_2$)-$\eta^5$:$\eta^1$-$C_9H_5SiMe_2N^tBu$}$TiCl_2$ | | $^1$H NMR, $^{29}$Si NMR[356] |
| ($\eta^5$:$\eta^1$-$C_5H_2Me_2CH_2CMe_2NH$)$_2$Ti | **188** | yellow crystalline solid, $^1$H NMR, $^{13}$C NMR, MS, UV−vis[196] |
| ($\eta^5$:$\eta^1$-$C_5HMe_3CH_2CMe_2NH$)$_2$Ti | **189** | yellow crystals, mp (dec), $^1$H NMR, $^{13}$C NMR, MS, IR[196] |
| $\eta^5$:$\eta^1$-$C_9H_6SiMe_2NR$}$TiCl_2$ | | |
| R = CHMePh | **190** | deep red crystals, $^1$H NMR, $^{13}$CNMR, EA, [α], X-ray[166], ($R_{Ti}$,$S_c$)$^1$H NMR,$^{13}$C NMR, ($S_{Ti}$,$S_c$)$^1$H NMR, EA, MS[182] |
| R = $C_6H_{11}$ | **191** | orange-red powder, $^1$H NMR,$^{13}$C NMR, EA[166] |
| [2-$R^1$-3-$R^2$-$\eta^5$:$\eta^1$-$C_9H_5SiMe_2N^tBu$]$TiCl_2$ | | |
| $R^1$ = $NMe_2$, $R^2$ = H | **192** | red-brown solid, $^1$H NMR, $^{13}$C{$^1$H} NMR, EA, HRMS, X-ray[201] |
| $R^1$ = OEt, $R^2$ = H | **193** | red-brown solid, $^1$H NMR, $^{13}$C{$^1$H} NMR, EA, HRMS, X-ray[201] |
| $R^1$ = H, $R^2$ = OMe | | $^1$H NMR, $^{13}$C{$^1$H} NMR, EA, HRMS, X-ray[201] |
| $R^1$ = H, $R^2$ = $C_4H_8N$ | | $^1$H NMR, $^{13}$C{$^1$H} NMR, EA, HRMS, X-ray[201] |
| {$\eta^5$:$\eta^1$-(2-$C_9H_6$)$SiMe_2N^tBu$}$TiCl_2$ | | red-brown crystals, mp, IR, $^1$H NMR, $^{13}$C{$^1$H} NMR, EA[204] X-ray[189] |

have a more "open" active site (Cp−Ti−N bite angle of 101.12°) and an increasing unsaturation of the Ti−N bond [length 1.857 Å (11)] indicating a significant property change.

The data of X-ray single-crystal diffraction for the ethylene-bridged cyclopentadienylamide titanium complexes show that this type of complex still belongs to the CGC class.[191] By studying the structures of [$C_5Me_4(SiMe_2)N^tBu$]$TiCl_2$ and [$C_5Me_4(CH_2)_2N^tBu$]-$TiCl_2$, it was found that the Cp(centroid)−Ti−N bite angle (and the Ti−N lengths) of the two complexes are practically identical, being 107.8° (2) for the $Me_2Si$ bridge and 107.9° for $(CH_2)_2$, (1.910 and 1.909 Å, respectively).[171,177] Teuben investigated the influence of the length of the spacer bridge group on the Ti−Cl, Ti−N, and Ti−C (centroid) distances and Cl−Ti−Cl angles of the two compounds [$\eta^5$:$\eta^1$-$C_5H_4$-$(CH_2)_2N^iPr$]$TiCl_2$ and [$\eta^5$:$\eta^1$-$C_5H_4(CH_2)_3N^iPr$]$TiCl_2$. The results showed that these parameters are hardly affected by variation of the length of the bridge.

However, from the crystal data in Figure 36 we may conclude that the short Ti−N distance [2, 1.864(2) Å; 5, 1.8668(15) Å] and the planar geometry of the nitrogen atom in both complexes indicated $sp^3$ hybridization of the N atom with the out-of-plane lone pair giving an N(p$\pi$)→Ti(d$\pi$) polarized Ti−N bond. The significant downfield shift (**182**, 5.92 ppm; **186**, 6.57 ppm) of the methine protons on the isopropyl group in the two complexes may be a direct consequence of the anisotropic effect caused by the titanium-amido nitrogen polarization, and the same phenomenon can also be observed in the case of ($\eta^5$:$\eta^1$-$C_5H_4SiMe_2N^iPr$)$TiCl_2$.[174] However, the key parameter (the Cp−Ti−N bite angle) changed a lot with the

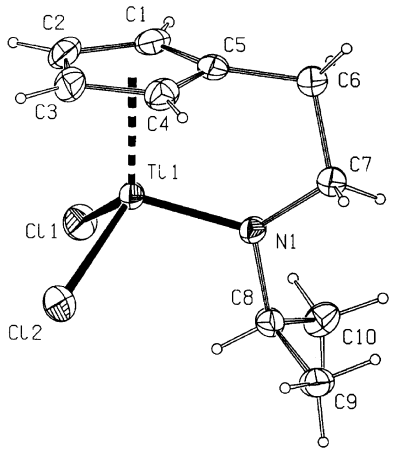


**Figure 37.** Structure of ($\eta^5$:$\eta^1$-$C_5H_4CH_2CH_2N^iPr$)$TiCl_2$ (**182**) in the crystal.[191] (Reprinted with permission from ref 191. Copyright 1997 American Chemical Society.)

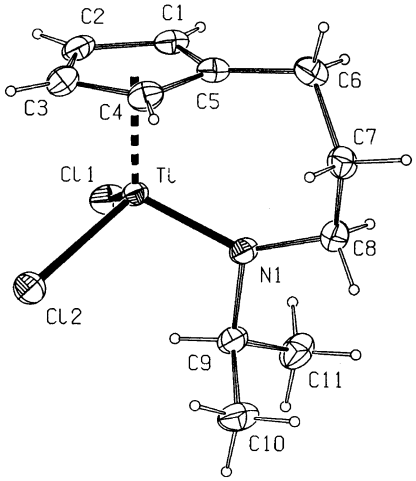


**Figure 38.** Structure of [$\eta^5$:$\eta^1$-$C_5H_4(CH_2)_3N^iPr_2$]$TiCl_2$ (**186**) in the crystal.[191] (Reprinted with permission from ref 191. Copyright 1997 American Chemical Society.)

variation of the length of spacer. In **186**, the Cp−Ti−N angle is 112.6(1)°, against only 104.47(1)° in **182** (Figures 37 and 38), which is even smaller than in the prototypical CGC complex ($\eta^5$:$\eta^1$-$C_5Me_4SiMe_2$-$N^tBu$)$TiCl_2$ (**137**) (107.8°). It is clear that the shorter $C_2$ spacer creates a much more open metal center than $C_3$ or the ubiquitous Si bridges.

In the ethylene-bridged "bis-CGC" titanocene **188** (Figure 39) a Ti−N bond length of similar distance [1.96(4)−1.969(4) Å] can also be seen with a N−Ti−Cp angle [100.6(2)−101.8°] caused probably as a result of the steric congestion around the Ti, leading to one of the smallest Cp−Ti−Cp angles of 87.2−87.6°, compared 132.60° in Cp metallocenes.[196,197]

Also, the introduction of additional pendant neutral coordination sites (OMe, $NMe_2$, and C=C) to the Cp or Ind moeity has been shown by X-ray structural analysis to produce metallocenes that are not different from ordinary unsubstituted ones.[201] No evidence of interaction between the potentially chelating pendant ligands and the central metal was observed (Figures 40 and 41).

The sheer volume of literature still pouring in on the linked-amido titanium complexes has established them presently as the most studied of the Cp- and

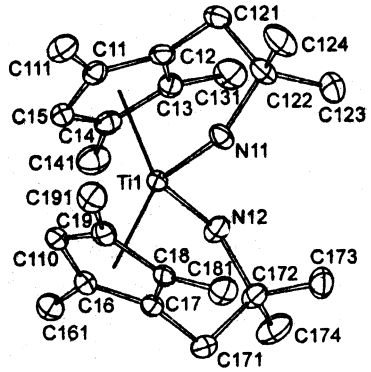


**Figure 39.** Structure of ($\eta^5$:$\eta^1$-$C_5H_2Me_2CH_2CMe_2NH)_2Ti$ (**188**) in the crystal.[196] (Reprinted with permission from ref 196. Copyright 2000 Elsevier Sequoia.)

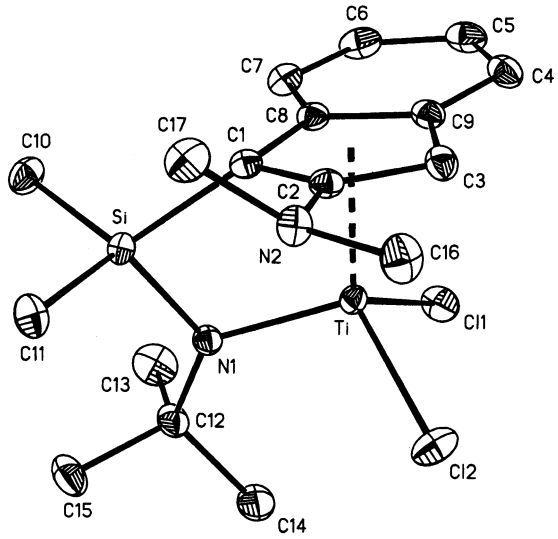


**Figure 40.** Structure of [2-$NMe_2$-$\eta^5$:$\eta^1$-$C_9H_6SiMe_2N^tBu$]-$TiCl_2$ (**192**) in the crystal.[201] (Reprinted with permission from ref 201. Copyright 2001 American Chemical Society.)

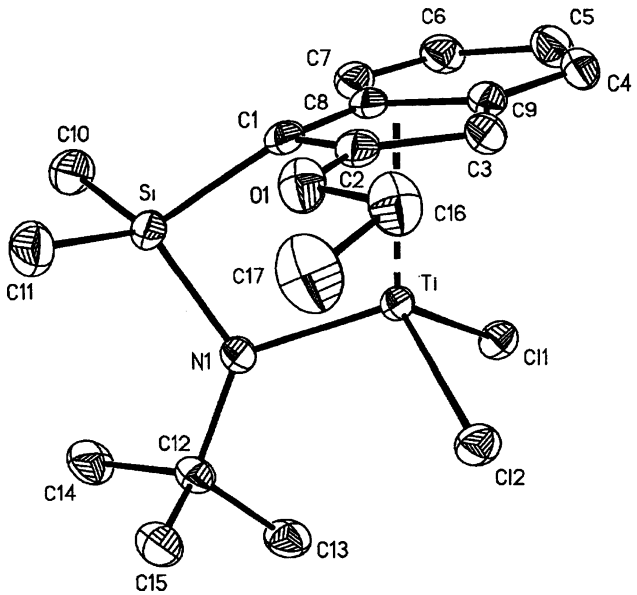


**Figure 41.** Structure of [2-OEt-$\eta^5$:$\eta^1$-$C_9H_6SiMe_2N^tBu$]-$TiCl_2$ (**193**) in the crystal.[201] (Reprinted with permission from ref 201. Copyright 2001 American Chemical Society.)

Ind-based titanium compounds. Hence, in Table 17 we present references, means of characterization, and

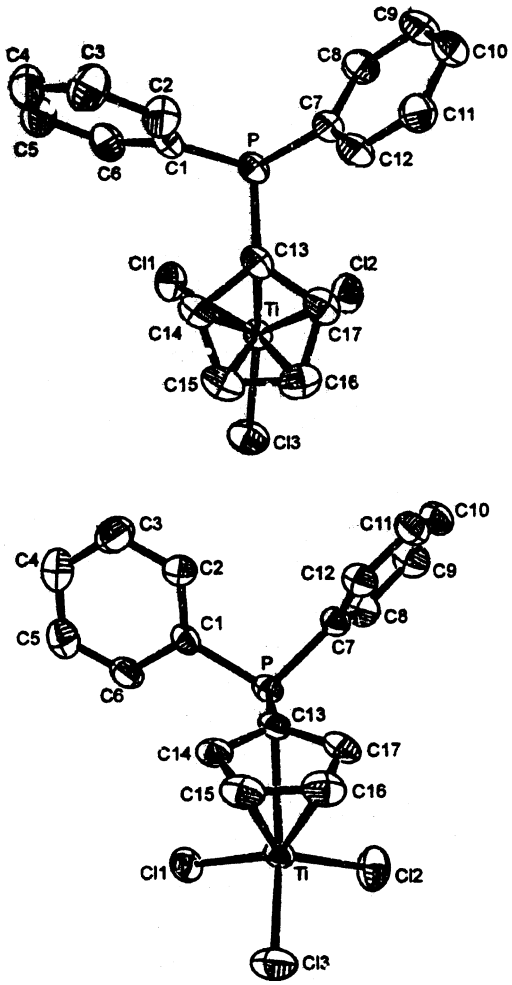


**Figure 42.** Structure of ($\eta^5$-$C_5H_4PPh_2$)$TiCl_3$ (**194**) in the crystal.[71] (Reprinted with permission from ref 71. Copyright 2000 Elsevier Sequoia.)

some physical property data on compounds reported to date.

### *4. Mono-Cp(Ind) Titanium Complexes Containing Pendant Phosphino Side Groups*

The air- and moisture-sensitive phosphinoalkyl-substituted complex **194** was prepared by the reaction of a trimethylsilyl cyclopentadiene derivative with $TiCl_4$ (Scheme 75) or by the reaction of thallium salt with $TiCl_4$ to give complex **195** (Scheme 76).[71]

The single crystal of **194** was successfully obtained through recrystallization with a $CH_2Cl_2$/hexane mixture.[71] The anticipated piano stool configuration around the titanium atom was confirmed (Figure 42); also, the Ti−Cl bond distances and the Cl−Ti−Cl angles are very similar to those of the unsubstituted ($\eta^5$-$C_5H_5$)$TiCl_3$.[205,206] There is no evidence to suggest any interaction between the phosphorus atom in the side chain and the central titanium atom with the Ti−P distance being 3.525(1) Å.

**Scheme 75**

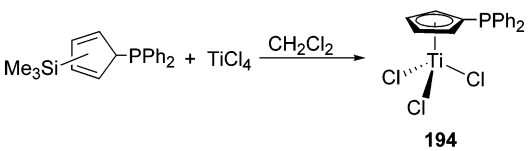


**194**

**Scheme 76**

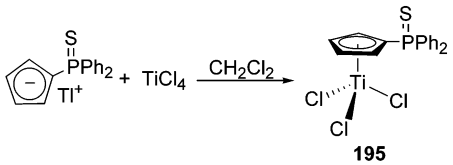


**195**

### *5. Mono-Cp(Ind) Titanium Complexes Functionalized by Bulky Side Groups*

Mono-cyclopentadienyl titanium complexes functionalized by bulky substituents (**196** and **197**) are synthesized directly from the trimethylsilylated bulky Cp ligand (or titanocene) and titanium tetrachloride (Schemes 77[207] and 78).[45] In addition, it is a common technique to use homoleptic metal amides $Ti(NR_2)_4$ via amine elimination followed by halogenation, similar to the earlier described route 2 (see section II.A.1) (Scheme 79).[31]

**Scheme 77**

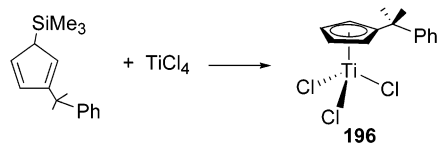


**196**

**Scheme 78**

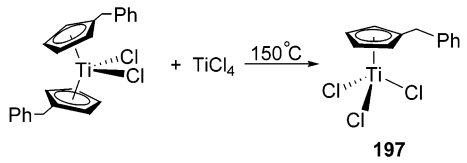


**197**

**Scheme 79**

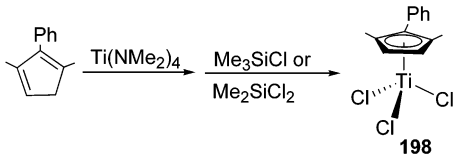


**198**

The molecular structure of ($\eta^5$-$C_5H_4CMe_2Ph$)$TiCl_3$ shows the piano-stool geometry typical of half-metallocenes and similar to that of the standard unsubstituted $CpTiCl_3$ complex in most respects (Figure 43). The phenyl ring is almost perpendicular to the Cp-ring plane, and no coordination between the phenyl ring and the central titanium atom was observed in this case.[207]

Following the observation that $IndTiCl_3$ is a significantly better olefin polymerization precursor than $CpTiCl_3$, researchers thought that by using bulkier substituents the result may even be further improved; hence, this finding resulted in massive interest in bulky aromatic substituted indenyltrichlorotitanium complexes.[208] Conversion of aromatic bearing (un)substituted benz[*e*]indene ligands into the corresponding titanium complexes was readily achieved by conventional metathetical procedures. Thus, the reaction between

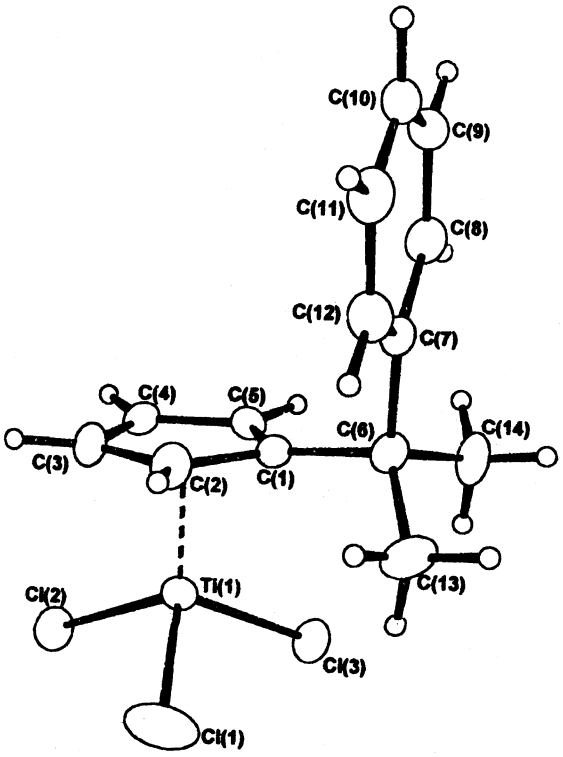


**Figure 43.** Structure of ($\eta^5$-$C_5H_4CMe_2Ph$)$TiCl_3$ (**196**) in the crystal.[207] (Reprinted with permission from ref 207. Copyright 1999 Elsevier Sequoia.)

**Scheme 80**

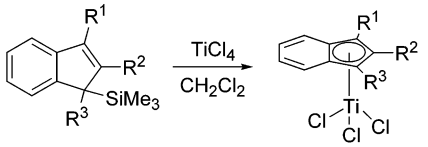


**199**: $R^1$ = Ph, $R^2$ = $R^3$ = H
**200**: $R^1$ = Ph, $R^2$ = H, $R^3$ = Ph
**201**: $R^1$ = $CH_2Ph$, $R^2$ = $R^3$ = H
**202**: $R^1$ = $CH_2CH_2Ph$, $R^2$ = $R^3$ = H

**Scheme 81**

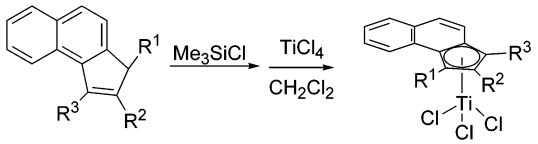


**203**: $R^1$ = $R^2$ = $R^3$ = H
**204**: $R^1$ = $R^3$ = H, $R^2$ = $CH_3$
**205**: $R^1$ = $R^2$ = $R^3$ = $CH_3$

(trimethylsilyl)benz[*f*]indene and $TiCl_4$ was carried out at −78 °C in both $CH_2Cl_2$ and toluene (Schemes 80−82).

Rausch[209] and Xu[210] independently reported the synthesis of tetrahydro-2-methylbenzindenyltitanium complexes as outlined in Schemes 83 and 84 respectively.

Britzinger and co-workers[211] synthesized cyclopenta[*l*]phenanthrene titanium trichloride and the corresponding 2-methyl and phenyl derivatives (Scheme 85). The crystal structure of **212** (R = Me) was determined by X-ray diffraction analysis (Figure 44), exhibiting the typical piano stool structure of half-titanocenes.

**Scheme 82**

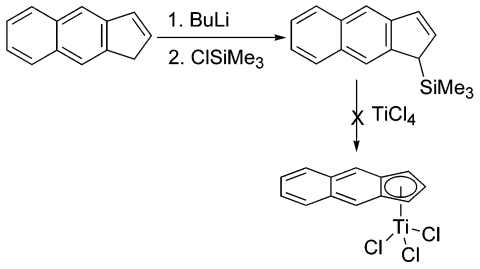


**Scheme 83**

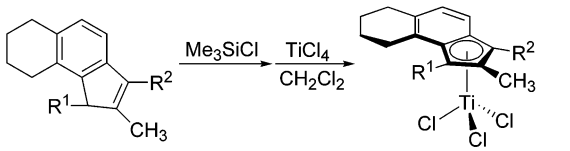


**206**: $R^1$ = $R^2$ = H
**207**: $R^1$ = H, $R^2$ = $CH_3$
**208**: $R^1$ = H, $R^2$ = Ph
**209**: $R^1$ = $CH_3$, $R^2$ = $CH_3$

**Scheme 84**

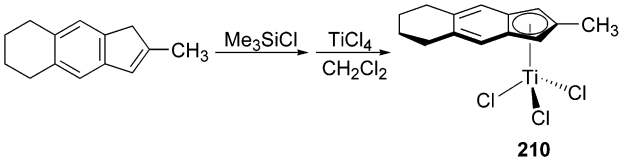


**210**

**Scheme 85**

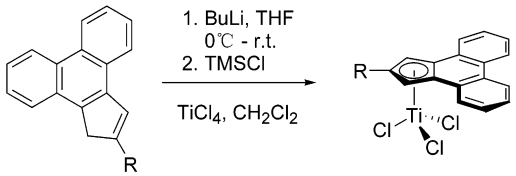


**211**: R = H
**212**: R = Me
**213**: R = Ph

Table 18 presents data on the physical properties, references, and methods of characterization for recently reported bulky group functionalized half-sandwich cyclopentadienyl titanium complexes.

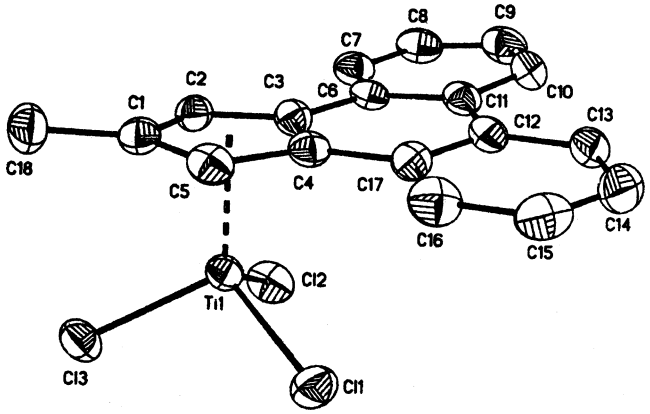


**Figure 44.** Structure of 2-methylcyclopenta-[*l*]-phenanthrene titanium trichloride (**212**) in the crystal.[211] (Reprinted with permission from ref 211. Copyright 1997 Elsevier Sequoia.)

**Table 18. Cp′TiCl$_3$ Containing a Bulky Group in the Side Chain**

| complex | | color, characterization, etc. |
|---|---|---|
| ($\eta^5$-$C_5H_4CMe_2Ph$)$TiCl_3$ | **196** | orange crystals, $^1$H NMR, $^{13}$C NMR, EA, X-ray[207] |
| ($\eta^5$-$C_5H_4CMe_2CH_2Ph$)$TiCl_3$ | | dark red oil, $^1$H NMR, $^{13}$C NMR[207] |
| ($\eta^5$-$C_5H_4SiMe_2Ph$)$TiCl_3$ | | yellow needles, $^1$H NMR, $^{13}$C NMR, EA, X-ray[207] |
| ($\eta^5$-$C_5H_4CHPh_2$)$TiCl_3$ | | orange crystals, $^1$H NMR, $^{13}$C NMR, EA, X-ray[207] |
| ($\eta^5$-$C_5H_4CH_2Ph$)$TiCl_3$ | **197** | orange solid, $^1$H NMR, MS, EA[45] |
| (1,3-$R^1_2$-2-$R^2$-$\eta^5$-$C_5H_2$)$TiCl_3$ | | |
| $R^1$ = Ph, $R^2$ = Bu | | reddish crystalline solid, $^1$H NMR, $^{13}$C NMR, EA, MS[31] |
| $R^1$ = Me, $R^2$ = Ph | **198** | red crystalline solid, $^1$H NMR, $^{13}$C NMR, EA, X-ray[31] |
| $R^1$ = $R^2$ = Ph | | $^1$H NMR, $^{13}$C NMR, EA[31] |
| ($\eta^5$-$C_5H_4CPh_3$)$TiCl_3$ | | bright yellow crystals, $^1$H NMR, X-ray[78] |
| ($\eta^5$-$C_5Me_4CH_2CH_2Ph$)$TiCl_3$ | | red needles, $^1$H NMR, $^{13}$C NMR, EA, X-ray[212] |
| ($\eta^5$-$C_5H_4C_6F_5$)$TiCl_3$ | | orange crystals, $^1$H NMR, EA[73] |
| [$\eta^5$-$C_5H_4CMe_2(C_{13}H_9)$]$TiCl_3$ | | yellow crystals, $^1$H NMR, $^{13}$C{$^1$H} NMR, MS, EA[213] |
| (1-$R^1$-2-$R^2$-3-$R^3$-$\eta^5$-$C_9H_4$)$TiCl_3$ | | |
| $R^1$ = Ph, $R^2$ = $R^3$ = H | **199** | purple crystals, $^1$H NMR, EA[208] |
| $R^1$ = H, $R^2$ = Ph, $R^3$ = H | | red solid, $^1$H NMR, EA[208] |
| $R^1$ = Ph, $R^2$ = H, $R^3$ = Ph | **200** | green crystals, $^1$H NMR, EA[208] |
| $R^1$ = $CH_2Ph$, $R^2$ = $R^3$ = H | **201** | purple crystals, $^1$H NMR, EA[208] |
| $R^1$ = $CH_2CH_2Ph$, $R^2$ = $R^3$ = H | **202** | burgundy solid, $^1$H NMR, EA[208] |
| [1-$R^1$-2-$R^2$-3-$R^3$-$\eta^5$-($C_{13}H_6$)[a]]$TiCl_3$ | | |
| $R^1$ = $R^2$ = $R^3$ = H | **203** | red-orange crystals, $^1$H NMR, EA[208] |
| $R^1$ = $R^3$ = H, $R^2$ = $CH_3$ | **204** | red crystals, $^1$H NMR, EA[208] |
| $R^1$ = $R^2$ = $R^3$ = $CH_3$ | **205** | purple crystals, $^1$H NMR, EA[208] |
| [1-$R^1$-2-Me-3-$R^2$-$\eta^5$-($C_{13}H_{10}$)[c]]$TiCl_3$ | | |
| $R^1$ = $R^2$ = H | **206** | red crystals, $^1$H NMR, EA,[209,210] MS[209] |
| $R^1$ = H, $R^2$ = $CH_3$ | **207** | brown/red crystals, $^1$H NMR, EA, MS[210] |
| $R^1$ = H, $R^2$ = Ph | **208** | red solid, $^1$H NMR, EA, MS[210] |
| $R^1$ = $CH_3$, $R^2$ = $CH_3$ | **209** | red/purple crystals, $^1$H NMR, EA, MS[210] |
| [2-Me-$\eta^5$-($C_{13}H_{12}$)[d]]$TiCl_3$ | **210** | red crystals, $^1$H NMR[209] |
| [2-R-$\eta^5$-($C_{17}H_{10}$)[b]]$TiCl_3$ | | |
| R = H | **211** | red solid, $^1$H NMR, $^{13}$C NMR, HMQC, EA, MS[211] |
| R = Me | **212** | red needles, $^1$H NMR, $^{13}$C NMR, HMQC, EA, MS, X-ray[211] |
| R = Ph | **213** | red solid, $^1$H NMR, $^{13}$C, HMQC, COSY, EA, MS[211] |

[a] a: 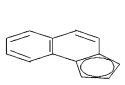 b: 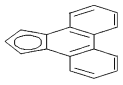 c: 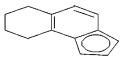 d: 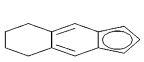

## C. Miscellaneous Titanium Complexes

The first cyclopentadienyl titanocene containing borane was synthesized by Jutzi and co-workers,[214] who prepared a series of titanium complexes ($\eta^5$-$C_5H_3RBX_2$)$TiCl_3$ (R = H, Me; X = Cl, Br, OEt, or Me) by the dehalosilylation of ($C_5H_3RBX_2$)$SiMe_3$. Since then, few investigations on titanium complexes containing the borane ligand have been reported. Recently, however, due to the potential for application in homogeneous olefin polymerization catalysis, there is renewed interest in their synthesis. Thus, with techniques similar to Jutzi's, a series of related catecholboryl- and phenylboryl-substituted titanium trichloride complexes[134b] and [$\eta^5$-$C_5H_4B(C_6F_5)_2$]$TiCl_3$ **214** have been reported (Scheme 86).[215]

**Scheme 86**

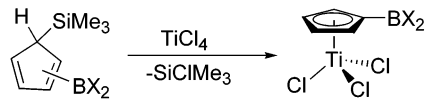


**214**: $BX_2$ = $B(C_6F_5)_2$
**215**: $BPh_2$
**216**: BPhCl
**217**: $B(O_2C_6H_4)$

The single-crystal X-ray diffraction indicated that the structure of the complex [$\eta^5$-$C_5H_4B(C_6F_5)_2$]$TiCl_3$ (**214**) is monomeric with the familiar piano stool geometry (Figure 45). The Ti−Cl bond distance [2.2240(7) Å] and Ti−Cp centroid distance (2.02 Å) are comparable to typical cyclopentadienyl titanium trichloride complexes.

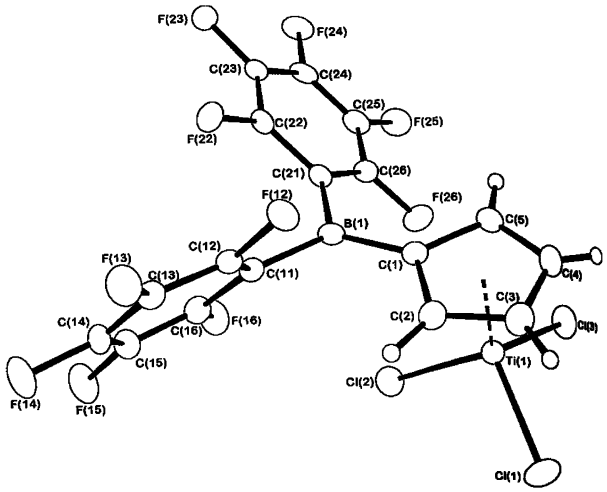


**Figure 45.** Structure of [$\eta^5$-$C_5H_4B(C_6F_5)_2$]$TiCl_3$ (**214**) in the crystal.[215] (Reprinted with permission from ref 215. Copyright 1997 American Chemical Society.)

Broussier[216] reported the synthesis of [$\eta^5$-$C_5Me_4SCH_2CH_2CH_3$]$_2TiCl_2$ (**218**) via the reaction of propylthio-substituted tetramethylcyclopentadienylsodium with $TiCl_3$·3THF in $CCl_4$ (Scheme 87).

**Table 19. Titanium Complexes Functionalized by Miscellaneous Ligands**

| complex | | color, characterization, etc. |
|---|---|---|
| $(\eta^5\text{-}C_5H_4BX_2)TiCl_3$ | | |
| $BX_2 = B(C_6F_5)_2$ | **214** | yellow-orange crystals, $^1$H NMR, $^{13}$C NMR, $^{11}$B NMR, EA, X-ray[215] |
| $BX_2 = BPh_2$ | **215** | lime green powder, $^1$H NMR, $^{13}$C NMR, $^{11}$B NMR, EA, EI-MS[134b,215] |
| $BX_2 = BPhCl$ | **216** | olive green powder, $^1$H NMR, $^{13}$C NMR, $^{11}$B NMR, EA, EI-MS[134b,215] |
| $BX_2 = B(C_6H_4O_2)$ | **217** | brick red solid, $^1$H NMR, $^{13}$C NMR, $^{11}$B NMR, EA, EI-MS[134b,215] |
| $(\eta^5\text{-}C_5Me_4SR)_2TiCl_2$ | | |
| $R = CH_2CH_2CH_3$ | **218** | black crystals, $^1$H NMR, $^{13}$C NMR, EA, MS, X-ray[216] |
| $(\eta^5\text{-}C_9H_6SCH_3)TiCl_3$ | | blue-green needles, $^1$H NMR, EA[137] |

**Scheme 87**

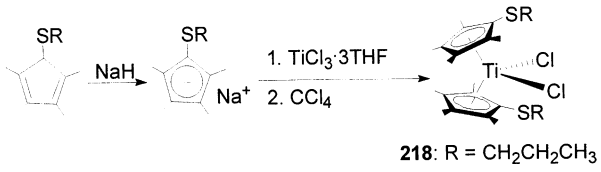


**218**: R = $CH_2CH_2CH_3$

The steric influence on the geometry of the titanocene exerted by the $C_5Me_4SPr$ ligands is similar to that of the $C_5Me_5$ and $C_5Me_4PPh_2$ ligands with comparable Cp−Ti−Cp bite angles. It is noteworthy to observe that the $C_5Me_4SPr$ are poorer donor ligands than $C_5Me_5$ because the Cl−Ti−Cl angle of 93.4° observed in the titanocene is intermediate between the values found for the permethylated complexes (92.9°) and the unsubstituted complexes (94.5°) (Table 19).

## *III. Catalytic Applications of Ring-Substituted Titanium(IV) Complexes*

Ziegler first made use of titanium-based compounds as catalysts in 1953, when he produced high-density polyethylene (HDPE) by employing diethylaluminum chloride as cocatalyst.[217] This was followed the finding by Natta that semicrystalline polypropylene was obtainable from titanium compounds, and this led to the creation of the traditional Ziegler−Natta (Z−N) catalysts.[218] For almost 50 years now further developments in polymer science have become closely entangled with breakthroughs in organometallic chemistry research. Z−N catalysts are heterogeneous multiple active site systems that afford little control over polymer microstructure and properties in some cases; hence, study of their mechanisms of action was very difficult. This has made development of new and more efficient catalyst systems almost impossible until the serendipitous discovery in 1977 by Sinn and Kaminsky[219,220] that hydrolyzed $Me_3Al$ called methylalumoxane (MAO) can activate titanocenes and other group IV metallocenes for the polymerization of ethylene and α-olefins stimulated a flurry of activity and renewed interest in both academia and industry into research on what may be termed second-generation catalysts. In comparison with Z−N catalysts, the metallocene catalysts are very attractive because they offer certain advantages. They are homogeneous single active site compounds of very high activity that may be heterogenized to provide added advantages in terms of control of polymer properties, activity, and microstructure. Their ability to polymerize α-olefins with a great deal of stereocontrol is unprecedented.

Despite all of the interest and efforts toward the development of metallocene-based catalysts, commercialization of the process suffers from some deficiencies such as the excessive amounts of expensive MAO required for activation (up to 15000 molar equiv of transition metal). This is impractical both commercially in terms of cost and technologically in terms of the amount of residues left in the polymer, because commercial Z−N catalysts require only an Al-to-catalyst ratio of 50−200:1. This shortcoming has opened the avenue for the development of the so-called third-generation catalysts. These are single-component catalysts that are self-activating without the need for either a cocatalyst or a stoichiometric amount of weakly binding non Al-based cocatalysts, such as the tetra(pentafluorophenyl) borate anion $[(C_6F_5)_4B]^-$ and its derivatives.[221] Also along this line is the development of the so-called CGC, hybrids of the sterically unsaturated, open-structured bis(amido) chelate complexes developed in 1990 by Bercaw and Shapiro[162,222,223] and the *ansa*-metallocenes developed by Brintzinger.[5,19] Further developments have seen the introduction of heterogenized catalyst systems supported on a porous inorganic support such as silica, alumina, or $MgCl_2$.[221] This generally brings down dramatically the amount of required MAO to 100−500 molar equiv.

In discussions involving catalyst systems (precursor + cocatalysts) the efficiency of the catalyst is generally expressed as the combination of the polymer yield, the activity, and the stereo- or regiospecificity when applicable. Different authors express activities in different ways, such as the weight (grams or kilograms) of polymer/[(moles (grams) of catalyst) × hours × (moles of monomer)]. In this paper the expression used by the source author will be maintained.

### A. Mechanism of Polymerization and Termination

The process of polymerization using bent metallocene catalysts is thought to be governed by the Cossee−Arlman mechanism (Scheme 88).[224,225] This very simple mechanism initially proposed in the early 1960s for the traditional Z−N system is still valid for almost all of the generations of catalyst systems discussed above.[226−228]

Referring to Scheme 88, the treatment of a solution of $Cp_2TiCl_2$ in a non-coordinating solvent such as toluene with MAO results in a fast ligand exchange producing the partially alkylated compound

**Scheme 88. Cossee−Arlman Mechanism**

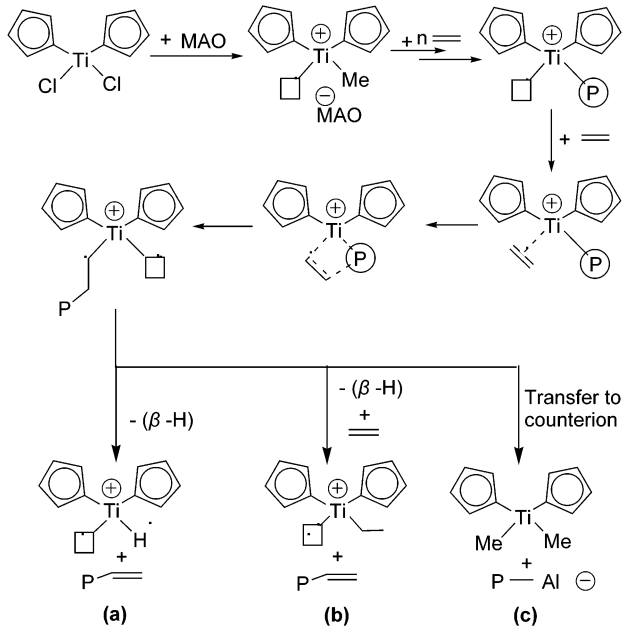


$Cp_2TiMeCl$, and the use of an excess of MAO ensures full alkylation to $Cp_2TiMe_2$. A rapid complexation reaction follows that produces the active species as an electron-deficient cation $[Cp_2TiMe]^+$ stabilized by a complex anion of MAO. Attack by a monomer ($CH_2{=}CH_2$) molecule produces an α-agostic $\pi$-complex, where it is coordinated by the insertion of its $\pi$-bond into the metal carbon $\sigma$-bond of the bound methyl group or growing polymer chain. Regio-(stereo)selectivity of α-olefin (co)polymerization occurs at this stage by either stereogenic site control or polymer chain-end control. Coates[20] has beautifully reviewed the subject of regio- and stereospecific control in single-site metallocene catalyst systems, so we will discuss only specific cases relevant to titanocenes that appeared in very recent literature. MAO (and especially free $Me_3Al$ in it) has been identified to function as a scavenger for impurities and moisture and also as a stabilizer against bimetallic deactivation of the active titanium species.

Chain transfer and termination may occur via a variety of pathways depending on the type of metallocene catalyst used, solvent type, and the presence or not of other additives in the system. The most common is by $\beta$-hydrogen transfer to the metal (agostic $\beta$-H...Ti interaction) (a) or to an incoming monomer (b) to produce a $CH_2{=}C(Me){\sim}P$-terminated polymer chain. Transfer to metal and to a monomer results in the production of new metal hydride and metal alkyl active sites, respectively. Similarly, crowded metallocenes favor $\beta$-methyl transfer, in the process also producing $CH_2{=}C(Me){\sim}P$-terminated polymer chain and new metal alkyl active sites. Transfer to Al produces a metal-crowned polymer unit ($Al{-}CH_2{-}CH_2{\sim}P$) that is also capable of further coordination to the transition metal (c). The relative rate of chain propagation to chain termination (and transfer) in olefin and related polymerization determines the chain length and molecular weight of the polymer.

The Cossee−Arlman mechanism is able to explain the path of most metallocene-catalyzed (co)polymerization to date but is unable to explain all experimental observations. The alternative carbocationic polymerization mechanism and the other mechanism for ring-opening melathesis polymerization (ROMP) and hydrogenation will be fully discussed in the corresponding section.

The role of counterions and cocatalysts in olefin polymerization is still a subject of discussion and research interest; several reviews, notably by Bochmann[229] and Chen and Marks,[221] have addressed some of the salient points and the gray areas as they relate to polymer chain growth and termination. Many theoretical studies have been conducted on the role of the cocatalyst and its counterion on the initiation, propagation, and termination steps in olefin polymerization by group IV metallocenes.[230−233]

## B. Polyethylene

Polymerization of ethylene (ethene) to polyethylene (PE) has a long history in polymer chemistry. Development of such catalyst systems as the Z−N and Phillips (a chromium-based) catalyst are centered on this simplest of all olefin monomers. Application of metallocenes to the production of PE, its developmental history, mechanisms, and the various uses of the polymer have been the subject of several reviews and books.[234,235] Here we shall discuss only the latest developments in utilizing titanocenes in this area over the period covered by the review as earlier reviews have covered most of the background information (Chart 18).

It is important to always remember that the data to be presented and discussed came from different sources using experimental conditions that are not uniform; therefore, it is very difficult and oftentimes misleading to arrive at general conclusions and establish trends merely on the basis of comparing these data because each laboratory employs its own experimental conditions and standards. Despite this, it has been possible to establish observable general patterns for metallocenes irrespective of the source of the data, and, with this in mind, we will try to establish some unambiguous and readily observable patterns for titanocenes in olefin and similar polymerization catalysis.

Generally, as a measure of quality of a catalyst system we will refer to the activity or productivity (reported by almost every researcher) and, to some extent, the molecular weight. For the polymerization of propylene and higher olefins and copolymerization reactions, the selectivity of a catalyst will be as crucial as its ability to produce tons of polymers.

### *1. Ethylene Polymerization Initiated by Sandwich Titanocenes*

Ethylene polymerization using sandwich titanocenes has been accomplished using MAO and perfluoro phenyl borane cocatalysts. Bridged complexes are found to exhibit higher catalytic efficiency compared to the unbridged counterparts in the case of ethylene

**Chart 18. (a) Sandwich Titanium Catalysts for Ethylene Polymerization; (b) Half-Sandwich Titanium Catalysts and Constrained Geometry Catalysts for Ethylene Polymerization**

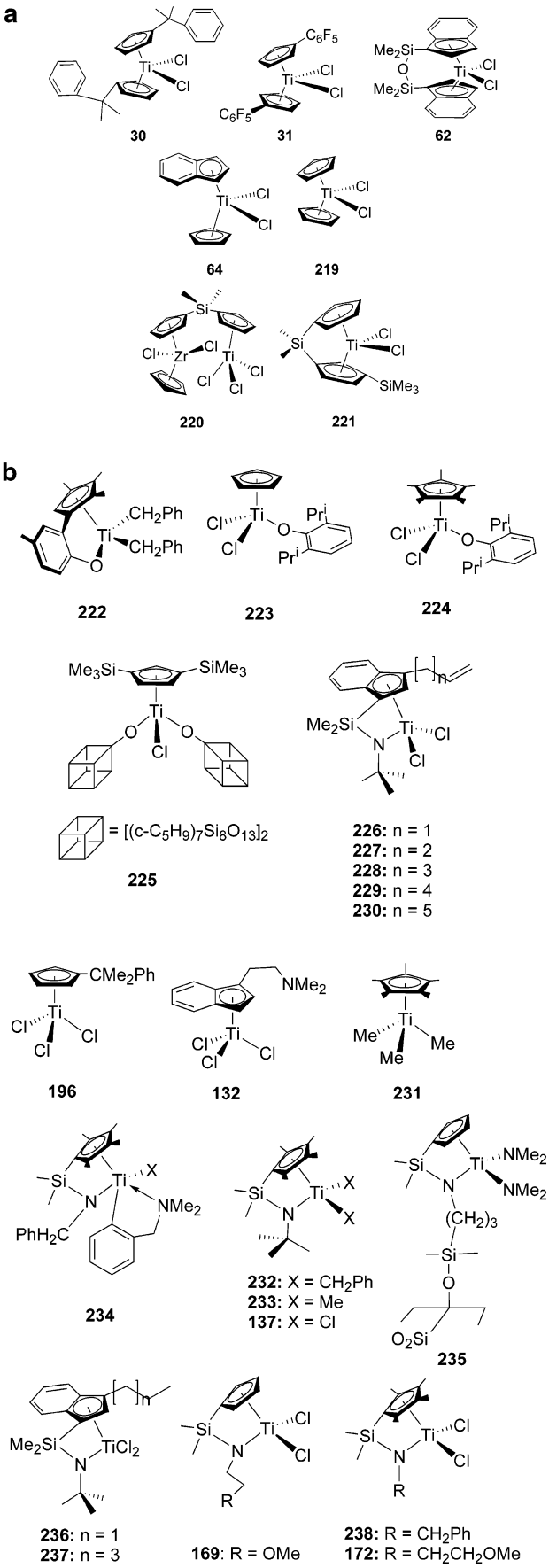


polymerization under a certain condition. Also, the nature of the bridging unit, the type of Cp or Ind ring substituents, and the conditions of polymerization such as the nature of the counterion and the amount of catalyst all affect catalytic activity. Low molecular weight polyethylene is produced by bridged complexes due to the large open bite angle at the active center that favors chain transfer.[16]

Chien, Rausch, and co-workers[114] demonstrated the effects of the nature of the counterion on ethylene polymerization by employing the first disiloxane-bridged bis(indenyl)titanium complex **62**. The triatomic bridged complex showed a moderate activity (*A*) of $4.91 \times 10^3$ kg of PE/mol of catalyst when MAO was the cocatalyst, but remarkably enough under similar conditions the $Ph_3C^+B(C_6F_5)_4^-$TIBA cocatalyst developed by the same group[236] showed no activity toward ethylene. As this was the first catalyst system showing such unusual behavior, the authors reasoned that the difference might be due to $\sigma$-donation from the bridging oxygen atom to the metal center. In the case of the inert and noncoordinating $Ph_3C^+B(C_6F_5)_4^-$TIBA cocatalyst, the titanocenium ion is exposed due to the absence of a counterion, a situation that greatly decreases the electrophilicity of the metal center, resulting in destabilization of the M−C bond. However, with MAO $\sigma$-complexation will restore the electron deficiency at the metal center and ethylene polymerization activity. Generally, the $C_2$ symmetric bridged substituted Cp-titanocenes showed moderate to low activity to the polymerization of ethylene.[89,237] The authors attribute such low activity to the presence of bulky substituents on the Cp ring. The $C_{2v}$ symmetric complex **31** synthesized by Rausch and coworkers[73] is probably an attempt at creating a single-component catalyst by incorporating the catalytic properties of the pentafluorophenyl ligand into a titanocene structure to mimic a titanocenium active species in solution. Due primarily to a steric reason, which is so strong as to prevail over any electronic benefits in unbridged complexes having bulky Cp[42,238] and Ind[239] substituents, the polymerization activities are much lower than in $Cp_2TiCl_2$ under similar conditions.

### *2. Ethylene Polymerization Initiated by Half-Sandwich Titanium Complexes*

The mono-Cp(Ind) titanium complexes are sterically less hindered and electronically less saturated than the sandwich complexes. Therefore, the active site is more accessible to incoming monomer, and this is a plus in ethylene polymerization because it is not governed by selectivity concerns as in the case of propylene and higher olefins. Among the mono-Cp titanium complexes, the constrained geometry catalysts functionalized by a side amido chain have received more attention recently. Both MAO and the perfluorinated boranes have been applied as cocatalysts to generate the 10-electron active species $[Cp'TiR_2]^+$.[240] For a better understanding of the kinetics of olefin polymerization at the molecular level, perfluoro aryl boranes and borates are used to generate the active species because they afford

intermediates that could be isolated and characterized, rather than the complicated and intractable species produced by MAO activation of $Cp^*TiMe_3$.[84] It has been shown[237,241] that a 1:1 molar reaction of $Cp^*TiMe_3$ with the perfluoro aryl borane $B(C_6F_5)_3$ forms a methyl-bridged species which forms the basic source of the active species $[Cp^*TiR_2]^+$. Understanding the kinetics and nature of this cation−anion pair gives much insight into catalyst molecular structure, activity, stereoregulation, and chain transfer/stability characteristics. Marks and co-workers have elucidated the intermediary ion pairs in the reaction of $CGCTi(CH_2Ph)_2$,[172] which, due to phenyl coordination, are more stable than $CGCTi(Me)_2$ and therefore could be isolated and analyzed, shedding light into the nature of the active species in perfluorophenyl borate cocatalyzed polymerization of ethylene.

On the influence of catalyst structure[181,168,242] on reactivity a systematic study by Alt et al.[168] has further confirmed that under similar conditions indenylidene complexes have much higher polymerization activities than the corresponding Cp compounds, because the weaker $\pi$-donor effect of the indenyl system increases the Lewis acidity at the central metal. General trends on the influence of Cp and Ind side chains on polymerization of olefins cannot be wholly explained on the basis of steric and electronic considerations alone. For example, steric and electronic considerations alone cannot fully explain the recent example of the ethylene polymerization catalyst that switches to ethylene trimerization (to 1-hexene) with a high activity by simply changing the ligand substituent R in $[(\eta^5\text{-}C_5H_4CMe_2R)TiCl_3]$/MAO from a methyl to a semilabile phenyl group.[243,244] In a similar situation using $B(C_6F_5)_3$ as the cocatalyst it was observed[245] that branched polyethylene having the features of LLDPE may be obtained by selecting the right experimental conditions that allow for both polymerization and trimerization by the multisite active species. Therefore, in addition catalyst symmetry, which may vary with ligand substitution and experimental conditions, is equally very important. In all, the generalization that stabilization of the active site by more electron-releasing substituents is important for high catalyst activity, lower weight distribution, and high molecular weight is fully established.[242]

In a further exploration of variables that are likely to influence catalyst activity in linked-amido catalysts, Okuda et al.[181] studied the influence of the substituent R″ in the $Ti(\eta^5{:}\eta^1\text{-}C_5R_4\text{-}ZNR'')Cl_2$ type complexes on the polymerization of ethylene and realized that the third donor groups ($-NMe_2$ and $-ROR'$), some of which are soft donor semilabile in nature, affect the activity at the active site by virtue of coordination abilities in competition with the ethylene molecule, hence the low activity. These tridentate CGC may form a link between Cp-based and the non-Cp catalysts.[246]

The nature of the cocatalyst on catalyst activity has been the subject of numerous studies, principally because it is responsible for producing the counterions that balance the active species.[169−175] The functions of the cocatalysts have been well studied and highlighted;[227,233] notably, it stabilizes the active titanium alkyl by preventing reductive ion pairing and also serves in some instances as a scavenger of impurities. In a study[172] employing various perfluoroborates and boranes as counterions under the same conditions, it was observed that when $B(C_6F_5)_4^-$ is the counterion, catalytic activity is 10-fold more than the situation utilizing $MeB(C_6F_5)_3^-$ and $PhCH_2\text{-}B(C_6F_5)_3^-$ counterions. In addition, the melting temperature of the polyethylene is higher, demonstrating the significant influence of the nature of the anion on catalytic activity. Generally, activity−structure relationships show that depending on the nature of the ligand framework, and the coordinating power of the cocatalysts, CGC form high molecular weight polyethylenes with long-chain branching, resulting from the incorporation of oligoethylene chains formed by $\beta$-hydride elimination into the open structure of the active species.[247] The ability of the counterion to coordinate to or form a complex with the active species largely determines the stability and hence efficiency of the pair as a catalyst system.

By far MAO has remained the cocatalyst of choice for olefin polymerization, and results of homogeneous polymerization of ethylene using various titanium compounds with MAO are summarized in Table 20. The application of various boron-based cocatalysts has also gained wide acceptance, especially for kinetic studies, and results of ethylene polymerization using various titanium compounds with boron salts as cocatalysts (sometimes with added aluminum alkyls) are presented in Table 21.

## C. Polypropylene (PP)

Propylene is a simple extension of ethylene, with a methyl group substituting for a proton. Although this transition is subtle, it is all that is needed to bring so much difference between the chemistry and technology of PE, on the one hand and propylene and other higher olefins, on the other. The first and major problem encountered when the transition from PE to PP is made is that of selectivity due to the hanging methyl group (see Chart 19); so for this process, in addition to activity, the catalyst has the added task of regio- and stereoselectivity. The added challenge is also responsible for the immense popularity of research in propylene and higher olefin polymerization. This subject has been thoroughly reviewed by Resconi et al.[29] with a particular emphasis on zirconium catalysts.

The general principles behind polyolefin stereochemistry and its precise control with particular reference to propylene polymerization have been the subject of several reviews.[20,21,253,254] A particular area of recent activity is the production of thermoplastic elastomers (TPE) for the tire and rubber industry. This is achieved through copolymerization or by the use of catalysts capable of introducing both hard and soft segments into the backbone of the same monomer. Rieger and Müller have very recently reviewed this area with particular emphasis on propene-based TPE catalyzed by group IV metallocenes.[255]

Ewen[83] first demonstrated the use of the bridged titanium complex ethylenebis(1-indenyl)titanium

**Table 20. Ethylene Polymerization Initiated by Titanocene−MAO Catalyst Systems**

| catalyst | polymerization conditions | A[a] ($10^{-3}$) | $M_w$ ($10^{-4}$) | $T_m$ (°C) | $M_w/M_n$ | ref |
|---|---|---|---|---|---|---|
| **64** | $n_{Ti-complex}$ = 8.4 μmol; $T_p$ = 30 °C; 10 bar $C_2H_4$ | 7.0 | | | | 117 |
| **238** | $n_{Ti-complex}$ = 5 μmol; [Al]/[Ti] = 500; $T_p$ = 23 °C; $t_p$ = 2 h; 3 bar $C_2H_4$ | 3090.0 | | 135.6 | | 167 |
| **234** | $n_{Ti-complex}$ = 5 μmol; [Al]/[Ti] = 500; $T_p$ = 23 °C; $t_p$ = 2 h; 3 bar $C_2H_4$ | 2060.0 | | 140.0 | | 167 |
| **224** | $n_{Ti-complex}$ = 4.2 μmol; $T_p$ = 60 °C; $t_p$ = 1 h; 4 kgf/cm$^2$ $C_2H_4$; [Al]/[Ti] = 2000 | 1240.0 | 13.8 | | 4.7 | 242 |
| **172** | $n_{Ti-complex}$ = 5 μmol; $T_p$ = 25 °C; $t_p$ = 1.5 h; 3 bar $C_2H_4$; [Al]/[Ti] = 500 | 12.0 | 466.0 | 132.3 | >10 | 169 |
| **225** | $n_{Ti-complex}$ = 20 μmol; [Al]/[Ti] = 1500 $T_p$ = 25 °C; $t_p$ = 5 min; 5 atm $C_2H_4$ | 5.7 | | | | 248 |
| **169** | $n_{Ti-complex}$ = 5 μmol; $T_p$ = 25 °C; $t_p$ = 2 h; 3 bar $C_2H_4$; [Al]/[Ti] = 500 | 12.0 | | 132.3 | | 181 |
| **30** | $T_p$ = 60 °C; $t_p$ = 1 h; 10 bar $C_2H_4$; [Al]/[Ti] = 3000 | 7.6 | 130[b] | | | 72 |
| **235** | $n_{Ti-complex}$ = 12.3 μmol; $T_p$ = 80 °C; $t_p$ = 20 min; 2 bar $C_2H_4$; [Al]/[Ti] = 5400 | 15.0 | | 128.9<br>133.9 | | 249 |
| **219** | $n_{Ti-complex}$ = 3 μmol; $T_p$ = 20 °C; $t_p$ = 30 min; 1 atm $C_2H_4$; [Al]/[Ti] = 2500 | 2130.0 | 76.9[b] | | 2.06 | 239 |
| **169** | $n_{Ti-complex}$ = 15 μmol; $T_p$ = 30 °C; $t_p$ = 30 min; 5 bar $C_2H_4$; [Al]/[Ti] = 1000 | 2787 | | | | 243 |
| **226** | $m_{Ti-complex}$ = 10 mg; $T_p$ = 60 °C; $t_p$ = 1 h; 10 bar $C_2H_4$; [Al]/[Ti] = 2500 | 9421 | | 136.6 | | 168 |
| **227** | $m_{Ti-complex}$ = 10 mg; $T_p$ = 60 °C; $t_p$ = 1 h; 10 bar $C_2H_4$; [Al]/[Ti] = 2500 | 3607 | | 141.5 | | 168 |
| **228** | $m_{Ti-complex}$ = 10 mg; $T_p$ = 60 °C; $t_p$ = 1 h; 10 bar $C_2H_4$; [Al]/[Ti] = 2500 | 3324 | | 138.3 | | 168 |
| **229** | $m_{Ti-complex}$ = 10 mg; $T_p$ = 60 °C; $t_p$ = 1 h; 10 bar $C_2H_4$; [Al]/[Ti] = 2500 | 2246 | | | | 168 |
| **236** | $m_{Ti-complex}$ = 10 mg; $T_p$ = 60°C; $t_p$ = 1 h; 10 bar $C_2H_4$; [Al]/[Ti] = 2500 | 3504 | | 137.1 | | 168 |
| **237** | $m_{Ti-complex}$ = 10 mg; $T_p$ = 60 °C; $t_p$ = 1 h; 10 bar $C_2H_4$; [Al]/[Ti] = 2500 | 2083 | | 136.9 | | 168 |
| **62** | [Ti] = 50 μM; [Al]/[Ti] = 4000; $T_p$ = 20 °C; $t_p$ = 10 min | 4910 | 3.9[b] | 135.6 | | 114 |
| **220** | $n_{Ti-complex}$ = 6.25 μmol; [Al]/[Ti] = 2500; $T_p$ = 30 °C; $t_p$ = 57 min; 2 bar $C_2H_4$ | 3300 | | 137.7 | | 250 |
| **221** | $n_{Ti-complex}$ = 5 μmol; [Al]/[Ti] = 290; $T_p$ = 30 °C; $t_p$ = 2 h; 10 bar $C_2H_4$ | 6710 | 0.75 | 137.9 | | 89 |
| **132** | [Ti] = 50 μM; $T_p$ = 21 °C; $t_p$ = 10 min; [Al]/[Ti] = 2000 | 9100 | 7.2 | 135.5 | | 154 |

[a] Activity = g of PE/(mol of Ti)·atm·h. [b] $M_n$ determined by viscometry. [c] Dry MAO (white solid) was obtained from in vacuo evaporation of a toluene solution; $m_{Ti-complex}$ = weight of catalyst; $n_{Ti-complex}$ = moles of catalyst.

**Table 21. Ethylene Polymerization Initiated by Titanocene−Borane Catalyst Systems**

| catalyst system | polymerization conditions | $A^a$ ($10^{-3}$) | $M_w$ ($10^{-5}$) | $T_m$ (°C) | $M_w/M_n$ | ref |
|---|---|---|---|---|---|---|
| **222**−$B(C_6F_5)_3$ | $n_{Ti-complex}$ = $n_{B-complex}$ = 15 μmol; $T_p$ = 25 °C; $t_p$ = 30 min; 1 atm $C_2H_4$; 100 mL toluene | 14.7 | 12.70 | 142.5 | >10 | 251 |
| **222**−$Ph_3C^+B(C_6F_5)_4^-$ | $n_{Ti-complex}$ = $n_{B-complex}$ = 15 μmol; $T_p$ = 25 °C; $t_p$ = 1 min; 1 atm $C_2H_4$; 100 mL toluene | 2100.0 | 11.40 | 142.4 | >10 | 251 |
| **232**−$MeB(C_6F_5)_3$ | $n_{Ti-complex}$ = $n_{B-complex}$ = 15 μmol; $T_p$ = 25 °C; $t_p$ = 7 min; 1 atm $C_2H_4$; 50 mL toluene | 114.0 | 10.60 | 136.8 | 9.54 | 172 |
| **233**−$PhCH_2B(C_6F_5)_3$ | $n_{Ti-complex}$ = $n_{B-complex}$ = 15 μmol; $T_p$ = 25 °C; $t_p$ = 1 min; 1 atm $C_2H_4$; 50 mL toluene | 131.0 | 20.00 | 142.1 | 6.77 | 172 |
| **137**−$B(C_6F_5)_3$ | $n_{Ti-complex}$ = 15 μmol, $n_{B-complex}$ = 45 μmol; $T_p$ = 140 °C; $t_p$ = 4 min; 500 psig $C_2H_4$; MMAO [Al] = 150 μmol | 10300 | 1.09 | | 2.00 | 252 |
| **223**−$Ph_3C^+B(C_6F_5)_4^-$ | $n_{Ti-complex}$ = $n_{B-complex}$ = 18.3 μmol; $T_p$ = 60 °C; $t_p$ = 1 h; 4 kgf/cm$^2$ $C_2H_4$; Al$^i$Bu$_3$ [Al]/[Ti] = 500 | 77.0 | | | | 242 |
| **224**−$Ph_3C^+B(C_6F_5)_4^-$ | $n_{Ti-complex}$ = $n_{B-complex}$ = 6.5 μmol; $T_p$ = 60 °C; $t_p$ = 1 h; 4 kgf/cm$^2$ $C_2H_4$; Al$^i$Bu$_3$ [Al]/[Ti] = 500 | 2220.0 | 0.917 | | 5.00 | 242 |
| **231**−$B(C_6F_5)_3$ | $n_{Ti-complex}$ = $n_{B-complex}$ = 88 μmol; $AlMe_3$ [Al]/[Ti] = 1.14; $T_p$ = 50 °C; $t_p$ = 20 min; 1 atm $C_2H_4$ | 104.0 | | 123.0 | 10.7 | 245 |
| **219**−$Ph_3C^+B(C_6F_5)_4^-$ | $n_{Ti-complex}$ = 50 μmol; [B]/[Ti] = 20; $T_p$ = 0 °C; $t_p$ = 15 min; 15 psig $C_2H_4$ | 6300 | | 130 | | 73 |

[a] Activity = g of PE/(mol of Ti)·atm·h; $n_{Ti-complex}$ = moles of catalyst; $n_{B-complex}$ = moles of cocatalyst.

**Chart 19. Selectivity in Propylene Polymerization**

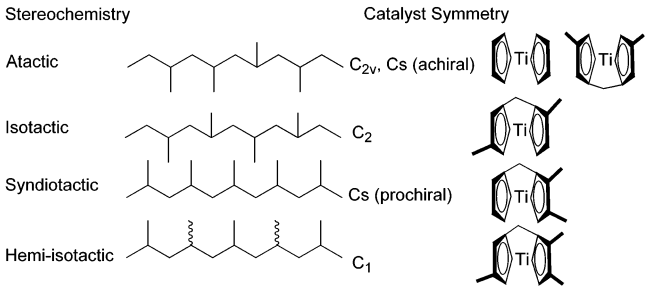


dichloride for the synthesis of a mixture of 63% isotactic and 37% atactic polypropylene, as the first example of a titanium-based isospecific propylene polymerization catalyst. This is in analogy to the chiral zirconocene synthesized by Britzinger.[84]

In the polymerization of propylene and higher alkenes, the tacticity or the relative configuration of adjacent stereocenters of the main polymer chain is as important as the activity. Therefore, a good catalyst in this instance should be able to not only convert the monomer to a polymer but also produce polymer of a given configuration. Chart 19 presents the different tacticities and the required metallocene configuration for obtaining such a configuration. Using a series of relationships credited to Ewen,[83] it is possible to predict and control very precisely the microstructure of polymers by employing a combination of polymerization variables and use of well-defined metallocenes. Syndiotactic polypropylene is produced when the neighboring stereocenters are regularly alternating, obtainable from a catalyst molecule with a center of asymmetry ($C_s$). When the two neighboring stereocenters are of the same configuration, as obtained from a catalyst with a $C_2$ symmetry, then an isotactic polypropylene is obtained. These are achieved by enantiomorphic site control, via a 1,2-insertion.[225] In a situation where the energy difference between the neighboring stereocenters is

**Chart 20. Catalysts Used for the Polymerization of Propylene**

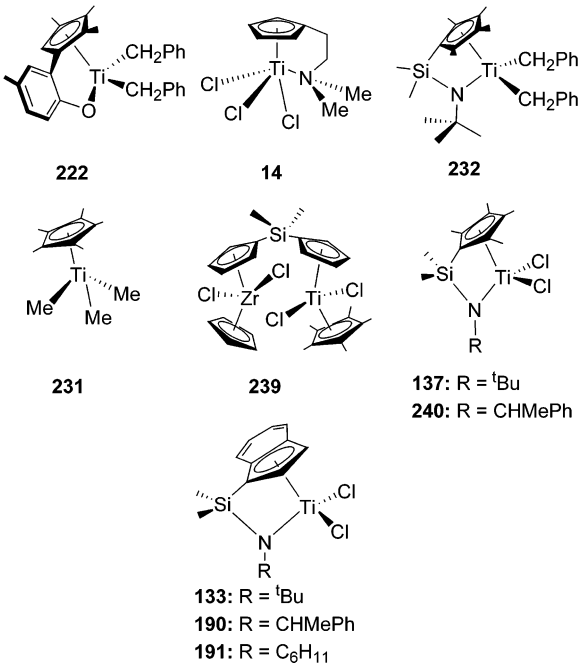


very small or zero, because the two sources of chirality are absent as obtainable from a catalyst with a $C_{2v}$ or *meso* $C_s$ symmetry, then a random or atactic polypropylene is obtained. The use of achiral $C_{2v}$ symmetric $Cp_2TiPh_2$/MAO to obtain isotactic polypropylene at low temperatures was explained to be governed by polymer chain-end control via a 1,2-insertion.[83] A hemi-isotactic polymer is obtained when an isotactic polymer is regularly interspersed by atactic stereocenters. When isotactic blocks of a polymer regularly alternate (syndiotactically), then it is referred to as stereoblock.

The period under review is one in which titanocene research is dominated by the CGC and Cp(or Ind)-$TiCl_3$ complexes due to the high interest generated by the former as a result of its high activity for (co)polymerization of olefins and the latter for syndiotactic polystyrene. Because of the lack of chirality in these catalyst systems, they give atactic polypropylenes via polymer chain-end control, but interest in atactic polypropylene, especially the high molecular weight type, is increasing because of their elastomeric properties.[256,257]

A syndiotactically enriched atactic polypropylene (*rr* 0.35−0.41) has been prepared using the catalyst systems **232**−$B(C_6F_5)_3$ and **233**−$Ph_3C^+B(C_6F_5)_4^-$ (see Chart 20), with the latter system an order of magnitude more active under the same conditions, although the amount of syndiotactic units is higher with the trityl counterion, underpinning the role of the counterion in determining catalyst activity and selectivity.[172] The subject of the role of cocatalysts in propylene polymerization has also been taken by Ikeda and co-workers,[175] who established that bulky trialkylaluminum additives [(octyl)$_3$Al; *i*-$Bu_3Al$] enhance the formation of the active species and hence improve catalyst activity.

In a study on a series of linked-amido catalysts, Waymouth et al.[166] have by statistical analysis arrived at the conclusion that the Bernoullian model for chain-end control is the dominant propagation mechanism for CGC because of the open nature of the achiral catalyst systems, except where ligand chirality is strong enough to influence stereospecificity. They also noted that under similar conditions $Me_4C_5$-based catalysts were generally more active and produce polymers of higher molecular weight than their indenyl analogues, due to more favorable electronic effects from the $Me_4C_5$ moiety leading to a decrease in chain termination by $\beta$-H elimination. It has been shown by $^{13}C$ NMR measurements that in these asymmetric mono-Cp catalyst systems the ligand environment[166] and the polymerization temperature[258] significantly affect the catalyst efficiency including the number of regioerrors as a result of 2,1-misinsertions. Hence, the effect of the ligand environment on catalyst efficiency is observable from the studies utilizing chelated[154] or weakly coordinated pendant groups[207] on the polymerization of propylene. It was found that steric bulk as well as electronic factors play a major role because the pendant anionic and neutral moeities ($NMe_2$, Ph, and OMe) may coordinate (although reversibly) to the metal center, giving comparably stable metallocenium complexes that are stronger than the coordination of counterion $[B(C_6F_5)_4]^-$, hence blocking the uptake of monomer and enhancing chain termination and resulting in decreased catalyst reactivity and selectivity as compared to complexes without potentially chelating side chains such as the $Cp^*TiMe_3$ precursor under the same conditions.[207]

Table 22 summarizes results of some propylene catalyst systems reported within the period covered by this review.

## D. Stereospecific Polymerizations of Styrene

Syndiotactic polystyrene (s-PS) is a relatively new material having the same glass transition temperature as atactic polystyrene in the range of 100 °C. However, unlike the atactic form prepared by anionic or free radical initiators, s-PS is stereoregular and is able to crystallize with a melting point of ∼270 °C, one of the highest known for a homopolymer. In addition, it has high dimensional stability, chemical resistance, and low water uptake, responsible for good electrical properties, while retaining the density of atactic polystyrene. These advantages coupled to its cheap cost make it attractive to industry for s-PS to replace some polyamides as a cheap engineering thermoplastic. These properties also contrast s-PS from the common isotactic polystyrene prepared by Z−N polymerization, which is characterized by a very low crystallization rate and is therefore useless for most industrial applications. The discovery of s-PS made in 1986 by Ishihara[259,260] at Idemitsu Kodan Co. has inspired a flurry of activity from researchers around the world.[261−266] Presently the polymerization mechanism[267,268] and the nature of the active species[269,270] have been elucidated. Half-sandwich titanium complexes of the general formulas $Cp'TiX_3$ and $Ind'TiX_3$ activated by MAO or $B(C_6F_5)_3$ have been identified to give best results.[261−264,266] Further research aimed at process optimization and extensive

**Table 22. Propylene Polymerization Initiated by Titanocene Catalyst Systems**

| catalyst system | conditions | $A^a$ | $M_w$ ($10^{-4}$) | $M_w/M_n$ | remarks | ref |
|---|---|---|---|---|---|---|
| **222**−$Ph_3C^+$ $B(C_6F_5)_4^-$ | $n_{Ti-complex}$ = 20 $\mu$mol; $T_p$ = 25 °C; $t_p$ = 5 min; 1 atm $C_3H_6$; [$Ph_3C^+$]/[Ti] = 1; 50 mL toluene | 3820 | 236 | 1.85 | [*mm*] = 0.224 [*mr*] = 0.512 [*rr*] = 0.264 | 251 |
| **14**−MAO | [Ti] = 25 $\mu$M; [Al]/[Ti] = 4000; $T_p$ = 20 °C; $t_p$ = 30 min; 20 psig $C_3H_6$; 50 mL toluene | 1900 | 45 | | | 153 |
| **14**−$Ph_3C^+$ $B(C_6F_5)_4^-$/TIBA | [Ti] = 100 $\mu$M; [$Ph_3C^+$]/[Ti]/[Al] = 1:1:20; $T_p$ = 20 °C; $t_p$ = 7 min; 20 psig $C_3H_6$; 50 mL toluene | 4820 | 45 | | | 153 |
| **232**−$B(C_6F_5)_4^-$ | $n_{Ti-complex}$ = 15 $\mu$mol; $T_p$ = 25 °C; $t_p$ = 5 min; 1 atm $C_3H_6$; [B]/[Ti] = 1; 50 mL toluene | 2120 | 14.2 | 3.80 | [*mm*] = 0.156 [*mr*] = 0.491 [*rr*] = 0.353 | 172 |
| **231**−$B(C_6F_5)_3$ | $n_{Ti-complex}$ = 20 $\mu$mol; $T_p$ = −45 °C; $t_p$ = 2 min; 1 bar $C_3H_6$; [B]/[Ti] = 1 | 5200 | 227.5 | 2.0 | | 207 |
| **239**−MAO | $n_{Ti-complex}$ = 31.3 $\mu$mol; [Al]/[Ti] = 2500; $T_p$ = 30 °C; $t_p$ = 404 min; 2 bar $C_3H_6$; 210 mL toluene | 35 | 0.059[b] | | [*mm*] = 0.22 [*mr*] = 0.48 [*rr*] = 0.30 | 250 |
| **137**−MAO | [Ti] = 38 $\mu$M; [Al]/[Ti] = 289; $T_p$ = 30 °C; $t_p$ = 1 h; 100 psig $C_3H_6$; 100 mL toluene | 380 | 40.0 | 1.68 | [*mmmm*] = 0.01 [*rrrr*] = 0.233 | 166 |
| **240**−MAO | [Ti] = 34 $\mu$M; [Al]/[Ti] = 350; $T_p$ = 30 °C; $t_p$ = 1 h; 100 psig $C_3H_6$; 100 mL toluene | 188 | 26.9 | 3.55 | [*mmmm*] = 0.043 [*rrrr*] = 0.104 | 166 |
| **133**−MAO | [Ti] = 39 $\mu$M; [Al]/[Ti] = 350; $T_p$ = 30 °C; $t_p$ = 1 h; 100 psig $C_3H_6$; 100 mL toluene | 19 | 3.7 | 2.29 | [*mmmm*] = 0.145 [*rrrr*] = 0.074 | 166 |
| **190**−MAO | [Ti] = 34 $\mu$M; [Al]/[Ti] = 350; $T_p$ = 30 °C; $t_p$ = 1 h; 100 psig $C_3H_6$; 100 mL toluene | 196 | 11.1 | 2.04 | [*mmmm*] = 0.055 [*rrrr*] = 0.129 | 166 |
| **191**−MAO | [Ti] = 36 $\mu$M; [Al]/[Ti] = 400; $T_p$ = 30 °C; $t_p$ = 1 h; 100 psig $C_3H_6$; 100 mL toluene | 239 | 16.5 | 2.20 | [*mmmm*] = 0.046 [*rrrr*] = 0.075 | 166 |

[a] Kilograms of PP/mol of Ti·h. [b] Determined by end group analysis from $^1$H NMR; $n_{Ti-complex}$ = moles of catalyst.

investigation of the substituent effects has resulted in very active and highly syndiospecific homogeneous catalysts that could be commercialized.[141] This is evidenced by the marketing of s-PS under trade names such as Idemitsu Kodan Co.'s XAREC and Dow Chemical Co.'s Questra Crystalline Polymers, with different grades targeted at the electrical, electronics, and the automotive industries.[271] Table 23 presents some catalyst systems reported for the syndiospecific polymerization of styrene within the period covered by this review.

The mechanism of syndiospecific polymerization of styrene (Scheme 89) has been determined by NMR measurements to progress through a Z−N type polyinsertion with $\beta$-H elimination being the main-chain termination mechanism, so that the polymer molecular weight ($M_w$) and degree of polymerization ($P_N$) are determined by the absolute ratio of monomer enchainment ($V_P$) to the rate of chain transfer by $\beta$-H elimination ($V_{TR}$). Chain-end stereocontrol is the main determinant of syndiotacticity as evidenced by NMR analysis, showing a significant amount of *rmr* tetrad fragments from polymer chain-end control and the near absence of *rmm* tetrads from metallocene site stereocontrol.[272]

Although the nature of the active species in syndiospecific polymerization of styrene is still a topic of debate among researchers, the more compelling evidence is in favor of a Ti(III) cationic species.[269,270,273−276] Zambelli and co-workers, on the basis of NMR, ESR, and kinetic studies, have considered the syndiospecific polymerization of styrene to be an "electronic" polyinsertion reaction at the metal center, suggesting that the real active species are Ti(III) cations of the type $CpTiP^+$ (P = polymeryl).[277,278] After a series of EPR spectral measurements, kinetic investigation, and polymerization experiments, Xu et al.[141,210,279] concluded that the Ti(III) complex $[Cp^*TiR]^+$ is the main active species in the syndiospecific polymerization of styrene, whereas Ti(IV) and Ti(II) have very little influence as active species, and the main termination process is by $\beta$-H elimination in the system examined. In a proposal for the involvement of a carbocationic mechanism (Scheme 90) in the polymerization of styrene, Baird et al.[280] have shown that reacting $Cp^*TiMe_3$ with the highly electrophilic borane $B(C_6F_5)_3$ results in the formation of the highly reactive methyl-bridged borane compound **241**. These is a good source of the 10-electron species $[Cp'TiR_2]^+$, which by slow reductive decomposition yield the 9-electron active species $[Cp'TiR]^+$.[273] This catalyst system initiates styrene to atactic polystyrene via the carbocationic polymerization mechanism only at −15 °C in aromatic solvents such as toluene.[265] The carbocationic theory will not be pursued any further, because the topic has been recently reviewed and the catalyst system follows a Z−N mechanism in toluene or bulk, at room temperature and above, the ripe conditions for s-SP polymerization.[281]

General conclusions of the extensive studies by researchers on the effects of polymerization condi-

**Table 23. Syndiospecific Polymerization of Styrene Initiated by Half-Sandwich Titanium Catalysts−MAO Catalyst Systems**

| catalyst | conditions | activity[a] × $10^{-7}$ | s-PS[b] (%) | $M_w$ ($10^{-4}$) | $T_m$[c] (°C) | ref |
|---|---|---|---|---|---|---|
| **242** | [Ti] = 50 $\mu$M; $T_p$ = 50 °C; $t_p$ = 30 min; [styrene] = 0.87 M; [Al]/[Ti] = 4000 | 1.40 | 67.4 | 43.5 | 259.7 | 137 |
| **243** | [Ti] = 50 $\mu$M; $T_p$ = 50 °C; $t_p$ = 30 min; [styrene] = 0.87 M; [Al]/[Ti] = 4000 | 3.70 | 98.2 | 72.0 | 270.8 | 137 |
| **206** | [Ti] = 83.3 $\mu$M; $T_p$ = 60 °C; $t_p$ = 15 min; [styrene] = 2.94 M; [Al]/[Ti] = 1000 | 13.61 | 95.2 | 9.5 | 270.0 | 210 |
| **207** | [Ti] = 83.3 $\mu$M; $T_p$ = 60 °C; $t_p$ = 15 min; [styrene] = 2.94 M; [Al]/[Ti] = 1000 | 12.70 | 96.1 | 17.9 | 272.0 | 210 |
| **207** | [Ti] = 83.3 $\mu$M; $T_p$ = 60 °C; $t_p$ = 15 min; [styrene] = 2.94M; [Al]/[Ti] = 1000 | 21.77 | 98.1 | 65.7 | 275.0 | 210 |
| **208** | [Ti] = 83.3 $\mu$M; $T_p$ = 60 °C; $t_p$ = 15 min; [styrene] = 2.94 M; [Al]/[Ti] = 1000 | 22.68 | 98.7 | 68.5 | 275.0 | 210 |
| **212** | [Ti] = 50 $\mu$M; $T_p$ = 60 °C; $t_p$ = 15 min; [styrene] = 2.94 M; [Al]/[Ti] = 1000 | 10.28 | 95.0 | 27.5 | 270.0 | 210 |
| **213** | [Ti] = 50 $\mu$M; $T_p$ = 60 °C; $t_p$ = 15 min; [styrene] = 2.94 M; [Al]/[Ti] = 1000 | 12.69 | 96.2 | 50.3 | 269.0 | 210 |
| **86** | [Ti] = 50 $\mu$M; $T_p$ = 50 °C; $t_p$ = 30 min; [styrene] = 0.88M; [Al]/[Ti] = 4000 | 16.6 | 90.2 | 66.0 | 272.2 | 282 |
| **199** | [Ti] = 50 $\mu$M; $T_p$ = 50 °C; $t_p$ = 30 min; [styrene] = 0.88 M; [Al]/[Ti] = 4000 | 7.70 | 90.0 | 42.0 | 260.7 | 282 |
| **200** | [Ti] = 50 $\mu$M; $T_p$ = 50 °C; $t_p$ = 30 min; [styrene] = 0.88 M; [Al]/[Ti] = 4000 | 3.60 | 94.8 | 49.0 | 262.0 | 282 |
| **203** | [Ti] = 50 $\mu$M; $T_p$ = 50 °C; $t_p$ = 30 min; [styrene] = 0.88 M; [Al]/[Ti] = 4000 | 17.00 | 92.5 | 54.0 | 270.4 | 282 |
| **204** | [Ti] = 50 $\mu$M; $T_p$ = 50 °C; $t_p$ = 30 min; [styrene] = 0.88 M; [Al]/[Ti] = 4000 | 18.00 | 92.8 | 42.0 | 275.2 | 282 |
| **205** | [Ti] = 50 $\mu$M; $T_p$ = 50 °C; $t_p$ = 30 min; [styrene] = 0.88 M; [Al]/[Ti] = 4000 | 2.00 | 96.0 | 32.0 | 276.0 | 282 |
| **213** | [Ti] = 50 $\mu$M; $T_p$ = 75 °C; $t_p$ = 30 min; [styrene] = 0.88 M; [Al]/[Ti] = 4000 | 75.00 | 92.0 | 13.0 | 265.2 | 211 |
| **205** | [Ti] = 50 $\mu$M; $T_p$ = 75 °C; $t_p$ = 30 min; [styrene] = 0.88 M; [Al]/[Ti] = 4000 | 76.00 | 89.0 | 9.0 | 267.8 | 211 |
| **244** | [Ti] = 50 $\mu$M; $T_p$ = 50 °C; $t_p$ = 30 min; [styrene] = 0.87 M; [Al]/[Ti] = 4000 | 3.80 | 97.7 | | 270.2 | 138 |
| **246** | [Ti] = 420 $\mu$M; $T_p$ = 50°C; $t_p$ = 5 min; [Al]/[Ti] = 3400 | 9.74 | 94.2 | | 259.4 | 283 |
| **245** | [Ti] = 600 $\mu$M; $T_p$ = 35°C; $t_p$ = 60 min; [styrene] = 1.28 M; [B][d]/[Ti] = 1 | 1.12 | 97.1 | | 270.0 | 284 |

[a] *A* (activity) = g of s-PS/mol of Ti·mol of S·h. [b] s-PS % = (g of polymer soluble in 2-butanone)/(g of total polymer) × 100%. [c] Melting point determined by DSC. [d] Cocatalyst = $B(C_6F_5)_3$.

**Scheme 89. Mechanism of Initiation, Chain Propagation, and Transfer**

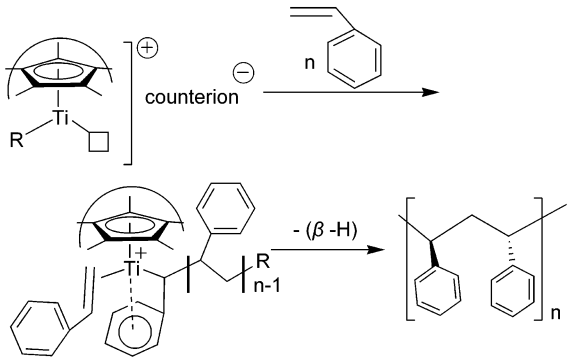


tions and Cp (or Ind) ring substitution on the activity, selectivity, and melting temperatures of s-PS can be summarized as follows:

• In cases where steric constraints are not pronounced, small electron-donating substituents increase catalyst activity, selectivity of s-PS, $M_w$, and polymer melting temperatures. This is evidenced by studies of a series of alkyl-substituted complexes of increasing steric size. Only the smaller electron-releasing alkyl substituent ($CH_3$) improves catalyst activity beyond the unsubstituted counterparts.[137,141,210]

**Scheme 90**

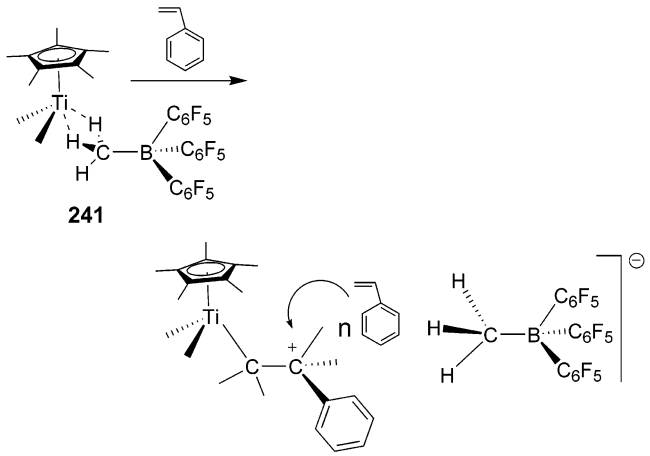


• Indenyl and substituted-indenyl complexes are more active than Cp and substituted-Cp complexes, due to the higher electron-donating ability of the indenyl moiety.[137,285]

• Fluorinated complexes are much more active than their chlorinated counterparts.[286] This is believed to be due to the higher electronegativity and hence polarizing effect of fluorine compared to chlorine,

**Chart 21. Catalysts for s-PS**

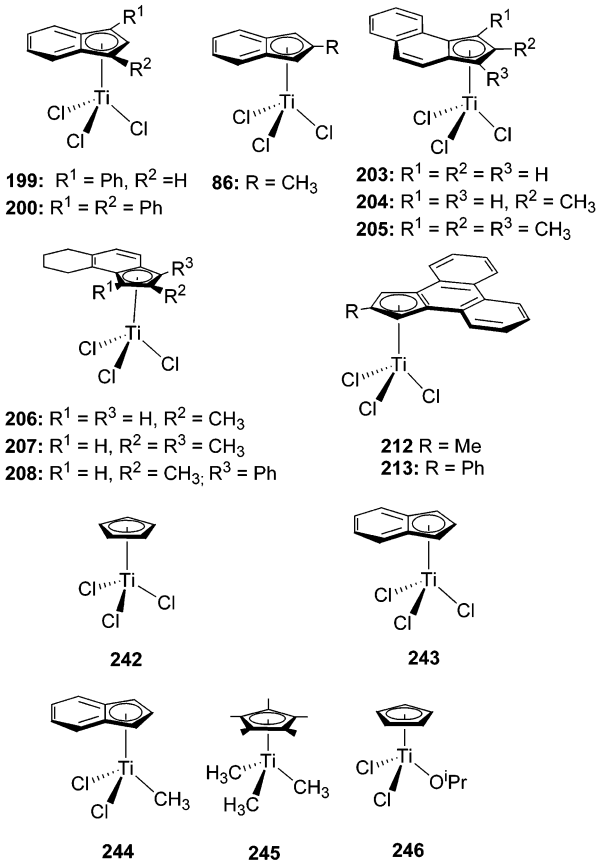


which makes it easier for the counterion to generate active species from the electrophilic Ti metal. High activities of fluorinated catalysts are reached at very low Al/Ti ratios (1:300), as compared to 1:2000−3000 for the chlorinated catalysts; this coupled with their better stability at higher temperatures makes them suitable for industrial applications.[141]

• Bulky annulated aromatic ligands are capable of stabilizing the active species and hence improving catalyst efficiency.[208,210] For example, the benz[*e*]-indenyl-$TiCl_3$ prepared by Chien et al.[208] has an extremely high activity of $1.7 \times 10^8$ g of PS/(mol of Ti·mol of styrene·h), 93% syndiotacticity, and $M_w = 5.5 \times 10^5$ and is stable up to 100 °C without any appreciable loss of quality. It is stable to air for several hours without decomposition, making it very attractive for industrial application. This observation was attributed to the steric congestion at the Ti center, which suppresses detrimental $\beta$-agostic interactions during propagation by promoting chain olefin insertion relative to chain termination by $\beta$-H transfer.[211,287]

• Except in a few cases ($Cp'TiF_3$) catalytic activity increases with an increase in MAO concentration or addition of trialkylaluminum compounds to systems cocatalyzed by borane/borate salts.[281]

• Up to the decomposition point of the active species, there is a general direct dependence of catalyst efficiency on polymerization temperature. This is because a rise in temperature will increase ion-pair dissociation and also increase the rate of polymer propagation, resulting in increased activity. At higher temperatures the $\pi$-complex formed by the growing chain and the active species (monomer→$Ti^+$−$P_n$) will dissociate and lead to reductive deactivation of the growing chain, resulting in a fall in activity and syndiotacticity.[138,288]

• In the syndiospecific polymerization of styrene, the s-PS percentage is usually reported as an integral part of expressing the quality of a catalyst system. This is usually expressed as a ratio [weight of methyl ethyl ketone (MEK) insoluble polymer/weight of total polymer (%)]. Although this methodology is very convenient and widespread, Kaminsky et al.[289] have demonstrated that it is not quite reliable because extraction with boiling MEK washes out low molecular weight s-PS as well as atactic polystyrene. The researchers have shown that part of the MEK soluble polymer they extracted actually contains s-PS as evidenced by $^{13}C$ NMR analysis and high melting temperatures unusual for atactic polystyrene. Therefore, analysis of triad and pentad sequences from NMR measurements remains the most absolute and unambiguous measure of tacticity.

## E. Copolymerizations

The ever-increasing desire by industry to create new and cheap materials with enhanced mechanical and chemical properties, ease of processability, compatibility with various additives, and fully improved end use and marketability is the driving force behind the push into the development of co- and terpolymers. Because the variety obtainable from homopolymers and polymer blends is very limited in scope and applications, the need to develop new homogeneous catalysts capable of copolymerizing two different monomers becomes very important. Due to different reactivity ratios between different monomers, numerous good homopolymerization catalysts show only very limited success in incorporating comonomers of different geometry or chemical composition. This situation is illustrated by the half-sandwich $Cp'TiX_3$ complexes that are very active styrene homopolymerization catalysts but exhibit very poor activity for ethylene homopolymerization or ethylene/styrene copolymerization. On the introduction of a linked-amido group to the $Cp'TiX_3$ through ligand modification, a new type of half-titanocene called constrained geometry catalysts (CGC) was born.[162,163] The CGC show a very poor activity for styrene homopolymerization but, in contrast, are extremely active in the copolymerization of ethylene with a variety of comonomers including styrene. The ability of these catalysts to incorporate bulky monomers has been attributed to the more open and "constrained" nature of the Cp−amido bond and the $\pi$-donating ability of the amido group. Very recently, the half-sandwich complex with the structure $Cp^*TiCl_2(O\text{-}2,6\text{-}{}^iPr_2C_6H_3)$ has been found to be an efficient catalyst precursor not only for ethylene polymerization but also for ethylene/α-olefin copolymerization in the presence of MAO.[290]

In summary, the suitability of a catalyst system for copolymerization is determined by high catalyst activity, its ability to incorporate a relatively high composition and uniform distribution of each comonomer, well-defined copolymer structures represented by high comonomer stereo- and regioselectivity, high

copolymer molecular weight, and narrow molecular weight distribution.

### 1. Ethylene–Styrene Copolymerization (E–S)

Oliva and co-workers found[291,292] that cyclopentadienyl titanium trichloride ($CpTiCl_3$) activated by MAO is able to promote the copolymerization of ethylene and styrene. The polymerization conditions play an important role in the composition and structure of the resultant copolymer. In the presence of a high Al/Ti molar ratio (1000:1), a blocker polymer is obtained together with a mixture of homopolymers (PE and s-PS), whereas with a low Al/Ti molar ratio (100:1), a copolymer containing an ESE sequence can be obtained. It has been reported that the oxidation state of the active titanium species is responsible either for homopolymerization or for copolymerization; $CpTiR_2^+$ is active in the polymerization of ethylene and the copolymerization of ethylene and styrene, whereas $CpTiR^+$ leads to the syndiospecific polymerization of styrene.

The CGC with a linked-amido group−MAO has proved to be the most successful catalyst system due to the aforementioned reasons and the fact that they present only a single site that enables the production of E−S copolymers free of homopolymer units (Scheme 91).[290,293,294] Recent research efforts in the copolymerization of ethylene with styrene are geared toward the synthesis of E−S copolymers with tailored microstructures and predictable properties via the modification of the ligands around the central metal.[290] The result is new products very suited as important components in novel polymer materials and composites. A new copolymer with perfect alternation between the styrene and olefin units was prepared by Xu[295] using the CGC [$Me_2Si(Flu)(N^tBu)TiMe_2$], which contains the bulky amido-fluorenyl ligand. A series of CGC complexes containing various substituent groups on the N and Cp ligands were prepared[170,296] to study the influence of ring and amido substitution on the ability of the catalysts in the processes of copolymerization. It was observed that small electron-donating groups on both ligands produce copolymers of overall best properties, due to high electron density, whereas tetramethylated Cp-based complexes are more active than the corresponding indenyl complexes for the same reason. Bulky substituents on the Cp ring will increase the steric hindrance and reduce the styrene incorporation but improve the long-term activity of the polymerization; the presence of a bulky $PhCH_2$ group on the amido ligand improves comonomer content and gives higher melting temperatures at very low activity levels.

**Scheme 91**

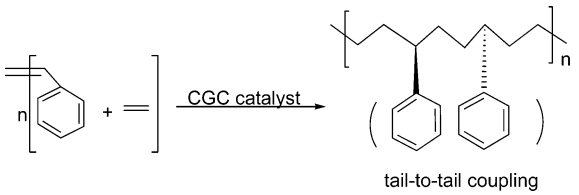


$^{13}C$ NMR spectroscopic analysis of an E−S copolymer microstructure shows exclusively an alternating tail-to-tail coupling (Scheme 91) of styrene units in the polymer backbone, thus limiting the maximum amount of styrene incorporation.[300]

Also, the crystal structure of an E−S copolymer synthesized using a zirconocene catalyst has recently been determined by Oliva et al.,[301,302] giving a possible insight into the mechanism of stereocontrol that was believed to be the alternation between the isotactic styrene insertion and the atactic ethylene insertion.[20]

Modification to the metal center of a half-sandwich complex by using an aryloxy ligand was an effective way to give a series of novel catalysts for ethylene/styrene copolymerization in the presence of MAO (see Chart 22). Nomura and co-workers[290,297,298] found that the substituents on cyclopentadienyl and aryloxy ligands play an important role in the copolymerization activity as well as the microstructure of the resultant copolymer. The styrene incorporation efficiency has a slight relationship with the substituted Cp fragment, whereas the microstructure of the resultant copolymer shows a strong relationship with the substituted Cp fragment. It was also found that the ease of styrene incorporation into the polyethylene backbone is attributed to the wide bond angles of ∼120° of Cp−Ti−O compared with that of the CGC complex $C^N$-18a (Cp−Ti−N, 107.6°), which improves the flexibility of rotation. Furthermore, internal rotation of the substituted Cp fragment will have an influence on the coordination or insertion of incoming styrene monomer.

**Chart 22**

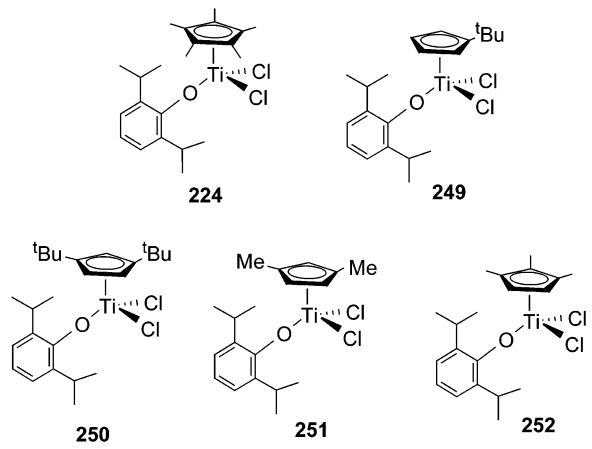


Alternating E−S copolymer prepared by a MAO-free half-sandwich titanium catalyst was obtained by Pellecchia and co-workers.[299] They used an $Me_5CpTi(CH_2Ph)_3-B(C_6F_5)_3$ catalytic system and obtained the alternating E−S copolymers together with some homopolymers (PE and s-PS). The regiospecificity of styrene insertion by analysis of $^{13}C$-enriched end groups in the initiation step is largely secondary insertion, rather than primary insertion.

As an extension of this process in an effort to introduce new functionality and prepare model compounds for LLDPE, terpolymers (containing three monomers) of ethylene-*co*-styrene and 1-octene, propene, norbonene, and 1,5-hexadiene have been prepared using a CGC−MAO catalyst system.[303,304] Mülhaupt and co-workers[303] found that no styrene/

1-octene sequences exist among the ethylene/styrene/1-octene terpolymer microstructure by using $^{13}C$ NMR analysis.

### *2. Ethylene–(α-Olefins) Copolymerization (E–O)*

The ability to prepare LLDPE with controllable properties such as narrow molecular weight distribution, high molecular mass, and uniform comonomer distribution is one of the major achievements of CGC−MAO catalyst systems. Prior to this, low-density polyethylene (LDPE) having long branches was prepared by radical polymerization at high pressure, and the LLDPEs produced by the copolymerization of ethylene with α-olefins initiated by ordinary Z−N catalysts suffer from wide property fluctuations due to the heterogeneity of the active species.[305−308] Recent research efforts are geared toward establishing a correlation between metallocene structure and polymerization behavior with a view toward optimization and design of new more efficient catalyst systems. The CGC−MAO catalyst system has been established to be superior to sandwich *ansa*-metallocenes[309−311] and CGC−borane/borate[172] catalyst systems in terms of activity and ability to incorporate the larger comonomers with high precision and regioselectivity.

Copolymerization of ethylene with higher olefins 1-hexene[242,312] and 1-octene[309,311,313] produces amorphous polymers with a substantially alternating structure as evidenced by a single glass transition temperature ($T_g$), and the level of amorphousity increases with an increase in the content of the higher olefin. Because, comparatively, substituted α-olefins are more difficult to incorporate especially in large amounts using homogeneous catalysts, there are many fewer studies citing them as comonomers. Sivaram and co-workers[314] have investigated the copolymerization of ethylene with aromatic vinyl monomers (styrene, allylbenzene, and 4-phenyl-1-butene) using a bridged titanocene $Me_2SiCp_2TiCl_2$/MAO system. It was found that the comonomer incorporation is <10 mol % and dependent on the incoming comonomer type as 4-phenyl-1-butene > allylbenzene > styrene, showing the incorporation is controlled by the substituent size to the olefinic bond of the comonomer.

In a recent systematic study involving a series of CGC having various Cp ligand substitutions, Xu[310] was able to establish that ligand substitution has a significant effect on the copolymerization of ethylene with 4-methyl-1-pentene (Scheme 92). Observed patterns were rationalized on the basis of the usual electronic and steric considerations as they affect stabilization of the active species, which affects the rate of monomer insertion as well as deactivation and chain transfer or termination. $^{13}C$ NMR analysis of the microstructure also reveals significant differences moving from one catalyst to the other, so that copolymers of varying microstructure and, hence, properties may be prepared by varying the ligand environment around the central Ti metal. Isobutylene,[247] propylene,[315] and 2-methyl-1-pentene[247] have also been successfully copolymerized with ethylene using CGC−MAO catalyst systems.

**Scheme 92. Copolymerization of Ethylene with 4-Methyl-1-pentene**

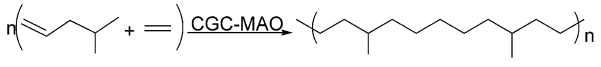


Besides CGC and *ansa*-titanocene as the prevailing catalysts for ethylene/α-olefin copolymerization, another type of catalyst [Cp′$TiCl_2$(O-2,6-$^i$Pr$_2$C$_6$H$_3$)] reported by Nomura and co-workers was worth with attention, particularly in the ethylene/1-hexene copolymerization of ethylene/α-olefin copolymerization.[312,316]

## F. Polymerization of Dienes

Polymers are useful materials for the production of synthetic rubber and have been paid great attention in the industrial field.[317] The stereoselectivity of reactions involving conjugated dienes is much more complex than the case of monoalkenes. This is because both the growing polymer chain and the incoming monomer may coordinate to the active species and have the mutual orientation of each component; the insertion pathway varies, leading to a multitude of product possibilities.[318] The general consensus is that, following a 1,2- or 1,4-insertion (Scheme 93), *endo*−*endo* or *exo*−*exo* arrangement of

**Scheme 93**

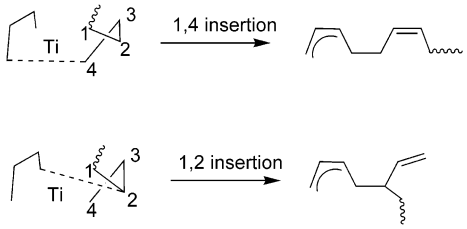


the monomer and growing polymer chain leads to a syndiotactic polymer, whereas *exo*−*endo* or *endo*−*exo* arrangement produces an isotactic polymer (Chart 23).[318]

**Chart 23. Possible Orientations of the Growing Polymer Chain and Monomer in the Polymerization of Dienes (Adapted from Reference 318)**

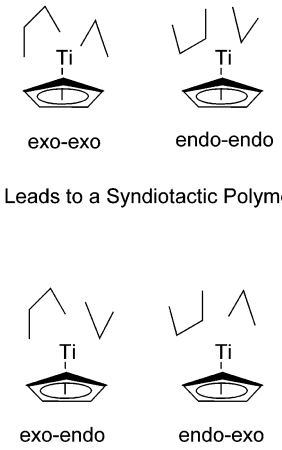

Soga et al.[319,320] performed the living polymerization of 1,3-butadiene using a $Cp'TiCl_3$−MAO catalyst system at low temperature (−25 °C) and reported nearly monodisperse polymers with up to 94% *cis* content, the predominant mode of enchainment being 1,4 chain insertion as determined by $^1H$ and $^{13}C$ NMR. The cis specificity was largely influenced by the steric bulkiness of the substituents attached to the Cp ring and the polymerization temperature.

Qian et al.[321,322] used a titanocene/$^i$PrMgX catalytic system for studying the polymerization of isoprene, but the main products were found to be the oligomers as shown in Scheme 94. The influence of Cp ring

**Scheme 94. Oligomerization of Diolefins**

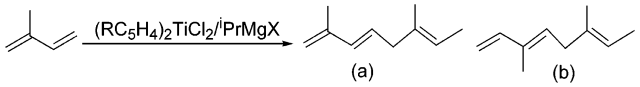


substitution on selectivity was also reported by studying a series of alkyl and $\omega$-alkenyl ring funtionalized titanocenes. The mechanism of the isomerization was proposed by introducing the catalytic species [$Cp_2TiH$], formed in situ from the reaction of titanocene dichloride with Grignard reagents as shown in Scheme 95. The copolymerization of iso-

**Scheme 95**

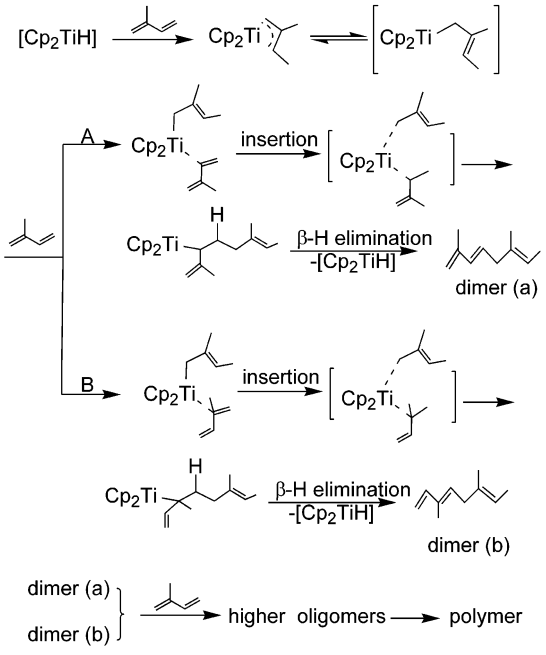


butylene and isoprene has also been initiated via a carbocationic mechanism to atactic products via a mechanism similar to Scheme 90,[323] incorporating by isoprene via *trans*-1,4-insertion.

## G. Polymerization Involving Cyclic Monomers

The heteropolymerization of cyclic monomers has been conducted after the discovery of the Ziegler catalysts. The addition polymerization of bulky cyclic monomers such as cyclopentene, cyclohexene, and norbornene has proven to be difficult for traditional heterogeneous Ziegler−Natta catalysts. These processes had many disadvantages including low activities and varying product properties, which were difficult to control. The first reported homogeneous catalysts for addition polymerization of norbornene were palladium(II) catalysts,[324] but the advanced homopolymerization of norbornene was achieved by Kaminsky[325,326] and co-workers with a zirconocene−MAO system. In comparison with heteropolymerization, the homopolymerization of norbornene and cyclopentene using metallocene can synthesize crystalline, insoluble polymers with high temperature and chemical resistance. According to the literature,[327] two models of reaction are known for the polymerization of norbornene (Scheme 96).

**Scheme 96. Possible Polymerization Reaction of Norbornene**

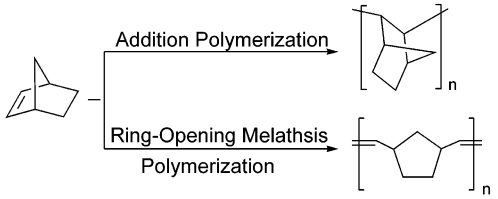


Unlike the ROMP catalyst, a metallocene−MAO catalyst system conducts exclusively polymerization by opening of the double bond only with the formation of the saturated, thermally stable polymer. However, polycyclo-olefins produced with the above-mentioned processes attract no commercial interest due to the absence of a melting point. In the 1990s, Kaminsky et al.[328] reported the preparation of ethane−cyclo-olefin copolymers, which show melting points together with other interesting properties despite their high transparency and chemical resistance. The main advantage of ethane−cyclo-olefin copolymers lies in their wide-ranging glass transition temperature, which can be varied from 20 to 260 °C with different ratios between norbornene and ethane. The ethane−norbornene copolymer can be used as compact disks, light-conducting fibers, and optical lenses due to the absence of polar, high transparency, and unsaturated or aromatic groups. Fink[329−332] and co-workers first reported the application of half-sandwich titanocene CGC in ethene−cyclo-olefin copolymerization (Scheme 97).

**Scheme 97. Poly(ethylene-*co*-norbonene)**

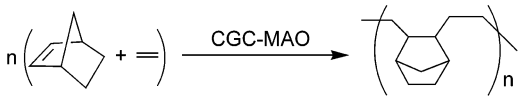


They found that the norbornene has been *cis*-2,3-*exo* inserted during the copolymerization with all of the metallocene and half-sandwich catalysts. The highest norbornene contents were achieved using metallocenes with a small substituent on the Cp ring. Unexpectedly, low norbornene contents (<50 mol %) were achieved with the half-sandwich CGC, although these types of catalysts had a relatively open active site, which can easily insert larger monomers. Another surprise result coming from the CGC is that increasing norbornene content decreases the molecular weight of the ethene−norbornene copolymers. Fink proposed that the norbornene unit, which is

inserted before an ethene molecule, supports the transfer reactions after an ethene insertion.

Waymouth et al.[333] also used various $C_s$ and $C_2$ symmetric CGC as catalysts for the copolymerization of norbornene. They get a similar result that although CGC possess a sterically less demanding ligand system and have less difficulty inserting larger monomers, norbornene homopolymerization appears to be much slower for CGC than for zirconocene.

Both Fink[329−332] and Waymouth[333] suggested that CGC might be good candidates for producing alternating microstructures, which is caused by the absence of norbornene dimers, trimers, and the high symmetry of the NENEN and ENENE pentads (N = norbornene, E = ethane). Fink further pointed that there is a difference in the trend of producing alternating sequences between the CGC and metallocene catalysts, although both copolymers are nearly of the same norbornene content. The CGC favor the formation of an isolated norbornene unit more than the alternating monomer sequence, whereas there are only slight differences in the tendency for alternating monomer sequences, according to analysis of the $^{13}C$ NMR spectrum.

Waymouth[333] also found that the copolymer productivity increases and norbornene incorporation decreases with the increase of reaction temperature and the decrease of norbornene concentration.

Wu[334] and co-workers investigated the polymerization behavior of $CpTiCl_3$, $CpTi(OBz)_3$, $Cp^*TiCl_3$, and $Cp^*Ti(OBz)_3$ for the addition polymerization of norbornene. The result shows that the activity of Cp-bearing catalysts is much higher than that of Cp*-bearing ones, due to the less steric obstacle to the coordination of the bulky cyclic monomer onto the active species. On the other hand, replacement of Cl with an OR group led to a remarkable increase in catalytic activity. Further study on the polymerization behavior of $CpTi(OBz)_3$ showed that the content of residual TMA in MAO plays a key role in the activity for norbornene polymerization. Less residual TMA led to higher activity.

As shown in Scheme 96, the type of catalyst is a major factor determining the course of reaction. The pioneering research works of Grubbs[335] and Schrock[336] have provided an important possible mechanism for ROMP, which led to the preparation of new polymeric materials.

The most effective catalysts for ROMP were alkylidene complexes (LnM=CHR) of molybdenum,[337] tungsten,[338] tantalum,[339] rhenium,[340] and ruthenium.[341] The titanium-based Tebbe reagent ($Cp_2Ti$=CHR) was also used for this kind of polymerization.[342]

Qian[343] and co-workers reported the result of titanium-based catalysts composed from $Cp_2TiCl_2$ and a series of Grignard agents RMgX for ROMP of norbornene. The results show that $Cp_2TiCl_2$−$CH_3MgI$ was the most effective catalytic system among the other catalyst systems. According to the mechanism of ROMP,[342] Tebbe reagent had been shown to be a titanium carbene precursor, which reacts with α-olifin and a Lewis base to form a stable, crystalline titanacyclobutane. Both titanium carbene and titancycles are the active species for ROMP (Scheme 98).

**Scheme 98. Mechanism of ROMP**

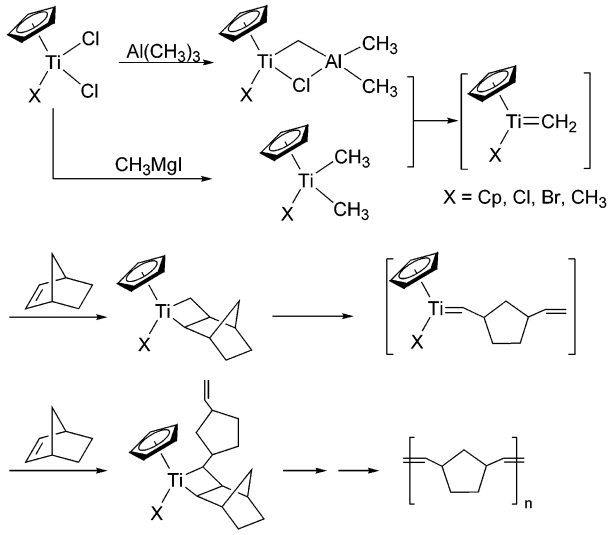


Petasis and co-workers found that dibenzyl,[344] bis-[(trimethylsilyl)methyl],[345] and bis(cyclopropyl)titanocenes[346] as well as dimethyltitanocene[342] behave similarly, although the formation for titanium carbene was via the different processes.

Qian et al.[343] also used $CpTiCl_2$−RMgX (R = $^i$Pr, $^n$Bu, *n*-hexanyl, 1-$C_3H_5$, or Ph) as catalyst system for polymerization of norbornene, resulting in polynorbornene with low activity. They assumed that these polymerizations followed a different mechanism with ROMP as the generation of titanocene hydride, allyl, and benzyl intermediates instead of a titanocene carbene complex during the reaction.

In some cases, copolymers may contain a ring unit via the isomerization of a linear olefin. MAO-activated complex **137** produced homopolymers and random copolymers of 1,5-hexadiene with ethylene, and the incorporation of styrene resulted in terpolymers with high hexadiene content and random distribution of *cis* and *trans* rings (Chart 24). The ratio of methylene−1,3-cyclopentane rings to vinyl side chains was controlled by 1,5-hexadiene concentration.[303,304]

**Chart 24. Terpolymer of Hexadiene:Poly(ethane-*co*-styrene-*co*-1,5-hexadiene)**

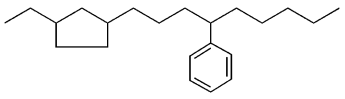

## H. Isomerization and Hydrogenation of Olefins

The isomerization of olefins is an important part in a great number of transition metal catalyzed reactions. Several mechanisms for the transition metal catalyzed isomerization of olefins have been well documented. Among these theories, the $\pi$-allylmetal hydride mechanism (a) and the metal hydride addition−elimination mechanism (b) are the two main reasonable mechanisms,[347] which undergo fundamentally different reactions. Mechanism a indicates that intramolecular 1,3-hydrogen isomerization is initiated by metal via an $\eta^3$-allylmetal hydride intermediate. Mechanism b is an intermolecular process, containing $\beta$-hydrogen elimination from a

**Scheme 99. Different Mechanisms for the Isomerization of Olefins: (a) $\pi$-Allyl Metal Hydride Mechanism; (b) Metal Hydride Addition−Elimination Mechanism**

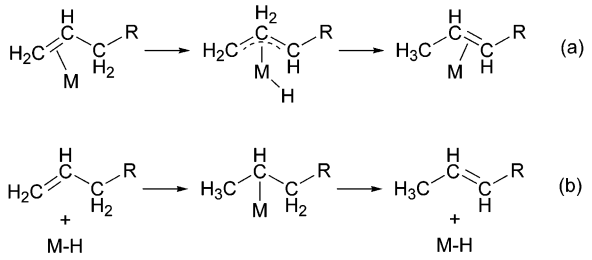

**Chart 25**

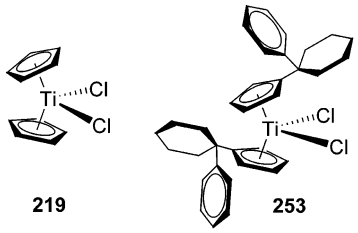

secondary metal alkyl, and requires a stable metal hydride as an active species (Scheme 99).

The low-valent cyclopentadienyl titanium complexes [$Cp_2TiH$], generated in situ from the reduction of dicyclopentadienyl titanium dichloride by various reducing agents such as Grignard reagents having a $\beta$-hydrogen ($i$-$C_3H_7MgBr$), have been regarded as the catalyst in a number of reactions, including the isomerization of olefins such as 1,5-hexadiene,[348−351] 1,5-cyclooctadiene,[352] and 4-vinyl-cyclohexene.[322]

Qian[348−351] et al. employed some ring-substituted titanocene as isomerization catalyst for 1,5-hexadiene, resulting in a mixture of 1,4-hexadiene, 1,3-hexadiene, 2,4-hexadiene, methylcyclopentane, and methylcyclopentene. The results indicated that those complexes containing an amino substituent on the Cp ring isomerize 1,5-hezadiene into methylenecyclopentane and methylcyclopentene with a cyclic selectivity as high as 92−97%. High selective cyclization of 1,5-hexadiene is reasonably attributed to the intramolecular coordination of N to Ti, which increases the electron density on titanium and hence favors another intramolecular coordination of a double bond to titanium. 4-Vinylcyclohexane (VCH) can be isomerized by ring-substituted titanocene (complex **253**) into 4-ethylidenecyclohexane with a conversion of nearly 99%, or its conjugated isomer may be obtained quantitatively by complex **219** by controlling the reaction condition (Chart 25 and Scheme 100). Introduction of substituents on the Cp ring decreases the activity due to the steric hindrance.[322]

**Scheme 100. Isomerization of VCH**

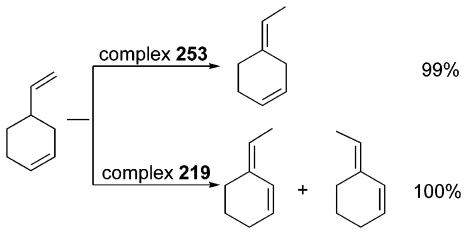

Monocyclopentadienyl and dicyclopentadienyl group 4 transition metal compounds using Ziegler−Natta catalysts for homogeneous olefin hydrogenation have been fully studied and well documented. In a published review, Royo et al.[353] summarized the different reactions for the formation of the active hydride species [LnM−H], including addition of $LiAlH_x(OR)_y$ or $AlR_3$, $MgH_2$ or RMgX, and NaH, KH, or LiR or Na, K, Mg, etc., to the metallocene dichloride, using dihydride or chlorohydride complexes or hydrogenolysis of monoalkyl or dialkyl complexes. They also pointed out that this type of catalyst did not hydrogenate aromatic double bonds and that the titanium complexes exhibited higher activity but poorer selectivity than the zirconium derivatives. We have now reviewed some selected literature about titanium catalysts for hydrogenation since 1995.

Asymmetric hydrogenation of imines was conducted in excellent conversion using chiral CGC complexes (complexes **142**−**155**), but their enantioselectivity was improved finitely. Okuda[180,182] et al. proposed that these CGC might not offer an active site capable of efficiently discriminating the enantiotopic side of the imine substrate in comparison with the Brintzinger-type *ansa*-titanocene.

Liao[354,355] et al. reported the hydrogenation of a terminal olefin was catalyzed by titanocenes with a bulk substituent on the Cp ring in the presence of nanometric sodium hydride. The steric hindrance of a substituent containing a six- or severn-membered ring may reduce the possibility of dimerization of low-valent titanium, which improved the stability of active species and resulted in the high activity for hydrogenation. These catalysts exhibited very high selectivity to the terminal olefins.

Buchwald[118] and co-workers investigated the catalytic activity of complexes **66** and **67** for the hydrogenation of 2-phenylpyrroline (Scheme 101).

**Scheme 101**

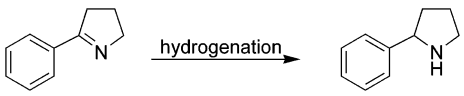

The result shows that the catalytic activity of a complex with one atom in the bridge (complexes **66** and **67**) was lower than that of complexes with two atoms in the bridge (Brintzinger type catalyst). Complex **67** catalyzed the hydrogenation reaction at a rate of ∼5 times that observed for complex **66**. Buchwald presumed the electron effect was the main factor as the steric difference was slight between the two complexes. The more electron-rich metal center of complex **67** exhibited an increasing reaction rate compared with the electron-deficient metal center of complex **66**.

## *IV. Conclusions and Outlook*

In this review, we have tackled the synthetic methodologies to various classes of titanocenes based on the nature of ring substitution. We have also appraised the application of these complexes as polymerization catalysts in the presence of various cocatalysts. The half-sandwich titanocenes and the

constrained geometry linked-amido cyclopentadienyl-(indenyl) titanium complexes remain the most active area of titanium research. The ability of these complexes to initiate the polymerization of a variety of monomers and to incorporate several monomers forming a co- or terpolymer is quite remarkable. Looking to the future, we expect to see a rapid expansion in the scope of titanocene applications. A frenzy of activity similar in magnitude to that witnessed over the past two decades that brought organometallic and polymer chemistry together will probably soon be repeated.

## V. List of Abbreviations

| | |
|---|---|
| Bn | benzenyl |
| bp | boiling point |
| Bu | butyl |
| Ce | centroid of Cp ring |
| CGC | constrained geometry catalysts |
| Cp(Ind) | cyclopentadienyl(indenyl) mixed ligand |
| Cp* | pentamethylcyclopentadiene, permethylated cyclopentadienyl ligand |
| Cp | cyclopentadiene, cyclopentadienyl ligand |
| Cp′ | substituted cyclopentadiene, substituted cyclopentadienyl ligand |
| CpLi | cyclopentadienyllithium salt |
| Et | ethyl |
| HDPE | high-density polyethylene |
| Ind* | permethylated indenyl ligand |
| Ind | indene, indenyl ligand |
| Ind′ | substituted indene, substituted indenyl ligand |
| IndLi | indenyllithium salt |
| LDPE | linear density polyethylene |
| LLDPE | linear low-density polyethylene |
| MAO | methylalumoxane |
| Me | methyl |
| MEK | methyl ethyl ketone (acetone) |
| $M_n$ | number-average molecular weight |
| mp | melting point |
| $M_w$ | weight-average molecular weight |
| Ph | phenyl |
| Pr | propyl |
| Py | pyridyl |
| s-PS | syndiotactic polystyrene |
| $T_m$ | melting temperature of s-PS |
| TM | transition metal(s) |
| $t_p$ | polymerization time |
| $T_p$ | polymerization temperature |
| Z−N | Ziegler−Natta catalyst |

## VI. Acknowledgments

We gratefully acknowledge financial support from the Special Funds for Major State Basic Research Projects (G 1999064801), the National Natural Science Foundation of China (NNSFC) (29871010, 9734145, 20072004). Such a big project would not have been successful without the input of many colleagues and associates; we extend our thanks to all current and past members of the Laboratory of Organometallic Chemistry for their contributions.

## VII. References

(1) *Metallocenes: Synthesis−Reactivity−Applications*; Togni, A., Halterman, R. L., Eds.; Wiley-VCH: New York, 1998; Vol. 1 and 2.
(2) Long, N. J. *Metallocenes*; Blackwell Science: Malden, MA, 1998.
(3) Yasuda, H. *Prog. Polym. Sci.* **2000**, *25*, 573.
(4) Boffa, L. S.; Novak, B. M. *Chem. Rev.* **2000**, *100*, 1479.
(5) Britovsek, G. J. P.; Gibson, V. C.; Wass, D. F. *Angew. Chem., Int. Ed. Engl.* **1999**, *38*, 428.
(6) Calhorda, M. J.; Veiros, L. F. *Coord. Chem. Rev.* **1999**, *185−186*, 37.
(7) *Applied Homogeneous Catalysis With Organometallic Compounds*; Corniels, B., Hermann, W. A., Eds.; VCH: Weinheim, Germany, 1996; Vol. I and II.
(8) Alt, H. G. *J. Chem. Soc., Dalton Trans.* **1999**, 1703.
(9) Hlatky, G. G. *Coord. Chem. Rev.* **1999**, *181*, 243.
(10) *Chem. Rev.* **2000**, *100* (4).
(11) *Chem. Rev.* **2002**, *102* (6).
(12) Möhring, P. C.; Coville, N. J. *J. Organomet. Chem.* **1994**, *479*, 1.
(13) Kaminsky, W. *Catal. Today* **2000**, *62*, 23.
(14) Kaminsky, W. *Macromol. Chem. Phys.* **1996**, *197*, 3907.
(15) Kaminsky, W. *J. Chem. Soc., Dalton Trans.* **1998**, 1413.
(16) Alt, H. G.; Köppl, A. *Chem. Rev.* **2000**, *100*, 1205.
(17) Ewen, J. A. *J. Mol. Catal., A: Chem.* **1998**, *128*, 103.
(18) McKnight, A. L.; Waymouth, R. M. *Chem. Rev.* **1998**, *98*, 2587.
(19) Brintzinger, H. H.; Fischer, D.; Mülhaupt, R.; Rieger, B.; Waymouth, R. M. *Angew. Chem., Int. Ed. Engl.* **1995**, *34*, 1143.
(20) Coates, G. W. *Chem. Rev.* **2000**, *100*, 1223.
(21) Coates, G. W.; Waymouth, R. M. In *Comprehensive Organometallic Chemistry II*; Abel, E. W., Stone, F. G. A., Wilkinson, G., Eds.; Pergamon Press: Oxford, U.K., 1995; Vol. 12, p 1193.
(22) Jutzi, P.; Redeker, T. *Eur. J. Inorg. Chem.* **1998**, 663.
(23) Müller, C.; Vos, D.; Jutzi, P. *J. Organomet. Chem.* **2000**, *600*, 127.
(24) Butenschön, H. *Chem. Rev.* **2000**, *100*, 1527.
(25) Siemeling, U. *Chem. Rev.* **2000**, *100*, 1495.
(26) Qian, Y.; Huang, J. *Chin. J. Chem.* **2001**, *19*, 1009.
(27) Jutzi, P.; Siemeling, U. *J. Organomet. Chem.* **1995**, *500*, 175.
(28) Hlatky, G. G. *Chem. Rev.* **2000**, *100*, 1247.
(29) Resconi, L.; Cavallo, L.; Fait, A.; Piemontesi, F. *Chem. Rev.* **2000**, *100*, 1253.
(30) Halterman, R. L. In *Metallocenes: Synthesis−Reactivity−Applications*; Togni, A., Halterman, R. L., Eds.; Wiley-VCH: New York, 1998; p 455.
(31) Lee, B. Y.; Han, J. W.; Seo, H.; Lee, I. S.; Chung, Y. K. *J. Organomet. Chem.* **2001**, *627*, 233.
(32) Nomura, K.; Naga, N.; Niki, M.; Yanagi, K.; Imai, A. *Organometallics* **1998**, *17*, 2152.
(33) Amor, J. I.; Cuenca, T.; Galakhov, M.; Royo, P. *J. Organomet. Chem.* **1995**, *497*, 127.
(34) King, W. A.; Bella, S. D.; Gulino, A.; Lanza, G.; Fragalà, I. L.; Stern, C. L.; Marks, T. J. *J. Am. Chem. Soc.* **1999**, *121*, 355.
(35) Butakoff, K. A.; Lemenovskii, D. A.; Mountford, P.; Kuz'mina, L. G.; Churakov, A. V. *Polyhedron* **1996**, *15*, 489.
(36) Okuda, J.; du Plooy, K. E.; Toscano, P. J. *J. Organomet. Chem.* **1995**, *495*, 195.
(37) Cheng, Y.; Yu, X.; Jin, G.; Jia, H. *Acta Polym. Sin. (Chinese)* **2001**, *2*, 139.
(38) Zhou, G.; Cheng, Y.; Jin, G. *Chin. J. Appl. Chem.* **2001**, *18*, 396.
(39) Grimmond, B. J.; Corey, J. Y.; Rath, N. P. *Organometallics* **1998**, *18*, 404.
(40) Zhang, J.; Xu, Z.; Chen, S. *Acta Sci. Nat. Univ. Pekin.* **2000**, *36*, 259.
(41) Hughes, R. P.; Lomprey, J. R.; Rheingold, A. L.; Haggerty, B. S.; Yap, G. P. A. *J. Organomet. Chem.* **1996**, *517*, 89.
(42) Licht, E. H.; Alt, H. G.; Karim, M. M. *J. Organomet. Chem.* **2000**, *599*, 275.
(43) Hart, S. L.; Duncalf, D. J.; Hastings, J. J.; McCamley, A.; Taylor, P. C. *J. Chem. Soc., Dalton Trans.* **1996**, 2843.
(44) Kerstig, M. In *Polymeric Materials Encyclopedia*; Salamone, J. C., Ed.; CRC Press: New York, 1996; p 8119.
(45) Qian, Y.; Huang, J.; Yang, J.; Chan, A. S. C.; Chen, W.; Chen, X.; Li, G.; Jin, X.; Yang, Q. *J. Organomet. Chem.* **1997**, *547*, 263.
(46) Huang, Q.; Qian, Y.; Li, G.; Tang, Y. *Trans. Met. Chem.* **1990**, *15*, 483.
(47) Plenio, H.; Warnecke, A. *J. Organomet. Chem.* **1997**, *544*, 133.
(48) Huang, J.; Zhang, Y.; Huang, Q.; Qian, Y. *Inorg. Chem. Commun.* **1999**, *2*, 104.
(49) Qian, Y.; Li, G. *Polyhedron* **1993**, *12*, 967.
(50) van der Zeijden, A. A. H.; Mattheis, C. *J. Organomet. Chem.* **1998**, *555*, 5.
(51) Piao, G.; Goto, H.; Akagi, K.; Shirakawa, H. *Polymer* **1998**, *39*, 3559.
(52) Huang, Q.; Qian, Y.; Tang, Y. *Trans. Met. Chem.* **1989**, *14*, 315.
(53) Tian, J.; Hu, N.; Sheng, Q.; Huang, B. *Chin. J. Struct. Chem. (Jiegou Huaxue)* **1995**, *14*, 83.
(54) Huang, Q.; Qian, Y,; Tang, Y. *J. Organomet. Chem.* **1989**, *368*, 277.
(55) Clearfield, A.; Warner, D. K.; Saldarriaga-Molina, C. H.; Ropal, R.; Bernal, I. *Can. J. Chem.* **1975**, *53*, 1622.
(56) Jutzi, P.; Kleimeier, J. *J. Organomet. Chem.* **1995**, *486*, 287.
(57) Jutzi, P.; Redeker, T.; Neumann, B.; Stammler, H.-G. *Organometallics* **1996**, *15*, 4153.

(58) Beckhaus, R.; Oster, J.; Ganter, B.; Englert, U. *Organometallics* **1997**, *16*, 3902.
(59) Jutzi, P.; Redeker, T.; Neumann, B.; Stammler, H.-G. *Chem. Ber.* **1996**, *129*, 1509.
(60) Flores, J. C.; Chien, J. C. W.; Rausch, M. D. *Macromolecules* **1996**, *29*, 8030.
(61) Qian, Y.; Guo, R.; Huang, J.; Jonas, K. *Chin. Chem. Lett.* **1996**, *7*, 1139.
(62) Jutzi, P.; Redeker, T.; Neumann, B.; Stammler, H.-G. *Chem. Ber.* **1996**, *129*, 1509.
(63) Enders, M.; Köhler, K.; Frosch, W.; Pritzkow, H.; Lang, H. *J. Organomet. Chem.* **1997**, *538*, 163.
(64) Carter, C. A. G.; McDonald, R.; Stryker, J. M. *Organometallics* **1999**, *18*, 820.
(65) Greidanus, G.; McDonald, R.; Stryker, J. M. *Organometallics* **2001**, *20*, 2492.
(66) Delgado, E.; Forniés, J.; Hernández, E.; Lalinde, E.; Mansilla, N.; Moreno, M. T. *J. Organomet. Chem.* **1995**, *494*, 261.
(67) Gendre, P. L.; Maubrou, E.; Blacque, O.; Boni, G.; Moïse, C. *Eur. J. Inorg. Chem.* **2001**, 1437.
(68) Delgado, E.; García, M. A.; Hernández, E.; Mansilla, N.; Martínez-Cruz, L. A.; Tornero, J.; Torres, R. *J. Organomet. Chem.* **1998**, *560*, 27.
(69) Gendre, P. L.; Richard, P.; Moïse, C. *J. Organomet. Chem.* **2000**, *605*, 151.
(70) Graham, T. W.; Llamazares, A.; McDonald, R.; Cowie, M. *Organometallics* **1999**, *18*, 3490.
(71) Flores, J. C.; Hernández, R.; Royo, P.; Butt, A.; Spaniol, T. P.; Okuda, J. *J. Organomet. Chem.* **2000**, *593*−*594*, 202.
(72) Lin, S.; Waymouth, R. M. *Acc. Chem. Res.* **2002**, *35*, 765.
(73) Maldanis, R. J.; Chien, J. C. W.; Rausch, M. D. *J. Organomet. Chem.* **2000**, *599*, 107.
(74) Horáček, M.; Polášek, M.; Kupfer, V.; Thewalt, U.; Mach, K. *Collect. Czech. Chem. Commun.* **1999**, *64*, 61.
(75) Qian, Y.; Qin, X.; Huang, J.; Chan, A. S. C.; Chen, S.; Wang, H. *Chin. J. Chem.* **2001**, *19*, 97.
(76) Dorado, I.; Flores, J. C.; Galakhov, M.; Sal, P. G.; Martín, A.; Royo, P. *J. Organomet. Chem.* **1998**, *563*, 7.
(77) Foster, P.; Chien, J. C. W.; Rausch, M. D. *Organometallics* **1996**, *15*, 4951.
(78) Rufanov, K. A.; Churakov, A. V.; Kazennova, N. B.; Brusova, G. P.; Lemenovskii, D. A.; Kuz'mina, L. G. *J. Organomet. Chem.* **1995**, *498*, 37.
(79) Kupfer, V.; Thewalt, U.; Tišlerová, I.; Štěpnička, P.; Gyepes, R.; Kubišta, J.; Horáček, M.; Mach, K. *J. Organomet. Chem.* **2001**, *620*, 39.
(80) Zhou, G.; Cheng, D.; Jin, G. *Chin. J. Appl. Chem.* **2001**, *18*, 128.
(81) Marechal, E.; Lepert, A. *Bull. Soc. Chim. Fr.* **1967**, 2954.
(82) Wild, F. R. W. P.; Zsolnai, J.; Huttner, G.; Brintzinger, H. H. *J. Organomet. Chem.* **1982**, *232*, 233.
(83) Ewen, J. A. *J. Am. Chem. Soc.* **1984**, *106*, 6355.
(84) Kaminsky, W.; Kulper, K.; Britzinger, H. H.; Wild, F. R. P. *Angew. Chem., Int. Ed. Engl.* **1985**, *24*, 507.
(85) Varga, V.; Hiller, J.; Gyepes, R.; Polášek, M.; Sedmera, P.; Thewalt, U.; Mach, K. *J. Organomet. Chem.* **1997**, *538*, 63.
(86) Tian, G.; Wang, B.; Xu, S.; Zhang, Y.; Zhou, X. *J. Organomet. Chem.* **1999**, *579*, 24.
(87) Sun, X.; Wang, B.; Xu, S.; Zhou, X. *Chem. J. Chin. Univ.* **2000**, *21*, 222.
(88) Tian, G.; Wang, B.; Dai, X.; Xu, S.; Zhou, X.; Sun, J. *J. Organomet. Chem.* **2001**, *634*, 145.
(89) Weiss, K.; Neugebauer, U.; Blau, S.; Lang, H. *J. Organomet. Chem.* **1996**, *520*, 171.
(90) Beagley, P.; Davies, P.; Adams, H.; White, C. *Can. J. Chem.* **2001**, *79*, 731.
(91) Miyake, S.; Henling, L. M.; Bercaw, J. E. *Organometallics* **1998**, *17*, 5528.
(92) Wang, B. Q.; Xu, S. S.; Zhou, X. Z.; Su, L. M.; Feng, R.; He, D. W. *Chem. J. Chin. Univ.* **1999**, *20*, 77.
(93) Luttikhedde, H. J. G.; Leino, R.; Wilén, C.; Laine, E.; Sillanpää, R.; Näsman, J. H. *J. Organomet. Chem.* **1997**, *547*, 129.
(94) Agarkov, A. Y.; Izmer, V. V.; Riabov, A. N.; Kuz'mina, L. G.; Howard, J. A. K.; Beletskaya, I. P.; Voskoboynikov, A. Z. *J. Organomet. Chem.* **2001**, *619*, 280.
(95) Halterman, R. L.; Combs, D.; Khan, M. A. *Organometallics* **1998**, *17*, 3900.
(96) Hitchcock, S. R.; Situ, J. J.; Covel, J. A.; Olmstead, M. M.; Nantz, M. H. *Organometallics* **1995**, *14*, 3732.
(97) Palandoken, H.; Wyatt, J. K.; Hitchcock, S. R.; Olmstead, M. M.; Nantz, M. H. *J. Organomet. Chem.* **1999**, *579*, 338.
(98) Halterman, R. L.; Ramsey, T. M. *J. Organomet. Chem.* **1997**, *530*, 225.
(99) Halterman, R. L.; Combs, D.; Kihega, J. G.; Khan, M. A. *J. Organomet. Chem.* **1996**, *520*, 163.
(100) Halterman, R. L.; Tretyakov, A.; Khan, M. A. *J. Organomet. Chem.* **1998**, *568*, 41.
(101) Chen, Z.; Halterman, R. L. *J. Am. Chem. Soc.* **1992**, *114*, 2276.
(102) Halterman, R. L.; Zhu, C.; Chen, Z.; Dunlap, M. S.; Khan, M. A.; Nicholas, K. M. *Organometallics* **2000**, *19*, 3824.
(103) Steinhorst, A.; Erker, G.; Grehl, M.; Fröhlich, R. *J. Organomet. Chem.* **1997**, *542*, 191.
(104) Urazowski, I. F.; Atovmyan, L. O.; Mkoyan, S. G.; Broussier, R.; Perron, P.; Gautheron, B.; Robert, F. *J. Organomet. Chem.* **1997**, *536*−*537*, 531.
(105) Jaquith, J. B.; Guan, J.; Wang, S.; Collins, S. *Organometallics* **1995**, *14*, 1079.
(106) Halterman, R. L.; Ramsey, T. M.; Pailes, N. A.; Khan, M. A. *J. Organomet. Chem.* **1995**, *497*, 43.
(107) Ellis, W. W.; Hollis, T. K.; Odenkirk, W.; Whelan, J.; Ostrander, R.; Rheingold, A. L.; Bosnich, B. *Organometallics* **1993**, *12*, 4391.
(108) Huttenloch, M. E.; Diebold, J.; Rief, U.; Brintzinger, H. H.; Gilbert, A. M.; Katz, T. J. *Organometallics* **1992**, *11*, 3600.
(109) Huttenloch, M. E.; Dorer, B.; Rief, U.; Prosenc, M. H.; Schmidt, K.; Brintzinger, H. H. *J. Organomet. Chem.* **1997**, *541*, 219.
(110) Halterman, R. L.; Tretyakov, A.; Combs, D.; Chang, J.; Khan, M. A. *Organometallics* **1997**, *16*, 3333.
(111) Zhou X. Z.; Wang, B. Q.; Xu, S. S. *Chem. J. Chin. Univ.* **1995**, *16*, 887.
(112) Ciruelos, S.; Sebastián, A.; Cuenca, T.; Gómez-Sal, P.; Manzanero, A.; Royo, P. *J. Organomet. Chem.* **2000**, *604*, 103.
(113) Deck, P. A.; Fisher, T. S.; Downey, J. S. *Organometallics* **1997**, *16*, 1193.
(114) Song, W.; Shackett, K.; Chien, J. C. W.; Rausch, M. D. *J. Organomet. Chem.* **1995**, *501*, 375.
(115) Alt, H. G.; Föttinger, K.; Milius, W. *J. Organomet. Chem.* **1998**, *564*, 109.
(116) Shin, J. H.; Hascall, T.; Parkin, G. *Organometallic* **1999**, *18*, 6.
(117) Schmid, M. A.; Alt, H. G.; Milius, W. *J. Organomet. Chem.* **1996**, *514*, 45.
(118) Willoughby, C. A.; Davis, W. M.; Buchwald, S. L. *J. Organomet. Chem.* **1995**, *497*, 11.
(119) Miyake, S.; Okumura, Y.; Inazawa, S. *Macromolecules* **1995**, *28*, 8, 3074.
(120) Gauthier, W. J.; Corrigan, J. F.; Taylor, N. J.; Collins, S. *Macromolecules* **1995**, *28*, 3771.
(121) Noh, S. K.; Byun, G.; Lee, C.; Lee, D.; Yoon, K.; Kang, K. S. *J. Organomet. Chem.* **1996**, *518*, 1.
(122) Jung, J.; Noh, S. K.; Lee, D.; Park, S. K.; Kim, H. *J. Organomet. Chem.* **2000**, *595*, 147.
(123) Ciruelos, S.; Cuenca, T.; Gómez-Sal, P.; Manzanero, A.; Royo, P. *Organometallics* **1995**, *14*, 177.
(124) Churakov, A. V.; Lemenovskii, D. A.; Kuz'mina, L. G. *J. Organomet. Chem.* **1995**, *489*, C81.
(125) Björgvinsson, M.; Halldorsson, S.; Arnason, I.; Magull, J.; Fenske, D. *J. Organomet. Chem.* **1997**, *544*, 207.
(126) Li, Z.; Huang, J.; Yao, T.; Qian, Y.; Leng, M. *J. Organomet. Chem.* **2000**, *598*, 339.
(127) Cano, A.; Cuenca, T.; Rodríguez, G.; Royo, P. *J. Organomet. Chem.* **1993**, *447*, 51.
(128) Nifant'ev, I. E.; Borzov, M. V.; Churakov, A. V.; Mkoyan, S. G.; Atovmyan, L. O. *Organometallics* **1992**, *11*, 3942.
(129) Huhmann, J. L.; Corey, J. Y.; Rath, N. P. *J. Organomet. Chem.* **1997**, *533*, 61.
(130) Ciruelos, S.; Cuenca, T.; Gómez, R.; Gómez-Sal, P.; Manzanero, A.; Royo, P. *Polyhedron* **1998**, *17*, 1055.
(131) Feng, R.; Su, L.; He, D.; Wang, B.; Tian, G.; Xu, S.; Zhou, X. *Acta Polym. Sin.* **1998**, *3*, 360.
(132) Lee, D.; Yoon, K.; Lee, E.; Noh, S.; Byun, G.; Lee, C. *Macromol. Rapid Commun.* **1995**, *16*, 265.
(133) Corey, J. Y.; Huhmann, J. L.; Rath, N. P. *Inorg. Chem.* **1995**, *34*, 3203.
(134) (a) Royo, B.; Royo, P.; Cadenas, L. M. *J. Organomet. Chem.* **1998**, *551*, 293. (b) Larkin, S. A.; Golden, J. T.; Shapiro, P. J.; Yap, G. P. A.; Foo, D. M. J.; Rheingold, A. L. *Organometallics* **1996**, *15*, 2393.
(135) Flores, J. C.; Ready, T. E.; Chien, J. C. W.; Rausch, M. D. *J. Organomet. Chem.* **1998**, *562*, 11.
(136) (a) Nifant'ev, I. E.; Borzov, M. V.; Churakov, A. V.; Mkoyan, S. G.; Atovmyan, L. O. *Organometallics* **1992**, *11*, 3942. (b) Huang, J.; Feng, Z.; Wang, H.; Qian, Y.; Sun. J.; Xu, Y.; Chen, W.; Zheng, G. *J. Mol. Catal. A: Chem.* **2002**, *189*, 187.
(137) Ready, T. E.; Chien, J. C. W.; Rausch, M. D. *J. Organomet. Chem.* **1996**, *519*, 21.
(138) Ready, T. E.; Chien, J. C. W.; Rausch, M. D. *J. Organomet. Chem.* **1999**, *583*, 11.
(139) Kim, Y.; Koo, B. H.; Do, Y. *J. Organomet. Chem.* **1997**, *527*, 155.
(140) Shaw, S. L.; Storhoff, J. J.; Cullison, S.; Davis, C. E.; Holloway, G.; Morris, R. J.; Huffman, J. C.; Bollinger, J. C. *Inorg. Chim. Acta* **1999**, *292*, 220.
(141) Xu, G. X.; Ruckenstein, E. *J. Polym Sci., Part A: Polym. Chem.* **1999**, *37*, 2481.
(142) Künzel, A.; Parisini, E.; Roesky, H. W.; Sheldrick, G. M. *J. Organomet. Chem.* **1997**, *536*−*537*, 177.
(143) van der Zeijden, A. A. H.; Mattheis, C.; Fröhlich, R. *Organometallics* **1997**, *16*, 2651.
(144) Rau, A.; Schmitz, S.; Luft, G. *J. Organomet. Chem.* **2000**, *608*, 71.

(145) Huang, J.; Huang, Q.; Qian, Y.; Chan, A. S. C.; Wong, W. T. *Polyhedron* **1998**, *17*, 2523.
(146) Trouvé, G.; Laske, D. A.; Meetsma, A.; Teuben, J. H. *J. Organomet. Chem.* **1996**, *511*, 255.
(147) Christie, S. D. R.; Man, K. W.; Whitby, R. J.; Slawin, A. M. Z. *Organometallics* **1999**, *18*, 348.
(148) Qian, Y.; Huang, J. Unpublished results.
(149) Foster, P.; Rausch, M. D.; Chien, J. C. W. *J. Organomet. Chem.* **1997**, *527*, 71.
(150) Tian, G.; Xu, S.; Zhang, Y.; Wang, B.; Zhou, X. *J. Organomet. Chem.* **1998**, *558*, 231.
(151) Qian, Y.; Li, G.; Chen, W.; Li, B.; Jin, X. *J. Organomet. Chem.* **1989**, *373*, 185.
(152) Bu, W.; Wang, J.; Ye, L.; Mu, Y.; Yang, G.; Fan, Y. *Acta Crystallogr.* **1999**, *C55*, 728.
(153) Flores, J. C.; Chien, J. C. W.; Rausch, M. D. *Organometallics* **1994**, *13*, 4140.
(154) Blais, M. S.; Chien, J. C. W.; Rausch, M. D. *Organometallics* **1998**, *17*, 3775.
(155) Jutzi, P.; Redeker, T.; Neumann, B.; Stammler, H.-G. *J. Organomet. Chem.* **1997**, *533*, 237.
(156) Herrmann, W. A.; Morawietz, M. J. A.; Priermeier, T.; Mashima, K. *J. Organomet. Chem.* **1995**, *486*, 291.
(157) Enders, M.; Rudolph, R.; Pritzkow, H. *Chem. Ber.* **1996**, *129*, 459.
(158) Enders, M.; Rudolph, R.; Pritzkow, H. *J. Organomet. Chem.* **1997**, *549*, 251.
(159) van der Zeijden, A. A. H. *J. Organomet. Chem.* **1996**, *518*, 147.
(160) Jutzi, P.; Kristen, M. O.; Dahlhaus, J.; Neumann, B.; Stammler, H. G. *Organometallics* **1993**, *12*, 2980.
(161) Wang, T.-F.; Lee, T.-Y.; Wen, Y.-S.; Liu, L.-K. *J. Organomet. Chem.* **1991**, *403*, 353.
(162) Shapiro, P. J.; Bunel, E.; Schaefer, W. P.; Bercaw, J. E. *Organometallics* **1990**, *9*, 867.
(163) Okuda, J. *Chem. Ber.* **1990**, *123*, 1649.
(164) Herrmann, W. A.; Morawietz, M. J. A. *J. Organomet. Chem.* **1994**, *482*, 169.
(165) du Plooy, K. E.; Moll, U.; Wocadlo, S.; Massa, W.; Okuda, J. *Organometallics* **1995**, *14*, 3129.
(166) McKnight, A. L.; Masood, M. A.; Waymouth, R. M.; Straus, D. A. *Organometallics* **1997**, *16*, 2879.
(167) Eberle, T.; Spaniol, T. P.; Okuda, J. *Eur. J. Inorg. Chem.* **1998**, 237.
(168) Alt, H. G.; Reb, A.; Milius, W.; Weis, A. *J. Organomet. Chem.* **2001**, *628*, 169.
(169) Amor, F.; Butt, A.; du Plooy, K. E.; Spaniol, T. P.; Okuda, J. *Organometallics* **1998**, *17*, 5836.
(170) Sernetz, F. G.; Mülhaupt, R.; Amor, F.; Eberle, T.; Okuda, J. *J. Polym. Sci., Part A: Polym. Chem.* **1997**, *35*, 1571.
(171) Zemánek, J.; Štěpnička, P.; Fejfarová, K.; Gyepes, R.; Císařová, I.; Horáček, M.; Kubišta, J.; Varga, V.; Mach, K. *Collect. Czech. Chem. Commun.* **2001**, *66*, 605.
(172) Chen, Y.-X.; Marks, T. J. *Organometallics* **1997**, *16*, 3649.
(173) Alt, H. G.; Föttinger, K.; Milius, W. *J. Organomet. Chem.* **1999**, *572*, 21.
(174) Okuda, J.; Eberle, T.; Spaniol, T. P. *Chem. Ber./Recueil* **1997**, *130*, 209.
(175) Ioku, A.; Hasan, T.; Shiono, T.; Ikeda, T. *Macromol. Chem. Phys.* **2002**, *203*, 748.
(176) Park, J. T.; Yoon, S. C.; Bae, B.-J.; Seo, W. S.; Suh, I.-H.; Han, T. K.; Park, J. R. *Organometallics* **2000**, *19*, 1269.
(177) Carpenetti, D. W.; Kloppenburg, L.; Kupec, J. T.; Petersen, J. L. *Organometallics* **1996**, *15*, 1572.
(178) Yoon, S. C.; Bae, B.-J.; Suh, I.-H.; Park, J. T. *Organometallics* **1999**, *18*, 2049.
(179) Ciruelos, S.; Cuenca, T.; Gómez, R.; Gómez-Sal, P.; Manzanero, A.; Royo, P. *Organometallics* **1996**, *15*, 5577.
(180) Okuda, J.; Verch, S.; Spaniol, T. P.; Stürmer, R. *Chem. Ber.* **1996**, *129*, 1429.
(181) Okuda, J.; Eberle, T.; Spaniol, T. P.; Piquet-Fauré, V. *J. Organomet. Chem.* **1999**, *591*, 127.
(182) Okuda, J.; Verch, S.; Stürmer, R.; Spaniol, T. P. *J. Organomet. Chem.* **2000**, *605*, 55.
(183) Jiménez, G.; Rodríguez, E.; Gómez-Sal, P.; Royo, P.; Cuenca, T.; Galakhov, M. *Organometallics* **2001**, *20*, 2459.
(184) Okuda, J.; du Plooy, K. E.; Massa, W.; Kang, H.-K.; Rose, U. *Chem. Ber.* **1996**, *129*, 275.
(185) Gómez, R.; Gómez-Sal, P.; Martín, A.; Núñez, A.; del Real, P. A.; Royo, P. *J. Organomet. Chem.* **1998**, *564*, 93.
(186) Jiménez, G.; Royo, P.; Cuenca, T.; Herdtweck, E. *Organometallics* **2002**, *21*, 2189.
(187) Amor, F.; Okuda, J. *J. Organomet. Chem.* **1996**, *520*, 245.
(188) Okuda, J.; Schattenmann, F. J.; Wocadlo, S.; Massa, W. *Organometallics* **1995**, *14*, 789.
(189) Nickias, P. N.; Devire, D. D.; Wilson, D. R. (Dow) PCT Int. Appl. WO 93/08199, 1993.
(190) van Leusen, D.; Beetstra, D. J.; Hessen, B.; Teuben, J. H. *Organometallics* **2000**, *19*, 4084.
(191) Sinnema, P.-J.; van der Veen, L.; Spek, A. L.; Veldman, N.; Teuben, J. H. *Organometallics* **1997**, *16*, 4245.
(192) Gomes, P. T.; Green, M. L. H.; Martins, A. M. *J. Organomet. Chem.* **1998**, *551*, 133.
(193) Gomes, P. T.; Green, M. L. H.; Martins, A. M.; Mountford, P. *J. Organomet. Chem.* **1997**, *541*, 121.
(194) Galakhov, M.; Gómez-Sal, P.; Martín, A.; Mena, M.; Yélamos, C. *Eur. J. Inorg. Chem.* **1998**, 1319.
(195) Lensink, C. *J. Organomet. Chem.* **1998**, *553*, 387.
(196) Rep, M.; Kaagman, J.-W. F.; Elsevier, C. J.; Sedmera, P.; Hiller, J.; Thewalt, U.; Horáček, M.; Mach, K. *J. Organomet. Chem.* **2000**, *597*, 146.
(197) Varga, V.; Mach, K.; Polášek, M.; Sedmera, P.; Hiller, J.; Thewalt, U.; Troyanov, S. I. *J. Organomet. Chem.* **1996**, *506*, 241.
(198) Pupi, R. M.; Coalter, J. N.; Petersen, J. L. *J. Organomet. Chem.* **1995**, *497*, 17.
(199) Minhas, R. K.; Scoles, L.; Wong, S.; Gambarotta, S. *Organometallics* **1996**, *15*, 1113.
(200) Bajgur, C. S.; Tikkanen, W. R.; Petersen, J. L. *Inorg. Chem.* **1985**, *24*, 2539.
(201) Klosin, J.; Kruper, W. J., Jr.; Nickias, P. N.; Roof, G. R.; Waele, P. D.; Abboud, K. A. *Organometallics* **2001**, *20*, 2663.
(202) Kamigaito, M.; Lal, T. K.; Waymouth, R. M. *J. Polym. Sci., A: Polym. Chem.* **2000**, *38*, 4649.
(203) Alt, H. G.; Reb, A.; Kundu, K. *J. Organomet. Chem.* **2001**, *628*, 211.
(204) Weiss, T.; Becke, S.; Sachse, H.; Rheinwald, G.; Lang, H. *Inorg. Chem. Commun.* **2002**, *5*, 159.
(205) Engelhardt, L. M.; Papasergio, P. I.; Raston, C. L.; White, A. H. *Organometallics* **1984**, *3*, 18.
(206) Alcock, N. W.; Toogood, G. E.; Wallbridge, M. G. H. *Acta Crystallogr., C: Cryst. Struct. Commun.* **1984**, *40*, 598.
(207) Sassmannshausen, J.; Powell, A. K.; Anson, C. E.; Wocadlo, S.; Bochmann, M. *J. Organomet. Chem.* **1999**, *592*, 84.
(208) Foster, P.; Chien, J. C. W.; Rausch, M. D. *Organometallics* **1996**, *15*, 2404.
(209) Foster, P.; Rausch, M. D.; Chien, J. C. W. *J. Organomet. Chem.* **1998**, *571*, 171.
(210) Xu, G.; Cheng, D. *Macromolecules* **2000**, *33*, 2825.
(211) Schneider, N.; Prosenc, M. H.; Brintzinger, H. H. *J. Organomet. Chem.* **1997**, *545*−*546*, 291.
(212) Flores, J. C.; Wood, J. S.; Chien, J. C. W.; Rausch, M. D. *Organometallics* **1996**, *15*, 4944.
(213) Dorado, I.; Flores, J. C.; Galakhov, M.; Sal, P. G.; Martín, A.; Royo, P. J. *Organomet. Chem.* **1998**, *563*, 7.
(214) Jutzi, P.; Seufert, A. *J. Organomet. Chem.* **1979**, *169*, 373.
(215) Duchateau, R.; Lancaster, S. J.; Thornton-Pett, M.; Bochmann, M. *Organometallics* **1997**, *16*, 4995.
(216) Broussier, R.; Bourdon, C.; Blacque, O.; Vallat, A.; Kubicki, M. M.; Gautheron, B. *J. Organomet. Chem.* **1997**, *538*, 83.
(217) Ziegler, K.; Holzkamp, E.; Breil, H.; Martin, H. *Angew. Chem.* **1955**, *67*, 541.
(218) Natta, G. *Angew. Chem.* **1956**, *68*, 393.
(219) Sinn, H.; Kaminsky, W. *Adv. Organomet. Chem.* **1980**, *18*, 99.
(220) Sinn, H.; Kaminsky, W.; Vollmer, H. J.; Woldt, R. *Angew. Chem., Int. Ed. Engl.* **1980**, *19*, 390.
(221) Chen, E. Y.; Marks, T. J. *Chem. Rev.* **2000**, *100*, 1391.
(222) Piers, W. E.; Shapiro, P. J.; Bunel, E.; Bercaw, J. E. *Synlett* **1990**, *2*, 74.
(223) Shapiro, P. J.; Cotter, W. D.; Schaefer, W. P.; Labinger, J. A.; Bercaw, J. E. *J. Am. Chem. Soc.* **1994**, *116*, 4623.
(224) Cossee, P. *J. Catal.* **1964**, *3*, 80.
(225) Arlman, E. J.; Cossee, P. *J. Catal.* **1964**, *3*, 99.
(226) Chen, Y. X.; Stern, C. L.; Yang, S. T.; Marks, T. J. *J. Am. Chem. Soc.* **1996**, *118*, 12451.
(227) Chen, Y. X.; Metz, M. V.; Li, L. T.; Stern, C. L.; Marks, T. J. *J. Am. Chem. Soc.* **1998**, *120*, 6287.
(228) Luo, L.; Marks, T. J. *Top. Catal.* **1999**, *7*, 97.
(229) Bochmann, M. In *Polymeric Materials Encyclopedia*; Salamone, J. C., Ed.; CRC Press: New York, 1996; p 4177.
(230) Chan, M. S. W.; Vanka, K.; Pye, C. C.; Ziegler, T. *Organometallics* **1999**, *18*, 4624.
(231) Woo, T. K.; Margl, P. M.; Ziegler, T.; Blöchl, P. E. *Organometallics* **1997**, *16*, 3454.
(232) Lanza, G.; Fragalà, I. L.; Marks, T. J. *J. Am. Chem. Soc.* **1998**, *120*, 8257.
(233) Deck, P. A.; Beswick, C. L.; Marks, T. J. *J. Am. Chem. Soc.* **1998**, *120*, 1772.
(234) Kaminsky, W.; Bark, A.; Spiehl, R.; Moller-Lindenhof, N.; Niedoba, S. In *Transition Metals and Organometallics as Catalysts for Olefin Polymerization*; Kaminsky, W., Sinn, H., Eds.; Springer: Berlin, Germany, 1988.
(235) *Ziegler Catalysts*; Fink, G., Mülhaupt, R., Britzinger, H. H., Eds.; Springer-Verlag: Berlin, Germany, 1995.
(236) Tsai, W.-M.; Rausch, M. D.; Chien, J. C. W. *Appl. Organomet. Chem.* **1993**, *7*, 71.
(237) Ewart, S. W.; Sarsfield, M. J.; Williams, E. F.; Baird, M. C. *Polym. Prepr.* **1999**, *40*, 385.

(238) Kim, M. W.; Hong, E.; Han, T. K.; Woo, S. I.; Do, Y. *J. Organomet. Chem.* **1996**, *523*, 211.
(239) Tian, G.; Wang, B.; Xu, S.; Zhou, X. *Trans. Metal. Chem.* **2000**, *25*, 568.
(240) Wang, Q.; Quyoum, R.; Gillis, D. J.; Jeremic, D.; Baird, M. C. *J. Organomet. Chem.* **1997**, *527*, 7.
(241) Wang, Q.; Quyoum, R.; Gillis, D. J.; Tudoret, M.-J.; Jeremic, D.; Hunter, B. K.; Baird, M. C. *Organometallics* **1996**, *15*, 693.
(242) Nomura, K.; Naga, N.; Miki, M.; Yanagi, K. *Macromolecules* **1998**, *31*, 7588.
(243) Deckers, P. J. W.; Hessen, B.; Teuben, J. H. *Angew. Chem., Int. Ed.* **2001**, *40*, 2516.
(244) Nandi, M.; Jin, J.; RajanBabu, T. V. *J. Am. Chem. Soc.* **1999**, *121*, 9899.
(245) Pellecchia, C.; Pappalardo, D.; Gruter, G. *Macromolecules* **1999**, *32*, 4491.
(246) Hultzsch, K. C.; Spaniol, T. P.; Okuda, J. *Organometallics* **1998**, *17*, 485.
(247) Shaffer, T. D.; Canich, J. A. M.; Squire, K. R. *Macromolecules* **1998**, *31*, 5145.
(248) Duchateau, R.; Abbenhuis, H. C. L.; van Santen, R. A.; Thiele, S. K.; van Tol, M. F. H. *Organometallics* **1998**, *17*, 5222.
(249) Juvaste, H.; Pakkanen, T. T. *Organometallics* **2000**, *19*, 4834.
(250) Ushioda, T.; Green, M. L. H.; Haggitt, J.; Yan, X. *J. Organomet. Chem.* **1996**, *518*, 155.
(251) Chen, Y.; Fu, P.; Stern, C. L.; Marks, T. J. *Organometallics* **1997**, *16*, 5958.
(252) Wang, W.; Yan, D.; Zhu, S.; Hamielec, A. E. *Macromolecules* **1998**, *31*, 8677.
(253) Angermund, K.; Fink, G.; Gensen, V. R.; Kleinschmidt, R. *Chem. Rev.* **2000**, *100*, 1457.
(254) Huang, B.; Tian, J. In *Polymeric Materials Encyclopedia*; Salamone, J. C., Ed.; CRC Press: New York, 1996; p 4191.
(255) Müller, G.; Rieger, B. *Prog. Polym. Sci.* **2002**, *27*, 815.
(256) Resconi, L.; Jones, R. L.; Rheingold, A. L.; Yap, G. P. A. *Organometallics* **1996**, *15*, 998.
(257) Hauptman, E.; Waymouth, R. M.; Ziller, J. W. *J. Am. Chem. Soc.* **1995**, *117*, 11586.
(258) Ewart, S. W.; Sarsfield, M. J.; Jeremic, D.; Tremblay, T. L.; Williams, E. F.; Baird, M. C. *Organometallics* **1998**, *17*, 1502.
(259) Ishihara, N.; Seimiya, T.; Kuramoto, M.; Uoi, M. *Macromolecules* **1986**, *19*, 2464.
(260) Ishihara, N.; Kuramoto, M.; Uoi, M. Eur. Patent 210615, 1987 (to Idemitsu Kosan Co.).
(261) Po, R.; Cardi, N. *Prog. Polym. Sci.* **1996**, *21*, 47.
(262) Vittoria, V. In *Handbook of Thermoplastics*; Olabisi, O., Ed.; Dekker: New York, 1997; p 81.
(263) Tomotsu, N.; Ishihara, N.; Newman, T. H.; Malanga, M. T. *J. Mol. Catal., A.: Chem.* **1998**, *128*, 167.
(264) Pellecchia, C.; Grassi, A. *Top. Catal.* **1999**, *7*, 125.
(265) Ewart, S. W.; Baird, M. C. *Top. Catal.* **1999**, *7*, 1.
(266) Ewart, S. W.; Baird, M. C. In *Metallocene Based Polyolefins, Preparations, Properties and Technology*; Scheirs, J., Kaminsky, W., Eds.; Wiley: New York, 2000; Vol. 1, p 119.
(267) Longo, P.; Proto, A.; Zambelli, A. *Macromol. Chem. Phys.* **1995**, *196*, 3015.
(268) Duncalf, D. J.; Wade, H. J.; Waterson, C.; Derrick, P. J.; Haddleton, D. M.; McCamley, A. *Macromolecules* **1996**, *29*, 6399.
(269) Grassi, A.; Saccheo, S.; Zambelli, A.; Laschi, F. *Macromolecules* **1998**, *31*, 5588.
(270) Grassi, A.; Zambelli, A.; Laschi, F. *Organometallics* **1996**, *15*, 480.
(271) Newman, T. H.; Borodychuk, K. K. *Polym. Prepr.* **1999**, *40*, 387.
(272) Zambelli, A.; Pellecchia, C.; Proto, A. *Macromol. Symp.* **1995**, *89*, 373.
(273) Grassi, A.; Pellecchia, C.; Oliva, L.; Laschi, F. *Macromol. Chem. Phys.* **1995**, *196*, 1093.
(274) Xu, G.; Lin, S. *Macromolecules* **1997**, *30*, 685.
(275) Pó, R.; Cardi, N.; Abis, L.; *Polymer* **1998**, *39*, 959.
(276) Williams, E. F.; Murray, M. C.; Baird, M. C. *Macromolecules* **2000**, *33*, 261.
(277) Pellecchia, C.; Longo, P.; Grassi, A.; Ammendola, P.; Zambelli, A. *Macromol. Chem. Rapid Commun.* **1978**, *8*, 277.
(278) Zambelli, A.; Pellecchia, C.; Oliva, L.; Longo, P.; Grassi, A. *Makromol. Chem.* **1991**, *192*, 223.
(279) Xu, G. *Macromolecules* **1998**, *31*, 586.
(280) Wang, Q.; Baird, M. C. *Macromolecules* **1995**, *28*, 8021.
(281) Baird, M. C. *Chem. Rev.* **2000**, *100*, 1471.
(282) Foster, P.; Ready, T. E.; Chien, J. C. W.; Rausch, M. D. *Polym. Prepr.* **1996**, *37*, 258.
(283) Liu, J.; Ma, H.; Huang, J.; Qian, Y.; Chan, A. S. C. *Eur. Polym. J.* **1999**, *35*, 543.
(284) Xu, G.; Chung, T. C. *Macromolecules* **2000**, *33*, 5803.
(285) Gassman, P. G.; Winter, C. H. *J. Am. Chem. Soc.* **1988**, *110*, 6130.
(286) Kaminsky, W.; Lenk, S.; Scholz, V.; Roesky, H. W.; Herzog, A. *Macromolecules* **1997**, *30*, 7647.
(287) Grubbs, R. H.; Coates, G. W. *Acc. Chem. Res.* **1996**, *29*, 85.
(288) Ma, H.; Zhang, Y.; Chen, B.; Huang, J.; Qian, Y. *J. Polym. Sci., Part A: Polym. Chem.* **2001**, *39*, 1807.
(289) Kaminsky, W.; Arrowsmith, D.; Strübel, C. *J. Polym. Sci., Part A: Polym. Chem.* **1999**, *37*, 2959.
(290) Nomura, K.; Okumura, H.; Komatsu, T.; Naga, N. *Macromolecules* **2002**, *35*, 5388.
(291) Longo, P.; Grassi, A.; Oliva, L. *Makromol. Chem.* **1990**, *191*, 2387.
(292) Pellecchia, C.; Oliva, L. *Rubber Chem. Technol.* **1999**, *72*, 553.
(293) Stevens, J. C.; Timmers, F. J.; Wilson, D. R.; Schmidt, G. F.; Nickias, P. N.; Rosen, R. K. Knight, G. W.; Lai, S.-Y. Eur. Patent 0 416 815 A2, 1990 (to Dow Chemical Co.).
(294) Devore, D. D. Eur. Patent 0 514 828 A1, 1992 (to Dow Chemical Co.).
(295) Xu, G. *Macromolecules* **1998**, *31*, 2395.
(296) Okuda, J.; Amor, F.; Eberle, T.; Hultzsch, K. C.; Spaniol, T. P. *Polym. Prepr.* **1999**, *40*, 371.
(297) Nomura, K.; Komatsu, T.; Imanishi, Y. *Macromolecules* **2000**, *33*, 8122.
(298) Nomura, K.; Oya, K.; Komatsu, T.; Imanishi, Y. *Macromolecules* **2000**, *33*, 3187.
(299) Pellecchia, C.; Pappalardo, D.; D'Arco, M.; Zambelli, A. *Macromolecules* **1996**, *29*, 1158.
(300) Sernetz, F. G.; Mülhaupt, R.; Amor, F.; Eberle, T.; Okuda, J. *J. Polym. Sci., Part A: Polym. Chem.* **1997**, *35*, 1571.
(301) Oliva, L.; Immirzi, A.; Tedesco, C.; Venditto, V.; Proto, A. *Macromolecules* **1999**, *32*, 2675.
(302) Venditto, V.; Tullio, G. D.; Izzo, L.; Oliva, L. *Macromolecules* **1998**, *31*, 4027.
(303) Sernetz, F. G.; Mülhaupt, R. *J. Polym. Sci., Part A: Polym. Chem.* **1997**, *35*, 2549.
(304) Sernetz, F. G.; Mülhaupt, R.; Waymouth, R. M. *Polym. Bull. (Berlin)* **1997**, *38*, 141.
(305) Cozewith, C.; ver Strate, G. *Macromolecules* **1971**, *4*, 482.
(306) Kakugo, M.; Naito, Y.; Mizunuma, K.; Miyatake, T. *Macromolecules* **1982**, *15*, 1150.
(307) Soga, K.; Shiono, T.; Doi, Y. *Polym. Bull. (Berlin)* **1983**, *10*, 168.
(308) Doi, Y.; Ohnishi, R.; Soga, K. *Makromol. Chem. Rapid Commun.* **1983**, *4*, 169.
(309) Wang, W.; Kolodka, E.; Zhu, S.; Hamielec, A. E. *J. Polym. Sci., Part A: Polym. Chem.* **1999**, *37*, 2949.
(310) Xu, G.; Cheng, D. *Macromolecules* **2001**, *34*, 2040.
(311) Soga, K.; Uozumi, T.; Nakamura, S.; Toneri, T.; Teranish, T.; Sano, T.; Arai, T.; Shiono, T. *Macromol. Chem. Phys.* **1996**, *197*, 4237.
(312) Imanishi, Y.; Nomura, K. *J. Polym. Sci., Part A: Polym. Chem.* **2000**, *38*, 4613.
(313) Xu, G.; Ruckenstein, E. *Macromolecules* **1998**, *31*, 4724.
(314) Kumar, K. R.; Sivaram, S. *Polym. Int.* **2001**, *50*, 367.
(315) Wang, W.; Zhu, S.; Park, S. *Macromolecules* **2000**, *33*, 5770.
(316) Nomura, K.; Komatsu, T.; Imanishi, Y. *J. Mol. Catal., A: Chem.* **2000**, *159*, 127.
(317) *Ulmann's Encyclopedia of Industrial Chemistry*; Elvers, B., Hawkins, S., Russell, W., Shulz, G., Eds.; VCH: Weinheim, Germany, 1993; Vol. 23.
(318) Peluso, A.; Improta, R.; Zambelli, A. *Organometallics* **2000**, *19*, 411.
(319) Miyazawa, A.; Kase, T.; Soga, K. *J. Polym. Sci., Part A: Polym. Chem.* **1999**, *37*, 695.
(320) Miyazawa, A.; Kase, T.; Soga, K. *Macromolecules* **2000**, *33*, 2796.
(321) Tao, X.; Qian, F.; Yong, L.; Qian, Y. *J. Mol. Catal., A: Chem.* **2000**, *156*, 121.
(322) Qian, Y.; Saleque, M. A.; Cai, L.; Hong, K.; Lu, J. *Chin. J. Catal.* **1999**, *20*, 389.
(323) Barsan, F.; Karam, A. R.; Parent, M. A.; Baird, M. C. *Macromolecules* **1998**, *31*, 8439.
(324) Satori, G.; Ciampelli, F.; Cameli, N. *Chim. Ind.* **1963**, *45*, 1479.
(325) Kaminsky, W.; Bark, A.; Dake, I. *Stud. Surf. Sci. Catal.* **1990**, *56*, 425.
(326) Kaminsky, W.; Arndt, M.; Beulich, I. *Polym. Mater. Sci. Eng.* **1997**, *76*, 18.
(327) Ruchatz, D.; Fink, G. *Macromolecules* **1998**, *31*, 4669.
(328) Kaminsky, W.; Bark, A.; Amdt, M. *Makromol. Chem., Macromol. Symp.* **1991**, *47*, 83.
(329) Ruchatz, D.; Fink, G. *Macromolecules* **1998**, *31*, 4670.
(330) Ruchatz, D.; Fink, G. *Macromolecules* **1998**, *31*, 4674.
(331) Ruchatz, D.; Fink, G. *Macromolecules* **1998**, *31*, 4681.
(332) Ruchatz, D.; Fink, G. *Macromolecules* **1998**, *31*, 4684.
(333) McKnight, A. L.; Waymouth, R. M. *Macromolecules* **1999**, *32*, 2816.
(334) Wu, Q.; Lu, Y.; Lu, Z. *Polym. Mater. Sci. Eng.* **1999**, *80*, 483.
(335) Grubbs, R. H.; Tumas, W. *Science* **1989**, *243*, 907.
(336) Schrock, R. R. *Acc. Chem. Res.* **1990**, *23*, 158.
(337) Schoettel, G.; Kress, J.; Osborn, J. A. *J. Chem. Soc., Chem. Commun.* **1989**, 1062.
(338) Schrock, R. R.; Feldman, J.; Cannizzo, L. F.; Grubbs, R. *Macromolecules* **1987**, *20*, 1169.
(339) Wsllsce, K. C.; Liu, A. H.; Dewan, J. C.; Schrock, R. R. *J. Am. Chem. Soc.* **1988**, *110*, 4964.

(340) Torcki, R.; Schrock, R. R.; Vale, M. G. *J. Am. Chem. Soc.* **1991**, *113*, 3610.
(341) Hamilton, J. G.; Marquess, D. G.; O'Neill, T. J.; Rooney, J. J. *J. Chem. Soc., Chem. Commun.* **1990**, 119.
(342) Petasis, N. A.; Fu, D.-K. *J. Am. Chem. Soc.* **1993**, *115*, 7208.
(343) Zhang, D.; Huang, J.; Qian, Y.; Chan, A. S. C. *J. Mol. Catal. A: Chem.* **1998**, *133*, 131.
(344) Petasis, N. A.; Bzowej, E. I. *J. Org. Chem.* **1992**, *57*, 1327.
(345) Petasis, N. A.; Akritopoulou, I. *Synlett* **1992**, 665.
(346) Petasis, N. A.; Bzowej. E. I. *Tetrahedron Lett.* **1993**, *34*, 943.
(347) Ohff, A.; Burlakov, V. V.; Rosenthal, U. *J. Mol. Catal. A: Chem.* **1996**, *105*, 103.
(348) Qian, Y.; Zhuang, J.; Lu, J.; Huang, Q.; Xu, W.; Chen, S. *J. Mol. Catal.* **1987**, *38*, 331.
(349) Qian, Y.; Li, G.; He, Y.; Chen, W.; Li, B.; Chen, S. *J. Mol. Catal.* **1990**, *60*, 19.
(350) Lehmkuhl, H.; Tsien, Y. (Qian, Y.) *Chem. Ber.* **1983**, *116*, 2437.
(351) Qian, Y.; Saleque, M. A.; Huang, J.; Li, Z. *Chin. J. Catal.* **2000**, *21*, 1.
(352) Qian, Y.; Lu, J.; Xu, W. *J. Mol. Catal.* **1986**, *34*, 31.
(353) Cuenca, T.; Carlos, J.; Royo, P. *J. Organomet. Chem.* **1993**, *462*, 191.
(354) Fan, Y.; Liao, S.; Xu, Y.; Qian, Y.; Huang, J. *Chin. J. Catal. (Chinese)* **1998**, *19*, 389.
(355) Fan, Y.; Liao, S.; Xu, J.; Wang, F.; Qian, Y.; Huang, J. *J. Catal.* **2002**, *205*, 294.
(356) Alt, H. G.; Weis, A.; Reb, A.; Ernst, R. *Inorg. Chimi. Acta* **2003**, *343*, 253.
(357) Noh, S. K.; Lee, J.; Lee, D. *J. Organomet. Chem.* **2003**, *667*, 53.

CR020002X